ISSN 2602-2575 • EISSN 2618-6144

EUROPEAN JOURNAL OF BIOLOGY

OFFICIAL JOURNAL OF ISTANBUL UNIVERSITY'S SCIENCE FACULTY

Volume: 81 • Issue: 1 • June 2022

https://iupress.istanbul.edu.tr/en/journal/ejb/home

ISTANBUL UNIVERSITY PRESS

EUROPEAN
JOURNAL OF
BIOLOGY

Indexing and Abstracting

Zoological Record - Clarivate Analytics

CAB Abstracts

CABI

- AgBiotechNet Database

- Animalscience Database

- VetMed Resource

- Environmental Impact Database

- Horticultural Science Database

- Nutrition and Food Sciences Database

Chemical Abstracts Service (CAS)

ULAKBIM TR Index

Scopus

DOAJ

EBSCO Central & Eastern European Academic Source

SOBIAD

EUROPEAN
JOURNAL OF
BIOLOGY

Owner
Prof. Dr. Tansel AK
Istanbul University, Istanbul, Turkey

Responsible Manager
Prof. Dr. Sehnaz BOLKENT
Istanbul University, Istanbul, Turkey
sbolkent@istanbul.edu.tr

Correspondence Address
Istanbul University, Faculty of Science,
Department of Biology,
34134 Vezneciler, Fatih, Istanbul, Turkey
Phone: +90 (212) 455 57 00 (Ext. 20318)
Fax: +90 (212) 528 05 27
E-mail: ejb@istanbul.edu.tr
https://iupress.istanbul.edu.tr/en/journal/ejb/home

Publisher
Istanbul University Press
Istanbul University Central Campus,
34452 Beyazit, Fatih, Istanbul, Turkey
Phone: +90 (212) 440 00 00

Printed by
İlbey Matbaa Kağıt Reklam Org. Müc. San. Tic. Ltd. Şti.
2. Matbaacılar Sitesi 3NB 3 Topkapı / Zeytinburnu,
Istanbul, Turkey
www.ilbeymatbaa.com.tr
Certificate No: 51632

The publication language of the journal is English.

This is a scholarly, international, peer-reviewed and open-access journal published biannually in June and December.

Publication Type: Periodical

EUROPEAN
JOURNAL OF
BIOLOGY

EDITORIAL MANAGEMENT BOARD

EUROPEAN
JOURNAL OF
BIOLOGY

EDITORIAL BOARD

EUROPEAN
JOURNAL OF
BIOLOGY

Aims and Scope

European Journal of Biology (Eur J Biol) is an international, scientific, open access periodical published in accordance with independent, unbiased, and double-blinded peer-review principles. The journal is the official publication of Istanbul University Faculty of Science and it is published biannually on June and December. The publication language of the journal is English. European Journal of Biology has been previously published as IUFS Journal of Biology. It has been published in continuous publication since 1940.

European Journal of Biology aims to contribute to the literature by publishing manuscripts at the highest scientific level on all fields of biology. The journal publishes original research and review articles, and short communications that are prepared in accordance with the ethical guidelines in all fields of biology and life sciences.

The scope of the journal includes but not limited to; animal biology and systematics, plant biology and systematics, hydrobiology, ecology and environmental biology, microbiology, cell and molecular biology, biochemistry, biotechnology and genetics, physiology, toxicology, cancer biology, developmental and stem cell biology.

The target audience of the journal includes specialists and professionals working and interested in all disciplines of biology.

The editorial and publication processes of the journal are shaped in accordance with the guidelines of the International Committee of Medical Journal Editors (ICMJE), World Association of Medical Editors (WAME), Council of Science Editors (CSE), Committee on Publication Ethics (COPE), European Association of Science Editors (EASE), and National Information Standards Organization (NISO). The journal is in conformity with the Principles of Transparency and Best Practice in Scholarly Publishing (doaj.org/bestpractice).

European Journal of Biology is currently indexed by Web of Science Zoological Record, CAB Abstracts (CABI), Chemical Abstracts Service (CAS), TUBITAK-ULAKBIM TR Index, Scopus, DOAJ, EBSCO Central & Eastern European Academic Source and SOBIAD.

Processing and publication are free of charge with the journal. No fees are requested from the authors at any point throughout the evaluation and publication process. All manuscripts must be submitted via the online submission system, which is available at dergipark.gov.tr/iufsjb. The journal guidelines, technical information, and the required forms are available on the journal's web page.

All expenses of the journal are covered by the Istanbul University.

Statements or opinions expressed in the manuscripts published in the journal reflect the views of the author(s) and not the opinions of the Istanbul University Faculty of Science, editors, editorial board, and/or publisher; the editors, editorial board, and publisher disclaim any responsibility or liability for such materials.

All published content is available online, free of charge at https://dergipark.org.tr/tr/pub/iufsjb. Printed copies of the journal are distributed free of charge.

OPEN ACCESS

Editor in Chief: Prof. Dr. Sehnaz BOLKENT
Address: Istanbul University, Faculty of Science, Department of Biology, 34134 Vezneciler, Fatih, Istanbul, TURKEY
Phone: +90 212 4555700 (Ext. 20318)
Fax: +90 212 5280527
E-mail: sbolkent@istanbul.edu.tr

EUROPEAN
JOURNAL OF
BIOLOGY

Instructions to Authors

European Journal of Biology (Eur J Biol) is an international, scientific, open access periodical published in accordance with independent, unbiased, and double-blinded peer-review principles. The journal is the official publication of Istanbul University Faculty of Science and it is published biannually on June and December. The publication language of the journal is English. European Journal of Biology has been previously published as IUFS Journal of Biology. It has been published in continuous publication since 1940.

European Journal of Biology aims to contribute to the literature by publishing manuscripts at the highest scientific level on all fields of biology. The journal publishes original research and review articles, and short communications that are prepared in accordance with the ethical guidelines in all fields of biology and life sciences.

The scope of the journal includes but not limited to; animal biology and systematics, plant biology and systematics, hydrobiology, ecology and environmental biology, microbiology, cell and molecular biology, biochemistry, biotechnology and genetics, physiology, toxicology, cancer biology, developmental and stem cell biology.

The editorial and publication processes of the journal are shaped in accordance with the guidelines of the International Council of Medical Journal Editors (ICMJE), the World Association of Medical Editors (WAME), the Council of Science Editors (CSE), the Committee on Publication Ethics (COPE), the European Association of Science Editors (EASE), and National Information Standards Organization (NISO). The journal conforms to the Principles of Transparency and Best Practice in Scholarly Publishing (doaj.org/bestpractice).

Originality, high scientific quality, and citation potential are the most important criteria for a manuscript to be accepted for publication. Manuscripts submitted for evaluation should not have been previously presented or already published in an electronic or printed medium. Manuscripts that have been presented in a meeting should be submitted with detailed information on the organization, including the name, date, and location of the organization.

Manuscripts submitted to European Journal of Biology will go through a double-blind peer-review process. Each submission will be reviewed by at least three external, independent peer reviewers who are experts in their fields in order to ensure an unbiased evaluation process. The editorial board will invite an external and independent editor to manage the evaluation processes of manuscripts submitted by editors or by the editorial board members of the journal. The Editor in Chief is the final authority in the decision-making process for all submissions.

An approval of research protocols by the Ethics Committee in accordance with international agreements (World Medical Association Declaration of Helsinki "Ethical Principles for Medical Research Involving Human Subjects," amended in October 2013, www.wma.net) is required for experimental, clinical, and drug studies. If required, ethics committee reports or an equivalent official document will be requested from the authors.

For manuscripts concerning experimental research on humans, a statement should be included that shows the written informed consent of patients and volunteers was obtained following a detailed explanation of the procedures that they may undergo. Information on patient consent, the name of the ethics committee, and the ethics committee approval number should also be stated in the Materials and Methods section of the manuscript. It is the authors' responsibility to carefully protect the patients' anonymity. For photographs that may reveal the identity of the patients, signed releases of the patient or of their legal representative should be enclosed.

European Journal of Biology requires experimental research studies on vertebrates or any regulated invertebrates to comply with relevant institutional, national and/or international guidelines. The journal supports the principles of Basel Declaration (basel-declaration.org) and the guidelines published by International Council for Laboratory Animal Science (ICLAS) (iclas.org). Authors are advised to clearly state their compliance with relevant guidelines.

European Journal of Biology advises authors to comply with IUCN Policy Statement on Research Involving Species at Risk of Extinction and the Convention on the Trade in Endangered Species of Wild IUCN Policy Statement on Research Involving Species at Risk of Extinction and the Convention on the Trade in Endangered Species of Wild Fauna and Flora.

All submissions are screened by a similarity detection software (iThenticate by CrossCheck).

In the event of alleged or suspected research misconduct, e.g., plagiarism, citation manipulation, and data falsification/fabrication, the Editorial Board will follow and act in accordance with COPE guidelines.

Each individual listed as an author should fulfil the authorship criteria recommended by the International Committee of Medical Journal Editors (ICMJE - www.icmje.org). The ICMJE recommends that authorship be based on the following 4 criteria:

1 Substantial contributions to the conception or design of the work; or the acquisition, analysis, or interpretation of data for the work; AND
2 Drafting the work or revising it critically for important intellectual content; AND
3 Final approval of the version to be published; AND
4 Agreement to be accountable for all aspects of the work in ensuring that questions related to the accuracy or integrity of any part of the work are appropriately investigated and resolved.

In addition to being accountable for the parts of the work he/she has done, an author should be able to identify which co-authors are responsible for specific other parts of the work. In addition, authors should have confidence in the integrity of the contributions of their co-authors.

All those designated as authors should meet all four criteria for authorship, and all who meet the four criteria should be identified as authors. Those who do not meet all four criteria should be acknowledged in the title page of the manuscript.

European Journal of Biology requires corresponding authors to submit a signed and scanned version of the authorship contribution form (available for download through the journal's web page) during the initial submission process in order to act appropriately on authorship rights and to prevent ghost or honorary authorship. If the editorial board suspects a case of "gift authorship," the submission will be rejected without further review. As part of the submission of the manuscript, the corresponding author should also send a short statement declaring that he/she accepts to undertake all the responsibility for authorship during the submission and review stages of the manuscript.

European Journal of Biology requires and encourages the authors and the individuals involved in the evaluation process of submitted manuscripts to disclose any existing or potential conflicts of interests, including financial, consultant, and institutional, that might lead to potential bias or a conflict of interest. Any financial grants or other supports received for a submitted study from individuals or institutions should be disclosed to the Editorial Board. To disclose a potential conflict of interest, the ICMJE Potential Conflict of Interest Disclosure Form should be filled and submitted by all contributing authors. Cases of a potential conflict of interest of the editors, authors, or reviewers are resolved by the journal's Editorial Board within the scope of COPE and ICMJE guidelines.

The Editorial Board of the journal handles all appeal and complaint cases within the scope of COPE guidelines. In such cases, authors should get in direct contact with the editorial office regarding their appeals and complaints. When needed, an ombudsperson may be assigned to resolve cases that cannot be resolved internally. The Editor in Chief is the final authority in the decision-making process for all appeals and complaints.

When submitting a manuscript to European Journal of Biology, authors accept to assign the copyright of their manuscript to Istanbul University Faculty of Science. If rejected for publication, the copyright of the manuscript will be assigned back to the authors. European Journal of Biology requires each submission to be accompanied by a Copyright Transfer Form (available for download at the journal's web page). When using previously published content, including figures, tables, or any other material in both print and electronic formats, authors must obtain permission from the copyright holder. Legal, financial and criminal liabilities in this regard belong to the author(s).

Statements or opinions expressed in the manuscripts published in European Journal of Biology reflect the views of the author(s) and not the opinions of the editors, the editorial board, or the publisher; the editors, the editorial board, and the publisher disclaim any responsibility or liability for such materials. The final responsibility in regard to the published content rests with the authors.

MANUSCRIPT SUBMISSION

European Journal of Biology endorses ICMJE-Recommendations for the Conduct, Reporting, Editing, and Publication of Scholarly Work in Medical Journals (updated in December 2015 - http://www.icmje.org/icmje-recommendations.pdf). Authors are required to prepare manuscripts in accordance with the CONSORT guidelines for randomized research studies, STROBE guidelines for observational original research studies, STARD guidelines for studies on diagnostic accuracy, PRISMA guidelines for systematic reviews and meta-analysis, ARRIVE guidelines for experimental animal studies, TREND guidelines for non-randomized public behaviour, and COREQ guidelines for qualitative research.

Manuscripts can only be submitted through the journal's online manuscript submission and evaluation system, available at the journal's web page. Manuscripts submitted via any other medium will not be evaluated.

Manuscripts submitted to the journal will first go through a technical evaluation process where the editorial office staff will ensure that the manuscript has been prepared and submitted in accordance with the journal's guidelines. Submissions that do not conform to the journal's guidelines will be returned to the submitting author with technical correction requests.

During the initial submission, authors are required to submit the following:

- Copyright Agreement Form,
- Author Contributions Form, and

ICMJE Potential Conflict of Interest Disclosure Form (should be filled in by all contributing authors). These forms are available for download at the journal's web page.

Preparation of the Manuscript

Title page: A separate title page should be submitted with all submissions and this page should include:

- The full title of the manuscript as well as a short title (running head) of no more than 50 characters,
- Name(s), affiliations, and highest academic degree(s) of the author(s),
- Grant information and detailed information on the other sources of support,
- Name, address, telephone (including the mobile phone number) and fax numbers, and email address of the corresponding author,
- Acknowledgment of the individuals who contributed to the preparation of the manuscript but who do not fulfil the authorship criteria.

Abstract: Abstract with subheadings should be written as structured abstract in submitted papers except for Review Articles and Letters to the Editor. Please check Table 1 below for word count specifications (250 words).

Keywords: Each submission must be accompanied by a minimum of three to a maximum of six keywords for subject indexing at the end of the abstract. The keywords should be listed in full without abbreviations.

Manuscript Types

Original Articles: This is the most important type of article since it provides new information based on original research. A structured abstract is required with original articles and it should include the following subheadings: Objective, Materials and Methods, Results and Conclusion. The main text of original articles should be structured with Introduction, Materials and Methods, Results, Discussion, and Conclusion subheadings. Please check Table 1 for the limitations of Original Articles.

Statistical analysis to support conclusions is usually necessary. Statistical analyses must be conducted in accordance with international statistical reporting standards. Information on statistical analyses should be provided with a separate subheading under the Materials and Methods section and the statistical software that was used during the process must be specified.

Units should be prepared in accordance with the International System of Units (SI).

Short Communications: Short communication is for a concise, but independent report representing a significant contribution to Biology. Short communication is not intended to publish preliminary results. But if these results are of exceptional interest and are particularly topical and relevant will be considered for publication.

Short Communications should include an abstract and should be structed with the following subheadings: "Introduction", "Materials and Methods", "Results and Discussion".

Editorial Comments: Editorial comments aim to provide a brief critical commentary by reviewers with expertise or with high reputation in the topic of the research article published in the journal. Authors are selected and invited by the journal to provide such comments. Abstract, Keywords, and Tables, Figures, Images, and other media are not included.

Review Articles: Reviews prepared by authors who have extensive knowledge on a particular field and whose scientific background has been translated into a high volume of publications with a high citation potential are welcomed. These authors may even be invited by the journal. Reviews should describe, discuss, and evaluate the current level of knowledge of a topic in clinical practice and should guide future studies. The main text should contain Introduction, Experimental and Clinical Research Consequences, and Conclusion sections. Please check Table 1 for the limitations for Review Articles.

Letters to the Editor: This type of manuscript discusses important parts, overlooked aspects, or lacking parts of a previously published article. Articles on subjects within the scope of the journal that might attract the readers' attention, particularly educative cases, may also be submitted in the form of a "Letter to the Editor." Readers can also present their comments on the published manuscripts in the form of a "Letter to the Editor." Abstract, Keywords, and Tables, Figures, Images, and other media should not be included. The text should be unstructured. The manuscript that is being commented on must be properly cited within this manuscript.

Tables

Tables should be included in the main document, presented after the reference list, and they should be numbered consecutively in the order they are referred to within the main text. A descriptive title must be placed above the tables. Abbreviations used in the tables should be defined below the tables by footnotes (even if they are defined within the main text). Tables should be created using the "insert table" command of the word processing software and they should be arranged clearly to provide easy reading. Data presented in the tables should not be a repetition of the data presented within the main text but should be supporting the main text.

Figures and Figure Legends

Figures, graphics, and photographs should be submitted as separate files (in TIFF or JPEG format with 1200 dpi for graphic and 600 dpi for colour images) through the submission system. The files should not be embedded in a Word document or the main document. When there are figure subunits, the subunits should be labeled merged to form a single image. Each subunit should be submitted separately through the submission system. Images

Table 1. Limitations for each manuscript type

Type of manuscript	Word limit	Abstract word limit	Reference limit	Table limit	Figure limit
Original Article	4500	250 (Structured)	No limit	6	Maximum 10
Short Communication	2500	200	30	3	4
Review Article	5500	250	No limit	5	6
Letter to the Editor	500	No abstract	5	No tables	No media

should be labeled (a, b, c, etc.) to indicate figure subunits. Thick and thin arrows, arrowheads, stars, asterisks, and similar marks can be used on the images to support figure legends. Like the rest of the submission, the figures too should be blind. Any information within the images that may indicate an individual or institution should be blinded. The minimum resolution of each submitted figure should be 300 DPI. To prevent delays in the evaluation process, all submitted figures should be clear in resolution and large in size (minimum dimensions: 100 × 100 mm). Figure legends should be listed at the end of the main document.

All acronyms and abbreviations used in the manuscript should be defined at first use, both in the abstract and in the main text. The abbreviation should be provided in parentheses following the definition.

When a drug, chemical, product, hardware, or software program is mentioned within the main text, product information, including the name of the product, the producer of the product, and city and the country of the company (including the state if in USA), should be provided in parentheses in the following format: "Discovery St PET/CT scanner (General Electric, Milwaukee, WI, USA)".

All references, tables, and figures should be referred to within the main text, and they should be numbered consecutively in the order they are referred to within the main text.

Limitations, drawbacks, and the shortcomings of original articles should be mentioned in the Discussion section before the conclusion paragraph.

References

While citing publications, preference should be given to the latest, most up-to-date publications. If an ahead-of-print publication is cited, the DOI number should be provided. Authors are responsible for the accuracy of references. Journal titles should be abbreviated in accordance with the journal abbreviations in Index Medicus/ MEDLINE/PubMed. When there are six or fewer authors, all authors should be listed. If there are seven or more authors, the first six authors should be listed followed by "et al." In the main text of the manuscript, references should be cited using Arabic numbers in parentheses. The reference styles for different types of publications are presented in the following examples.

Journal Article: Rankovic A, Rancic N, Jovanovic M, Ivanović M, Gajović O, Lazić Z, et al. Impact of imaging diagnostics on the budget – Are we spending too much? Vojnosanit Pregl 2013; 70: 709-11.

Book Section: Suh KN, Keystone JS. Malaria and babesiosis. Gorbach SL, Barlett JG, Blacklow NR, editors. Infectious Diseases. Philadelphia: Lippincott Williams; 2004.p.2290-308.

Books with a Single Author: Sweetman SC. Martindale the Complete Drug Reference. 34th ed. London: Pharmaceutical Press; 2005.

Editor(s) as Author: Huizing EH, de Groot JAM, editors. Functional reconstructive nasal surgery. Stuttgart-New York: Thieme; 2003.

Conference Proceedings: Bengisson S. Sothemin BG. Enforcement of data protection, privacy and security in medical informatics. In: Lun KC, Degoulet P, Piemme TE, Rienhoff O, editors. MEDINFO 92. Proceedings of the 7th World Congress on Medical Informatics; 1992 Sept 6-10; Geneva, Switzerland. Amsterdam: North-Holland; 1992. pp.1561-5.

Scientific or Technical Report: Cusick M, Chew EY, Hoogwerf B, Agrón E, Wu L, Lindley A, et al. Early Treatment Diabetic Retinopathy Study Research Group. Risk factors for renal replacement therapy in the Early Treatment Diabetic Retinopathy Study (ETDRS), Kidney Int: 2004. Report No: 26.

Thesis: Yılmaz B. Ankara Üniversitesindeki Öğrencilerin Beslenme Durumları, Fiziksel Aktiviteleri ve Beden Kitle İndeksleri Kan Lipidleri Arasındaki Ilişkiler. H.Ü. Sağlık Bilimleri Enstitüsü, Doktora Tezi. 2007.

Epub Ahead of Print Articles: Cai L, Yeh BM, Westphalen AC, Roberts JP, Wang ZJ. Adult living donor liver imaging. Diagn Interv Radiol. 2016 Feb 24. doi: 10.5152/dir.2016.15323. [Epub ahead of print].

Manuscripts Published in Electronic Format: Morse SS. Factors in the emergence of infectious diseases. Emerg Infect Dis (serial online) 1995 Jan-Mar (cited 1996 June 5): 1(1): (24 screens). Available from: URL: http:/ www.cdc.gov/ncidodlElD/cid.htm.

REVISIONS

When submitting a revised version of a paper, the author must submit a detailed "Response to the reviewers" that states point by point how each issue raised by the reviewers has been covered and where it can be found (each reviewer's comment, followed by the author's reply and line numbers where the changes have been made) as well as an annotated copy of the main document. Revised manuscripts must be submitted within 30 days from the date of the decision letter. If the revised version of the manuscript is not submitted within the allocated time, the revision option may be cancelled. If the submitting author(s) believe that additional time is required, they should request this extension before the initial 30-day period is over.

Accepted manuscripts are copy-edited for grammar, punctuation, and format. Once the publication process of a manuscript is completed, it is published online on the journal's webpage as an ahead-of-print publication before it is included in its scheduled issue. A PDF proof of the accepted manuscript is sent to the corresponding author and their publication approval is requested within 2 days of their receipt of the proof.

Editor in Chief: Prof. Dr. Sehnaz BOLKENT
Address: Istanbul University, Faculty of Science, Department of Biology, 34134 Vezneciler, Fatih, Istanbul, TURKEY
Phone: +90 212 4555700 (Ext. 20318)
Fax: +90 212 5280527
E-mail: sbolkent@istanbul.edu.tr

EUROPEAN
JOURNAL OF
BIOLOGY

Contents

ISTANBUL UNIVERSITY PRESS

RESEARCH ARTICLE

Eur J Biol 2022; 81(1): 1-10

Chemical Profiling and Wetting Behaviors of Endemic *Salvia absconditiflora* Greuter & Burdet (Lamiaceae) Collected from Gypsum Areas

Aysenur Kayabas[1], Ertan Yildirim[2]

[1]Cankiri Karatekin University, Faculty of Science, Department of Biology, Cankiri, Turkiye
[2]Gazi University, Faculty of Science, Department of Chemistry, Ankara, Turkiye

ORCID IDs of the authors: A.K. 0000-0003-3555-4399; E.Y. 0000-0002-4083-3408

Please cite this article as: Kayabas A, Yildirim E. Chemical Profiling and Wetting Behaviors of Endemic *Salvia absconditiflora* Greuter & Burdet (Lamiaceae) Collected from Gypsum Areas. Eur J Biol 2022; 81(1): 1-10. DOI: 10.26650/EurJBiol.2021.1011530

ABSTRACT

Objective: *Salvia absconditiflora* Greuter & Burdet is an endemic plant and survives in nature by adapting to extreme conditions. The aims of this study are to characterize and compare the diversity in the spectral-chemical structure of *S. absconditiflora*'s plant parts using the FTIR spectroscopy technique, to determine the wettability of the adaxial and abaxial epidermal surfaces of *S. abscontidiflora* leaves and to interpret whether there is a difference between the contact angle (CA) measurements at the points determined in the surface area of the leaves from the part close to the petiole to the leaf tip.

Materials and Methods: The ATR-FTIR spectra for the chemical content of *S. absconditiflora* were obtained from six different plant parts and information about their chemical compositions was obtained. CA measurements were carried out for the natural events of the leaf area, especially for the water holding capacity or hydrophilic-hydrophobic characteristics.

Results: The biochemical fingerprint of *S. absconditiflora* was determined by the analysis of chemical groups in vegetative and generative plant parts using ATR-FTIR spectroscopy. The CAs showed that the leaf had a hydrophobic character. In addition, leaf hysteresis was determined for each plant part, and it was understood that the lotus effect also appeared in *S. absconditiflora*.

Conclusion: Detailed biochemical profiling, wettability, and hysteresis reports of *S. absconditiflora* were created for the first time. With this study, important clues about the adaptation of plants to harsh conditions were obtained.

Keywords: ATR-FTIR spectroscopy, contact angle, gypsum, hysteresis, *Salvia* leaf

INTRODUCTION

Lamiaceae is a family rich in wild aromatic plant species and antioxidant compounds beneficial to humans (1). The Lamiaceae family is divided into seven subfamilies: Ajugoideae, Lamioideae, Nepetoideae, Scutellarioideae, Viticoideae, Symphorematoideae and Prostantheroideae, the first five of which are grown in Turkey (1). *Salvia* L. is one of the largest belonging to the Lamiaceae (2) and is known as 'adaçayı (sage)' in Turkey (3). It is known that *Salvia* taxa, which have antibacterial, carminative, stimulant, diuretic, and spasmolytic properties, have been used for treatment since the earliest times (4-6). *Salvia*, the diversity of which varies according to leaf shapes, calyx structure, length, and color of petals, has 100 species and 107 taxa in the flora of Turkey (7-10), and Turkey is very important in terms of its import and use (11). *Salvia absconditiflora* Greuter & Burdet (Synonym: *S. cryptantha* Montbret & Aucher ex Bentham) is a perennial and endemic plant. The life form is the whole adaptation of the plant to the climate, and it is assumed in the literature that it develops in response to

Corresponding Author: Aysenur Kayabas E-mail: aysenurkayabas@karatekin.edu.tr
Submitted: 18.10.2021 • **Revision Requested:** 02.11.2021 • **Last Revision Received:** 03.11.2021 • **Accepted:** 04.11.2021 • **Published Online:** 27.01.2022

environmental conditions (12). The life form of *S. absconditiflora*, which generally spreads on rocky limestone slopes, dry steppes, fallow fields, and roadsides, is hemicryptophyte (13) and its flowering time is from May to August.

Gypsum habitats with rare, threatened, and endemic plants are one of the most illustrative examples of natural stressful environments (14). Depending on the substrate factor, gypsum plants are faced with both the physical and chemical stress of the soil and arid climatic conditions. For plants growing in gypsum soils containing $CaSO_4.2H_2O$, soil salinity is also a consideration (14). When plants are exposed to salinity, certain biochemical changes occur in plant tissues which maintain an osmotic balance between soil and these tissues. These changes cause the accumulation or loss of biochemicals such as carbohydrates, amines, and lipids (15). Plants develop morphological, physiological, ecophysiological, and biochemical adaptations to tolerate substrate factors such as soil salinity. Examining the properties of leaves under salt stress is an important way to study abiotic stress situations (16).

The use of infrared (IR) spectroscopy in biological samples dates to the 1950s (17). After the development of IR spectroscopy, Fourier transform infrared (FTIR) spectroscopy became a valuable instrument for distinguishing and identifying different samples (18). Attenuated total reflection-Fourier transform infrared (ATR-FTIR) spectroscopy is also a tool with many advantages due to features such as being able to perform the analysis in a short time without the need for sample dilution and more frequent reproducibility (19). Furthermore, in ATR-FTIR spectroscopy, ATR measurement is independent of sample thickness and can be measured even when the biological sample is small (20).

The fact that FTIR spectroscopy allows the investigation of biological samples as well as gases, liquids, and solids, has made it powerful (18). FTIR provides effective data on the molecular structure and chemical composition of biological samples. These fingerprints even make it possible to trace changes in the molecular composition of human cancer diseases today (21).

In addition to its use in human health, FTIR is also used to monitor plant physiological processes such as environmental stress, leaf senescence, and aging (22). Wahab et al. reported that FTIR helped identify the use of *Cactus* leaves fibers in wastewater treatment for ammonium removal as a recycling strategy (23). Palacio et al. investigated the ability of gypsum plants to distinguish groups by comparing the main chemical groups in the leaves of plant groups specialized for gypsum habitats with the help of FTIR spectroscopy (24). Woutersen et al. interpreted the evolutionary history of *Nitraria* by determining the chemical composition of pollen walls with FTIR spectroscopy (25). To understand the osmotic balance between the roots, which are the most important organs in the connection of plants with the soil, and the soil solution, biochemicals are determined with expensive equipment such as HPLC and GS-MS (26), together with xylem sap analysis (27). However, the use of FTIR spectroscopy in stress studies is recommended more due to its advantages such as time efficiency and cheapness (15).

Wetting, which occurs because of the interaction of water with a surface, has a critical importance in plants. The water contact angle (CA) with the surface is the angle at which water, air, and solid meet, and it is also a measure that represents the probability of the surface being wetted by water (28). Leaf wetting is effective in reducing water loss from intense transpiration, thus limiting water depression by keeping the relations between the plant and water in balance (29-30). The plant surfaces exhibit hydrophobic or hydrophilic properties depending on their affinity for wetness (31). As the surface hydrophobicity increases, the contact angle hysteresis (CAH) decreases in parallel with the increase in water contact angles (CAs) (32). Super hydrophobicity is very important in wetting studies, where both the water contact angle is greater than 150° and the hysteresis is less than 10°. Super hydrophobicity is often associated with very low adhesive surfaces. The best example of a low stickiness surface and super hydrophobicity is the lotus effect, which comes from the waterproofing of the lotus leaf. The lotus effect was first described by Neinhuis and Barthlott (33), and it was reported that the water-repellent effect of the lotus leaf resulted from its complex morphology. Studies on hydrophobic natural surfaces were generally inspired by the lotus leaf (34) and *Salvia* was interpreted for the first time.

In this study, endemic *S. absconditiflora* Greuter & Burdet growing in gypsum habitats was examined. To the best of our knowledge, there are no literature reports regarding the FTIR spectroscopy analysis and CA measurements of *S. absconditiflora*. Two main objectives of this study were: (i) to characterize and compare the diversity in the spectral-chemical structure of vegetative and generative organs of *S. absconditiflora* using the FTIR spectroscopy technique; and (ii) to determine the wettability of the adaxial and abaxial epidermal surfaces of *S. abscontidiflora* leaves and to interpret whether there is a difference between the CAs at the points determined in the surface area of the leaves.

MATERIALS AND METHODS

Species Selection and Study Area

The endemic *Salvia absconditiflora* samples were collected from around the Aşağıpelitözü village (950-1000 m a.s.l., 40°29′ N, 33°41′ E) in the Çankırı province in the northern part of Central Anatolia from May to June 2021 (Figure 1). In this study, *S. absconditiflora* was taken from gypsum areas (Figure 1d). After it was brought to the laboratory, it was freed from residues. Damaged plant parts were not included in the analysis. The plant was identified taxonomically according to Davis et al. (35). The plant material identification was determined by the author (A. Kayabaş). After plant identification, the vegetative and generative parts were dried in a shady and ventilated room. The plant samples were stored in Çankırı Karatekin University as part of a personal collection. When evaluated climatically, the climate in Çankırı, which is approximately 250 km away from the sea, is continental and a semi-arid climate prevails (36). When examined geologically, gypsum formations are common in the Çankırı province and its surroundings (36).

Figure 1. *Salvia absconditiflora* Greuter & Burdet (Photos by A. Kayabaş) a. Plant habit, b. Early-stage of plant, c. Late-stage of plant d. Gypsum habitat in which the species grows.

ATR-FTIR Spectroscopic Analysis

The infrared spectra of the dried root, stem, leaf, petiole, and flower were obtained using ATR-FTIR spectroscopy, model Thermo Nicolet 6700, supplied by OMNIC software and recorded at room temperature in the wavenumber range from 400 to 4000 cm^{-1} at a resolution of 4 cm^{-1}, accumulating 32 scans per spectrum.

Leaf CAs Measurement

The CA measurements of the *S. absconditiflora* leaves were carried out at room temperature using a Krüss DSA 100 goniometer. A drop of deionized water (4 µL, 18 MΩ cm resistivity) was used as the wetting liquid. Three contact angle values were obtained from three different parts between the petiole and the leaf tip and then averaged. The leaf veins were avoided in the measurements.

RESULTS

ATR-FTIR spectroscopy gave detailed results for the analysis of organic matter chemical groups in the vegetative and generative plant parts of *S. absconditiflora*. The results contributed to the determination of the biochemical fingerprint of *S. absconditiflora*. Starting from the root of *S. absconditiflora*, the ATR-FTIR spectra of each plant part were taken. The ATR-FTIR spectra of the root, stem, petiole, leaf, sepal, and petal are shown in Figure 2. Although there were partial shifts in the band regions seen in the ATR-FTIR spectra, it was determined that there was not much change. It was found that the chemical groups of the ATR-FTIR spectra for each segment were similar and the band regions were close (Table 1). It was determined that there were changes in the intensities of only some chemical groups ranging from the root to the petal.

It was determined that the S-O bending bands in the ATR-FTIR spectrum were caused by gypsum and sulphate, and the range of these bands was between 602-595, 680-675, and 690-630 cm^{-1} respectively. The bands of calcium carbonate and alkane groups were found in the range of 730-710 cm^{-1}. Calcium oxalate, lignin, and calcium carbonate sourced bands were seen in 780-775 (COO^- bending), 832-825 (aromatic CH out of plane) and 879-872 cm^{-1} (C-O plane banding) bands, respectively. The band C-O stretching, and O-H deformation band of polysaccharides were detected at 1015-1005 cm^{-1}. Stretching bands in silicates, phosphates and sulphates were seen significantly at 1150-950

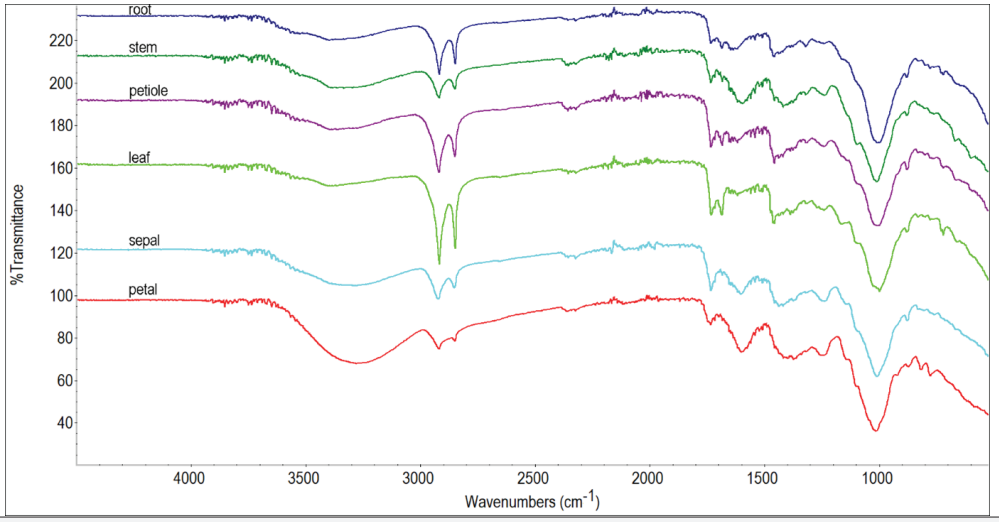

Figure 2. ATR-FTIR spectra of different parts of *Salvia absconditiflora*.

Table 1. Characteristic bands of ATR-FTIR spectra at *Salvia absconditiflora.*

Salvia absconditiflora						**Wavenumbers (cm^{-1})/ Chemical Group/ Compound type**	**Ref.**
Root (cm^{-1})	**Stem (cm^{-1})**	**Petiole (cm^{-1})**	**Leaf (cm^{-1})**	**Sepal (cm^{-1})**	**Petal (cm^{-1})**		
(669, 600)	(667, 600)	(667, 600)	(668, 598)	(667, 597)	(665, 599)	669, 597 S-O bending, Gypsum	(38)
(680-630)	x	(690-650)	(690-650)	(680-650)	(680-650)	680-610 S-O bending, Sulphates	(37)
(720)	x	(720)	(717)	(715)	(710)	715 C-O in-plane bending, Calcium carbonate	(39)
(730)	(729)	(729)	(730)	(730)	x	720 CH_2 wag, Long chain (> C4) alkanes	(24)
(775)	(779)	(775)	(780)	(780)	(778)	780 COO^- bending, Calcium oxalate	(42)
(830)	(832)	(830)	(827)	(825)	(820)	835 Aromatic CH out of plane, Lignin	(40)
(875)	(876)	(875)	(879)	(879)	(872)	874 C-O plane bending, Calcium carbonate	(41)
(1015)	(1010)	(1008)	(1020)	(1008)	(1010)	1050 (1030-1080) Combination of C-O stretching and O-H deformation, Polysaccharides	(43)
(1085-910)	(1080-920)	(1080-920)	(1080-930)	(1090-910)	(1090-950)	1100-950 Si-O stretching, Silicates	(44)
(1080-915)	(1080-920)	(1080-915)	(1080-930)	(1090-910)	(1090-950)	1100-1000 P-O stretching, Phosphates	(44)
(1135-1080)	(1130-1080)	(1160-1130)	(1180-1130)	(1170-1135)	(1180-1030)	1140-1080 S-O stretching, Sulphates	(44)
(1265-1220)	(1280-1200)	(1260-1205)	(1260-1215)	(1280-1200)	(1280-1210)	1265-1240 C-O-C stretching Esters …….. C-N stretching Amide III	(45)
(1265-1220)	(1280-1200)	(1260-1205)	(1260-1215)	(1280-1200)	(1280-1210)		(46)
(1268)	x	(1268)	(1271)	(1250)	(1260)	~1265 C-O stretching of phenolic and/or aryl-methyl ethers, Indicative of lignin backbone	(48)
(1318)	(1318)	(1316)	(1318)	(1317)	(1316)	1312 C-O stretching, Calcium oxalate	(47)

Table 1. Characteristic bands of ATR-FTIR spectra at *Salvia absconditiflora*. **(continued)**

Salvia absconditiflora						**Wavenumbers (cm^{-1})/ Chemical Group/ Compound type**	**Ref.**
Root (cm^{-1})	**Stem (cm^{-1})**	**Petiole (cm^{-1})**	**Leaf (cm^{-1})**	**Sepal (cm^{-1})**	**Petal (cm^{-1})**		
(1450, 1370)	(1458, 1373)	(1455, 1374)	(1457, 1373)	(1450, 1375)	(1453, 1372)	1371-1450 C-H deformations, Phenolic (lignin) and aliphatic structures	(24)
(1429)	(1430)	(1434)	(1434)	(1435)	(1420)	1426 Symmetric C-O stretch from COO^- or stretch and OH deformation, Carboxylate/Carboxylic structures (humic acids)	(49)
(1440-1410)	(1450-1425)	(1445-1425)	(1470-1435)	(1450-1425)	(1450-1420)	1450-1410 C-O stretching, Calcium carbonate	(51)
(1510-1505)	(1510-1500)	(1511-1502)	(1510-1504)	(1511-1502)	(1512-1505)	1505-1515 Aromatic C = C stretching, Lignin/Phenolic backbone	(24)
(1555)	(1550)	(1555)	(1558)	(1557)	(1558)	1550 N-H in plane (amide-II), Proteinaceous origin	(50)
(1600-1650)	(1630-1580)	(1630-1580)	(1630-1585)	(1620-1590)	(1640-1600)	1600-1650 (1610) Aromatic C = C stretching and/or asymmetric C-O strech in COO^-, Lignin and other aromatics, or aromatic or aliphatic carboxylates	(61)
(1617)	(1617 cm^{-1})	(1617 cm^{-1})	(1614 cm^{-1})	(1617 cm^{-1})	(1622 cm^{-1})	1615 C = O streching, Calcium oxalate	(52)
(1653)	(1655)	(1651)	(1655)	(1647)	(1652)	1653 C = O of amide I, Proteinaceous origin	(53)
(1707-1703)	(1720-1710)	(1720-1710)	(1710-1700)	(1710-1700)	(1710-1695)	1710-1707 C = O stretch of COOH, Carboxylic acids	(61)
(1735-1730)	(1740-1720)	(1740-1720)	(1740-1720)	(1740-1718)	(1740-1720)	1740-1720 C = O strech of COOR, Esters	(45)
(2850)	(2850)	(2850)	(2850)	(2850)	(2850)	2850 symmetric CH_2 stretching Fats, waxes, lipids	(56)
(2920)	(2920)	(2920)	(2920)	(2925)	(2925)	2920 antisymmetric CH_2 stretching Fats, waxes, lipids	(57)
x	x	x	x	x	x	3340 O-H stretching, Cellulose	(55)
(3500-3000)	(3500-3000)	(3500-3000)	(3500-3000)	(3500-3000)	(3620-3000)	3600, 3400 O-H stretching, Gypsum	(54)

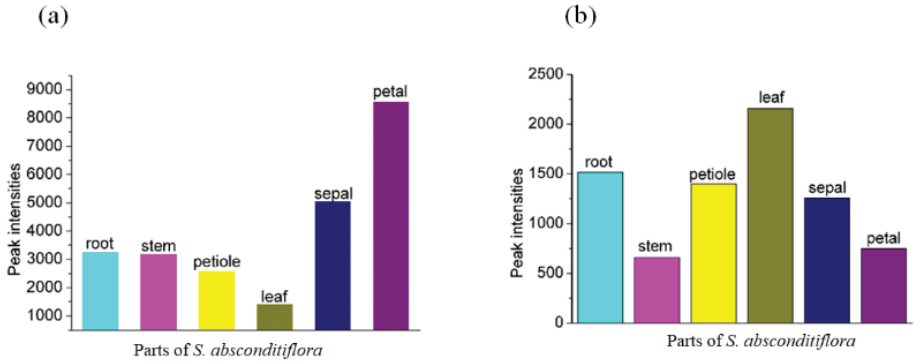

Figure 3. Peak intensities of hydroxyl (a) and aliphatic groups (b) at *Salvia absconditiflora*.

cm^{-1}. It is thought that these bands overlap each other since these bands are seen distinctly and are also in the fingerprint region. C-O-C and C-N stretch bands in lignin and amide-III structures were detected at 1280-1200 cm^{-1}. Lignin, calcium oxalate, phenolic and aliphatic structures, carboxylate structures were referred to C-O stretch (1275-1265 cm^{-1}), C-H deformation (1450-1371 cm^{-1}), symmetrical C-O, COO^- and OH deformation bands (1434-1426 cm^{-1}). C-O stretching, aromatic C=C stretching, and N-H bands, which belong to calcium carbonate, lignin/phenolic, and proteinaceous origin, were determined at 1450-1410, 1505-1502, and 1560-1550 cm^{-1}, respectively. The aromatic C=C band containing lignin and other aromatic structures, carbonyl band originating from calcium oxalate, and protein bands known as carbonyl amides were detected at 1640-1580, 1620-1615, and 1655-1650 cm^{-1}. The carboxylic acid carbonyl stretch band and carbonyl band of esters were also determined at 1710-1700 and 1750-1715 cm^{-1}.

Bands of hydroxyl chemical groups originating from gypsum and cellulose were seen in plant parts from root to flower. The intensity change graph of the hydroxyl bands is shown in Figure 3a. Accordingly, the hydroxyl band intensity from root to petal was calculated as 3240, 3170, 2570, 1410, 5040, and 8560 a.u. (arbitrary units), respectively. Band intensities were determined to be different for each region. The bands belonging to symmetric and antisymmetric aliphatic carbon groups, which are considered as the main source of oils, waxes, and lipids were also observed at 2920 and 2850 cm^{-1} (Figure 3b). The intensity of these bands also differed according to the regions of the plant. Band intensities were measured as 1520, 660, 1400, 2160, 1260, and 750 a.u. from root to petal. These results show that the band intensity changes for each part, which is valid for the hydroxyl band.

CA measurements were taken to understand the chemical composition of the leaf surfaces and their hydrophobic-hydrophilic interactions. The leaves were measured at regular intervals for CA measurements. The CA of the leaves divided into three regions from the petiole to the tip of the leaf was measured. According to these measurements, the CA measurements of the abaxial surface of the leaf from the petiole to the leaf tip were found to be 99.14±3.05°, 98.42±4.41° and 97.78±2.18°, respectively (Figure 4).

Three regions were selected for the adaxial surface of the leaf, and CA measurements were made for these regions. In this context, the CA measurement results were measured as 98.02±4.42°, 95.09±4.17° and 89.98±4.04° in the regions determined from the petiole to the leaf tip (Figure 5). The CA measurement values on the adaxial surface differed more than the abaxial surface.

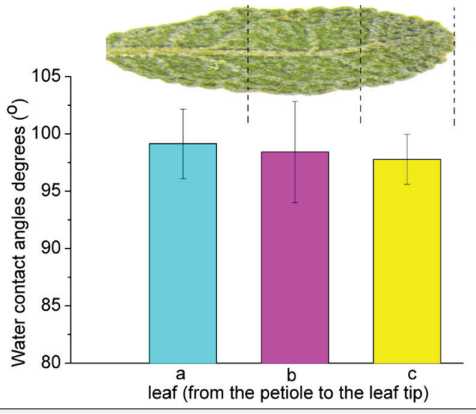

Figure 4. Contact angle measurements of the leaf abaxial surface at *Salvia absconditiflora*.

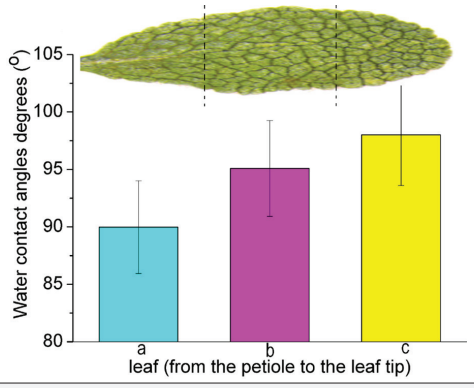

Figure 5. Contact angle measurements of the leaf adaxial surface at *Salvia absconditiflora*.

Table 2. Hysteresis values.

Abaxial		**Adaxial**	
Regions	**Hysteresis values**	**Regions**	**Hysteresis values**
Leaf tip	6.25	Leaf tip	8.20
Middle region of the leaf	1.05	Middle region of the leaf	1.67
Petiole	2.17	Petiole	4.06

Contact angle hysteresis (CAH) values, a measure of surface roughness that can be determined by CA measurements, were also calculated. Leaf surfaces were considered for hysteresis values. For the CAH of the abaxial and adaxial surfaces, the differences between the values of the advancing and receding CAs taken from three different regions of each surface were taken. The CAH values of the adaxial and abaxial surfaces of the leaf were different (Table 2).

This study aims to investigate the chemical profile and wettability of *S. absconditiflora*. In this context, a series of results based on ATR-FTIR spectroscopy and CA measurements were obtained. With the help of ATR-FTIR, the chemical profile of the *S. absconditiflora* was obtained and the types of possible chemical structures in this plant were determined. In particular, the ATR-FTIR spectra taken from the root, stem, petiole, leaf, sepal, and petal of the *S. absconditiflora* were compared, and which chemical components were more abundant was determined by the change of band intensities.

In the ATR-FTIR spectra from the plant parts of *S. absconditiflora*, the bands were similar, but there were variations in the intensities and wavenumbers of some bands. The values of the shifts in the bands are given in Table 1. It is thought that the shifts in the number of waves seen in the bands detected in the ATR-FTIR spectra do not change much chemically, but the change in band values may be because of the extreme habitat in which this plant species lives.

The changes in band intensities show that *S. absconditiflora* contains different amounts of chemicals in each plant part. The intensities of the bands belonging to the hydroxyl and aliphatic groups, in which the band area can be easily detected, were compared among the spectra. It was calculated that the hydroxyl band had different areas ranging from the root to the petal. This proves that the amount of gypsum or cellulose in the plant varies according to the plant parts (Table 1, Figure 3a). Band intensities for the relative amounts of oils, lipids and waxes compounds were calculated from the ATR-FTIR spectra. It was determined that the band intensities changed according to the chemical amounts in each plant part (Table 1, Figure 3b).

As a result of the CA measurements taken from different parts of the *S. absconditiflora* leaf, it was observed that there were more changes, especially on the adaxial surface compared to the abaxial surface. The difference between the CAs changed more from region to region on the adaxial surface. The CA on the abaxial surface showed a change of about 10° from petiole to leaf tip. Contrary to this situation, on the abaxial surface, a 2° change was observed in the CAs. It can be said that the stability of the CA in the abaxial part of the leaf is due to less contact with environmental conditions than the adaxial surface. The source of the changes in the CA on the adaxial surface may be because the sun's rays do not touch the leaf surface at the same angle. It is thought that the sun's rays remove the water on the leaf, making it more hydrophobic than the abaxial surface.

When the hydrophobicity of the *S. absconditiflora* leaf is examined in detail, CAs on the adaxial surface of the leaf is average ~ 94°, while it is average ~ 98° on the abaxial surface ($Adaxial_{CA}$<$Abaxial_{CA}$). It can be said that the adaxial and abaxial surfaces of the *S. absconditiflora* leaf are hydrophobic according to the results of the CAs ($Adaxial_{hidrofobicity}$< $Abaxial_{hidrofobicity}$). However, while the CA was higher on the adaxial surface of the leaf, the hysterization of the abaxial surface of the leaf was higher ($Adaxial_{hysterise}$>$Abaxial_{hysterise}$). The hysterization of the adaxial surface of the leaf averages ~4.6°, while the abaxial surface averages ~3.2°.

DISCUSSION

The chemical groups and band intensities of the root, stem, leaf, petiole, sepal, and petal of *S. absconditiflora* were measured by using ATR-FTIR. In the literature, bands have been reported for calcium, sulphate, silicate, phosphate, polysaccharide, lipid, aromatic compounds, phenolic compounds, and protein-based structures in the ATR-FTIR spectra taken especially for gypsum plants (24,37-53). Band intensities varied between plant parts from root to flower. Palacio et al. reported that band densities of wide and narrow gypsum plants varied between ecological plant groups (24). In this study, it was understood that the band types did not change much in the ATR-FTIR spectra taken for the vegetative and generative plant parts of the *S. absconditiflora,* but the band intensities differed. In this case, where the hydroxyl band of gypsum (54,55), whose intensity can be measured, differs for each plant parts, it was shown that the amount of gypsum varied in the root, stem, leaf, petiole, and flower. Likewise, the observation of differences in the band intensities of symmetric and asymmetrical aliphatic carbons, which are the basis of oils, waxes, and lipids, showed that the plant parts have different chemical contents (56,57). In general, the presence of each specific band was detected in the ATR-FTIR spectra taken,

but it was understood that the same trend was observed for all plant parts where the band intensities were different.

Since gypsum plants grow in gypsum soils, they have the potential to be an accumulator of calcium and sulfur (58). Ozdemir et al. reported the presence of the calcium mineral in *Gypsophila* taxa and that it can be used as an accumulator (59). The presence of chemical bands in calcium carbonate and calcium oxalate compounds, which are thought to be calcium sources for each plant part in the ATR-FTIR spectra, indicates that *S. absconditiflora* may be an accumulator in terms of calcium content. Another mineral frequently seen in gypsum plants is sulfur and it has been reported that it can act as an accumulator (58). Sulfur-derived bands, especially in the structure of sulphates, were detected in each of the plant parts and it was understood from the band intensities that this plant species is rich in terms of the sulfur mineral. In addition to these two minerals, the presence of organic compounds (aromatic, phenolic, etc.) and protein-based structures revealed that the plant species is also rich in organic compounds (24). The high intensities of the hydroxyl bands originating from gypsum indicate that the water content and gypsum content of *S. absconditiflora* are high. In terms of adaptation to harsh conditions, the presence of important minerals in *S. absconditiflora*, as well as the presence of organic compounds, will help in the process of understanding adaptation.

Wang et al. observed that the CAs and hysterization of the adaxial and abaxial surfaces on the lotus leaf were also different and mentioned two types of surface descriptions of plants with hydrophobic properties and stated that leaves such as lotus exhibited a typical feature in investigating the hydrophobicity of various plant leaves (32). The hydrophobicity and hysterization of the *S. absconditiflora* leaf support the results in the lotus leaf. Legrand et al. also recorded the hydrophobicity and hysteresis of three natural leaves, describing their wetting behavior, and modeled the relationship between surface roughness, wettability, and leaf behavior (34). Hysteresis values also help to prove the existence of inorganic compounds in the plant. Katata and Held tested the presence of inorganic compounds in a spruce forest with the hysteresis effect (60). The structure of superhydrophobic surfaces such as lotus leaves and rose petals is due to the fine architectural features created by nature, and the superhydrophobic behavior of these organic surfaces in fields such as chemistry has also inspired the creation of surfaces with synthetic molecules (62). This study, inspired by the lotus effect of the *S. absconditiflora* plant, which has a surface feature like a lotus leaf, can contribute to the formation of synthetic surfaces in other fields of science. As well as contributing to the formation of synthetic molecules, knowing the morphology and wettability of the leaf also guides the retention of pesticides used in sustainable agriculture on the leaf (63). Similar studies are also important in agriculture as well as plant ecology.

CONCLUSION

In summary, in the first step of this study, the chemical profile of the root, stem, petiole, leaf, sepal, and petal of *S. absconditiflora* was extracted using the ATR-FTIR technique. Using this technique, possible compounds that might be found in the structure of the plant were determined. Due to the different band intensities of each plant part in terms of compound content, it was understood that the compound amounts of each structure was different from region to region. In the second stage, detailed wettability, and hysteresis results of the abaxial and adaxial surfaces of the leaves were evaluated. The leaves were divided into three different regions on the petiole up to the tip, and CA measurements were made for both sides (adaxial and abaxial). It was determined that the adaxial surface was more hydrophobic than the abaxial surface, and the CAs were less stable. It was discussed that this situation will play a key role in understanding the adaptation of the *S. absconditiflora* plant to extreme conditions. At the same time, by calculating the hysteresis results of the surfaces, it was announced that this plant species has similar characteristics as the lotus plant. As a result, detailed wettability, and hysteresis profiles of both chemical and leaves of the *S. absconditiflora* plant were created for the first time in the literature. With this study, important clues about the adaptation of plants to harsh conditions were obtained. Thus, this study paves the way for many future studies to determine what kinds of chemical structures and wettability parameters are required to prevent the future extinction of plant species that cannot keep up with extinction or difficult conditions in the world.

Acknowledgements: The authors would like to thank the Gazi University Academic Writing and Research Center for their help and valuable support in the proofreading of this study.

Informed Consent: Written consent was obtained from the participants.

Peer Review: Externally peer-reviewed.

Author Contributions: Conception/Design of Study- A.K., E.Y.; Data Acquisition- A.K., E.Y.; Data Analysis/Interpretation- A.K., E.Y.; Drafting Manuscript- A.K., E.Y.; Critical Revision of Manuscript- A.K., E.Y.; Final Approval and Accountability- A.K., E.Y.

Conflict of Interest: Authors declared no conflict of interest.

Financial Disclosure: Authors declared no financial support.

REFERENCES

1. Fırat M. *Stachys semsurensis* (Lamiaceae), a new species from Adıyaman province (Turkey) belonging to section. Infrarosularis. Phytotaxa 2021; 511: 275-82.
2. Hedge IC. Lamiaceae of south-west Asia: diversity, distribution and endemism. Proc Royal Soc B 1986; 89: 23-5.
3. Yaris E, Adsız LB, Yener I, Tuncay E, Yilmaz MA, et al. Isolation of secondary metabolites of two endemic species: *Salvia rosifolia* Sm. and *Salvia cerino-pruinosa* Rech. f. var. *elazigensis* (Lamiaceae). J Food Meas 2021; 1-10.
4. Baytop T. Therapy with medicinal plants in Turkey. Istanbul: Nobel Medical Press; 1999.

5. Singh B, Singh B, Kishor A, Singh S, Bhat MN, et al. Exploring plant-based ethnomedicine and quantitative ethnopharmacology: Medicinal plants utilized by the population of Jasrota Hill in Western Himalaya. Sustainability 2020; 12: 7526.
6. Tundis R, Leporini M, Bonesi M, Rovito S, Passalacqua NG. *Salvia officinalis* L. from Italy: A comparative chemical and biological study of its essential oil in the mediterranean context. Molecules 2020; 25: 5826.
7. Hedge IC. *Salvia* L. Davis PH, editor. Flora of Turkey and the East Aegean Islands. Edinburgh: Edinburgh University Press; 1982. p. 400-61.
8. Davis PH, Mill RR, Tan K. Flora of Turkey and the East Aegean Islands (Vol X). Edinburgh: Edinburgh University Press; 1988.
9. Vural M, Adıgüzel N. A new species from Central Anatolia: *Salvia aytacii* M. Vural & N. Adıgüzel (Labiatae). Turk J Bot 1996; 20: 531-34.
10. Celep F, Raders E, Drew B. Two new hybrid species of *Salvia* (*S.*× *karamanensis* and *S.*×*doganii*) from Turkey: Evidence from molecular and morphological studies. Turk J Bot 2020; 44: 647-60.
11. Akkol EK, Göger F, Koşar M, Başer KHC. Phenolic composition and biological activities of *Salvia halophila* and *Salvia virgata* from Turkey. Food Chem 2008; 108: 942-49.
12. Sindhuja R, Rajendran A, Jayanthi P. Herbaceous life forms of Maruthamalai Hills, Southern Western Ghats, India. Int J Med Aromat Plants 2012; 2: 625-31.
13. Ozbey BG, Ozdeniz E, Bolukbaşi A, Oktem M, Keleş Y, et al. The role of free proline and soluble carbonhydrates in serpentine stress on some serpetinophyte and serpentinovag plants. Acta Biologica Turcica 2017; 30: 146-51.
14. Soriano P, Moruno F, Boscaiu M, Vicente O, Hurtado A, et al. Is salinity the main ecologic factor that shapes the distribution of two endemic Mediterranean plant species of the genus *Gypsophila*? Plant Soil 2014; 384: 363-79.
15. Westworth S, Ashwath N, Cozzolino D. Application of FTIR-ATR spectroscopy to detect salinity response in Beauty Leaf Tree (*Calophyllum inophyllum* L). Energy Procedia 2019; 160: 761-68.
16. Acosta-Motos JR, Ortuño MF, Bernal-Vicente A, Diaz-Vivancos P, Sanchez-Blanco MJ, et al. Plant responses to salt stress: Adaptive mechanisms. Agronomy 2017; 7: 18.
17. Barer R, Cole ARH, Thompson HW. Infra-red spectroscopy with the reflecting microscope in physics, chemistry and biology. Nature 1949;163:198-201.
18. Legner N, Meinen C, Rauber R. Root differentiation of agricultural plant cultivars and proveniences using FTIR spectroscopy. Front Plant Sci 2018; 9: 748.
19. Götz A, Nikzad-Langerodi R, Staedler Y, Bellaire A, Saukel J. Apparent penetration depth in attenuated total reflection Fourier-transform infrared (ATR-FTIR) spectroscopy of *Allium cepa* L. epidermis and cuticle. Spectrochim Acta A Mol Biomol Spectrosc 2020;224:117460.
20. Kazarian SG, Chan KLA. Applications of ATR-FTIR spectroscopic imaging to biomedical samples. Biochim Biophys Acta Biomembr 2006;1758:858-67.
21. Ferreira IC, Aguiar EM, Silva AT, Santos LL, Cardoso-Sousa L, et al. Attenuated Total Reflection-Fourier Transform Infrared (ATR-FTIR) spectroscopy analysis of saliva for breast cancer diagnosis. J Oncol 2020; 4343590.
22. Ivanova DG, Singh BR. Nondestructive FTIR monitoring of leaf senescence and elicitin-induced changes in plant leaves. Biopolymers: Original Research on Biomolecules 2003; 72: 79-85.
23. Wahab MA, Boubakri H, Jellali S, Jedidi N. Characterization of ammonium retention processes onto Cactus leaves fibers using FTIR, EDX and SEM analysis. J Hazard Mater 2012; 241: 101-9.
24. Palacio S, Aitkenhead M, Escudero A, Montserrat-Martí G, Maestro M et al. Gypsophile chemistry unveiled: Fourier transform infrared (FTIR) spectroscopy provides new insight into plant adaptations to gypsum soils. PLoS One 2014; 9: e107285.
25. Woutersen A, Jardine PE, Bogotá-Angel RG, Zhang HX, Silvestro D, et al. A novel approach to study the morphology and chemistry of pollen in a phylogenetic context, applied to the halophytic taxon *Nitraria* L. (Nitrariaceae). PeerJ 2018; 6: e5055.
26. Debnath M, Ashwath N, Hill CB, Callahan DL, Dias DA, et al. (2018). Comparative metabolic and ionomic profiling of two cultivars of *Stevia rebaudiana* Bert. (Bertoni) grown under salinity stress. Plant Physiol Biochem 2018; 129: 56-70.
27. Aswathappa N, Munns R, Bachelard EP, Tonnet ML. Ion concentrations in the xylem sap of two *Casuarina* species differing in salt tolerance. Proceedings of the 7th International Workshop on Plant Membrane Transport (Membrane Transport in Plants and Fungi). Sydney: University of Sydney Publication; 1986. p. 486-489.
28. Huhtamäki T, Tian X., Korhonen JT, Ras RH. Surface-wetting characterization using contact-angle measurements. Nat Protoc 2018; 13: 1521-38.
29. Yokoyama G, Yasutake D, Tanizaki T, Kitano M. Leaf wetting mitigates midday depression of photosynthesis in tomato plants. Photosynthetica 2019; 57: 740-7.
30. Yokoyama G, Yasutake D, Minami K, Kimura K, Marui A, et al. Evaluation of the physiological significance of leaf wetting by dew as a supplemental water resource in semi-arid crop production. Agric Water Manag 2021;255:106964.
31. Roy T, Sabharwal TP, Kumar M, Ranjan P, Balasubramaniam R. Mathematical modelling of superhydrophobic surfaces for determining the correlation between water contact angle and geometrical parameters. Precis Eng 2020; 61: 55-64.
32. Wang J, Chen H, Sui T, Li A, Chen D. Investigation on hydrophobicity of lotus leaf: Experiment and theory. Plant Sci 2009;176:687-95.
33. Neinhuis C, Barthlott W. Characterization and distribution of water-repellent, self-cleaning plant surfaces. Ann Bot 997; 79: 667-77.
34. Legrand Q, Benayoun S, Valette S. Biomimetic approach for the elaboration of highly hydrophobic surfaces: Study of the links between morphology and wettability. Biomimetics 2021; 6: 38.
35. Davis PH, Mill RR, Tan K. Flora of Turkey and the East Aegean Islands (Vol XII). Edinburgh: Edinburgh University Press; 1982.
36. Ozcan AU, Aytaş I. Temporal landscape change in biodiversity hotspot and geological heritage karst landscapes: Çankırı gypsum hills case. Yuzuncu Yil Univ J Agric Sci 2019; 29: 618-27.
37. Boke H, Akkurt S, Ozdemir S, Goktürk EH, Saltik ENC. Quantification of $CaCO_3$-$CaSO_3$·0.5 H_2O-$CaSO_4$·$2H_2O$ mixtures by FTIR analysis and its ANN model. Mater Lett 2004; 58: 723-6.
38. Shillito LM, Almond MJ, Nicholson J, Pantos M, Matthews W. Rapid characterisation of archaeological midden components using FT-IR spectroscopy, SEM-EDX and micro-XRD. Spectrochim Acta A Mol Biomol Spectrosc 2009; 73: 133-9.
39. Ennaciri Y, Bettach M, Cherrat A, Zegzouti A. Conversion of phosphogypsum to sodium sulfate and calcium carbonate in aqueous solution. J Mater Environ Sci 2016; 7: 1925-33.
40. Zaccheo P, Cabassi G, Ricca G, Crippa L. Decomposition of organic residues in soil: Experimental technique and spectroscopic approach. Org Geochem 2002; 33: 327-45.
41. Liu D, Tian H, Jia X, Zhang L. Effects of calcium carbonate polymorph on the structure and properties of soy protein-based nanocomposites. Macromol Biosci 2008; 8: 401-9.
42. Ma F, Huang AM, Zhang SF, Zhou Q, Zhang QH. Identification of three *Diospysros* species using FT-IR and 2DCOS-IR. J Mol Struct 2020; 1220: 128709.

43. Ferreira ML, Gerbino E, Cavallero GJ, Casabuono AC, Couto AS, et al. Infrared spectroscopy with multivariate analysis to interrogate the interaction of whole cells and secreted soluble exopolimeric substances of *Pseudomonas veronii* 2E with Cd (II), Cu (II) and Zn (II). Spectrochim Acta A Mol Biomol Spectrosc 2020; 228: 117820.
44. Jastrzębski W, Sitarz M, Rokita M, Bułat K. Infrared spectroscopy of different phosphates structures. Spectrochim Acta A Mol Biomol Spectrosc 2011; 79: 722-27.
45. Smidt E, Meissl K. The applicability of fourier transform infrared (FT-IR) spectroscopy in waste management. Waste Manage 2007; 27: 268-76.
46. Li C, Du C, Ma F, Zhou J. Diagnosis of nitrogen status in Chinese cabbage (*Brassica rapa chinensis*) using the ratio of amide II to amide I in leaves based on mid-infrared photoacoustic spectroscopy. J Plant Nutr Soil Sci 2015; 178: 888-95.
47. Frost RL, Yang J, Ding Z. Raman and FTIR spectroscopy of natural oxalates: Implications for the evidence of life on Mars. Chin Sci Bull 2003; 48: 1844-52.
48. Sun XF, Jing Z, Fowler P, Wu Y, Rajaratnam M. Structural characterization and isolation of lignin and hemicelluloses from barley straw. Ind Crops Prod 2011; 33(3): 588-98.
49. Parvan L, Dumitru M, Sîrbu C, Cioroianu T. Fertilizer with humic substances. Rom Agric Res 2013; 30: 205-12.
50. Centeno SA, Guzman MI, Yamazakikleps A, Védova COD. Characterization by FTIR of the effect of lead white on some properties of proteinaceous binding media. J Am Inst Conserv 2004; 43: 139-50.
51. Jamarun N, Yuwan S, Juita R, Rahayuningsih J. Synthesis and characterization carbonate apatite from bukit tui limestone padang Indonesia. J Appl Chem 2015; 4: 542-9.
52. Valarmathi D, Abraham L, Gunasekaran S. Growth of calcium oxalate monohydrate crystal by gel method and its spectroscopic analysis. Indian J Pure Appl Phys 2010; 48: 36-8.
53. De Campos Vidal B, Mello MLS. Collagen type I amide I band infrared spectroscopy. Micron 2011; 42: 283-89.
54. Mandal PK, Mandal TK. Anion water in gypsum ($CaSO_4 \cdot 2H_2O$) and hemihydrate ($CaSO_4 \cdot 1/2H_2O$). Cem Concr Res 2002; 32: 313-16.
55. Terpáková E, Kidalová L, Eštoková A, Čigášová J, Števulová N. Chemical modification of hemp shives and their characterization. Procedia Eng 2008; 42: 931-41.
56. Xin X, Si W, Yao Z, Feng R, Du B, et al. Adsorption of benzoic acid from aqueous solution by three kinds of modified bentonites. J Colloid Interface Sci 2011; 359: 499-504.
57. Johnston A, Rogers K. A study of the intermolecular interactions of lipid components from analogue fingerprint residues. Sci Justice 2018; 58: 121-7.
58. Bolukbasi A, Kurt L, Palacio S. Unravelling the mechanisms for plant survival on gypsum soils: an analysis of the chemical composition of gypsum plants from Turkey. Plant Biol 2016; 18(2): 271-9.
59. Ozdemir C, Ozkan M, Kandemir A. The morphological and anatomical properties of *Gypsophila lepidioides* Boiss (Caryophyllaceae) endemic to Turkey. Int Res J Plant Sci 2010; 1: 69-74.
60. Katata G, Held A. Combined measurements of microscopic leaf wetness and dry-deposited inorganic compounds in a spruce forest. Atmos Pollut Res 2021; 12: 217-24.
61. Utami SNH, Suswati D. Chemical and spectroscopy of peat from West and Central Kalimantan, Indonesia in relation to peat properties. Int J Environ Agric Res 2016; 2: 45-52.
62. Mukhopadhyay RD, Vedhanarayanan B, Ajayaghosh A. Creation of "Rose Petal" and "Lotus Leaf" effects on alumina by surface functionalization and metal-ion coordination. Angew Chem 2017; 129(50): 16234-8.
63. Wei J, Tang Y, Wang M, Hua G, Zhang Y, Peng R. Wettability on plant leaf surfaces and its effect on pesticide efficiency. Int J Precis Agric Aviat 2020; 3(1): 30-7.

ISTANBUL UNIVERSITY PRESS

RESEARCH ARTICLE

Eur J Biol 2022; 81(1): 11-17

The Effects of SARS CoV-2 nsp13 Mutations on the Structure and Stability of Helicase in Chinese Isolates

Ekrem Akbulut[1]

[1]Malatya Turgut Özal University, Department of Bioengineering, Malatya, Turkiye

ORCID IDs of the authors: E.A. 0000-0002-7526-9835

Please cite this article as: Akbulut E. The Effects of SARS CoV-2 nsp13 Mutations on the Structure and Stability of Helicase in Chinese Isolates. Eur J Biol 2022; 81(1): 11-17. DOI: 10.26650/EurJBiol.2022.1061858

ABSTRACT

Objective: Coronavirus Disease 2019 (COVID19) is a viral disease caused by Severe Acute Respiratory Syndrome Coronavirus-2 (SARS CoV-2). The high mutation propensity of the SARS CoV-2 genome is one of the biggest threats to the long-term validity of treatment options. Helicases are anti-viral targets because of the vital role they play in the viral life cycle. In this study, changes in the protein structure caused by SARS CoV-2 nsp13 mutations were investigated to contribute to the development of effective antiviral drugs.

Materials and Methods: Genome data of 298 individuals located in the China location were examined. The mutant model was built using deep learning algorithms. Model quality assessment was done with QMEAN. Protein stability analyses were performed with DynaMut2 and Cutoff Scanning Matrix stability. Changes in substrate affinity were performed with Haddock v2.4.

Results: In this study, twenty-eight mutations in nsp13 were identified (23 sense, 5 missense). The changes in protein structure caused by the five missense mutations (Leu14Phe, Arg15Ser, Arg21Ser, Leu235Phe, Ala454Thr) were modeled. The mutations caused a decrease in the stability of SARS CoV-2 helicase (-0.99, -1.66, -1.15, -0.54, and -0.73 for Leu14Phe, Arg15Ser, Arg21Ser, Leu235Phe, Ala454Thr, respectively). The mutations reduced the helicase's affinity to the substrate. The docking scores for wild-type and mutant helicase were -84.4±1.4 kcal.mol^{-1} and -71.1±6.7 kcal.mol^{-1}, respectively.

Conclusion: Helicase mutations caused a decrease in the protein stability and nucleic acid affinity of the SARS CoV-2 helicase. The results provide important data on the development of potential antivirals and the effect of mutation on the functions of viral proteins.

Keywords: COVID19, helicase, mutation, protein stability, SARS CoV-2 genome, substrate affinity

INTRODUCTION

The Corona Virus Disease 2019 (COVID-19) is characterized by a variety of clinical features ranging from asymptomatic acute respiratory distress to multi-organ dysfunction (1,2). The SARS CoV-2, which has a high risk of transmission and death rate, caused 289 million people to become ill and 5.44 million people to die in the last two years (3). The etiological agent of COVID-19, the SARS CoV-2 virus is positive polarity, single-strand RNA virus with a genome of 29.9 kb (4). The SARS CoV-2 genome consists of two overlapping open reading frames (ORF1ab and ORF1a), four structural proteins (spike, envelope, nucleocapsid, membrane) and six accessory proteins (ORF3a, ORF6, ORF7a, ORF7b, ORF8 and ORF10) (5). Open reading frames are involved in the continuous synthesis of 16 non-structural proteins (nsps) that play important roles in the viral life cycle (6). SARS CoV-2 helicase (non-structural protein 13/nsp13) catalyzes a 5′–3′ direction unwinding process in the presence of nucleotide three phosphate to transform duplex oligonucleotides (RNA or DNA) into single strands. Helicase, which is essential for the life cycle of the virus, is one of the important structural targets for therapeutic agents

Corresponding Author: Ekrem Akbulut E-mail: ekremakbulut@gmail.com

Submitted: 23.01.2022 • **Revision Requested:** 17.02.2022 • **Last Revision Received:** 19.02.2022 • **Accepted:** 21.03.2022 • **Published Online:** 13.04.2022

(7,8). Helicase plays an active role in the replication process of the SARS CoV-2 in the host together with RNA-dependent RNA polymerase. Helicases have additional biological roles such as transcription, mRNA splicing, mRNA export, RNA stability, translation, mitochondrial gene expression, and nucleic acid packaging into virions (9). The high mutation risk of the SARS CoV-2 genome, like with other RNA viruses, poses a major threat to the validity of therapeutic options. Modeling changes induced by mutations in the viral proteome supports the development of potent antivirals (10-12).

The changes in the helicase structure caused by nsp13 mutations of SARS CoV-2 were investigated to develop robust and valid therapeutics, in this study.

MATERIALS AND METHODS

Sequence Data and Mutation Analysis

The genome sequence data for the samples were obtained from the NCBI Virus database. The genome data of 12,218 individuals located on the Asian continent were examined and the sequence data from 298 individuals from the China location was used for analysis in this study. Reference sequence data for the genome and protein was used NC_045512.2 and YP_009725308.1, respectively (4). The sequence data was aligned with the MAFFT (v7.490) multiple sequence alignment program FFT-NS-i algorithm (13). The scoring matrix BLOSUM 80, and 1 PAM was chosen for the amino acid sequences, and nucleotide, respectively (14,15). The gap opening penalty was used as 2.0. The mutated residues were analyzed MegaX (16).

Tertiary Structure of Mutant Protein and Protein Stability Analysis

The tertiary structure of mutant nsp13 was generated by the method of homology modeling using RoseTTAFold (17). The 7NIO (pdb accession code) was selected as a template (18). The QMEAN was used for structural validation and model of mutant nsp13 (19). Superimpose and conformational analyses of the wild-type and mutant helicase were performed with the PyMOL (ver2.4.1) and NGL viewer (20). Topological differences of wild-type and mutant nsp13 proteins were calculated with the i-Tasser TM-Score and root mean square deviation (RMSD) algorithm (21). An analysis of changes in protein stability was performed using the DynaMut2 and mutation Cutoff Scanning Matrix (mCSM) (22,23). The mCSM provides graph-based structural signatures, which is used to examine the effect of mutations on protein stability and interaction. The mCSM, extending the inter-residual signature to an atomic level, is a protein structural tool used for large-scale protein function prediction and structural classification. The mCSM workflow consists of: collection and preprocessing of thermodynamic and structural data, extraction of residue environments, signature calculation and noise reduction, supervised learning, and mutation effect estimation and validation (24,25). Another approach used to analyze missense mutations' impact on protein stability was DynaMut2, which uses protein dynamics, wild-type residue environment, substitution trends and contact potential scores, and interatomic distance data to train and test machine learning algorithms (22). Non-covalent molecular interactions were calculated using Arpeggio (26).

Docking

The change in helicase – nucleic acid affinity after the mutation was evaluated using the Haddock version 2.4 (27). The active site for the helicase were residues number 288, 289, 290, 320, 374, 375, 404, 442, 443, 540, 567. A number of structures for rigid body docking was set to 1000. A number of trials for rigid body minimization was set to 5. A number of structures for semi-flexible refinement was set to 200. Refined with short molecular dynamics in open solvent using water. The clustering method was selected Fraction of Common Contacts (FCC). The RMSD cutoff for clustering was set to 0.6 Å. The Kyte-Doolittle hydrophobicity scale method was used for solvating. A cutoff distance (proton-acceptor) to define a hydrogen bond was set to 2.5 Å. A cutoff distance (carbon-carbon) to define a hydrophobic contact was set to 3.9 Å. The docking results were visualized with Discovery SV (ver20.1, DDS Biovia).

RESULTS

A mutation analysis revealed that there were 23 sense and 5 missense (Leu14Phe, Arg15Ser, Arg21Ser, Leu235Phe, and Ala454Thr) mutations in the helicase of SARS CoV-2 from Chinese isolates (Table 1). The mutant nsp13 protein was modeled using the deep learning-based modeling approach, RoseTTAFold. The Tm-score was 0.9787. The mutations caused changes in protein conformation and topological structure (rmsd 0.325 Å) (Figure 1). The five mutations causing amino acid changes showed a destabilizing effect in the helicase structure (-0.99, -1.66, -1.15, -0.54, and -0.73 kcal.mol^{-1} respectively). The mutations changed the bond conformation between the residues, forming the tertiary structure (Figure 2). After the Leu14Phe mutation, two interactions (Phe14-Cys26 and Phe14-Cys27) that were not in the wild-type appeared in the tertiary structure of the mutant helicase (Figures 2a and b). Increased inter-residual bond interaction may limit the movement of the helicase N-terminal domain. The Arg15Ser mutation reduced the local tertiary conformation provided by seven hydrophobic, nine polar, and one Van der Walls interactions in the wild protein to four polar and one hydrogen bond in the mutant protein (Figures 2c and d). The Arg21Ser mutation revealed the most striking reduction in terms of tertiary structure bond formation. The wild-type helicase, which demonstrated nine different interactions with five amino acids at position twenty-one, made single amino acid and single bond interaction in the mutant protein (Figures 2e and f). Although the Leu235Phe mutation abolished the hydrogen bonds between 235-Leu132 and 235-Ser385, it revealed an increase in polar and hydrophobic interactions (Figures 2g and h). The Ala454Thr mutation introduced an additional Asn459 polar interaction, which was not in wild-type (Figures 2i and j).

Table 1. SARS CoV-2 helicase mutations in Chinese isolates.

Genomic Location	Codon Change	Mutation	Sense/Missense
16255	GTA > GTT	Val6Val	sense
16279	TTT > TTA	Leu14Phe	missense
16280	CGA > AGA	Arg15Arg	sense
16282	AGT > AGA	Arg15Ser	missense
16297	ATT > ATA	Ile20Ile	sense
16298	AGT > CGT	Arg21Ser	missense
16300	CGG > CGT	Arg21Arg	sense
16342	ATT > ATA	Ile35Ile	sense
16364	CTG > TTG	Leu43Leu	sense
16420	ACA > ACT	Thr61Thr	sense
16450	TAC > TAT	Tyr71Tyr	sense
16498	GGT > GGA	Gly87Gly	sense
16567	GCT > GCA	Ala110Ala	sense
16601	CTA > TTA	Leu122Leu	sense
16762	CCT > CCA	Pro175Pro	sense
16769	AGA > CGA	Arg178Arg	sense
16879	ACT > ACA	Thr214Thr	sense
16894	TTG > TTA	Leu219Leu	sense
16921	ACC > ACA	Thr228Thr	sense
16942	TTT > TTA	Leu235Phe	missense
16978	GTG > GTT	Val247Val	sense
17377	ACT > ACA	Thr380Thr	sense
17416	GCA > GCT	Ala393Ala	sense
17530	ACA > ACT	Thr431Thr	sense
17597	ACT > GCT	Ala454Thr	missense
17990	CTG > TTG	Leu585Leu	sense
18020	CGG > AGG	Arg595Arg	sense
18031	GCT > GCA	Ala598Ala	sense

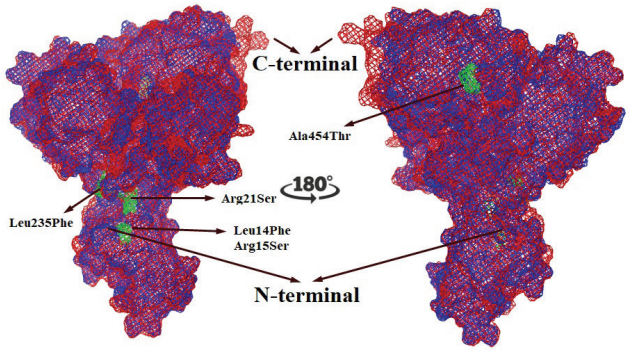

Figure 1. Display of changes caused by mutations in helicase in superimpose mode blue: wild-type helicase, red: mutant helicase, green: mutant residues

The mutations caused a decrease in the nucleic acid affinity of helicase (lowest ΔΔG -84.4±1.4 kcal.mol^{-1} and -71.1±6.7 kcal.mol^{-1} for wild-type and mutant, respectively) (Table 2). The Z-scores suggested that the mutant docking pattern was more accurate and successful (-1.4 and -2.1 for wild-type and mutant, respectively). This result showed a nice correlation between the intermolecular energy of our solutions and the FCC between these solutions and the target (Figure 3).

DISCUSSION

The helicase enzyme, a motor protein, causes the unwinding of double-stranded nucleic acids along the 5′-3′ direction during biological processes such as recombination, replication, and repair (28). The SARS CoV-2 helicase interacts with

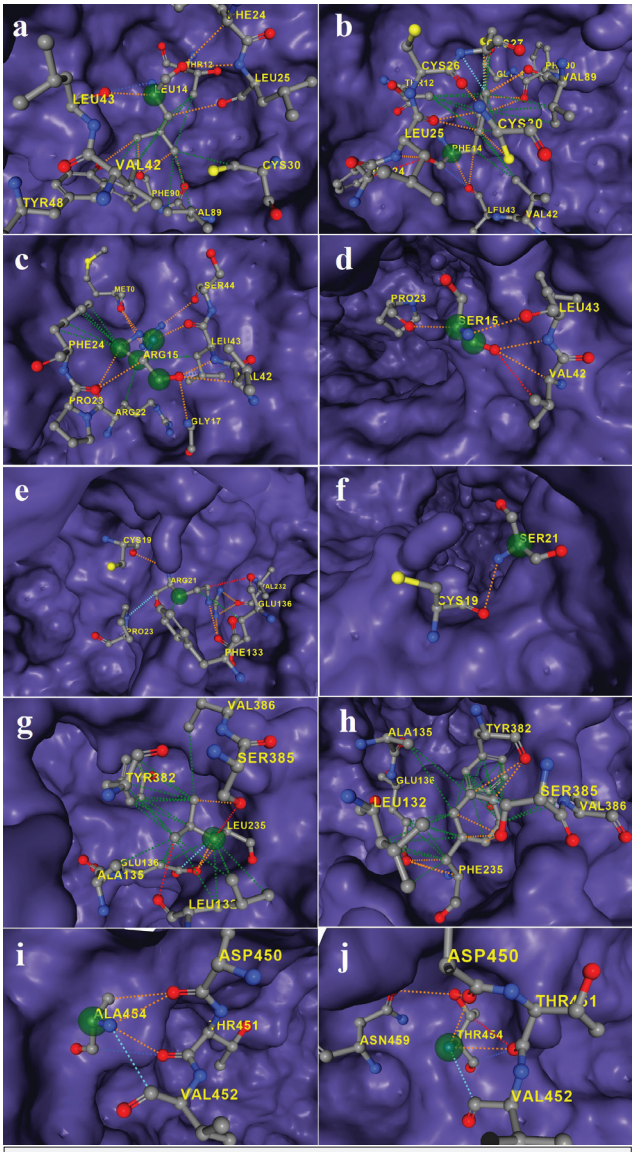

Figure 2. The change of inter-residual interaction in the tertiary structure of Helicase by mutations. Dashes indicates; red: hydrogen bond, orange: polar, green: hydrophobic, blue: Van der Walss. a: Leu14-wild-type, b: Phe14-mutant, c: Arg15-wild-type, d: Ser15-mutant, e: Arg21-wild-type, f: Ser21-mutant, g: Leu235-wild-type, h: Phe235-mutant, i: Ala454-wild-type, j: Phe454-mutant

human serine/threonine-protein kinase (TBK1). This interaction inhibits TBK1 phosphorylation and reduces interferon regulatory factor-3 phosphorylation by 75%, resulting in a reduction in the production of interferon-beta, one of the barriers to the viral invasion process (29,30). This study revealed that mutations in the SARS CoV-2 helicase, which is an important antiviral target, cause a decrease in substrate affinity and change in protein stability. The functional roles of proteins are formed by the dynamic movement and stability of their molecules (10,22). Mutations in the primary sequences of proteins change tertiary structure, stability, and function (31–33). A location-based evaluation of mutations is important in terms of the behavior of the virus in the cellular invasion process, the progression of the epidemic, and the specification of treatment options (34,35). The SARS CoV-2 has undergone thousands of mutations since the outbreak began, resulting in significant changes in its genome and protein structure (36,37). These changes manifested as various characteristics such as more virulence, increased affinity for the angiotensin converting enzyme-2 receptor, and faster host transition (38–40). The increase of the virus in the host cell is associated with an increased replication cycle and helicase activity. The opposite is also possible. Virus proteome rearrangements caused by mutations can increase or decrease virulence. Feroza et al. revealed two mutations with opposing effects on RNA-binding affinity with helicase (41). They reported that the Tyr541Cys substitution is a destabilizing mutation that increases molecular flexibility and leads to the reduced binding affinity for RNA and helicase, while the Phe504Leu substitution results in increased affinity (41). This study revealed that the Ala454Thr substitution in the 2A domain resulted in a decrease in protein stability (ΔΔG -0.73 kcal.mol^{-1}).

The interaction of active protein molecules and target nucleic acid sequence in the activation and regulation of replication and translation processes occurs with the contribution of special structural motifs such as zinc fingers (42,43). Zinc finger domain mutations result in alterations/weakening of target nucleic acid/protein and protein/protein interactions (44–46). According to the findings, three mutations (Leu14Phe, Arg15Ser, and Arg21Ser) in the zinc finger domain of the SARS CoV-2 helicase caused a decrease in protein stability (ΔΔG -0.99, -1.66, and -1.15 kcal.mol^{-1}, respectively) and a change in its conformation (Figure 2). Given the functional roles of the SARS CoV zinc finger structural motifs located in the N-terminus, it is clear that these mutations will result in significant changes in the functional properties of the helicase (47,48). The helicase-nucleic acid docking results indicated a decreased affinity of the SARS CoV-2 helicase (from -84.4 to -71.1 kcal.mol^{-1}). It is thought that the change in the bond interaction network of the residue in the zinc finger motif (^{26}Cys4), after the mutation affects the positive charge area, causes a weakening in the nucleic acid interaction (Figures 2a and b).

This study found that the Leu235Phe substitution located on the coil structure extending from the beta barrel formation to the nucleotide binding site between the 1A and 2A domains causes a decrease in protein stability (ΔΔG -0.54 kcal.mol^{-1}). This region of Leu235Phe substitution, located between the two domains responsible for nucleotide binding and hydrolysis, has been identified as a binding pocket for many candidate helicase inhibitors (49,50). Mutations are not only a threat to the functional roles of viral proteins, but also important for the validity of existing therapeutics. With mutations, the effectiveness of inhibitors can either increase or decrease.

Table 2. The change in helicase-nucleic acid interaction.

		Z-Score	DocSc	i-RMSD	Evdw	Eelec
1	**W**	-1.4	-84.4±1.4	16.8±4.2	-37.7±5.9	-322.8±19.7
	M	-2.1	-71.1±6.7	0.7±0.4	-40.9±13.3	-250.9±33.7
2	**W**	-1.4	-84.3±5.5	0.7±0.5	-36.3±5.0	-362.8±24.7
	M	-0.9	-57.0±2.5	7.7±0.7	-32.7±11.7	-180.4±47.7
3	**W**	-0.7	-71.2±9.0	7.4±1.4	-39.8±8.2	-245.5±47.5
	M	-0.8	-54.8±3.4	22.7±2.4	-26.9±3.8	-187.0±5.6
4	**W**	-0.6	-69.5±1.7	13.8±4.4	-31.0±3.7	-296.8±11.1
	M	0.2	-43.2±2.0	6.2±0.9	-20.1±6.3	-190.3±5.5
5	**W**	-0.1	-61.9±5.5	20.6±1.2	-34.8±4.4	-221.3±46.2
	M	0.3	-42.2±4.8	24.7±0.4	-43.1±8.4	-95.6±16.3
6	**W**	-0.1	-59.8±7.6	22.3±0.5	-32.0±3.9	-237.2±27.3
	M	0.4	-40.9±8.0	11.4±4.3	-19.3±8.1	-174.9±26.4
7	**W**	0.6	-49.3±5.1	24.8±3.8	-26.5±5.6	-185.9±23.0
	M	0.6	-38.1±7.2	23.9±0.5	-31.7±9.1	-92.2±14.0
8	**W**	0.9	-44.9±3.7	26.2±3.7	-34.2±5.7	-108.7±17.2
	M	1.1	-32.1±2.8	22.3±0.7	-17.4±4.5	-115.1±10.7
9	**W**	1.0	-43.1±1.3	24.8±3.8	-29.1±5.5	-150.4±28.4
	M	1.3	-29.5±5.1	28.9±2.0	-21.6±1.8	-54.3±24.1
10	**W**	1.7	-29.9±5.2	24.6±0.4	-23.2±4.2	-125.0±20.3
	M	-	-	-	-	-

W: wild, M: mutant, DocSc: docking score, i-RMSD: interface RMSD (from the overall lowest-energy structure), Evdw: Van der Waals energy, Eelec: electrostatic energy.

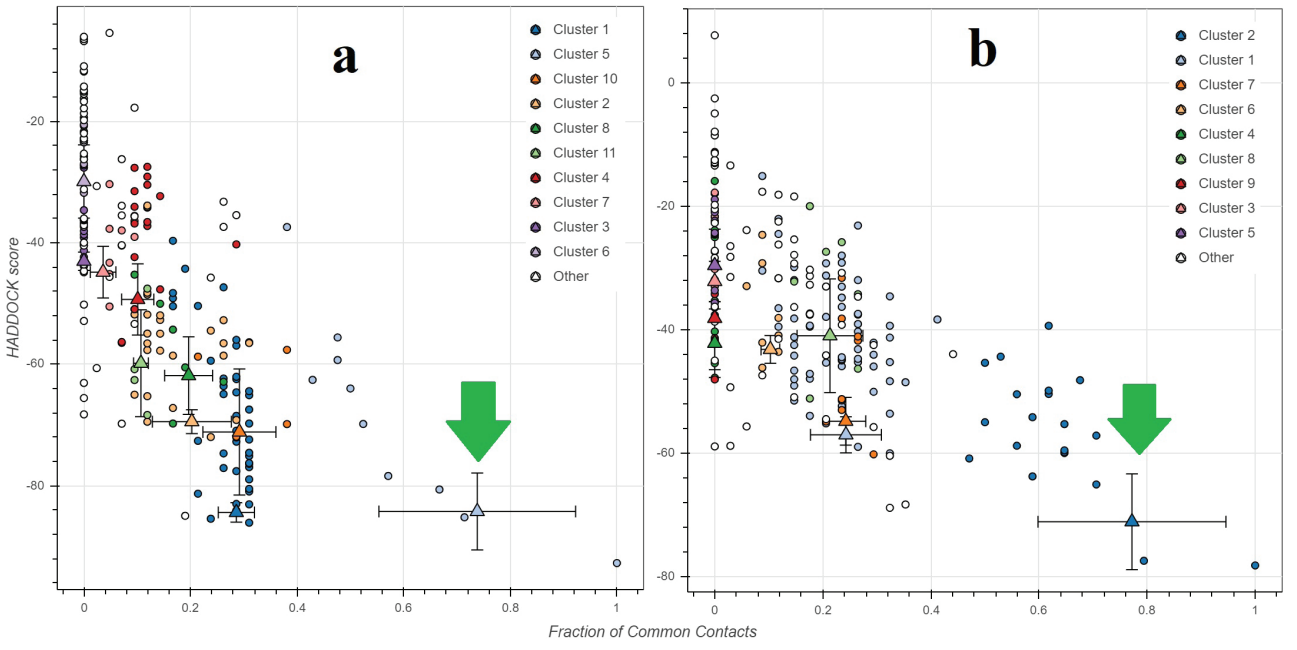

Figure 3. Evaluation of binding quality for wild-type helicase/nucleic acid and mutant helicase/nucleic acid complexes. a: wild-type helicase-nucleic acid complex, b: mutant helicase-nucleic acid complex.

CONCLUSION

The SARS CoV-2 nsp13 mutations decreased protein stability and nucleic acid affinity of helicase. The decreased helicase activity limits the replication and spread of SARS CoV-2 in the host cells. In China, which is the origin of the epidemic and the source of the isolates analyzed in this study, it is thought that successful epidemic control policies, as well as mutations in viral proteins in favor of the host, contributed to the decrease in the number of cases. The results provide important data on the development of potential antivirals and the effects of mutations on the functional behavior of viral proteins.

Acknowledgment: Genome data of Chinese isolates were obtained from the NCBI Virus database. Thanks to the NCBI Virus database for its open-source data sharing policy.

Peer Review: Externally peer-reviewed.

Conflict of Interest: Author declared no conflict of interest.

Financial Disclosure: Author declared no financial support.

REFERENCES

1. Singhal T. A Review of Coronavirus Disease-2019 (COVID-19). Indian J Pediatr 2020; 87: 281-6.
2. Zhou P, Yang X Lou, Wang XG, Hu B, Zhang L, Zhang W, et al. A pneumonia outbreak associated with a new coronavirus of probable bat origin. Nature 2020; 579: 270-3.
3. Worldometer. Coronavirus case report. WwwWorldometersInfo/Coronavirus 2022.
4. Wu F, Zhao S, Yu B, Chen YM, Wang W, Song ZG, et al. A new coronavirus associated with human respiratory disease in China. Nature 2020; 579: 265-9.
5. Zito Marino F, De Cristofaro T, Varriale M, Zannini G, Ronchi A, La Mantia E, et al. Variable levels of spike and ORF1ab RNA in post-mortem lung samples of SARS-CoV-2-positive subjects: comparison between ISH and RT-PCR. Virchows Arch 2022: 1-11.
6. Finkel Y, Mizrahi O, Nachshon A, Weingarten-Gabbay S, Morgenstern D, Yahalom-Ronen Y, et al. The coding capacity of SARS-CoV-2. Nature 2021; 589: 125-30.
7. Habtemariam S, Nabavi SF, Banach M, Berindan-Neagoe I, Sarkar K, Sil PC, et al. Should We Try SARS-CoV-2 Helicase Inhibitors for COVID-19 Therapy? Arch Med Res 2020; 51: 733-5.
8. Singleton MR, Dillingham MS, Wigley DB. Structure and mechanism of helicases and nucleic acid translocases. Annu Rev Biochem 2007; 76: 23-50.
9. Ahmad S, Waheed Y, Ismail S, Bhatti S, Abbasi SW, Muhammad K. Structure-based virtual screening identifies multiple stable binding sites at the RecA domains of SARS-CoV-2 helicase enzyme. Molecules 2021; 26: 1446.
10. Akbulut E. Mutations in the SARS CoV-2 spike protein may cause functional changes in the protein quaternary structure. Turkish J Biochem 2021; 46: 137-44.
11. Akbulut E. Comparative Genomic and Proteomic Analysis of SARS CoV-2 - with Potential Mutation Probabilities and Drug Targeting. Erzincan Univ J Sci Technol 2020; 13: 1187-97.
12. Zahradník J, Marciano S, Shemesh M, Zoler E, Harari D, Chiaravalli J, et al. SARS-CoV-2 variant prediction and antiviral drug design are enabled by RBD in vitro evolution. Nat Microbiol 2021; 6: 1188-98.
13. Katoh K. MAFFT: a novel method for rapid multiple sequence alignment based on fast Fourier transform. Nucleic Acids Res 2002; 30: 3059-66.
14. Mount DW. Using BLOSUM in sequence alignments. Cold Spring Harb Protoc 2008; 3: pdb-top39.
15. Jones DT, Taylor WR, Thornton JM. The rapid generation of mutation data matrices from protein sequences. Bioinformatics 1992; 8: 275-82.
16. Kumar S, Stecher G, Li M, Knyaz C, Tamura K. MEGA X: Molecular evolutionary genetics analysis across computing platforms. Mol Biol Evol 2018; 35: 1547-9.
17. Mirdita M, Ovchinnikov S, Steinegger M. ColabFold - Making protein folding accessible to all. BioRxiv 2021: 2021.08.15.456425.
18. Newman JA, Douangamath A, Yadzani S, Yosaatmadja Y, Aimon A, Brandão-Neto J, et al. Structure, mechanism and crystallographic fragment screening of the SARS-CoV-2 NSP13 helicase. Nat Commun 2021; 12.
19. Benkert P, Biasini M, Schwede T. Toward the estimation of the absolute quality of individual protein structure models. Bioinformatics 2011; 27: 343-50.
20. Rose AS, Bradley AR, Valasatava Y, Duarte JM, Prlic A, Rose PW. NGL viewer: Web-based molecular graphics for large complexes. Bioinformatics 2018; 34: 3755-8.
21. Xu J, Zhang Y. How significant is a protein structure similarity with TM-score = 0.5? Bioinformatics 2010; 26: 889-95.
22. Rodrigues CHM, Pires DEV, Ascher DB. DynaMut2: Assessing changes in stability and flexibility upon single and multiple point missense mutations. Protein Sci 2021; 30: 60-9.
23. Pires DEV, Ascher DB, Blundell TL. MCSM: Predicting the effects of mutations in proteins using graph-based signatures. Bioinformatics 2014; 30: 335-42.
24. Pires DEV, de Melo-Minardi RC, dos Santos MA, da Silveira CH, Santoro MM, Meira W. Cutoff Scanning Matrix (CSM): Structural classification and function prediction by protein inter-residue distance patterns. BMC Genomics, vol. 12, Springer; 2011, p. 1–11.
25. Pires DEV, De Melo-Minardi RC, Da Silveira CH, Campos FF, Meira W. ACSM: Noise-free graph-based signatures to large-scale receptor-based ligand prediction. Bioinformatics 2013; 29: 855-61.
26. Jubb HC, Higueruelo AP, Ochoa-Montaño B, Pitt WR, Ascher DB, Blundell TL. Arpeggio: A Web Server for Calculating and Visualising Interatomic Interactions in Protein Structures. J Mol Biol 2017; 429: 365-71.
27. Van Zundert GCP, Rodrigues JPGLM, Trellet M, Schmitz C, Kastritis PL, Karaca E, et al. The HADDOCK2.2 Web Server: User-Friendly Integrative Modeling of Biomolecular Complexes. J Mol Biol 2016; 428: 720-5.
28. Chen J, Malone B, Llewellyn E, Grasso M, Shelton PMM, Olinares PDB, et al. Structural Basis for Helicase-Polymerase Coupling in the SARS-CoV-2 Replication-Transcription Complex. Cell 2020; 182: 1560-1573.e13.
29. Leulier F, Parquet C, Pili-Floury S, Ryu JH, Caroff M, Lee WJ, et al. IK-Kepsilon and TBK1 are essential components of the IRF3 signaling pathway. Nat Immunol 2003; 4: 478-84. doi: 10.1038/ni922.
30. Xia H, Cao Z, Xie X, Zhang X, Chen JYC, Wang H, et al. Evasion of Type I Interferon by SARS-CoV-2. Cell Rep 2020; 33: 108234.
31. Nguyen TT, Chang SC, Evnouchidou I, York IA, Zikos C, Rock KL, et al. Structural basis for antigenic peptide precursor processing by the endoplasmic reticulum aminopeptidase ERAP1. Nat Struct Mol Biol 2011; 18: 604-13.
32. Wu S, Tian C, Liu P, Guo D, Zheng W, Huang X, et al. Effects of SARS-CoV-2 mutations on protein structures and intraviral protein–protein interactions. J Med Virol 2021; 93: 2132-40.

33. Akbulut E, Kar B. SARS CoV-2 nsp1 Mutasyonlarının Protein Yapıda Ortaya Çıkardığı Değişimler. Int J Pure Appl Sci 2020; 6: 68-76.
34. Farkas C, Fuentes-Villalobos F, Garrido JL, Haigh J, Barría MI. Insights on early mutational events in SARS-CoV-2 virus reveal founder effects across geographical regions. PeerJ 2020; 2020: e9255.
35. Garvin MR, T. Prates E, Pavicic M, Jones P, Amos BK, Geiger A, et al. Potentially adaptive SARS-CoV-2 mutations discovered with novel spatiotemporal and explainable AI models. Genome Biol 2020; 21: 1-26.
36. Alouane T, Laamarti M, Essabbar A, Hakmi M, Bouricha EM, Chemao-Elfihri MW, et al. Genomic diversity and hotspot mutations in 30,983 SARS-CoV-2 genomes: Moving toward a universal vaccine for the "confined virus"? Pathogens 2020; 9: 1-19.
37. Akbulut E. SARS CoV-2 Spike Glycoprotein Mutations and Changes in Protein Structure. Trak Univ J Nat Sci 2020; 22: 1-11.
38. Matyášek R, Kovařík A. Mutation patterns of human SARS-CoV-2 and bat RATG13 coronavirus genomes are strongly biased towards C>U transitions, indicating rapid evolution in their hosts. Genes (Basel) 2020; 11: 1-13.
39. Wang R, Hozumi Y, Zheng YH, Yin C, Wei GW. Host immune response driving SARS-CoV-2 evolution. Viruses 2020; 12: 1095.
40. Seyran M, Takayama K, Uversky VN, Lundstrom K, Palù G, Sherchan SP, et al. The structural basis of accelerated host cell entry by SARS-CoV-2†. FEBS J 2021; 288: 5010-20.
41. Feroza B, Banerjee AK, Tripathi PP, Ray U. Two mutations P/L and Y/C in SARS-CoV-2 helicase domain exist together and influence helicase RNA binding. BioRxiv 2020.
42. Jen J, Wang YC. Zinc finger proteins in cancer progression. J Biomed Sci 2016; 23: 1-9.
43. Iuchi S. Three classes of C2H2 zinc finger proteins. Cell Mol Life Sci 2001; 58: 625-35.
44. Filippova GN, Ulmer JE, Moore JM, Ward MD, Hu YJ, Neiman PE, et al. Tumor-associated zinc finger mutations in the CTCF transcription factor selectively alter its DNA-binding specificity. Cancer Res 2002; 62: 48-52.
45. Takaku M, Grimm SA, Roberts JD, Chrysovergis K, Bennett BD, Myers P, et al. GATA3 zinc finger 2 mutations reprogram the breast cancer transcriptional network. Nat Commun 2018; 9: 1-14.
46. Munro D, Ghersi D, Singh M. Two critical positions in zinc finger domains are heavily mutated in three human cancer types. PLoS Comput Biol 2018; 14: e1006290.
47. Ma J, Chen Y, Wu W, Chen Z. Structure and Function of N-Terminal Zinc Finger Domain of SARS-CoV-2 NSP2. Virol Sin 2021; 36: 1104-12.
48. Ma Y, Wu L, Shaw N, Gao Y, Wang J, Sun Y, et al. Structural basis and functional analysis of the SARS coronavirus nsp14-nsp10 complex. Proc Natl Acad Sci U S A 2015; 112: 9436-41.
49. Halder UC. Predicted antiviral drugs Darunavir, Amprenavir, Rimantadine and Saquinavir can potentially bind to neutralize SARS-CoV-2 conserved proteins. J Biol Res 2021; 28: 1-58.
50. Berta D, Badaoui M, Martino SA, Buigues PJ, Pisliakov A V., Elghobashi-Meinhardt N, et al. Modelling the active SARS-CoV-2 helicase complex as a basis for structure-based inhibitor design. Chem Sci 2021; 12: 13492-505.

ISTANBUL UNIVERSITY PRESS

RESEARCH ARTICLE

Eur J Biol 2022; 81(1): 18-25

Leptin Enhances Nitric Oxide Production and Decreases Blood Flow in Rat Skeletal Muscle

Savas Ustunova[1], Aysegul Kapucu[2], Cihan Demirci Tansel[2]

[1]Bezmialem Vakif University, School of Medicine, Department of Physiology, Istanbul, Turkiye
[2]Istanbul University, Faculty of Science, Department of Biology, Istanbul, Turkiye

ORCID IDs of the authors: S.U. 0000-0003-1870-229X; A.K. 0000-0002-0946-1407; C.D.T. 0000-0001-7926-3089

Please cite this article as: Ustunova S, Kapucu A, Demirci Tansel C. Leptin Enhances Nitric Oxide Production and Decreases Blood Flow in Rat Skeletal Muscle. Eur J Biol 2022; 81(1): 18-25. DOI: 10.26650/EurJBiol.2022.1082814

ABSTRACT

Objective: There are a few studies related to nitric oxide (NO) and leptin interaction in the regulation of physiological events in skeletal muscle. Therefore, the aim of the present study is to investigate the interaction of leptin and NO in response to blood flow and nitric oxide synthase (NOS) distribution on rat skeletal muscle.

Materials and Methods: Twenty-four adult-male Wistar albino rats were divided into 4 groups: control (C), Leptin (LP) (50 µg/kg), L-NG-nitroarginine methyl ester (LN) (a non-specific nitric oxide synthase inhibitor, 10 mg/kg,) and L-NAME+Leptin (LN+LP) administrated groups. Drugs were administered via the right jugular vein. Hemodynamic parameters: mean arterial pressure, heart rate and blood flow were recorded during the experiment and at the end blood samples for biochemical analyses of leptin and nitrite/nitrate levels and gastrocnemius muscle tissues from the right hindlimb for NOS distribution were taken.

Results: Leptin infusion after L-NAME administration significantly decreased heart rate and blood flow ($p<0.05$, $p<0.001$). In addition, there was no change in the mean arterial pressure in the leptin group and leptin-administered L-NAME group. Leptin levels were the highest in the LP+LN group ($p<0.01$). Decreased nitrate/nitrate levels with L-NAME administration ($p<0.01$ vs C) reached control values by leptin infusion. Both endothelial NOS (eNOS) and neuronal NOS (nNOS) distributions were observed in the skeletal muscle cells of the leptin group.

Conclusion: Although NO synthesis is inhibited by L-NAME, it is concluded that leptin partially enhances NO production and leptin uses NO as a mediator in its physiological effects.

Keywords: Blood flow, leptin, nitric oxide, rat; skeletal muscle

INTRODUCTION

Leptin, a polypeptide hormone, which is coded by the obesity (*Ob*) gene, is mainly released from white adipose tissue and belongs to the cytokine family. The best-known function of leptin is the regulation of food intake and energy expenditure (1). In addition, leptin is functional in many metabolic events such as angiogenesis, hematopoiesis, and lipid/carbohydrate metabolism. It is also effective on functions of reproductive, cardiovascular, and immune systems (2). Leptin shows its effect through membrane-bound leptin receptors (OBR). The OBR gene expresses in the central nervous system (CNS) and in many peripheral tissues including skeletal muscle (3). When leptin binds to OBR, thermogenesis is stimulated through the PI3K and AMPK signaling pathways in the skeletal muscle, enhancing glucose and fatty acid metabolism. Therefore, leptin-mediated increase in the fatty acid oxidation reduces the formation of triacylglycerol and fat deposits to prevent lipotoxicity (4, 5).

Furthermore, when leptin in circulation crosses the blood-brain barrier, it acts on the hypothalamus to regulate energy balance acting and increases the sympathetic nerve activity in brown adipose tissue to provide

Corresponding Author: Savas Ustunova E-mail: sustunova@bezmialem.edu.tr
Submitted: 04.03.2022 • **Revision Requested:** 21.03.2022 • **Last Revision Received:** 23.03.2022 • **Accepted:** 04.04.2022 • **Published Online:** 29.04.2022

thermogenesis. In addition, because of sympathetic nervous system stimulation, leptin increases arterial blood pressure, which is correlated to high levels of leptin in continuous hypertension (6, 7).

The binding sites of leptin in the brain are also important in the control of the cardiovascular system. Therefore, it is suggested that leptin may affect cardiovascular system functions through its effects on the CNS. Furthermore, functionally active OBRs have been demonstrated to be present in endothelial cells, suggesting that endothelium, which plays an important role in the regulation of blood pressure, is one of the main targets of leptin (8-10).

Nitric oxide (NO), a gaseous transmitter and intracellular second messenger in biological systems, is one of the substances released by the endothelium to cause vasodilatation for regulating blood pressure. Previous studies have also shown that NO plays an important role in platelet aggregation, cytotoxicity, hypertension, diabetes, atherosclerosis, learning and memory function, and regulation of male sexual function (11). In addition, NO has many functions in skeletal muscle. These are stimulation and contraction of muscle, mitochondrial energy production, glucose metabolism and autoregulation of blood flow. Although expression of OBRs is present in endothelial cells, its effect on NO production is controversial (12-14).

There have also been some studies demonstrating that leptin increases NO release from endothelial cells (9, 10, 15). Although there have been studies to demonstrate leptin and NO interaction, the relationship between leptin and NO has not been fully explained in the regulation of physiological events in skeletal muscle. Therefore, this study was carried out to determine the relationship between leptin and NO in response to blood flow and NOS distribution on rat skeletal muscle.

MATERIALS AND METHODS

Animals and Study Groups

In the present study, 24 adult-male Wistar albino rats weighing 250-300 g were used. All animals were housed in a light- (12/12 hours light and dark period) and temperature-controlled room (22±2°C), fed with standard lab chow and tap water *ad libitum* until the day of the experiment. The study was reviewed and approved by the Experimental Animals Ethics Committee of Experimental Medicine Research Institute of Istanbul University (Date:18.10.2005, Number: 36).

The rats were divided into 4 groups, each including 6 rats as follows: control (C), Leptin (LP) (50 µg/kg, #sc-471278, Santa Cruz Biotechnology, Texas, USA), L-NG-nitroarginine methyl ester (LN) (L-NAME, a non-specific nitric oxide synthase inhibitor, 10 mg/kg, Sigma-Aldrich Chemie Gmbh Munich, Germany) and L-NAME+Leptin (LN+LP) administrated groups. The control group had saline in the same volume at the same time points of drug administrations. All drugs and saline were administrated intravenously (IV) via an infusion pump (KDS 200/200P LEGACY, KD Scientific, Holliston, MA, USA) at a rate of 0.166 ml/min, so the total volume was 0.5 ml for each administration.

Experimental Design

The animals received intraperitoneal (ip) sodium pentothal (90 mg/kg) anesthesia. During the experiment, the rats were placed on a heating pad to control body temperature via a rectal probe (MLT1403, ADInstruments, Sydney, AUS) and body temperature was maintained at approximately 37°C. Tracheostomy was performed and spontaneous breathing was provided. Right carotid artery and right jugular vein were cannulated with a polyethylene (PE 50) cannula. Blood pressure was monitored via a pressure transducer (MLT0380/D, ADInstruments, Sydney, AUS) from the right carotid artery. All drugs were administered via a venous catheter which was attached to the right jugular vein. A small incision was made on the gastrocnemius muscle of the left hindlimb without causing any bleeding. To determine intramuscular blood flow, the needle probe of the laser Doppler flowmeter (Blood FlowMeter INL 191, ADIsntruments, Sydney, AUS) was carefully placed on the muscle surface. After a 30-min stabilization period the first drugs were applied and 20 min after the first drug administration, the second drugs were administered (Figure 1). All hemodynamic parameters were recorded during the experiment by a data acquisition unit (PowerLab 8/30, ADInstruments, Sydney, AUS) and then analyzed offline every 10 min.

At the end of the experiment, blood samples were collected directly from the heart for biochemical analyses and the tissue samples of the gastrocnemius muscle from the right hindlimb, which not had any intervention, were taken to determine the distribution of NOS enzymes, immunohistochemically.

Immunohistochemical Analysis

Gastrocnemius muscle tissues were fixed in 10% formalin and embedded in paraffin. In 4 µm sections taken from paraffin blocks, the distributions of eNOS and nNOS were examined immunohistochemically. For this purpose, the sections were kept overnight at 56°C, then passed through xylene and alcohol series and brought up to the water. The sections were incubated for antigen retrieval in citrate buffer (pH 6.0) (Thermo Scientific, AP-9003-500) for 10 minutes by microwaving slides and then allowed to cool to room temperature for 20 min and rinsed with distilled water. En-

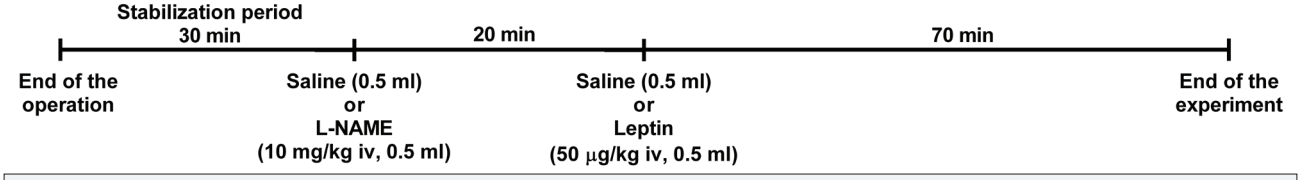

Figure 1. The timeline of experimental design.

dogenous peroxidase activity was eliminated with 0.3% H_2O_2 (Lab Vision, TA-060-HP) at room temperature for 10 min. The sections were rinsed with distilled water and washed for 10 min in phosphate buffered saline (PBS) three times in each step.

After washing, the sections were treated with blocking serum (Ultra V Block, Lab Vision, TA-60-UB, Värmdö, Sweden) for 5 min at room temperature. The muscle sections were then incubated with anti-eNOS (RB- 1711-P, NeoMarkers Fremont, CA) and nNOS (KAP-NO003, NeoMarkers Fremont, CA) antibodies at 4°C overnight. Antibodies were diluted in a ratio of 1:100 with an antibody diluent (UltrAb Diluent, Lab Vision, TA-125-UD, Värmdö, Sweden). Then, the sections were processed by the StrepABC procedure, following the manufacturer's instructions, using a goat anti-rabbit IgG (Labvision, TR- 125-BN and TR-125-HR, Värmdö, Sweden). The activity was demonstrated by the AEC (3-amino-9-ethyl carbazole) substrate kit (Labvision, TA-004-HAC, Värmdö, Sweden). The sections were counterstained with Mayer hematoxylin. The results of the immunohistochemistry were examined by two independent observers using a light microscope (Leica, Wetzlar, Germany) and photographed by Image Pro-Plus system.

Slides were blindly analyzed with ImageJ software (National Institutes of Health, Bethesda, Maryland, U.S.A.) by using a color deconvolution plug-in. For staining intensity, every section was assessed in 3 similar fields of view under 400X magnification. Images were analyzed to calculate the mean intensity of AEC, ranging from 0 (black) to 255 (total white). The final AEC intensity was calculated according to the formula $f = 255 - i$, (i = mean DAB intensity) with data acquired from the software; i ranges from 0 (zero = deep brown, highest expression), to 255 (total white) (16).

Biochemical Analysis

Leptin and nitrite/nitrate levels were measured in blood samples which were drawn from the hearts of animals at the end of the experiment. Blood samples were centrifuged at 1500 *g* for 10 min at 4°C and the serum samples were used for analysis. Serum leptin levels were studied by an enzyme-linked immunosorbent assay (ELISA) using the Rat Leptin ELISA kit (DRG Instruments GmbH, Germany) according to the manufacturer's notes. Nitrite/nitrate levels in the serum were determined by the Griess method (17, 18). According to this reaction, nitrate is reduced in nitrite in the presence of nitrate reductase enzyme. Then, the mixture containing the sulfanilamide and N-(1-naphthyl) ethylene diamine dihydrochloride compounds, named the Griess reactive, is added into nitrite to obtain the colored diazo product. The resulting-colored product is measured spectrophotometrically at 540 nm.

Statistical Analysis

Data were analyzed using the GraphPad Prism 6.0 (GraphPad Prism, Version 6, Software Program, San Diego, CA) and were expressed as mean ± standard error of means (SEM). The time dependent results of hemodynamic parameters were compared by two-way ANOVA, while biochemical results of blood samples in different groups and area under the curves (AUC) for hemodynamic parameters were compared by one-way ANOVA followed with post-hoc Bonferroni's multiple comparison test. A value of $p \leq 0.05$ was considered as statistically significant.

RESULTS

Hemodynamic Results

There was no significant difference in the Mean Arterial Pressure (MAP) in the leptin administrated group when compared with the values of the C group at the same time intervals during the experiment. MAP was significantly increased within the first 10 minutes of L-NAME infusion in LN and LN+LP groups ($p<0.001$). Although these high levels tend to decrease, they were maintained until the end of the experiment which did not change much more with leptin administration in the LN+LP group. At the end of the experimental procedure (at the 90th min) MAP of the LN and LN+LP groups were still significantly higher than MAP levels of the C and LP groups ($p<0.001$, Figure 2A). Leptin and L-NAME also showed similar effects on systolic and diastolic pressure, both of which were compatible with

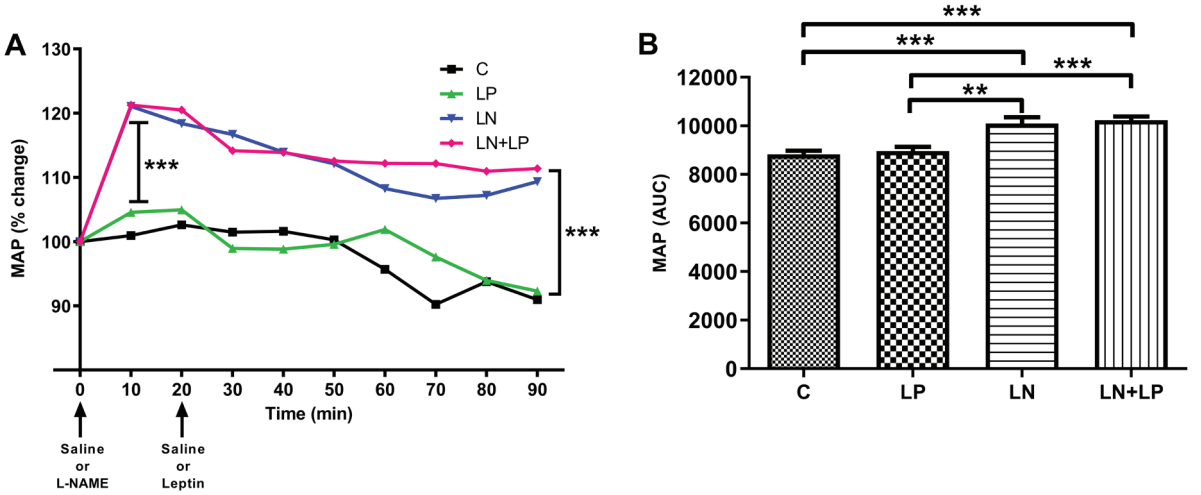

Figure 2. Comparison of % changes in mean arterial pressure during the experiment (A) and differences of area under curve (B) between the groups. MAP: mean arterial pressure, AUC: area under curve, C: Control, LP: Leptin, LN: L-NAME, LN+LP: L-NAME+Leptin groups (Data are expressed as mean±SEM, **p<0.01, ***p<0.001 statistically significance).

MAP (data not shown). To compare the cumulative difference between the groups during the experimental time, the AUC of hemodynamic parameters were calculated. AEC of both LN and LN+LP groups were very close to each other, as seen in the same way between the C and LP groups. However, the area under the curves of both LN and LN+LP was found to be significantly higher according to the control and leptin groups ($p<0.01$ and $p<0.001$ respectively, Figure 2B).

The heart rate (HR) was significantly decreased with L-NAME infusion in the LN and LN+LP groups ($p<0.05$). While these low levels slowly increased in the LN group and were close to that of the C levels at the end of the experiment, leptin administration slowed down this increase with respect to the LN group. Leptin and control groups had similar values during the experiment. At the end of the experimental procedure (at the 90th min) the LN+LP group had significantly lower HR according to all other groups ($p<0.05$, Figure 3A). When the AUC were analyzed, both C and LP groups had proximate values, which also were observed between LN and LN+LP groups. So, there was no significant difference in the HR during the experiment in the leptin administrated group when compared with the control group. On the other hand, the AUC of the LN+LP group was found to be significantly higher according to the C and LN groups ($p<0.05$, Figure 3B)

After administration of L-NAME, a statistically significant decrease in the blood flow, especially at the 20th minute of treatment, was observed in the LN and LN+LP groups, according to the C and LP groups ($p<0.001$). These low blood flow levels persisted over the duration of the experiment. Administration of leptin did not cause significant changes in blood flow compared to the C group until the 60th minute of the experiment. After that point, blood flow was significantly decreased ($p<0.001$). Leptin administration resulted in low blood flow in the LN+LP group until the end of the experiment and that was statistically

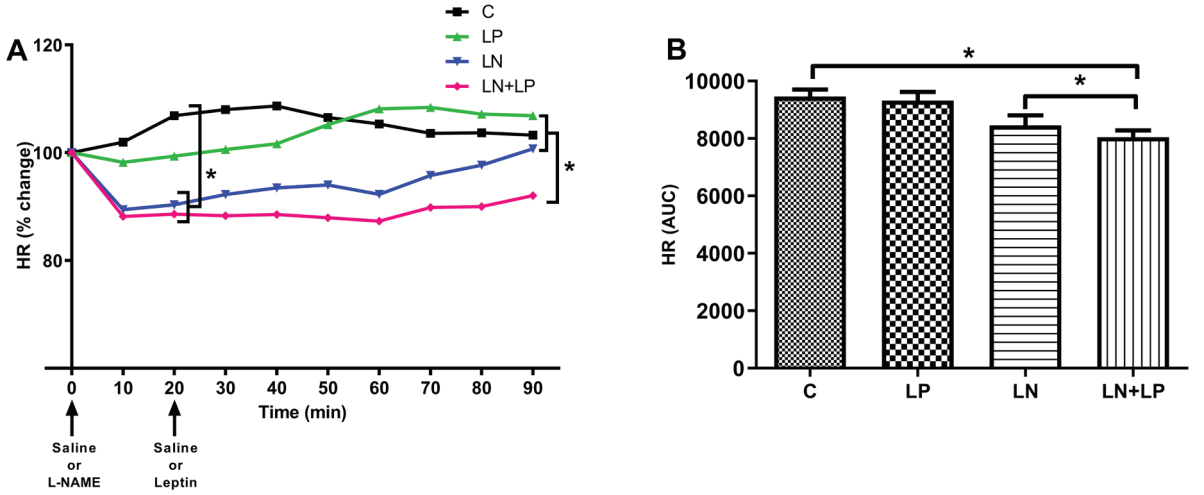

Figure 3. Comparison of % changes in heart rate during the experiment (A) and differences of area under curve (B) between the groups. HR: heart rate, AUC: area under curve, C: Control, LP: Leptin, LN: L-NAME, LN+LP: L-NAME+Leptin groups, C: Control, LP: Leptin, LN: L-NAME, LN+LP: L-NAME+Leptin groups (Data are expressed as mean±SEM, *p<0.05 statistically significance).

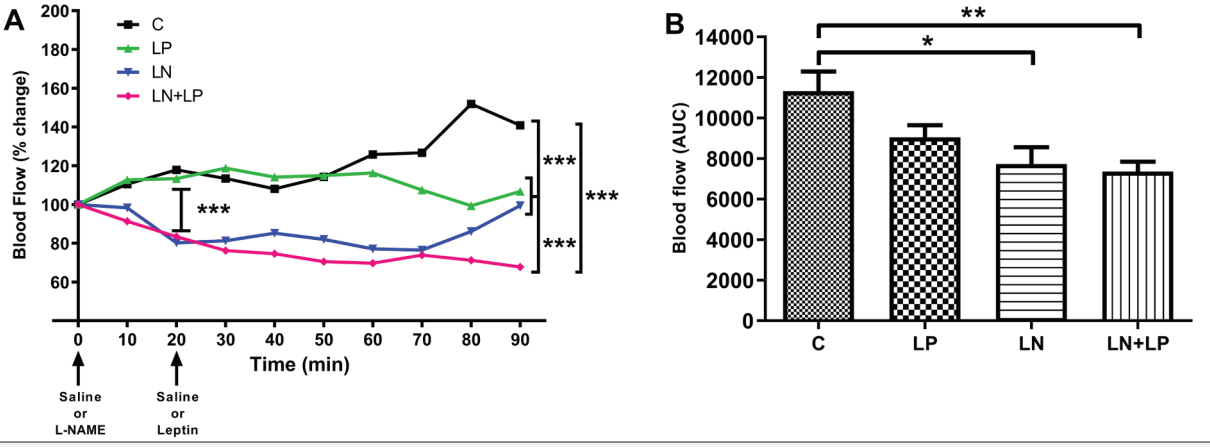

Figure 4. Comparison of % changes in blood flow during the experiment (A) and differences of area under curve (B) between the groups. AUC: area under curve, C: Control, LP: Leptin, LN: L-NAME, LN+LP: L-NAME+Leptin groups (Data are expressed as mean±SEM, *p<0.05, **p<0.01, ***p<0.001 statistically significance).

significant in accordance with other groups (p<0.001). However, in the LN group alone, blood flow returned to baseline levels at the end of the experiment (Figure 4A). When the area under the curves was examined, it was determined that the control group had a higher blood flow than that of all groups and this was statistically significant in both LN and LN + LP groups (p<0.001). L-NAME administration gave rise to a significant reduction in AUC of both LN and LN+LP groups when compared to LP group (p<0.001) (Figure 4B).

Biochemical Results

Serum leptin and nitrite/nitrate levels were measured in blood samples at the end of the experiment. It was determined that leptin levels of the LP, LN, and LN+LP groups were significantly increased according to that of the C group (p<0.05). The elevation in the LN+LP group was more significant (p<0.01) (Figure 5A). When the nitrite/nitrate levels were compared, the increase in the LP group was not significant, but there was a statistically significant decrease in the LN group compared to both C and LP groups (p<0.01, p<0.001, respectively). In the LN+LP group, the nitrite/nitrate levels were significantly higher than that of the LN group (p<0.01) but less than that of the LP group in a statistically insignificant manner and close to that of the C group values. In addition, nitrite/nitrate levels of the LP group were significantly elevated according to the LN group (p <0.001) (Figure 5B).

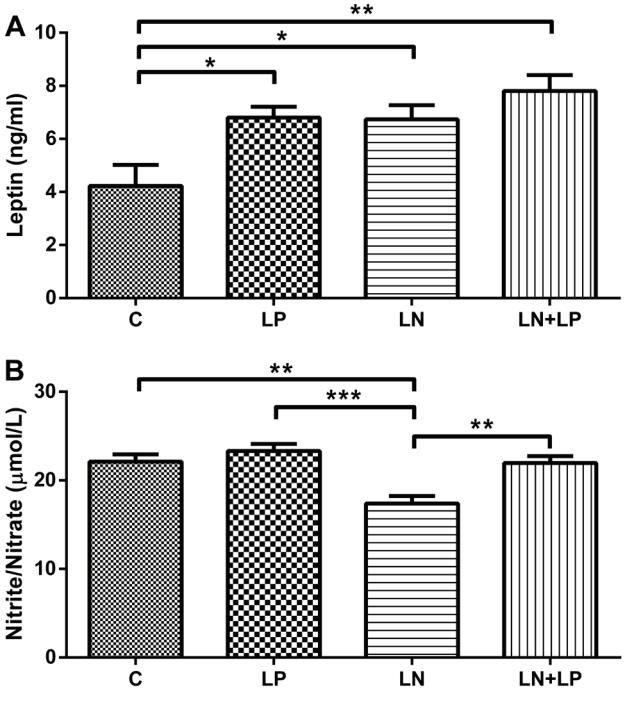

Figure 5. Serum leptin (A) and nitrite/nitrate (B) levels. C: Control, LP: Leptin, LN: L-NAME, LN+LP: L-NAME+Leptin groups (Data are expressed as mean±SEM, * p<0.05, **p<0.01, ***p<0.001).

Immunohistochemical Results

The distributions of eNOS and nNOS were investigated by immunohistochemical methods in the paraffin sections of control and drug administrated animals. In the control group, the reaction of eNOS and nNOS was determined in the perimysium, sarcolemma, and irregular connective tissue (Figure 6). In the leptin treated group, although the eNOS reaction was observed to be slightly dense in sarcolemma and more intense in the perimysium, the reaction was more pronounced around of the peripheral position of nuclei. The nNOS reaction was found to be similar in the same regions of the eNOS reaction, but at a lower density (Figure 6). The mean intensity of eNOS and nNOS reactions were significantly more than those of the C and LN groups (p<0.01, p<0.001, respectively) and were also denser from that of the LN+LP group which was significantly elevated in nNOS (Figures 7A-B). Both reactions were suppressed in the LN group. The eNOS reaction was denser in the sarcolemma whereas almost no nNOS reaction was observed in the control (Figure 6). After L-NAME administration, the eNOS reaction in the leptin-treated group was found to be mild in the sarcolemma and more in the vicinity of nuclei. The eNOS reaction was less than that of the leptin group and more than that of the control and L-NAME groups. The nNOS reaction was similar to that of the control values (Figures 6 and 7).

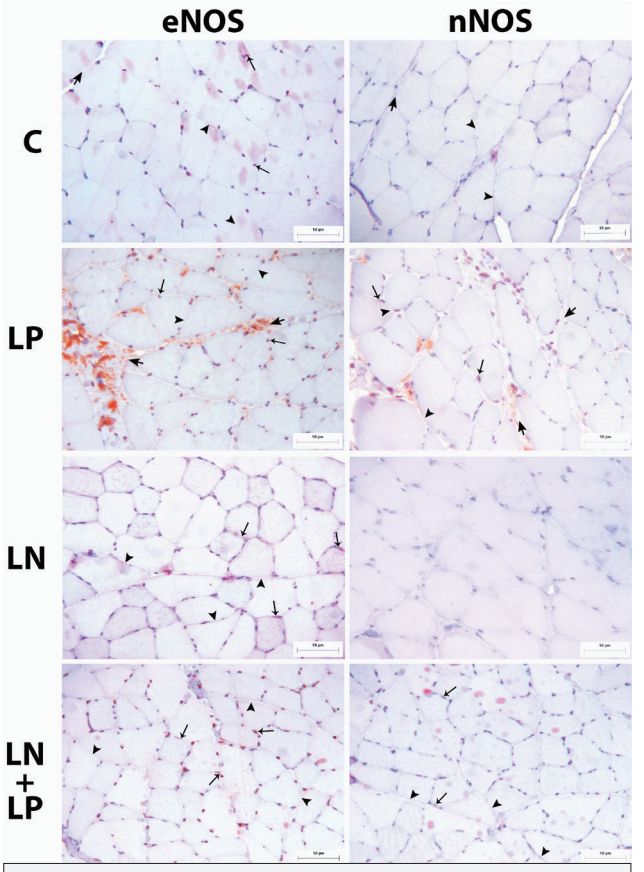

Figure 6. Immunohistochemically demonstrated eNOS and nNOS reactions in sarcolemma (➤), peripherally located nuclei (↑) and perimisium (↑) in gastrocnemius muscle. C: Control, LP: Leptin, LN: L-NAME, LN+LP: L-NAME+Leptin groups (Bar = 50 µm).

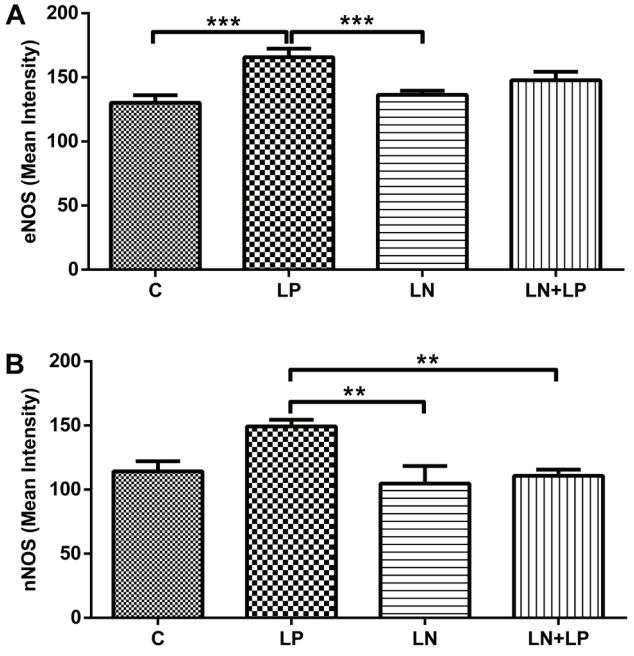

Figure 7. Mean intensity levels of eNOS (A) and nNOS (B) reactions in gastrocnemius muscle. C: Control, LP: Leptin, LN: L-NAME, LN+LP: L-NAME+Leptin groups (Data are expressed as mean±SEM, **p<0.01, ***p<0.001).

DISCUSSION

The understanding of the effects of leptin on the CNS and peripheral systems was led to thinking that there may be links between leptin and obesity, hypertension, and cardiovascular diseases (2). Experiments in ob/ob mice have shown that the absence of leptin causes abnormalities in the vascular endothelium and in the contraction-relaxation functions of vessels (19). Expression of leptin in fibroblasts and the presence of OBRs in vascular endothelium and cardiac muscle cells suggest that leptin has cardiovascular effects which might be mediated by NO (20). Therefore, in this study, we aimed to find out whether leptin exerts its cardiovascular effects through NO.

Leptin increases sympathetic nerve activity in rodents and humans; however, leptin only consistently increases BP chronically in rodents. The ability of leptin to increase BP in rodents is via both hypothalamic and extrahypothalamic regions.

It has been reported that administration of high dose intracerebroventricular leptin increases arterial blood pressure and HR by central neural mechanisms (21). In another study, no significant change in arterial pressure, HR, renal blood flow or renal cortical blood flow was observed by administration of leptin or saline in rats with similar initial values. It has also been suggested that leptin has no effect on systemic blood pressure and arterial blood flow (22). In our study, after a single dose of IV 50 µg/kg leptin administration, MAP and HR were found to be similar to that of the saline-administered control group, and there was no significant difference between them during the entire experiment. Similarly, Frühbeck (15) reported that after 90 minutes of administration of a single dose of IV saline and 10, 100, 1000 µg/kg of leptin, there was no change in blood pressure and an insignificant increase in HR. Mitchell et al. (23) reported that there was no significant change in MAP and HR between leptin-administered and non-administered animals when they infused a total of 1 mg/kg leptin to animals for 3 hours, while blood pressure decreased regularly in both groups during the experiment. Frühbeck (15) also reported an increase in MAP and a decrease in HR after the first 10 minutes of NOS inhibition, which was performed with L-NAME (30 mg/kg). In our study, when we used 10 mg/kg L-NAME, we found that MAP in this group was significantly higher, and HR was significantly lower than the control values at the same time intervals throughout the experiment. However, the HR was close to the control at the end of the experiment. In the leptin-administered L-NAME group, the increase in the MAP values was more dramatic and the changes in blood pressure were similar to the L-NAME group. The low values of HR after L-NAME administration were maintained until the end of the experiment in animals treated with leptin after L-NAME. HR levels in the LN+LP group was the lowest at the end of the experiment according to others. In addition, Dunbar et al. (24) reported that leptin administration decreased the blood flow in the iliac and mesenteric arteries without a change in the renal artery, and increased the MAP by decreasing the blood flow in the splanchnic vascular beds and skeletal muscle. It has also been reported in other studies that leptin did not cause a significant change in mesenteric, hindlimb and renal blood flow (9, 23). However, Mitchell et al. (23) also reported that L-NAME significantly increased regional blood flow when they applied it for 3 hours. In addition, it was noted that there was no significant change in renal and hindlimb blood flow when leptin was administered (23). In our study, no change in blood flow was observed in the one-hour period after leptin administration. However, after this period, there was a significant decrease in blood flow of the leptin-administered group until the end of the experiment. In addition, in our study, a regular decrease in blood flow was observed after L-NAME administration. In leptin and L-NAME administered animals, while the hindlimb blood flow decreased over time, this decrease reached a significant level only at the end of the experiment.

Bełtowski et al. (22) compared plasma leptin concentrations in the leptin (single dose, IV, 1000 µg/kg) administered groups at the different time intervals. The highest plasma leptin level was obtained at the 15th minute; after this minute the values began to decrease, tending to approach the control, and reached the control value at the 195th minute. Our samples were taken at the 90th minute, and in parallel with Beltowski's data, the serum leptin levels of the animals in the leptin and L-NAME groups were significantly higher. However, the increase in serum leptin levels was more dramatic in the leptin administered L-NAME group. Bełtowski et al. (25) suggested that NO products increased because of leptin administration, but the leptin values of the groups were close to each other. It was stated that there was no change in plasma leptin level in the group that was administered only L-NAME. In our study, on the

contrary, serum leptin levels were observed to be significantly higher in the L-NAME and leptin-administered L-NAME groups compared to the control group. It has been suggested in different studies that leptin exerts its effects not only through NO, but also through the sympathetic nervous system and endothelial-derived hyperpolarizing factor (25-27). In rodents, there is strong evidence for the role of leptin in an increase in SNA (28). Therefore, we think that leptin levels were also increased in the L-NAME group in order to compensate for the suppression of NO levels and to activate other possible pathways. Indeed, it was observed that inhibition of NO synthesis caused an increase in leptin level as expected.

In vitro studies have demonstrated that leptin stimulates NO production from the endothelium and causes NO-mediated vascular relaxation (10). However, the results of *in vivo* studies are not so conclusive. While some investigators reported the presence of NO in leptin-induced vascular relaxation (15), some investigators found the opposite (23, 29). Frühbeck and Gómez-Ambrosi (30) and Mastronardi et al. (31) observed an increase in plasma concentrations of nitrite/nitrate, the NO metabolites, after leptin administration. However, the source of NO has not been determined exactly. In our study, it was determined that serum nitrite/nitrate levels were significantly decreased in the L-NAME group compared to the control animals, as expected. When leptin was given to L-NAME treated animals, it was observed that there was a significant increase in serum nitrite/nitrate levels compared to that of the L-NAME group, and this value approached the control values. In the study by Bełtowski et al. (22) the highest nitrite/nitrate levels were obtained at the 45th and 75th minutes, respectively, after the administration of leptin (1000 µg/kg). At the 105th minute, this rate dropped to about one third. In our study, the failure to observe the expected increase in the leptin-administered group may be due to the time the blood samples were taken (after the 90th minute) and the dose of leptin administered.

NO is a mediator produced in endothelial cells that regulates vascular tone in a paracrine manner. There are studies showing NO production and NOS expression via leptin and its effects. It has been demonstrated that IV administration of leptin to Wistar albino rats increases serum NO level by 90% (15). In addition, it has been shown that administration of a single dose of leptin increases the level of nitrite/nitrate and cGMP, which is the secondary messenger of NO, in plasma and urine (22). In many different studies using L-NAME, it has been suggested that leptin increases NO production in ventricular cells, which in turn regulates cardiac contraction (32). It has also been indicated that expression of NOS isoforms is made in skeletal muscles of all mammals, including a muscle-specific type, nNOS. Immunohistochemical methods have shown that nNOS is found in the sarcolemma of muscle fibers, eNOS in the microvascular endothelium, and iNOS in leukocytes near muscle fibers and some endothelial cells (12, 33-37). In our study, nNOS and eNOS were also observed in the sarcolemmas of the fibrils, but the distribution ratios vary between groups. The increase in eNOS reactions in animals treated with leptin alone and L-NAME+Leptin may be due to the stimulatory effects of exogenous leptin administration on NO production.

In our study, when eNOS and nNOS distributions in the tissues were evaluated immunohistochemically, the strongest reaction was observed around the nuclei of the cells in the leptin group compared to all other groups. The fact that the reactions are intense around the nuclei suggests that NO plays a role in cellular transcription processes. Carbó et al. (38) suggested that protein synthesis was stimulated in the skeletal muscle, which they isolated 3.5 hours after 100 µg/kg IV leptin administration, and this was accomplished via an unknown mediator by leptin. In our study, the presence of eNOS and nNOS reactions around the nucleus after the leptin-administered groups strengthens the possibility that eNOS and nNOS may be the possible mediators that were not clearly known in the above-mentioned study. It was also determined that the distribution of eNOS in the tissue increased with the application of leptin after L-NAME while nNOS also showed a distribution like the control. The results here indicate that L-NAME may exert its inhibitory effect predominantly through nNOS. The eNOS reaction around the nuclei in the leptin-administrated L-NAME group, similar to the leptin group, suggests that leptin maintains its effect in various cellular events by stimulating eNOS.

In summary, with this study we demonstrated that a single dose IV leptin infusion did not cause any difference in mean arterial pressure with or without NO inhibition. Leptin administration significantly decreased heart rate and blood flow with the inhibition of NO. Both eNOS and nNOS distributions in skeletal muscle and nitrite/nitrate levels in serum samples were increased with leptin treatment which indicates that leptin induces NO production.

CONCLUSION

As a conclusion, the effect of leptin on blood flow, blood pressure and heart rate were investigated in the presence and absence of NO. Although NO synthesis is inhibited by L-NAME, we conclude that leptin partially enhances NO production and leptin uses NO as a mediator in its physiological effects.

Peer Review: Externally peer-reviewed.

Author Contributions: Conception/Design of Study- S.U., C.D.T.; Data Acquisition- S.U., A.K.; Data Analysis/Interpretation- S.U., A.K., C.D.T.; Drafting Manuscript- S.U., C.D.T.; Critical Revision of Manuscript- S.U., C.D.T.; Final Approval and Accountability- S.U., A.K., C.D.T.

Conflict of Interest: Authors declared no conflict of interest.

Financial Disclosure: This work was supported by the Research Fund of Istanbul University [grant number T-744/13092005].

REFERENCES

1. Paz-Filho G, Mastronardi CA, Licinio J. Leptin treatment: facts and expectations. Metabolism 2015; 64(1): 146-56.

2. Zhang Y, Chua S, Jr. Leptin Function and Regulation. Compr Physiol 2017; 8(1): 351-69.
3. Kokta TA, Dodson MV, Gertler A, Hill RA. Intercellular signaling between adipose tissue and muscle tissue. Domest Anim Endocrinol 2004; 27(4): 303-31.
4. Sletten AC, Peterson LR, Schaffer JE. Manifestations and mechanisms of myocardial lipotoxicity in obesity. J Intern Med 2018; 284(5): 478-91.
5. Minokoshi Y, Toda C, Okamoto S. Regulatory role of leptin in glucose and lipid metabolism in skeletal muscle. Indian J Endocrinol Metab 2012; 16(Suppl 3): S562.
6. Ciriello J. Leptin in nucleus of the solitary tract alters the cardiovascular responses to aortic baroreceptor activation. Peptides 2013; 44: 1-7.
7. Smith PM, Ferguson AV. Cardiovascular actions of leptin in the subfornical organ are abolished by diet-induced obesity. J Neuroendocrinol 2012; 24(3): 504-10.
8. Hassan MJM, Bakar NS, Aziz MA, Basah NK, Singh HJ. Leptin-induced increase in blood pressure and markers of endothelial activation during pregnancy in Sprague Dawley rats is prevented by resibufogenin, a marinobufagenin antagonist. Reprod Biol 2020; 20(2): 184-90.
9. Rahmouni K, Jalali A, Morgan DA, Haynes WG. Lack of dilator effect of leptin in the hindlimb vascular bed of conscious rats. Eur J Pharmacol 2005; 518(2-3): 175-81.
10. Winters B, Mo Z, Brooks-Asplund E, Kim S, Shoukas A, Li D, et al. Reduction of obesity, as induced by leptin, reverses endothelial dysfunction in obese (Lepob) mice. J Appl Physiol 2000; 89(6): 2382-90.
11. Robbins RA, Grisham MB. Nitric oxide. Int J Biochem Cell Biol 1997; 29(6): 857-60.
12. Buchwalow IB, Minin EA, Samoilova VE, Boecker W, Wellner M, Schmitz W, et al. Compartmentalization of NO signaling cascade in skeletal muscles. Biochem Biophys Res Commun 2005; 330(2): 615-21.
13. Grozdanovic Z. NO message from muscle. Microsc Res Tech 2001; 55(3): 148-53.
14. Stamler JS, Meissner G. Physiology of nitric oxide in skeletal muscle. Physiol Rev 2001; 81(1): 209-37.
15. Frühbeck G. Pivotal role of nitric oxide in the control of blood pressure after leptin administration. Diabetes 1999; 48(4): 903-8.
16. Fuhrich DG, Lessey BA, Savaris RF. Comparison of HSCORE assessment of endometrial beta3 integrin subunit expression with digital HSCORE using computerized image analysis (ImageJ). Anal Quant Cytopathol Histpathol 2013; 35(4): 210-6.
17. Arneth W, Herold B. Nitrate nitrite determination in sausages after enzymatic reduction. Fleischwirtschaft 1988; 68(6): 761-4.
18. Goshi E, Zhou G, He Q. Nitric oxide detection methods in vitro and in vivo. Med Gas Res 2019; 9(4): 192.
19. Ren J. Leptin and hyperleptinemia-from friend to foe for cardiovascular function. J Endocrinol 2004; 181(1): 1-10.
20. Castracane VD, Henson MC. Leptin. Endocrine Updates: Springer; 2006.
21. Correia MLG, Morgan DA, Sivitz WI, Mark AL, Haynes WG. Leptin acts in the central nervous system to produce dose-dependent changes in arterial pressure. Hypertension 2001; 37(3): 936-42.
22. Bełtowski J, Jochem J, Wójcicka G, Żwirska-Korczala K. Influence of intravenously administered leptin on nitric oxide production, renal hemodynamics and renal function in the rat. Regul Pept 2004; 120(1-3): 59-67.
23. Mitchell JL, Morgan DA, Correia MLG, Mark AL, Sivitz WI, Haynes WG. Does leptin stimulate nitric oxide to oppose the effects of sympathetic activation? Hypertension 2001; 38(5): 1081-6.
24. Dunbar JC, Hu Y, Lu H. Intracerebroventricular leptin increases lumbar and renal sympathetic nerve activity and blood pressure in normal rats. Diabetes 1997; 46(12): 2040-3.
25. Bełtowski J, Wójcicka G, Jamroz-Wiśniewska A. Role of nitric oxide and endothelium-derived hyperpolarizing factor (EDHF) in the regulation of blood pressure by leptin in lean and obese rats. Life Sci 2006; 79(1): 63-71.
26. Kang K-W, Ok M, Lee S-K. Leptin as a key between obesity and cardiovascular disease. Journal of Obesity & Metabolic Syndrome 2020; 29(4): 248.
27. Jamroz-Wiśniewska A, Gertler A, Solomon G, Wood ME, Whiteman M, Bełtowski J. Leptin-induced endothelium-dependent vasorelaxation of peripheral arteries in lean and obese rats: role of nitric oxide and hydrogen sulfide. PLoS One 2014; 9(1): e86744.
28. Simonds SE, Pryor JT, Cowley MA. Does leptin cause an increase in blood pressure in animals and humans? Current opinion in nephrology and hypertension 2017; 26(1): 20-5.
29. Lembo G, Vecchione C, Fratta L, Marino G, Trimarco V, d'Amati G, et al. Leptin induces direct vasodilation through distinct endothelial mechanisms. Diabetes 2000; 49(2): 293-7.
30. Frühbeck G, Gómez-Ambrosi J. Modulation of the leptin-induced white adipose tissue lipolysis by nitric oxide. Cell Signal 2001; 13(11): 827-33.
31. Mastronardi CA, Yu WH, McCann SM. Resting and circadian release of nitric oxide is controlled by leptin in male rats. Proc Natl Acad Sci 2002; 99(8): 5721-6.
32. Sweeney G. Leptin signalling. Cell Signal 2002; 14(8): 655-63.
33. Brevetti LS, Chang DS, Tang GL, Sarkar R, Messina LM. Overexpression of endothelial nitric oxide synthase increases skeletal muscle blood flow and oxygenation in severe rat hind limb ischemia. J Vasc Surg 2003; 38(4): 820-6.
34. Punkt K, Naupert A, Wellner M, Asmussen G, Schmidt C, Buchwalow IB. Nitric oxide synthase II in rat skeletal muscles. Histochem Cell Biol 2002; 118(5): 371-9.
35. Punkt K, Zaitsev S, Park JK, Wellner M, Buchwalow IB. Nitric oxide synthase isoforms I, III and protein kinase-Cθ in skeletal muscle fibres of normal and streptozotocin-induced diabetic rats with and without Ginkgo biloba extract treatment. Histochem J 2001; 33(4): 213-9.
36. Vranić TS, Bobinac D, Jurisić-Erzen D, Muhvić D, Sandri M, Jerković R. Expression of neuronal nitric oxide synthase in fast rat skeletal muscle. Coll Antropol 2002; 26: 183-8.
37. Yan Z, Chen Z. Modulation of nitric oxide synthase isoenzymes in reperfused skeletal muscle. Chin J Traumatol 2000; 3(2): 76-80.
38. Carbó N, Ribas V, Busquets S, Alvarez B, López-Soriano FJ, Argilés JM. Short-term effects of leptin on skeletal muscle protein metabolism in the rat. J Nutr Biochem 2000; 11(9): 431-5.

ISTANBUL UNIVERSITY PRESS

RESEARCH ARTICLE

Eur J Biol 2022; 81(1): 26-30

Benzyl Alcohol Increases Diffusion Limit of Nuclear Membrane in *Saccharomyces cerevisiae* Cells

Bengu Erguden[1]

[1]Gebze Technical University, Department of Bioengineering, Kocaeli, Turkiye

ORCID IDs of the authors: B.E. 0000-0002-8621-3474

Please cite this article as: Erguden B. Benzyl Alcohol Increases Diffusion Limit of Nuclear Membrane in *Saccharomyces cerevisiae* Cells. Eur J Biol 2022; 81(1): 26-30. DOI: 10.26650/EurJBiol.2022.1058174

ABSTRACT

Objective: Fungi are invasive species responsible for infections in many people around the world and which severely affect the immune system. The opportunistic pathogenic species, such as Candida species and *Aspergillus fumigatus*, can cause death in people with weakened immune systems. Natural medicines derived from plants are often used to treat fungal diseases. In connection with our efforts to unearth possible cellular targets of antimicrobial agents, in this study, we aimed to determine the functional consequences of benzyl alcohol treatment on the nuclear membrane.

Materials and Methods: We analysed the nuclear membrane distortions caused by benzyl alcohol in *Saccharomyces cerevisiae* cells using Nup49-GFP reporter strain. We also studied cellular distributions of various fluorescently tagged nuclear-cytoplasmic shuttling proteins to determine any functional disturbances in nuclear pore complexes upon benzyl alcohol treatment. Localization of 51.5 kDa protein LexA-NES-GFP and 61.8 kDa protein Pho4(Δ157-164)-GFP to the nucleus in yeast cells was key for evaluating the effect upon diffusion limit of pores.

Results: By analyzing the distribution of fluorescently tagged nuclear localization signal or nuclear export signals bearing reporter proteins between the nucleus and cytoplasm, we have shown that the nuclear membrane becomes leaky upon benzyl alcohol treatment.

Conclusion: The diffusion limit across the nuclear membrane in yeast cells is increased upon benzyl alcohol treatment. We believe that these findings not only increase our understanding of the mode of action of benzyl alcohol bearing antifungal agents, but also help widening their use.

Keywords: Benzyl alcohol, yeast, antifungal activity, nuclear membrane, nuclear pore complex

INTRODUCTION

Fungal infections are among the common causes of death, especially in individuals with a weakened immune system. These infections may be neglected, but they can be dangerous, contrary to common belief. There are few and limited treatments available to treat invasive fungal infections. A number of natural medicines derived from plants are used to treat the fungal diseases. Discovery of antifungal agents is much slower than antibacterial agents. Because fungi are eukaryotes, fungal-damaging substances can also often damage the host, so the antifungal agent developments are usually slow.

As a hallmark of eukaryotic cells, the genetic material is separated in a compartment surrounded by the nuclear membrane. The nuclear membrane separates DNA and translation, allowing transcription to be regulated in various ways. It also allows for differential processing and selective export of the synthesized mRNA.

The nuclear envelope consists of double lipid bilayers, the outer and inner nuclear membranes (1). The outer layer is continuous with the endoplasmic reticulum, which hosts ribosomes that carry out translation. Nuclear pore complexes (NPCs), which are large multiprotein structures that pass through the double bilayer structure, allow and regulate the passage of substances into

Corresponding Author: Bengu Erguden E-mail: b.sezen@gtu.edu.tr

Submitted: 15.01.2022 • **Revision Requested:** 29.03.2022 • **Last Revision Received:** 01.04.2022 • **Accepted:** 05.04.2022 • **Published Online:** 29.04.2022

and out of the nucleus. They are the gatekeepers mediating the exchange of essential compounds between the nucleoplasm and the cytoplasm (2-6). Ions and small metabolites can freely diffuse through NPCs. However, for the transport of large molecules with MW >40 kDa, active transport is necessary (7-12). This active transport into and out of the nucleus is governed by a large family of transport receptors called karyopherins in yeast (7, 13, 14). Although NPC structures differ between species such as size and variation in individual proteins, their overall structures are conserved from yeasts to mammals (3, 5, 10).

Benzyl alcohol is a known membrane fluidizer, and recently we demonstrated that it is active against yeast cells (15). In this study, we set out to determine its cellular target in *Saccharomyces cerevisiae* cells. For this purpose, we studied possible defects in the yeast nuclear membrane structure and function upon treatment with benzyl alcohol. We believe that these studies not only increase our understanding of the mechanism of action of alcoholic antifungal agents, but also open up new possibilities for the therapy of fungal infections.

MATERIALS AND METHODS

Strains and Growth Conditions

YPH499 (*MATa ura3-52 lys2-801_amber ade2-101_ochre trp1-Δ63 his3-Δ200 leu2-Δ1*) (16) was used as the *Saccharomyces cerevisiae* strain in this study. pRS315-GFP-*NUP49,* pADH1-*NLS-2*GFP-TRP1, pADH1-*NES*-YFP-TRP1, pRS315-*npl3*[S411A]-GFP, pRS314-*LexA-NES*-GFP and pRS314-*Pho4*(Δ157-164)-GFP reporters were a generous gift from Prof. Karsten Weis, and used according to the previously described protocols (20). Yeast cells were grown until the early exponential phase in yeast extract peptone glucose medium (YPD) at 25°C while shaking. Then cells were treated with 1% benzyl alcohol for 15 minutes and analysed using fluorescence microscopy as explained below. 1% benzyl alcohol corresponds to 10xMIC value.

Minimum Inhibitory Concentration (MIC) Measurement

The minimum inhibitory concentration (MIC) measurement was performed in a similar procedure in our previous study (15). *S. cerevisiae* cells were cultured overnight at 25°C in YPD broth and were suspended in YPD to give a final density of 1×10^6 CFU/mL. Benzyl alcohol dissolved in dimethyl sulfoxide (DMSO) was prepared with the serial dilution method and put in a 24-well microtiter plate. After that, *S. cerevisiae* cells were added to each well. Suspension of yeast cells in the medium without benzyl alcohol or any other additives as well as yeast cells in the medium with only DMSO were tested as controls. 24-well microtiter plates were incubated at 25 °C. The MIC was determined after 48 h. Viability of yeasts was deduced based on turbidity.

Extracellular pH Measurement

S. cerevisiae cells were incubated at 25°C in 20 mL of YPD until the exponential growth phase, harvested and washed twice with sterilized dH_2O. The pellet was then resuspended in sterilized dH_2O. About 50 mg wet weight of yeast cells were used for each experiment. 2% glucose was added and incubated for 20 min while shaking. At this point, 5 and 10 mM benzyl alcohol was added, and extracellular pH was recorded using an HI 98127 water proof pH meter (HANNA, USA).

Fluorescence Microscopy

Still images of non-fixed cells were captured at room temperature with a wide-field epifluorescence microscope (Axio Imager.A1; Carl Zeiss MicroImaging) equipped with 100x NA 1.45 oil immersion objective (Plan-Fluar; Carl Zeiss MicroImaging), a Cascade:1K camera (Photometrics) and Metamorph software (Universal Imaging). At least 1000 cells were analysed for each data set. Representative figures for each analysis were combined together after adjusting contrast and brightness.

MTT Mitochondrial Functionality Assay

Yeast cells were incubated at 25°C in 20 mL of YPD until the exponential growth phase, harvested and then resuspended in sterilized dH_2O, 1:1 (w/v). 0.05 M glucose, 0.4 mg/ml MTT, 1% benzyl alcohol was added to yeast cells and incubated at 30 °C for 15 min. The MTT reduction was determined using a spectrophotometer at 570 nm.

RESULTS

Nuclear Membrane is Distorted in Benzyl Alcohol Treated Yeast Cells

We have previously reported the antifungal activities of various terpenoids as well as benzyl alcohol (with MIC value of 5-10 mM) against yeast *Saccharomyces cerevisiae* (15). Recently, we extended our studies on the mode of action of benzyl alcohol. We have shown that the fungal cell wall is impaired by the action of benzyl alcohol and the cell membrane integrity is disrupted (17). The damage on the cell membrane triggers H^+ ion intake, revealed by an increase in extracellular pH (Figure 1).

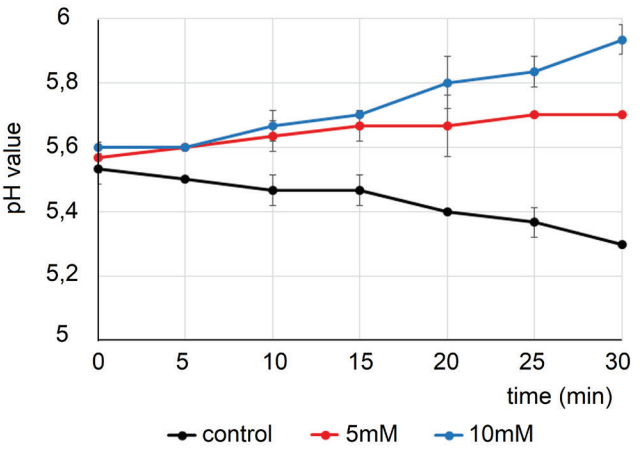

Figure 1. Effect of benzyl alcohol on the extracellular pH of yeast cells. Control corresponds to the measurements without any benzyl alcohol addition. The data represent the average of at least three independent experiments.

Furthermore, visualization of the nuclear membrane by means of labelling the nuclear pore complex protein Nup49 with GFP, revealed that yeast cells had highly deformed nuclear membranes (Figure 2) (17, 18). The effect of benzyl alcohol on the nuclear envelope can be seen as early as 15 min after its application.

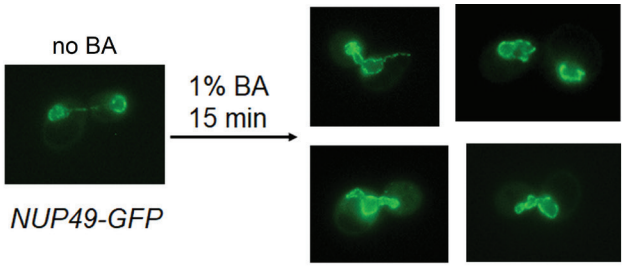

Figure 2. Nuclear envelope phenotype of benzyl alcohol treated cells. a) Yeast cells were transformed with pRS315-GFP-*NUP49* and analyzed using fluorescence microscopy. b) Yeast cells, transformed with pRS315-GFP-*NUP49,* were treated with 1% benzyl alcohol for 15 min and analyzed with fluorescence microscopy. Bars, 5 µm.

Transport through the Nuclear Membrane is Compromised in Benzyl Alcohol Treated Yeast Cells

Later, we tested whether the benzyl alcohol treated cells mislocalize the NLS-GFP (SV40 nuclear localization signal reporter protein fused with GFP) and NES-YFP (SV40 nuclear export signal reporter protein fused with YFP) reporters (Figure 3). In wild type cells with functional NPC, we expect the NLS reporter protein to be found entirely in the nucleus and the NES reporter protein to be excluded from the nucleus and found in the cytoplasm (20). As shown in Figure 2, both reporters were mislocalized upon benzyl alcohol treatment in some yeast cells, pointing to a defect in NPC function (21, 22). Note that mislocalization of these reporters takes somewhat longer than (ca. 1h) the morphological changes observed at the nuclear envelope (15 min).

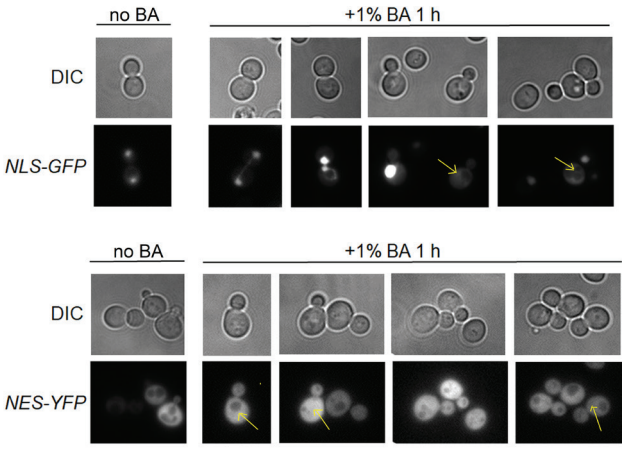

Figure 3. NLS-GFP and NES-YFP reporters were mislocalized in benzyl alcohol treated cells. Wild type cells were transformed with pADH1-NLS-2GFP-TRP1 and pADH1-NES-YFP-TRP1 reporters, and analyzed before and after benzyl alcohol treatment, with fluorescence microscopy. Arrows show the nucleus. Bars, 5 µm.

In order to demonstrate defects in NPC function in benzyl alcohol treated cells in a more quantitative manner, we used a reporter based on the yeast shuttling protein Npl3 described by Madrid et al. (20, 23). Npl3 is mainly nuclear and Npl3-GFP localizes correctly to the nucleus both in the absence and presence of benzyl alcohol (data not shown). However, while Npl3[S411A]-GFP reporter localizes mainly to the nucleus before treatment, benzyl alcohol treated cells show a marked increase in cells with cytoplasmic Npl3[S411A]-GFP reporter signal (Figure 4).

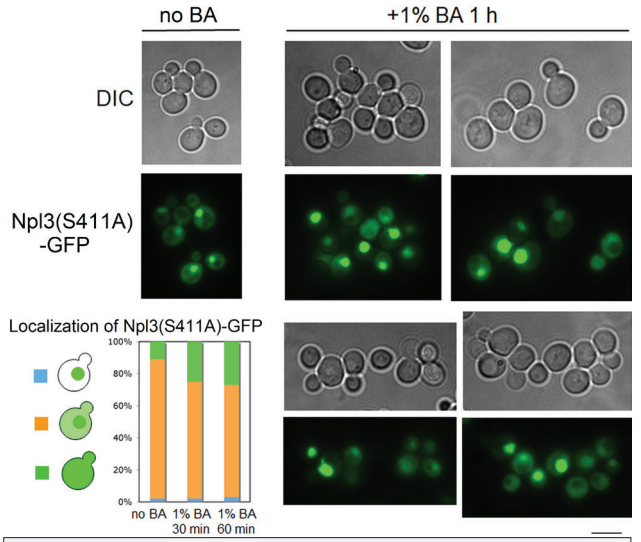

Figure 4. Npl3[S411A]-GFP reporter was mislocalized in benzyl alcohol treated cells. Wild type cells were transformed with pRS315-*npl3*[S411A]-GFP reporter, and analyzed before and after benzyl alcohol treatment, with fluorescence microscopy. Bars, 5 µm.

Diffusion Limit through the Nuclear Membrane is Increased in Benzyl Alcohol Treated Yeast Cells

In order to test the diffusion limit through NPCs, we used reporter proteins LexA-NES-GFP and Pho4(Δ157-164)-GFP. Both 51.5 kDa protein LexA-NES-GFP and 61.8 kDa protein Pho4(Δ157-

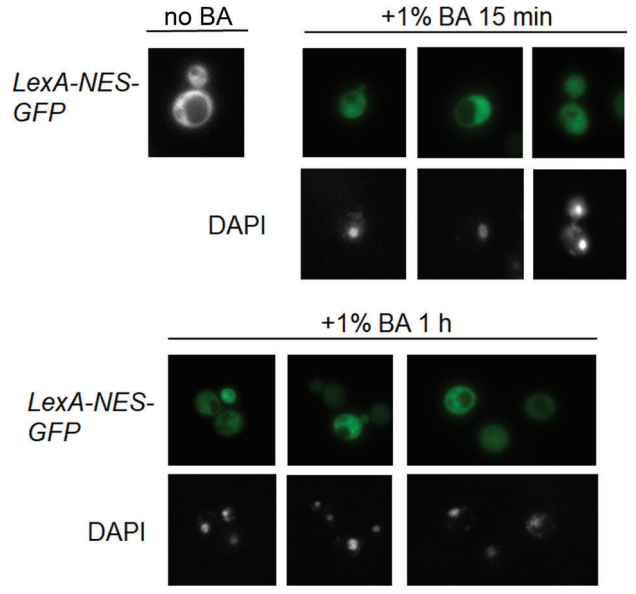

Figure 5. Diffusion limit is increased in wild type cells upon benzyl alcohol treatment. Wild type cells were transformed with pRS314-*LexA-NES*-GFP reporter, and analyzed before and after benzyl alcohol treatment, with fluorescence microscopy. Bars, 5 µm.

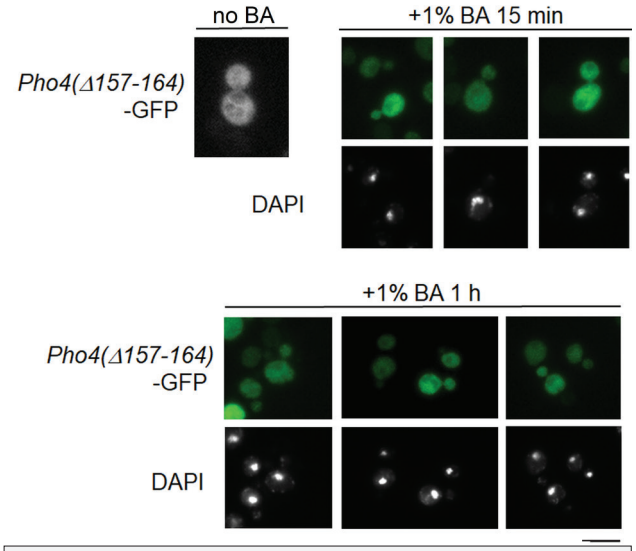

Figure 6. Diffusion limit is increased in wild type cells upon benzyl alcohol treatment. Wild type cells were transformed with pRS314-*Pho4*(Δ157-164)-GFP reporter, and analyzed before and after benzyl alcohol treatment, with fluorescence microscopy. Bars, 5 µm.

164)-GFP were excluded from the nucleus in yeast cells, but mislocalized inside the nucleus upon benzyl alcohol treatment (Figures 5 and 6). Thus, the diffusion limit increased upon benzyl alcohol application.

Mitochondria is Intact in Benzyl Alcohol Treated Yeast Cells

Disruption of the cell membrane as well as defects in nuclear pore function raises the question whether other organelles are also affected. In order to test this question, we performed an MTT mitochondrial functionality assay (24). This analysis revealed that benzyl alcohol treated cells have functional mitochondria, with no detectable loss in MTT activity (Figure 7).

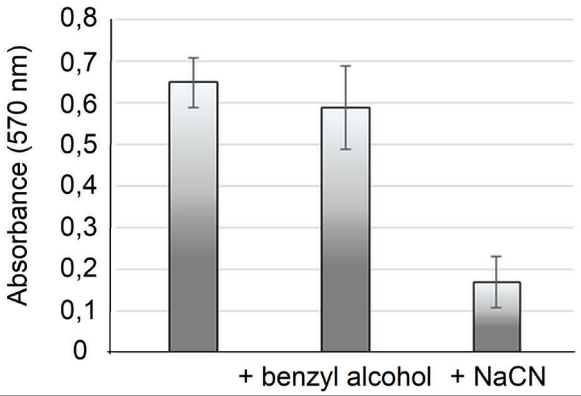

Figure 7. Mitochondria remains intact upon benzyl alcohol treatment. Optical density was measured at 570 nm using a spectrophotometer in order to determine the MTT reduction by yeast cells.

DISCUSSION

We have previously shown that benzyl alcohol acts as an antifungal agent against *S. cerevisiae* cells (15), and causes defects in the cell wall and cell membrane structures (17). In this study, we wanted to unearth any effects of benzyl alcohol on the organelle membranes of yeast cells. Visualization of the nuclear membrane by means of labelling the Nup49 protein a protein in the structure of nuclear pore complex that is embedded to the nuclear membrane with GFP, revealed that benzyl alcohol treated yeast cells had highly deformed nuclear membranes (Figure 2).

We have recently reported that certain stress conditions, including benzyl alcohol treatment, cause a reduction in Pom34 protein levels in up to 20% of untreated cells after incubation with the compound (19). Benzyl alcohol treatment mislocalized *POM34* mRNA towards the cytoplasmic fraction, reducing the translation of Pom34 protein. Since Pom34 is a protein in the structure of nuclear pore complexes (NPC), the gateways between the nucleus and cytoplasm, we asked whether benzyl alcohol treatment might affect NPC function. We first tested whether the benzyl alcohol treated cells mislocalized the NLS-GFP (SV40 nuclear localization signal reporter protein fused with GFP) and NES-YFP (SV40 nuclear export signal reporter protein fused with YFP) reporters (Figure 3). In wild type cells with functional NPC, we expect NLS reporter protein to be found entirely in the nucleus and the NES reporter protein to be excluded from the nucleus and found in the cytoplasm (20). However, both reporters were mislocalized upon benzyl alcohol treatment in some yeast cells, pointing to a defect in NPC function (21, 22).

In order to demonstrate defects in NPC function in benzyl alcohol treated cells in a more quantitative manner, we used a reporter based on the yeast shuttling protein Npl3 described by Madrid et al. (20, 23). Npl3 is a nuclear protein, and accordingly Npl3-GFP is exclusively nuclear in yeast cells, spectroscopically no detectable cytoplasmic signal in wild-type cells is observed. The Npl3[S411A]-GFP mutant, which cannot undergo Ser411 phosphorylation, in contrast, partially mislocalizes to the cytoplasm (20, 23). Although Npl3[S411A]-GFP reporter localized mainly to the nucleus in wild type cells before treatment, benzyl alcohol treatment caused an increase in cells with cytoplasmic Npl3[S411A]-GFP (Figure 4). This result is similar to the mislocalization of the same reporter in NPC defective cells (20).

Ions and small metabolites can freely diffuse through NPCs; however, molecules possessing a mass >40 kDa cannot diffuse and have to be actively transported (25). In order to test the diffusion limit through NPCs, we used reporter proteins LexA-NES-GFP and Pho4(Δ157-164)-GFP, having an MW greater than the diffusion limit in yeast cells (26, 27). Both 51.5 kDa protein LexA-NES-GFP and 61.8 kDa protein Pho4(Δ157-164)-GFP were excluded from the nucleus in wild type cells, but mislocalized inside the nucleus upon benzyl alcohol treatment (Figure 5 and 6). This result is also similar to the mislocalization of the same

reporters in NPC defective cells (20). Thus, we conclude from these observations that wild type cells treated with benzyl alcohol show various defects in nuclear pore function and diffusion limit is increased in these cells.

CONCLUSION

Considering our previous results showing that benzyl alcohol inhibits translation of Pom34 protein, a transmembrane protein in the structure of NPC, we propose that this antifungal agent targets NPC structures. Benzyl alcohol causes structural and functional defects in the NPC, which perhaps contributes to the antifungal activity of this molecule (28). These observations extend our understanding of the mechanism of action of membrane fluidizer alcohols against yeast cells.

Acknowledgement: pRS315-GFP-*NUP49,* pADH1-*NLS-2*GFP-TRP1, pADH1-*NES*-YFP-TRP1, pRS315-*npl3*[S411A]-GFP, pRS314-*LexA-NES*-GFP and pRS314-*Pho4*(Δ157-164)-GFP reporters are generous gift of Prof. Karsten Weis (20).

Peer Review: Externally peer-reviewed.

Conflict of Interest: Author declared no conflict of interest.

Financial Disclosure: Author declared no financial support.

REFERENCES

1. D'Angelo MA and Hetzer MW. The role of the nuclear envelope in cellular organization. Cell Mol Life Sci 2006; 63: 316-32.
2. Cook A, Bono F, Jinek M, Conti E. Structural biology of nucleocytoplasmic transport. Annu Rev Biochem 2007; 76: 647-71.
3. Yang Q, Rout MP, Akey CW. Three-dimensional architecture of the isolated yeast nuclear pore complex: functional and evolutionary implications. Mol Cell 1998; 1: 223-34.
4. Rout MP, Aitchison JD, Suprapto A, Hjertaas K, Zhao Y, Chait BT. The yeast nuclear pore complex: composition, architecture, and transport mechanism. J Cell Biol 2000; 148: 635-51.
5. Cronshaw JM, Krutchinsky AN, Zhang W, Chait BT, Matunis MJ. Proteomic analysis of the mammalian nuclear pore complex. J Cell Biol 2002; 158: 915-27.
6. Reichelt R, Holzenburg A, Buhle EL Jr, Jarnik M, Engel A, Aebi U. Correlation between structure and mass distribution of the nuclear pore complex and of distinct pore complex components. J Cell Biol 1990; 110: 883-94.
7. Mosammaparast N, Pemberton LF. Karyopherins: from nuclear-transport mediators to nuclear-function regulators. Trends Cell Biol 2004; 14: 547-56.
8. Mansfeld J, Guttinger S, Hawryluk-Gara LA, Pante N, Mall M, Galy V, Haselmann U, Muhlhausser P, Wozniak RW, Mattaj IW, Kutay U, Antonin W. The conserved transmembrane nucleoporin NDC1 is required for nuclear pore complex assembly in vertebrate cells. Mol Cell 2006; 22: 93-103.
9. Stavru F, Hulsmann BB, Spang A, Hartmann E, Cordes VC, Görlich D. NDC1: a crucial membrane-integral nucleoporin of metazoan nuclear pore complexes. J Cell Biol 2006; 173: 509-19.
10. Schwartz TU. Modularity within the architecture of the nuclear pore complex. Curr Opin Struct Biol 2005; 15: 221-6.
11. Alber F, Dokudovskaya S, Veenhoff LM, Zhang W, Kipper J, Devos D, Suprapto A, Karni-Schmidt O, Williams R, Chait BT, Rout MP, Sali A. Determining the architectures of macromolecular assemblies. Nature 2007; 450: 683-94.
12. Alber F, Dokudovskaya S, Veenhoff LM, Zhang W, Kipper J, Devos D, Suprapto A, Karni-Schmidt O, Williams R, Chait BT, Sali A, Rout MP. The molecular architecture of the nuclear pore complex. Nature 2007; 450: 695-701.
13. Suntharalingam M, Wente SR. Peering through the pore: nuclear pore complex structure, assembly, and function. Dev Cell 2003; 4: 775-89.
14. Macara IG. Transport into and out of the nucleus. Microbiol Mol Biol Rev 2001; 65: 570-94.
15. Konuk HB, Ergüden B. Phenolic –OH group is crucial for the antifungal activity of terpenoids via disruption of cell membrane integrity. Folia Microbiololica 2020; 65: 775-83.
16. Sikorski RS, Hieter P. A system of shuttle vectors and yeast host strains designed for efficient manipulation of DNA in *Saccharomyces cerevisiae*. Genetics 1989; 122: 9-27.
17. Ergüden B. *Saccharomyces cerevisiae* Outer and Inner Membranes are Compromised upon Benzyl Alcohol Treatment. Int J Memb Sci Tech 2021; 8: 35-9.
18. Thaller DJ, Lusk CP. Fantastic nuclear envelope herniations and where to find them. Biochem Soc Trans 2018; 46: 877-89.
19. Sezen B. Reduction of Saccharomyces cerevisiae Pom34 protein level by SESA network is related to membrane lipid composition. FEMS Yeast Research 2015; 15: fov089.
20. Madrid AS, Mancuso J, Cande WZ, Weis K. The role of the integral membrane nucleoporins Ndc1p and Pom152p in nuclear pore complex assembly and function. J Cell Biol 2006; 173: 361-71.
21. Meseroll RA, Cohen-Fix O. The Malleable Nature of the Budding Yeast Nuclear Envelope: Flares, Fusion, and Fenestrations. J Cell Physiol 2016; 231: 2353-60.
22. Brown JT, Alexandra JH, Christopher MW, Belanger KD. Characterization of nuclear pore complex targeting domains in Pom152 in Saccharomyces cerevisiae. Biology Open 2021; 10: bio057661.
23. Gilbert W, Siebel CW, Guthrie C. Phosphorylation by Sky1p promotes Npl3p shuttling and mRNA dissociation. RNA 2001; 7: 302-13.
24. Sanchez NS, Königsberg M. Using Yeast to Easily Determine Mitochondrial Functionality with 1-(4,5-Dimethylthiazol-2-yl)-3,5-diphenyltetrazolium Bromide (MTT) Assay. Biochem Mol Biol Edu 2006; 34: 209-12.
25. Frey S, Richter RP, Gorlich D. FG-rich repeats of nuclear pore proteins form a three-dimensional meshwork with hydrogel-like properties. Science 2006; 314: 815-17.
26. Ribbeck K, Gorlich D. The permeability barrier of nuclear pore complexes appears to operate via hydrophobic exclusion. EMBO J 2002; 21: 2664-71.
27. Ribbeck K, Gorlich D. Kinetic analysis of translocation through nuclear pore complexes. EMBO J 2001; 20: 1320–30.
28. Takahashi U, Hamada K, Iwahashi H. Critical Damage to the Cellular Organelles of *Saccharomyces cerevisiae* Under Sublethal Conditions Upon High Pressure Carbon Dioxide Treatment. High Pressure Res 2019; 39: 273-9.

ISTANBUL UNIVERSITY PRESS

RESEARCH ARTICLE

Eur J Biol 2022; 81(1): 31-40

Dodder (*Cuscuta* sp.) Extract Ameliorates Liver Fibrosis in Bile Duct-Ligated Rats

Omercan Albayrak[1], Dilek Ozbeyli[2], Ali Sen[3], Ozge Cevik[4], Omer Erdogan[4], Feriha Ercan[5], Fatma Kanpalta[5], Seren Ede[1], Goksel Sener[6]

[1]Marmara University, School of Pharmacy, Department of Pharmacology, Istanbul, Turkiye
[2]Marmara University, Vocational School of Health Services, Department of Medical Pathology Techniques, Istanbul, Turkiye
[3]Marmara University, School of Pharmacy, Department of Pharmacognosy, Istanbul, Turkiye
[4]Adnan Menderes University, School of Medicine, Department of Biochemistry, Aydın, Turkiye
[5]Marmara University, School of Medicine, Department of Histology & Embriology, Istanbul, Turkiye
[6]Fenerbahçe University, Vocational School of Health Sciences, Istanbul, Turkiye

ORCID IDs of the authors: O.A. 0000-0002-6254-3786; D.O. 0000-0002-0250-9535; A.S. 0000-0002-2144-5741; O.C. 0000-0002-9325-3757; O.E. 0000-0002-8327-7077; F.E. 0000-0003-2339-5669; F.K. 0000-0001-9832-6938; S.E. 0000-0002-3195-4064; G.S. 0000-0001-7444-6193

Please cite this article as: Albayrak O, Ozbeyli D, Sen A, Cevik O, Erdogan O, Ercan F, Kanpalta F, Ede S, Sener G. Dodder (*Cuscuta* sp.) Extract Ameliorates Liver Fibrosis in Bile Duct-Ligated Rats. Eur J Biol 2022; 81(1): 31-40. DOI: 10.26650/EurJBiol.2022.1097509

ABSTRACT

Objective: The aim is to examine the possible protective effect of *Cuscuta* sp. extract against liver damage induced by biliary obstruction in rats.

Materials and Methods: To induce biliary obstruction, the bile duct ligation (BDL) method was used. Sprague Dawley rats were allocated to 4 groups: Control (C), *Cuscuta* (CUS), bile duct ligation (BDL), and bile duct ligation + *Cuscuta* (BDL+CUS). Control and BDL rats were given physiological saline (SF), while CUS and BDL+CUS groups were administered 250 mg/kg of *Cuscuta* extract by oral gavage. At the end of 28th day, the rats were decapitated, serum and tissue samples were collected, and aspartate aminotransferase (AST), alanine transaminase (ALT), and direct and total bilirubin (DB and TB) levels were determined in blood samples. In liver tissues, transforming growth factor-β (TGF-β), 8-hydroxyguanosine (8-OHdG), hydroxyproline, and sodium–potassium ATPase (Na^+/K^+-ATPase) levels were determined.

Results: Serum samples of rats with cholestasis had high ALT, AST, DB, and TB levels, while TGF-β, 8-OHdG, and hydroxyproline concentrations were found to be significantly high in tissues. Hepatic Na^+/K^+-ATPase levels were decreased through biliary obstruction. Biochemical parameters were drastically reversed by *Cuscuta* care; also, this was supported histologically.

Conclusion: Results showed that *Cuscuta* extract, through its antioxidant and anti-inflammatory properties, provided protection against oxidative injury by biliary obstruction. Also, these results confirm the traditional use of *Cuscuta* sp. as hepatoprotective.

Keywords: Liver damage, Dodder, Inflammation, Oxidative injury

INTRODUCTION

Chronic liver disease is the most important disease globally (1). Fibrosis is a wound healing state that develop as a result of a response to liver injury due to different etiological causes, and are also a dynamic process involving unbalanced synthesis and destruction of extracellular matrix (2-5). Chronic liver disease is caused by liver fibrosis, hepatocyte damage, aggregation of platelet and inflammatory cells, stimulation of Kupffer cells, and finally discharge of cytokines and growth factors, respectively (6,7).

Obstruction in the bile duct preventing the flow of bile acids causes the accumulation of toxic bile components, which leads to the formation of reactive oxygen/nitro-

Corresponding Author: Goksel Sener E-mail: goksel.sener@fbu.edu.tr
Submitted: 02.04.2022 • **Revision Requested:** 27.04.2022 • **Last Revision Received:** 02.05.2022 • **Accepted:** 02.05.2022 • **Published Online:** 17.05.2022

gen derivatives in the liver (8). *In vitro* studies have shown that these harmful derivatives are formed when hepatocytes are treated with bile acids (9). Mitochondria is the main organelle from which reactive products are produced. Free radicals originating from hepatic mitochondria cause damage to liver cells and constitute the underlying causes of fibrosis (10). Considering that these factors have a momentous impact on pathogenesis, suppression of radical formation can prevent inflammation and fibrosis. Although various models have been used to develop liver fibrosis, bile duct ligation has the most clinical relevance.

The adverse effects of drugs lead researchers to look for new drugs. Recently, drugs obtained from natural sources have been studied and new alternatives with anti-fibrotic properties continue to be sought. It has been reported that some herbs are used in traditional medicine for liver-biliary disorders. Along these lines, one of these herbs is the *Cuscuta* species, used by the public in the treatment of jaundice in Turkey (11). The species of *Cuscuta*, known by the name Bostanbozan, are perennial, chlorophyll-free, and parasitic plants (12,13). *Cuscuta* species are used in the treatment of jaundice in Denizli, Diyarbakır, and Manisa, as well as in the province of Mardin. It has also been reported that these species have traditional uses as diuretics, carminative, laxatives, and cholagogues (14-16). They contain several secondary metabolites, such as flavonoids (quercetin, hiperoside etc.), alkaloids (cuscutamine, lupanine etc.), steroids and sterols (campesterol, sesamin etc.), triterpenes (Lupeol, ursolic acid etc.), carotenoids (Lutein, lycopene), fatty acids (oleic acid, linolenic acid etc.), and other compounds (cuscutalin, amarvelin etc.) (17).

In this experiment, the aim is to examine the possible therapeutic effect of *Cuscuta* sp. extract against liver damage induced by bile duct ligation (BDL).

MATERIALS AND METHODS

Animals and Ethics

In this experiment, all procedures related to experimental animals were performed according to NIH guidelines (NIH Publications No. 8023, revised 1978). Male Sprague Dawley rats (weighing 200-300 g) were kept at a constant temperature of 22±2°C, 50%±5 humidity, and a light/dark cycle (12/12h). Animals were allowed ad libitum feeding. This experiment was guided with the approval of Animal Experiments Ethics Committee (03/03/2021, Decision No: 40.2021mar).

Groups and Experimental Protocol

Rats were arbitrarily separated into 4 groups. The Control (C) and *Cuscuta* (CUS) groups were sham operated; Bile duct ligation (BDL) and BDL+CUS groups were subjected to the BDL procedure. C, CUS, and BDL+CUS groups consisted of 12 animals, while the BDL group had 14 animals. Animals in the C and BDL groups were given 1 ml of saline orally, while methanol extract dissolved in distilled saline was given by oral gavage at a dose of 250 mg/kg for 28 days in the CUS and BDL+CUS groups. The *Cuscuta* dose was based on previous studies (15). Animals were weighed twice, at the beginning and end of the study (before decapitation). On the 28th day, the rats were decapitated, and blood and liver tissue samples were collected. Aspartate aminotransferase (AST), alanine transaminase (ALT), and direct and total bilirubin (DB and TB) levels were analyzed in blood samples, while transforming growth factor-β (TGF-β), 8-hydroxyguanosine (8-OHdG), and hydroxyproline and sodium-potassium ATPase (Na^+/K^+-ATPase) were determined in liver tissues. In addition, histological examinations of liver tissue sections were performed under a light microscope.

Bile Duct Ligation for Induction of Cholestasis

Under anesthesia (100 mg/kg ketamine and 0.75 mg/kg chlorpromazine; i.p.), midline laparotomy was performed. By exposing the common bile duct, a double ligation was applied. One of the ligatures was underneath the hepatic duct junctions and the other one was over the access to the pancreatic ducts. Bile ducts were cut between ligations (18).

Formulation of Plant Extract

The aerial parts of *Cuscuta* sp. were purchased from an herbalist in the Midyat district of Mardin in May 2018. The plant was identified by Asst. Prof. Dr. Ahmet Doğan; a sample of the plant was made into a suitable herbarium sample and recorded by assigning it an herbarium number in the Herbarium of the Faculty of Pharmacy of Marmara University (MARE No: 22668).

After the dried aerial parts of the plant were dusted, approximately 757.06 g was weighed and macerated with 1600 mL of methanol for 10 days. The solvent of methanol extract obtained after filtration was vaporized using a rotary evaporator (Rotavapor® R-300). The methanol extract obtained with a yield of 10.83% was kept at +4°C until analysis.

Biochemical Analysis

Determination of the DPPH (2,2-diphenyl-1-picrylhydrazyl) Radical Scavenging Activity of Plant Extract

The antioxidant level of *Cuscuta* sp. extract was designated in compliance with the method of Zou et al (19). The percent free radical scavenging of the extract was computed according to the formula below.

DPPH radical scavenging percent (%): (A control - A sample / A control) x 100

The Control contained $DPPH^{\cdot}$ solution and dimethyl sulfoxide (DMSO). The sample contained $DPPH^{\cdot}$ solution and sample solutions. The inhibition concentrations (IC_{50}) of extract that scavenge 50% of DPPH radical were calculated by plotting an inhibition graph based on concentrations of extract using the GraphPad Prism 6 program. Ascorbic acid was used as a reference standard. Measurements were repeated three times.

ABTS (2,2'-azinobis-(3-ethylbenzothiazoline-6-sulfonic acid)) Radical Cation Scavenging Activity Determination of Plant Extract

To produce $ABTS^{\cdot+}$ used in the determination of total antioxidant capacity of the extract, 7 mM ABTS was mixed with 2.45 mM $K_2S_2O_8$ and left in the dark for 16 hours at room tempera-

ture (23°C) to complete reaction. The $ABTS^{\cdot+}$ solution was diluted with an ethanol (96%) solvent of analytical purity to give an optical density value of 0.700±0.050 at 734 nm. From the stock solution prepared in DMSO at a concentration of 5 mg/mL from extract, solutions at different concentrations were prepared by making 1:8 dilutions. 10 µl of each prepared solution was moved to the assay plates. 190 µl $ABTS^{\cdot+}$ solution was added. Immediately, the solution was placed at room temperature and kept there for thirty minutes; optical density was measured at 734 nm. Trolox was used as a standard and outcomes were expressed as IC_{50} value. The test was repeated three times (19).

Anti-inflammatory Activity of Plant Extract

For the detection of anti-inflammatory activity, Phosrithong et al.'s method was used with revisions (20, 21). 20 µL of ethanol, 20 µL of BBS (Borate buffered saline), and 25 µL of type 5 soy lipoxygenase solution (20.000 U/mL) were added to 10 µL of extract/standard at different concentrations. After the mixture was incubated for five minutes at 25°C, 100 µL of 0.6 mM linoleic acid solution was added, the mixture was thoroughly mixed, and the absorbance change at 234 nm was noted for six minutes. Indomethacin was used as a reference standard. Percent (%) inhibition was computed with the formula below.

% Inhibition: [(A control – A sample) / A control] × 100

A dose-response curve was charted to conclude IC_{50} values. IC_{50} is outlined as enough concentration to obtain 50% of the maximum anti-inflammatory activity. All analyses were executed in triplicate.

Determination of Total Phenol Compound of Plant Extract

The total phenol content (TFB) of the extract was determined using the Folin-Ciocalteau solution, according to Gao's method (21.22). Solutions of various concentrations were prepared by dilutions made from stock solution prepared in DMSO at a concentration of 5 mg/mL from extract. 10 µL of these solutions were taken into microplates, and then 20 µL of Folin-Ciocalteau solution, 200 µL of ultrapure water, and 100 µL of 15% Na_2SO_4 were added, respectively. Solutions were read against a blank formed by replacing only extract with the same amount of DMSO, with the other components remaining constant at 765 nm optical density. For standard curve plot, optical density corresponding to each concentration was measured using gallic acid (500-0.977 µg/mL). The amount of TFB of extract was calculated from this graph and scores were determined as mg GAE (Gallic Acid Equivalent)/g plant extract. The measurements of extract were repeated three times and the measurements of standard curve were repeated five times.

Examination of the Serum Samples

Liver enzymes (ALT and AST), TB, and DB were surveyed to assess BDL-induced liver injury using commercial kits (BT Laboratory, Shanghai) (23).

Examinations of Tissue Samples

Na^+/K^+-ATPase activity in tissue were determined using a commercial kit (AFG, EK720668) in accordance with the manufacturer's procedure. After tissue samples were homogenized in a phosphate-buffered saline (PBS) with pH 7.4, they were centrifugated at 3000 rpm at +4°C and used aiming at upper phase. The measuring range of the kit is 50-1000 pg/mL, and the sensitivity is 20 pg/mL. Standard solution in the range of 900 pg/mL-75 pg/mL was set by diluting stock standard in the kit (1350 pg/mL).

TGF-β levels in the tissue were determined using a commercial kit (AFG, EK720060) in accordance with the manufacturer's procedure. After tissue samples were homogenized in PBS (pH 7.4), they were centrifugated at 3000 rpm at +4°C and used aiming at upper phase. The measuring range of the kit is 10 ng/mL-200 ng/mL, and the sensitivity is 3 ng/mL. The standard solution in the range of 150 ng/mL-12.5 ng/mL was set by diluting stock standard (225 ng/mL) in the kit.

Hydroxyproline levels in the tissue were determined in accordance with manufacturer's procedure using a commercial kit (AFG, EK720734). After tissue samples were homogenized in PBS (pH 7.4), they were centrifugated at 3000 rpm at +4°C and used aiming at upper phase. The measuring range of the kit is 1 ug/mL-20 ug/mL and the sensitivity is 0.5 ug/mL. Standard solution in the range of 15 ug/mL-1.25 ug/mL was set by diluting the stock standard (22.5 ug/mL) in the kit.

8-OHdG concentration in the tissue was determined using a commercial kit (AFG, EK720424) in accordance with the manufacturer's procedure. After the tissue samples were homogenized in PBS (pH 7.4), they were centrifugated at 3000 rpm at +4°C and used aiming at upper phase. The measuring range of the kit is 0.625 ng/mL-20 ng/mL, and the sensitivity is 0.078 ng/mL. The standard solution in the range of 15 ng/mL-1.25 ng/mL was set by diluting stock standard (22.5 ng/mL) in the kit.

Light Microscopic Preparation

For light microscopic examinations, samples from the liver were fixed with 10% formaldehyde, diluted alcohol was then cleared using toluene, and they were embedded in paraffin and cut in 5 µm in thickness. Liver tissue slices were stained with hematoxylin for histopathological evaluation, then inspected and shot with the digital camera (Olympus, Tokyo, Japan) of a photomicroscope (Olympus BX51, Tokyo, Japan).

Statistical Analysis

GraphPad Prism 5.0 (GraphPad Software, San Diego; CA; USA) was utilized to perform statistical evaluations. All numeric records were expressed as means±SEM. ANOVA was used to compare groups of data followed by Tukey's multiple comparison tests. Values of $p<0.05$ were considered significant.

RESULTS

Anti-Inflammatory, Antioxidant Activities and Total Compound Contents of Dodder (*Cuscuta sp.*) Methanol Extract

Low IC_{50} value obtained in the measurements (the concentration that removes 50% of the radical or halts the enzyme's activity by 50%) implies high activity. When Table 1 is examined,

CUS extract showed remarkable antioxidant activity against the DPPH radical, with an IC_{50} value of 125.5 µg/ml. The obtained extract also exhibited significant antioxidant activity against the ABTS radical, with an IC_{50} value of 138.9 µg/ml. It was observed to have noteworthy anti-inflammatory activity against the 5-LOX (5-Lipoxygenase) enzyme, with an IC_{50} value of 103.5 µg/ml. The total amount of phenolic compounds of dodder plant extract was found to be 38.58 mg/g, equivalent to gallic acid in g extract (Table 1).

Cirrhosis Caused by Liver Damage and Related Urine Color Changes

As shown in Figure 1, changes occurred due to cirrhosis developing as a result of liver damage.

Evaluation of Body Weight

When body weights were compared at the beginning (t1) and the end of study (t2), there were significant differences between the groups' own t1 and t2 values (***p<0.001), and it was seen that there was weight gain in all groups. However, there was no statistically significant difference between both t1 and t2 of groups (Table 2). It is expected that there will be weight gain due to acid that develops in the body, so we measured the weights to observe this, but there was an increase in other groups because there was normal physiological weight gain in the process.

Findings of Serum Samples

The serum AST, ALT, DB, and TB levels of the BDL group were found to be significantly greater (p<0.001) compared to the C

Table 1. Antioxidant/anti-inflammatory activity and total phenolic compound content of methanol extract-obtained *Cuscuta* sp.

Experiments	*Cuscuta* sp. methanol extract	Ascorbic Acid	Trolox	Indomethacin
DPPH radical scavenging activity (IC_{50} µg/mL)	125.5±0.14[b]	17.6 ±0.37[a]		
ABTS radical scavenging activity (IC_{50} µg/mL)	138.9±0.28[b]		13.00 ±0.21[a]	
Anti-lipoxygenase activity (IC_{50} µg/mL)	103.5±4.72[b]			22.39±0.26[a]
Total phenolic compound content (mg GAE/g extract)*	38.58±0.39[b]			

* Total phenolic content was expressed as gallic acid equivalent (GAE).
Each value in the table is given as mean±SD (n=3). Different letter superscripts in the same line indicate a statistically significant difference (p<0.05).

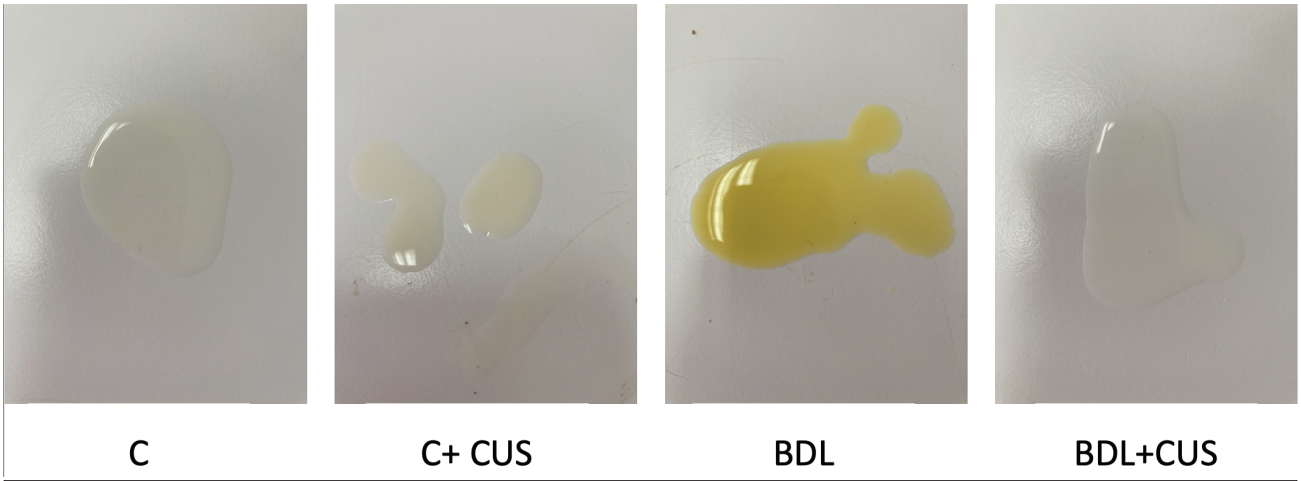

Figure 1. The urine colors of treated groups at the end of the experiment. C: Control, BDL: Bile duct ligation, CUS: *Cuscuta* sp.

Table 2. The body weights (g) of groups measured at the beginning of experiment (t1) and at the end of experiment (t2).

Body Weights	C	CUS	BDL	BDL+CUS
t1	224±7.1	220±4.6	235±4.7	239±5.1
t2	279±6.3 ***	266±10.1***	280±10.5***	285±5.8***

C: Control, BDL: Bile duct ligation, CUS: *Cuscuta* sp. ***p<0.001: comparisons between t1 and t2

Table 3. Serum AST, ALT, DB, TB values.

Serum	C	CUS	BDL	BDL+CUS
AST (U/L)	137.8±5.5	133.0±7.6	435.5±28.8***	304.3±4.318$^{***,+++}$
ALT (U/L)	55.3±4.8	52.3±4.4	142.0±5.6***	91.3±5.8$^{***,+++}$
DB (mg/dl)	0.4±0.2	0.4±0.2	4.8±0.3***	3.5±0.3$^{***,++}$
TB (mg/dl)	0.4±0.04	0.5±0.04	5.5±0.4***	4.2±0.32$^{***,++}$

Serum AST (Aspartate Aminotranferase), ALT (Alenine transaminase), DB (Direct Bilirubin), TB (Total Bilirubin) values. *p<0.05, **p<0.01, ***p<0.001 compared to control group, +p<0.05, ++p<0.01, +++p<0.001 compared to BDL group.

group, while the AST, ALT, DB, and TB levels of the treated group were significantly lower than the BDL group (p<0.01-0.001). However, the serum AST, ALT, DB, and TB levels of CUS-treated BDL group were found to be significantly (p<0.001) greater than those of the C group (Table 3).

Biochemical Findings of Liver

TGF-β, 8-OHdG, and hydroxyproline levels were significantly greater (p<0.05, p<0.01) in the liver tissues of the BDL (saline-treated) group compared to the C group, while these levels were significantly lower in the CUS-treated BDLgroup compared to the BDL group (p<0.05-0.01) (Figures 2a, 2b, 2d).

Na^+/K^+-ATPase activity were found to be significantly lower (p<0.05) in the liver tissues of the BDL group compared to the C group. On the other hand, Na^+/K^+-ATPase activity tended to increase, but this was not significant (Figure 2c).

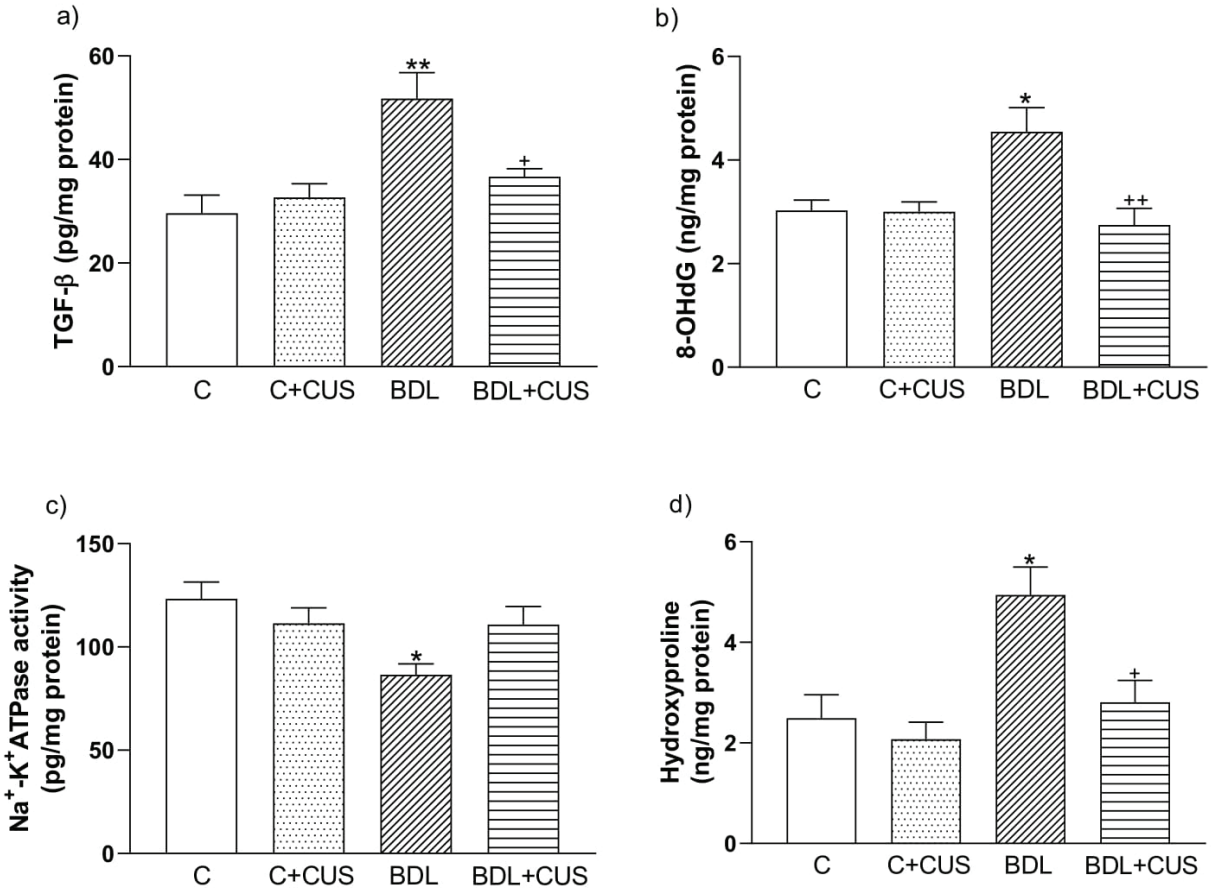

Figure 2. TGF-β, 8-OHdG, Na^+/K^+-ATPase, and Hydroxyproline results of liver tissue. TGF-β: Transforming growth factor, 8-OHdG: 8-hydroxy-2'-deoxyguanosine, Na^+/K^+-ATPase: Sodium-Potassium adenosine triphosphatase, C: Control group, BDL: Bile duct ligation, CUS: *Cuscuta* sp. ANOVA for statistical analysis. *p<0.05, **p<0.01; Compared to control group, +p<0.05, ++p<0.01; Compared to BDL group.

Histological Evaluations

The light microscopic assessment of the control group (Figure 3a) showed a steady form of liver parenchyma through intact hepatic cells, sinusoids, and the portal tract. A steady form of liver parenchyma through intact hepatic cells and portal tract, mild sinusoidal obstruction was detected in the C+CUS group (Figure 3b). Disorganized hepatic cords, severe increase of degenerated hepatocytes, bile duct proliferation, and inflammatory cell infiltration were seen in the saline-treated BDL group (Figure. 3c). Moderate decrease in the count of deteriorated hepatocytes, disorder of hepatic cords, drop in bile duct proliferation (ductular reaction), and inflammatory cell infiltration were observed in the BDL+CUS group (Figure. 3d).

DISCUSSION

The liver is a vital organ that plays an important role in the configuration and secretion of bile, as well as the excretion of toxic substances through bile ducts (24). Liver fibrosis is a reversible wound-healing response characterized by extracellular matrix (ECM) deposition and develops after liver injury (25). Delay in treatment can lead to life-threatening hyperammonemia, hepatic encephalopathy, and cirrhosis with high morbidity and mortality rates (26-28).

Different experimental studies have been conducted to slow or reverse the development of liver fibrosis; however, no effective treatment has been found for clinical use (29). There are many studies using anti-fibrogenic agents. However, in traditional

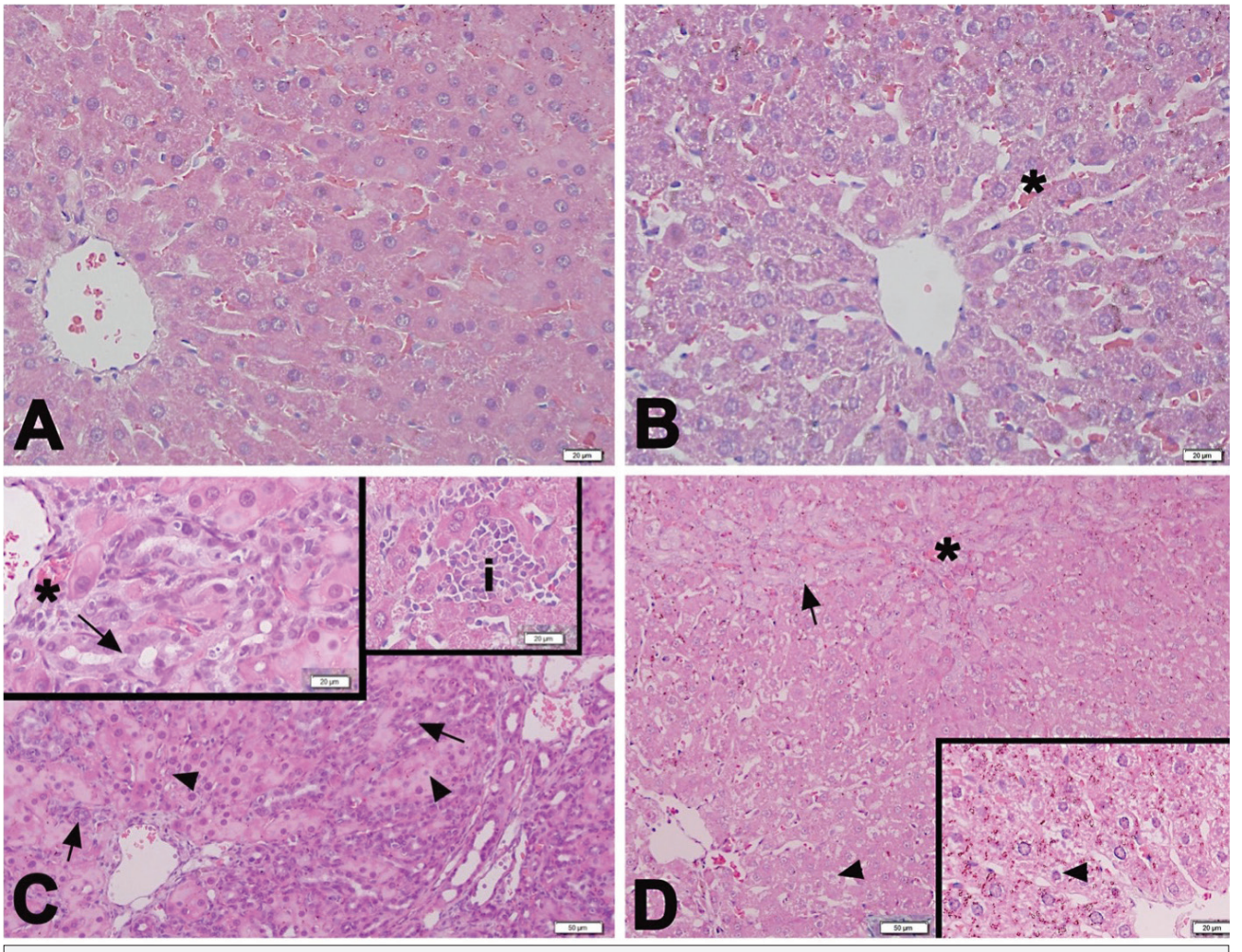

Figure 3. The representative light micrographs of liver samples in experimental groups. Normal liver parenchyma with hepatocytes, sinusoids, and portal tracts are seen in the C group (A). Normal liver parenchyma with hepatocytes, portal tracts, and mild sinusoidal congestion (*) are seen in the C+ CUS group (B). Disorganization of hepatic cords, sinusoidal congestion (*), increased number of degenerated hepatocytes (arrowhead), bile duct proliferation within portal tract and within acini (arrow), and inflammatory cell infiltration (i) in parenchyma (C) are seen in the BDL group. Mild sinusoidal congestion (*), disorganization of hepatic cords, decrease in degenerated hepatocytes (arrow), and decreased bile duct proliferation (arrow) are seen in the BDL+CUS group (D). Hematoxylin and eosin staining, Scale bars: A, B and insets in C and D: 20 µm, C and D: 50 µm. BDL: Bile duct ligation, CUS: *Cuscuta* sp., C: Control

medicine, natural products that are less toxic and cause side effects are also used instead of chemical anti-fibrotic drugs. These natural products are still in the experimental stage and are counted as therapeutic interventions (30).

Today, medicinal plants and products are being researched in the treatment of various diseases (31). In a detailed literature review, different types of *Cuscuta* (dodder) were found to have various biological effects, such as antitumor, antimicrobial, hepatoprotective, anticonvulsant, immunostimulant, antioxidant, α-glucosidase inhibitor, anti-inflammatory, diuretic, analgesic, antipyretic, neuroprotective, antiulcer, antispasmodic, antihypertensive, cardiotonic, and muscle relaxant (12,13,32). Similarly, in Turkey, it has been reported that some plants in traditional medicine are used in liver-biliary disorders. These species are used by the public in the treatment of jaundice (12,32). One of these species is the *Cuscuta* species (i-iv). Accordingly, in this study, liver damage was developed by creating cholestasis with BDL, and the treatment effect was investigated with an extract prepared from a traditional plant, the *Cuscuta* species.

Blood ALT and AST concentrations are well known as sensitive indicators of potential tissue damage, mainly liver toxicity (33). ALT and AST are known as aminotransferases involved in gluconeogenesis (34,35). AST is found in both cytosol and mitochondria of hepatocytes, while ALT is found only in cytosol (36-39). These enzymes leak into blood as a result of damage to hepatocytes (40). Metabolic factors such as drug use, toxins, viruses, ischemia, and autoimmune liver damage may affect liver parenchyma and increase AST and ALT values (23). Bilirubin, which is an important indicator of liver disease due to cholestasis, is the final breakdown product of hemoglobin and is directly or indirectly present in serum (41). According to scientific studies, direct bilirubin concentration increases due to BDL and in addition to the ALT, AST and bilirubin concentration in the BDL group were found to be remarkably greater than in the control group (42-44). In this study, the ALT, AST, and bilirubin concentration in the BDL group were found out to be greater than in the control group. According to another study on the curative effects of dodder plant extract on hepatotoxicity in rats, it was detected that ALT, AST, and bilirubin concentration were lower in groups treated with dodder plant extract compared to the model group (32). In agreement with these previous studies, in our study, the ALT, AST, and bilirubin levels of the BDL group were greater than those of the control group. Furthermore, in the BDL+CUS group, treatment with dodder plant extract, although not as high as control levels, significantly decreased these levels.

Sodium/potassium adenosine triphosphatase enzyme takes part in the structure and physiology of liver cells by providing sodium and potassium balance in all cell membranes (45). According to studies, it has been observed that BDL reduces the levels of Na^+/K^+-ATPase in liver tissue (46,47). In our study, the Na^+/K^+-ATPase activity of liver tissues of the BDL group were found to be lower than those of the control group. Shin et al demonstrated that decrease in renal Na^+/K^+-ATPase enzyme synthesis in a rat model of ischemia/reperfusion, while it was reversed by using dodder plant extract (48). In our study, the obtained hepatic Na^+/K^+-ATPase activities consistent with the literature were found to be significantly lower in cholestatic rats compared to the control group, while Na^+/K^+-ATPase activities were observed to be increased in the group treated with dodder plant extract.

Although free radicals are formed continuously in organisms during metabolic activities, they are scavenged by the endogenous antioxidant system. However, they have very harmful effects when they occur at a level that exceeds antioxidant system capacity. They are known to damage macromolecules, especially lipids, proteins, and nucleic acids, and are responsible for the pathogenesis of many diseases (49). The most widely used oxidative DNA damage indicator is 8-OHdG (50,51). Studies in cholestatic rats, and increased levels of 8-OHdG in liver tissue demonstrate oxidative damage in tissue due to BDL (52-54). In parallel with this information, in our study, the 8-OHdG levels of the liver tissues of the BDL group were found to be greater than those of the control group. According to a study, Ganoderma lucidum, an antioxidant and medicinal plant, ameliorates high 8-OHdG enzyme levels in liver tissues due to BDL (55). Likewise, in our study, a significant increase was seen in the concentration of 8-OHdG in the BDL group, and a significant reduction was observed in the level of the relevant damage marker in the rats treated with an antioxidant-effective dodder plant extract.

TGF-β is a regulator that has an essential role in the physiological and pathological changes of the liver, as well as in liver damage, inflammation, and fibrosis (56). Various studies have reported that TGF-β concentration is greater in the BDL group than in the control group and contributes to development of fibrosis as a proinflammatory cytokine (57-59). In parallel with this information, TGF-β concentration of liver tissues in the BDL group was found to be greater than in the control group in our study. According to a study examining its possible therapeutic effects on liver damage, the application of dodder plant extract was reported to be a hepatoprotective agent and alleviated an increase in TGF-β levels (21). In our study, it was found that TGF-β level was significantly greater in the BDL group compared to the control group. In addition, a diminution in TGF-β concentration was seen in the group treated with dodder plant extract.

Active hepatic stellate cells transforming into myofibroblasts increase hydroxyproline levels, which then cause collagen protein production and fibrosis (60,61). Consequently, hydroxyproline is used as a marker to assess the level of liver damage. According to studies on liver fibrosis in the BDL rat model, the hydroxyproline level of the BDL group was found to be significantly greater than in the control group (62-64). Similarly, in our study, the hydroxyproline concentration of liver tissues of the rats with BDL was found to be significantly greater, while a significant drop was observed in the hydroxyproline concentration of CUS treatment. It is thought that, as shown in our *in vitro* analyses, the anti-inflammatory properties of the CUS extract contribute to this effect, and thus it protects the tissue by

suppressing both TGF-β and collagen formation. Our histological findings also supported biochemical results, as significant damage was seen in the liver tissue of the BDL group and this damage was healed in liver tissue of the BDL group treated with dodder plant extract (32).

In vitro studies in the current study also supported *in vivo* studies. It has been found that the *Cuscuta* species have good antioxidant and anti-inflammatory activity as well as total phenolic content. A review study also confirmed that the plant has a DPPH radical scavenging effect and a good total phenol content (13). It has been reported that *Cuscuta* species are rich in phenolic compounds, especially flavonoids (17). Phenolic compounds have a hepatoprotective effect (65). Therefore, this group of compounds may be responsible for the hepatoprotective effect of the *Cuscuta* sp.

As a result, through the findings of the study, it has been seen that dodder plant extract has a possible protective effect against liver fibrosis caused by the BDL technique. This protective effect of dodder plant extract can be explained by its antioxidant, anti-inflammatory, and hepatoprotective effects. For this reason, it is thought that dodder plant extract may have a promising role in the treatment of liver fibrosis, with the support of clinical studies in future.

CONCLUSION

Our biochemical and histological results, obtained with the investigated parameters, suggest that *Cuscuta* sp. methanol extract may be beneficial for liver diseases and needs more detailed studies in the future. Accordingly, we concluded that it may have a role in the treatment of liver fibrosis if supported by future clinical studies. Also, these results confirm the traditional use of *Cuscuta* sp. in the treatment of liver disease.

Acknowledgements: The authors would like to thank Asst. Prof. Dr. Ahmet Doğan for his help in identification of the plant material.

Peer Review: Externally peer-reviewed.

Author Contributions: Conception/Design of Study- G.S., O.A.; Data Acquisition- A.S., O.C., O.E., F.E., F.K.; Data Analysis/Interpretation- G.S., A.S., O.C., F.E.; Drafting Manuscript- O.A., S.E.; Critical Revision of Manuscript- G.S.; Final Approval and Accountability- G.S., O.A., F.E., F.K., O.C., O.E., D.O., S.E., A.S.

Conflict of Interest: Authors declared no conflict of interest.

Financial Disclosure: Authors declared no financial support.

REFERENCES

1. Lai M, Afdhal NH. Liver Fibrosis Determination. Gastroenterol Clin North Am 2019; 48(2): 281-9.
2. Han JM, Kim HG, Choi MK, Lee JS, Park HJ, Wang JH, et al. Aqueous extract of *Artemisia iwayomogi* Kitamura attenuates cholestatic liver fibrosis in a rat model of bile duct ligation. Food Chem Toxicol 2012; 50(10): 3505-13.
3. Noll C, Raaf L, Planque C, Benard L, Secardin L, Petit E, et al. Protection and reversal of hepatic fibrosis by red wine polyphenols in hyperhomocysteinemic mice. J Nutr Biochem 2011; 22(9): 856-64.
4. Tsukada S, Parsons CJ, Rippe RA. Mechanisms of liver fibrosis. Clin Chim Acta 2006; 364(1-2): 33-60.
5. Xu R, Zhang Z, Wang FS. Liver fibrosis: Mechanisms of immune-mediated liver injury. Cell Mol Immunol 2012; 9(4): 296-301.
6. Dulundu E, Ozel Y, Topaloglu U, Toklu H, Ercan F, Gedik N, et al. Grape seed extract reduces oxidative stress and fibrosis in experimental biliary obstruction. J Gastroenterol Hepatol 2007; 22(6): 885-92.
7. Işeri SÖ, Şener G, Saglam B, Ercan F, Gedik N, Yeğen BÇ. Ghrelin alleviates biliary obstruction-induced chronic hepatic injury in rats. Regul Pept 2008; 146(1-3): 73-9.
8. Li S, Tan HY, Wang N, Zhang ZJ, Lao L, Wong CW, et al. The role of oxidative stress and antioxidants in liver diseases. Int J Mol Sci 2015; 16(11): 26087-124.
9. Sokol RJ, Devereaux M, Khandwala R, O'Brien K. Evidence for involvement of oxygen free radicals in bile acid toxicity to isolated rat hepatocytes. Hepatology 1993; 17(5): 869-81.
10. Videla LA, Rodrigo R, Orellana M, Fernandez V, Tapia G, Quiñones L, et al. Oxidative stress-related parameters in the liver of non-alcoholic fatty liver disease patients. Clin Sci 2004; 106(3): 261-8.
11. Koca-Caliskan U, Yilmaz I, Taslidere A, Yalcin FN, Aka C, Sekeroglu N. *Cuscuta* arvensis Beyr "dodder": *In Vivo* Hepatoprotective Effects Against Acetaminophen-Induced Hepatotoxicity in Rats. J Med Food 2018; 21(6): 625-31.
12. Erecevit Sönmez P, Kirbağ S, İnci Ş. Antifungal and antibacterial effect of dodder (*Cuscuta campestris*) used for hepatitis treatment of mothers and newborn infants in Province Mardin in Turkey. Yuz Yil Univ J Agric Sci 2019; 29(4): 722-30.
13. Noureen S, Noreen S, Ghumman SA, Batool F, Bukhari SNA. The genus *Cuscuta* (Convolvolaceae): An updated review on indigenous uses, phytochemistry, and pharmacology. Iran J Basic Med Sci 2019; 22(11): 1225-52.
14. Şekeroğlu N, Koca U, Meraler SA. Geleneksel Bir Halk İlacı:Iksut. YYÜ TAR BİL DERG 2012; 22(1): 56-61.
15. Bulut G, Biçer M, Tuzlaci E. The folk medicinal plants of Yüksekova (Hakkari-Turkey). J Pharm Istanbul Univ 2016; 46(2): 115-24.
16. Sari AO, Üniversitesi E, Fakültesi F, Bölümü B, Anabilim B. Ege ve Güney Marmara Bölgelerinde Halk İlacı Olarak Kullanılan Bitkiler. Anadolu 2010; 20(2): 1-21.
17. Ahmad A, Tandon S, Xuan TD, Nooreen Z. A Review on Phytoconstituents and Biological activities of *Cuscuta* species. Biomed Pharmacother 2017; 92: 772-95.
18. Criado M, Flores O, Ortíz MC, Hidalgo F, Rodríguez-López AM, Eleno N, et al. Elevated glomerular and blood mononuclear lymphocyte nitric oxide production in rats with chronic bile duct ligation: Role of inducible nitric oxide synthase activation. Hepatology 1997; 26(2): 268-76.
19. Zou Y, Chang SKC, Gu Y, Qian SY. Antioxidant activity and phenolic compositions of lentil (*Lens culinaris* var. *morton*) extract and its fractions. J Agric Food Chem 2011; 59(6): 2268-76.
20. Phosrithong N, Nuchtavorn N. Antioxidant and anti-inflammatory activites of *Clerodendrum* leaf extracts collected in Thailand. Eur J Integr Med 2016; 8(3): 281-5.
21. Şen A, Yıldırım A, Bitis L, Doğan A. Antioxidant and anti-inflammatory activity of capitula, leaf and stem extracts of *Tanacetum cilicicum* (Boiss.) Grierson. Int J Second Metab 2019; 6(2): 211-22.
22. Gao X, Ohlander M, Jeppsson N, Björk L, Trajkovski V. Changes in antioxidant effects and their relationship to phytonutrients in fruits of sea buckthorn (*Hippophae rhamnoides* L.) during maturation. J Agric Food Chem 2000; 48(5): 1485-90.

23. Limdi JK, Hyde GM. Evaluation of abnormal liver function tests. Postgrad Med J 2003; 79: 307-12.
24. Strazzabosco M. Transport systems in cholangiocytes: Their role in bile formation and cholestasis. Yale J Biol Med 1997; 70(4): 427-34.
25. Hernandez-Gea V, Friedman SL. Pathogenesis of liver fibrosis. Annu Rev Pathol Mech Dis 2011; 6: 425-56.
26. Goldbecker A, Buchert R, Berding G, Bokemeyer M, Lichtinghagen R, Wilke F, et al. Blood-brain barrier permeability for ammonia in patients with different grades of liver fibrosis is not different from healthy controls. J Cereb Blood Flow Metab 2010; 30(7): 1384-93.
27. Khan A, Ayub M, Khan WM. Hyperammonemia Is Associated with Increasing Severity of Both Liver Cirrhosis and Hepatic Encephalopathy. Int J Hepatol 2016; 2016.
28. Zhangdi HJ, Su SB, Wang F, Liang ZY, Yan YD, Qin SY, et al. Crosstalk network among multiple inflammatory mediators in liver fibrosis. World J Gastroenterol 2019; 25(33): 4835-49.
29. Tahan G, Akin H, Aydogan F, Ramadan SS, Yapicier O, Tarcin O, et al. Melatonin ameliorates liver fibrosis induced by bile-duct ligation in rats. Can J Surg 2010; 53(5): 313-8.
30. Gedik N, Kabasakal L, Şehirli Ö, Ercan F, Sirvanci S, Keyer-Uysal M, et al. Long-term administration of aqueous garlic extract (AGE) alleviates liver fibrosis and oxidative damage induced by biliary obstruction in rats. Life Sci 2005; 76(22): 2593-606.
31. Singh U, Singh S, Kochhar A. Therapeutic potential of antidiabetic nutraceuticals. Phytopharmacology 2012; 2(1): 144-69.
32. Koca-Caliskan U, Yilmaz I, Taslidere A, Yalcin FN, Aka C, Sekeroglu N. *Cuscuta arvensis* Beyr "dodder": *In Vivo* Hepatoprotective Effects Against Acetaminophen-Induced Hepatotoxicity in Rats. J Med Food 2018; 21(6): 625-31.
33. Ramaiah SK. A toxicologist guide to the diagnostic interpretation of hepatic biochemical parameters. Food Chem Toxicol 2007; 45(9): 1551-7.
34. Kobayashi A, Yokoyama H, Kataoka J, Ishida T, Kuno H, Sugai S, et al. Effects of spaced feeding on gene expression of hepatic transaminase and gluconeogenic enzymes in rats. J Toxicol Sci 2011; 36(3): 325-37.
35. Qian K, Zhong S, Xie K, Yu D, Yang R, Gong D-W. Hepatic ALT isoenzymes are elevated in gluconeogenic conditions including diabetes and suppressed by insulin at the protein level Kun. Diabetes Metab Res Rev 2015; 31(6): 562-71.
36. Horio Y, Tanaka T, Taketoshi M, Uno T, Wada H. Rat cytosolic aspartate aminotransferase: Regulation of its mRNA and contribution to gluconeogenesis. J Biochem 1988; 103(5): 805-8.
37. Jadaho SB, Yang RZ, Lin Q, Hu H, Anania FA, Shuldiner AR, et al. Murine Alanine Aminotransferase: cDNA Cloning, Functional Expression, and Differential Gene Regulation in Mouse Fatty Liver. Hepatology 2004; 39(5): 1297-302.
38. Tomkiewicz C, Muzeau F, Edgar AD, Barouki R, Aggerbeck M. Opposite regulation of the rat and human cytosolic aspartate aminotransferase genes by fibrates. Biochem Pharmacol 2004; 67(2): 213-25.
39. Yang RZ, Park S, Reagan WJ, Goldstein R, Zhong S, Lawton M, et al. Alanine aminotransferase isoenzymes: Molecular cloning and quantitative analysis of tissue expression in rats and serum elevation in liver toxicity. Hepatology 2009; 49(2): 598-607.
40. Raval N, Kalyane D, Maheshwari R, Tekade RK. Surface Modifications of Biomaterials and Their Implication on Biocompatibility. Biomaterials and Bionanotechnology. Elsevier Inc 2019; 639-674.
41. Jo J, Yun JE, Lee H, Kimm H, Jee SH. Total, direct, and indirect serum bilirubin concentrations and metabolic syndrome among the Korean population. Endocrine 2011; 39(2): 182-9.
42. Lim JH, Kim TW, Song IB, Park SJ, Kim MS, Cho ES, et al. Protective effect of the roots extract of *Platycodon grandiflorum* on bile duct ligation-induced hepatic fibrosis in rats. Hum Exp Toxicol 2013; 32(11): 1197-205.
43. Şener G, Kabasakal L, Şehirli Ö, Ercan F, Gedik N. 2-Mercaptoethane sulfonate (MESNA) protects against biliary obstruction-induced oxidative damage in rats. Hepatol Res 2006; 35(2): 140-6.
44. Yada K, Ishibashi H, Mori H, Morine Y, Zhu C, Feng R, et al. The Kampo medicine "daikenchuto (TU-100)" prevents bacterial translocation and hepatic fibrosis in a rat model of biliary atresia. Surg 2016; 159(6): 1600-11.
45. Atalay S, Soylu B, Aykaç A, Oğünç AV, Çetinel Ş, Ozkan N, et al. Protective effects of St. John's wort in the hepatic ischemia/ reperfusion injury in rats. Turkish J Surg 2018; 34(3): 198-204.
46. Muriel P. Interferon-α preserves erythrocyte and hepatocyte atpase activities from liver damage induced by prolonged bile duct ligation in the rat. J Appl Toxicol 1995; 15(6): 449-53.
47. Muriel P, Suarez OR, Gonzalez P, Zuñiga L. Protective effect of S-adenosyl-l-methionine on liver damage induced by biliary obstruction in rats: a histological, ultrastructural and biochemical approach. J Hepatol 1994; 21(1): 95-102.
48. Shin S, Lee YJ, Kim EJ, Lee AS, Kang DG, Lee HS. Effect of *Cuscuta chinensis* on renal function in ischemia/reperfusion- induced acute renal failure rats. Am J Chin Med 2011; 39(5): 889-902.
49. Forman HJ, Zhang H. Targeting oxidative stress in disease: promise and limitations of antioxidant therapy. Nat Rev Drug Discov 2021; 20(9): 689-709.
50. Atmaca E, Aksoy A. Oksidatif DNA Hasarı ve Kromatografik Yöntemlerle Tespit Edilmesi. YYU Veteriner Fakultesi Dergisi 2009; 20(2): 79-83.
51. Li P, Ramm GA, Macdonald GA. Value of the 8-oxodG/dG ratio in chronic liver inflammation of patients with hepatocellular carcinoma. Redox Biol 2016; 8: 259-70.
52. Huang YT, Hsu YC, Chen CJ, Liu CT, Wei YH. Oxidative-stress-related changes in the livers of bile-duct-ligated rats. J Biomed Sci 2003; 10(2): 170-8.
53. Maeda K, Koda M, Matono T, Sugihara T, Yamamoto S, Ueki M, et al. Preventive effects of ME3738 on hepatic fibrosis induced by bile duct ligation in rats. Hepatol Res 2008; 38(7): 727-35.
54. Matono T, Koda M, Tokunaga S, Sugihara T, Ueki M, Murawaki Y. The effects of the selective mineralocorticoid receptor antagonist eplerenone on hepatic fibrosis induced by bile duct ligation in rat. Int J Mol Med 2010; 25: 875-82.
55. Aydin S, Aytac E, Uzun H, Altug T, Mansur B, Saygili S, et al. Effects of *Ganoderma lucidum* on obstructive jaundice-induced oxidative stress. Asian J Surg 2010; 33(4): 173-80.
56. Fabregat I, Moreno-Càceres J, Sánchez A, Dooley S, Dewidar B, Giannelli G, et al. TGF-β signalling and liver disease. FEBS J 2016; 283: 2219-32.
57. Asakawa T, Yagi M, Tanaka Y, Asagiri K, Kobayashi H, Egami H, et al. The herbal medicine Inchinko-to reduces hepatic fibrosis in cholestatic rats. Pediatr Surg Int 2012; 28(4): 379-84.
58. Du JX, Sun MY, Du GL, Li FH, Liu C, Mu YP, et al. Ingredients of Huangqi decoction slow biliary fibrosis progression by inhibiting the activation of the transforming growth factor-beta signaling pathway. BMC Complement Altern Med 2012; 12: 1-11.
59. Sharawy MH, Abdel-Rahman N, Megahed N, El-Awady MS. Paclitaxel alleviates liver fibrosis induced by bile duct ligation in rats: Role of TGF-β1, IL-10 and c-Myc. Life Sci 2018; 211: 245-51.
60. Mu M, Zuo S, Wu RM, Deng KS, Lu S, Zhu JJ, et al. Ferulic acid attenuates liver fibrosis and hepatic stellate cell activation via inhibition of TGF-β/Smad signaling pathway. Drug Des Devel Ther 2018; 12: 4107-15.

61. Wang R, Song F, Li S, Wu B, Gu Y, Yuan Y. Salvianolic acid A attenuates CCl4-induced liver fibrosis by regulating the PI3K/AKT/mTOR, Bcl-2/Bax and caspase-3/cleaved caspase-3 signaling pathways. Drug Des Devel Ther 2019; 13: 1889-900.
62. Lee TY, Chang HH, Chen JH, Hsueh ML, Kuo JJ. Herb medicine Yin-Chen-Hao-Tang ameliorates hepatic fibrosis in bile duct ligation rats. J Ethnopharmacol 2007; 109(2): 318-24.
63. Nan J-X, Park E-J, Kim Y-C, Ko G, Sohn DH. *Scutellaria baicalensis* inhibits liver fibrosis induced by bile duct ligation or carbon tetrachloride in rats. J Pharm Pharmacol 2010; 54(4): 555-63.
64. Tian X, Zhao C, Guo J, Xie S, Yin F, Huo X, et al. Carvedilol Attenuates the Progression of Hepatic Fibrosis Induced by Bile Duct Ligation. Biomed Res Int 2017; 2017.
65. Yadav RK, Nandy BC, Maity S, Sarkar S, Saha S. Phytochemistry, pharmacology, toxicology, and clinical trial of Ficus racemosa. Pharmacogn Rev 2015; 9(17): 73-80.

ISTANBUL UNIVERSITY PRESS

RESEARCH ARTICLE

Eur J Biol 2022; 81(1): 41-49

Serotyping of *Legionella* Bacteria Isolated from Various Water Systems in the Central Anatolia Region

Betul Gumusluoglu[1,2], Nesrin Ozsoy Erdas[2]

[1]Public Health National Respiratory Pathogens Legionella Reference Laboratory, Ankara, Turkiye
[2]Ankara University, Faculty of Science, Department of Biology, Ankara, Turkiye

ORCID IDs of the authors: B.G. 0000-0003-3951-5599; N.O.E. 0000-0002-0470-3745

Please cite this article as: Gumusluoglu B, Ozsoy Erdas N. Serotyping of *Legionella* Bacteria Isolated from Various Water Systems in the Central Anatolia Region. Eur J Biol 2022; 81(1): 41-49. DOI: 10.26650/EurJBiol.2022.1054161

ABSTRACT

Objective: *Legionella* bacteria are waterborne environmental pathogens that are considered a public health problem because they cause Legionnaires' disease, which is a nationally notifiable disease.

Materials and Methods: *Legionella* analysis was performed in a total of 651 water samples collected during the years 2015 (450) – 2016 (201). Water samples were collected from hospitals (64.66%), hotels (15.05%), the automotive industry (14.43%) and from the buildings (5.83%) in the Central Anatolia Region. After the isolation of *Legionella* by the filtration and culturing method, serogroup and subtypes were determined via latex agglutination tests and the direct fluorescent antibody method.

Results: In 2015, the *Legionella* positivity rate was 8.6%, where 28.2% of detections were from *L. pneumophila* serogroup-1. Six isolates were found to be Philadelphia, four were Olda, and one was Bellingham subgroup. Overall, 64.1% were *L. pneumophila* serogroup 2-14. Moreover, 14 isolates were SG-5, 10 were SG-6, and one was SG-10. 7.7% were unidentified *Legionella* species. The *Legionella* species identified were *L. micdadei* and *L. longbeachae*. In 2016, the *Legionella* positivity rate was 10.4%, with 28.6% of them being from *L. pneumophila* serogroup-1. Four were found to be Olda and two were Philadelphia subgroups. Overall, 66.6% of them were *L. pneumophila* serogroup 2-14. Moreover, six of them were SG-5, four were SG-6, and four were SG-2. 4.7% were unidentified *Legionella* species. There was only one species detected as *L. micdadei*.

Conclusion: It has been observed that the distribution of *Legionella* has exhibited diversity in different water systems throughout the Central Anatolia Region.

Keywords: *Legionella*, water systems, DFA method, virulence, serotyping

INTRODUCTION

Legionella causes either influenza-like Pontiac fever or Legionnaires' disease, which is more dangerous due to the potential for pneumonia developing in the lungs. In 1976, during the Legion Congress, epidemic diseases and deaths were revealed in a hotel in the city of Philadelphia, USA. It was thought the outbreak was caused by the water used in the hotel. In 1977, a bacterium isolated from the hotel's water was revealed to be pathogenic and called *Legionella* by McDade et al. (1). Additionally, the disease was called *Legionnaires' disease* by Fraser et al. (1). *Legionella* is recognized as a waterborne environmental pathogen (2, 3). *Legionella* lives and proliferates by forming colonies in the biofilms of water systems (2-4). Thus, they represent a great danger to humans (5, 6). Additionally, they can resist environmental conditions by forming an exopolysaccharide matrix or by entering a "viable but non-culturable" state. These are important strategies that enable *L. pneumophila* to adapt to different environmental characteristics such as water temperature, flora, nutrients, chemicals, and chlorination, while also gaining resistance to disinfectants (7). For this reason,

Corresponding Author: Betul Gumusluoglu E-mail: gumusluoglu@ankara.edu.tr
Submitted: 26.01.2022 • **Revision Requested:** 28.03.2022 • **Last Revision Received:** 25.04.2022 • **Accepted:** 05.05.2022 • **Published Online:** 07.06.2022

the European Legionnaires' Disease Surveillance Net and the World Health Organization emphasized that it is necessary for potentially dangerous water systems to be checked for *Legionella* at regular intervals.

The number of reported *Legionnaires' disease* cases has increased in the United States and in Europe (1). The industrialization of cities and the use of pools, spas, jacuzzis, air conditioning, shower systems, sports centers, and elderly care centers have caused the increased pollution of water resources, which has increased *Legionnaires' disease* prevalence (4). It has been reported that *Legionella* especially affects elderly patients (8). Also, it more effectively invades suppressed immune systems and chronic disease patients. Additionally, health workers, smokers, agricultural workers, car washers, frequent travelers, and those staying in hotels are at risk (9, 10).

Legionella has 62 different species (11) and more than 80 serogroups (12), at least 21 of which cause infections in humans (3, 4). *L. pneumophila* is the most well-characterized strain, which causes 70-90% of all cases of legionellosis (13). The SG-1 serogroup of *L. pneumophila* is the most prevalent disease-causing variant (2), while serogroups 1, 4 and 6 are the causative agents of 85% of human infections (14). Other *Legionella* types that cause disease are *L. micdadei, L. bozemanii, L. dumoffii, L. gormanii,* and *L. longbeachae* (9). Additionally, *L. pneumophila* SG-1, SG-6, SG-7, and the species L. *micdadei, L. feeleii,* and *L. anisa* cause Pontiac fever (15).

In 2014, the largest *Legionella* outbreak occurred in Portugal. During this outbreak, 14 out of 400 cases resulted in death. It was reported that the disease was transmitted from person to person and involved the *L. pneumophila* SG-1 1905 strain (16). Moreover, in Japan, there were four major outbreaks caused by public baths (17). Notably, hot springs and baths are more common sources of *L. pneumophila* than cooling towers, according to the Japan National Center for Epidemiological Surveillance and Infectious Diseases (18). In Poland, although it has been a nationally notifiable disease since 2002, low-cost techniques are preferred for the diagnosis of *Legionella*. Thus, cases of disease are only usually noticed in an advanced stage, which has resulted in a paucity of relevant data (8). In Turkey, *Legionnaires' disease* was accepted as a nationally notifiable disease with the circular published by the Ministry of Health in 1996, and Turkey was included in the European *Legionella* Infections Working Group in 2001 (19). Detection of Legionella species in domestic, hotel and hospital hot water systems is very important (20).

Legionella bacteria are pleomorphic structures and thus have different morphological and physiological characteristics in the same species, and this results in varied virulence characteristics (21). Additionally, they have advanced mechanisms to reproduce and survive in different hosts and environmental conditions (22). For this reason, it is important to understand the virulence characteristics so that the disease can be detected more quickly and easily to apply necessary treatments.

The aim of this study is the determination of the species, serogroups, and subtypes of *Legionella* bacteria found in the water systems of hospitals, hotels, auto industry buildings, and buildings in different cities in the Central Anatolian Region. For this purpose, the serological typing of *Legionella* found in water systems was performed to detect *Legionella* contamination.

MATERIALS AND METHODS

Sample Collection

Legionella analysis in water systems has been routinely conducted in Turkey by the National Respiratory Pathogens *Legionella* Reference Laboratories of the General Directorate of Public Health in Ankara. In the present study, water samples were taken in 2015 and 2016 from hospitals, hotels, automotive industry buildings, and other buildings. The samples were then analyzed for *Legionella*. Water samples were collected from cooling towers, water tanks, and faucets/showerheads by qualified personnel in sterile containers. All samples were labeled, stored in a cool box at a temperature of up to 5 (±3)°C, and delivered directly to the laboratory within 24 h. Detailed information about water sample collection is available in the *Legionnaires' Disease* Laboratory Diagnosis Guide (23).

Filtration and Culture

Since water samples were taken from different water systems (cooling towers, water tanks, and faucets/showerheads), the filtration methods performed were also different. The filtration processes for water were carried out in accordance with standardized methods by the General Directorate of Public Health (previously known as the Refik Saydam Hygiene Center Presidency) National Respiratory Pathogens *Legionella* Reference Laboratories, 1999 (19-23). According to this method, the filtration of the 50 ml water samples was performed in three different ways. Each sample was inoculated on two different media. One medium is inhibitor-free Buffered Charcoal Yeast Extract (BCYE), while the other is BCYE-based agar with dyes, vancomycin, polymyxin B, and glycine (a chemical used to prevent the growth of environmental flora in water systems). We prepared all media for cultivating *Legionella* in our laboratory as described in the *Legionnaires' Disease* Control Program guide. After cultivation, plates were incubated at 37°C in a humidity incubator. For determination, suspected colonies were randomly chosen for subculture on both BCYE and 5% sheep blood medium (non-cysteine) at the same time. If colonies only grew on BCYE but did not grow on the blood medium, they were considered to be *Legionella*.

Isolation of *Legionella*

Firstly, gray-green and bright colonies that are similar to *Legionella* were examined under a colony microscope (Olympus SZ-40) for morphological assessment. After confirming the characteristic *Legionella* bacteria under the colony microscope, a second identification was made according to the protocol of the commercial agglutination kit (Oxoid, Latex; Oxoid Limited, UK). The latex agglutination test was performed for the identification of predominant *Legionella* species grown on plate

media with suspected *Legionella* bacteria. The Oxoid *Legionella* Latex Test allows the separate identification of *Legionella pneumophila* serogroup 1 and serogroups 2–14, as well as the detection of seven other *Legionella* species (*L. longbeachae*-1 and 2, *L. bozemanii*-1 and 2, *L. dumoffii*, *L. gormanii*, *L. jordanis*, *L. micdadei*, and *L. anisa*). The kit contains blue latex particles that are sensitive to *Legionella* species and serotypes. It allows specific *Legionella* cell walls to bind together and form visible clusters. This ensures that the test is completed rapidly and easily for pathogenic *Legionella* species and serotypes identification. The result is positive if the agglutination of blue latex particles occurs within one minute and with no agglutination in the control circle. A positive reaction indicates the presence of antigens against the suspected *Legionella* in the sample and which serogroup or species it belongs to.

Direct Fluorescence Antibody Testing

Following identification, direct fluorescence antibody (DFA) testing was applied to identify serogroups 2–14, subtypes, and *Legionella* spp. using an m-TECH assay kit (m-TECH, Monoclonal Technologies Inc. Milton, GA). The DFA test is particularly useful for a rapid microscopic diagnosis to detect the presence of specific antigens of bacteria based on fluorescent-labeled antibodies binding to the target antigen of *Legionella*. According to the manufacturer's protocol, *Legionella* bacteria are tagged with a monoclonal antibody treated with a fluorescein dye to form labeled antibody reagents against *Legionella* antigens. After the antibody binds to the antigen on the bacterial cell wall, it glows green under a fluorescence microscope. Firstly, *Legionella* sp. specimens were plated onto BCYE agar. The plates were then incubated at 37°C in 2.5% CO_2 and in a humidified environment for 24–48 h. A clear suspension (McFarland No.1) in phosphate buffer from pure *Legionella* cultures were made to assist in the attachment of the cells to the diagnostic microscope slides, which have a black epoxy coating that includes a few circles. The bacterial isolates to be tested were fixed to a microscope glass slide, air dried, gently fixed with heat, and overlaid with the Fluorescein isothiocyanate (FITC)-labeled antibody reagents directed against *Legionella* antigens. The diagnostic microscope slides were incubated for 20–30 min at 37°C in 2.5% CO_2 and in a humidified environment. They were then gently and individually rinsed with phosphate buffered saline (PBS) to remove the conjugates, resulting in the unbound antibodies being washed away. The slides were then immersed in individual jars containing PBS for five min. All slides were then rinsed with distilled water and air-dried. A mounting medium was then dropped onto the slides and coverslips were applied. The slides were then examined using a fluorescence microscope without delay (24). Both a polyvalent positive control antigen and a negative control conjugate were run with each test.

Fluorescence Microscopy

The microscope slides were examined under a fluorescence microscope (Leica DM1000). The FITC-labeled antibody binds specifically to any *Legionella* antigen in the sample isolate. If no *Legionella* antigen is present, the antibody reagent does not bind and is removed during the washing steps. The FITC-labeled antibody-antigen complex is detected by glowing a bright green color, and *Legionella* cells appear to glow as green bacilli under a fluorescence microscope.

RESULTS

Microscopy and Isolation of *Legionella*

Overall, 651 water samples were examined for *Legionella* between 2015 and 2016. In 2015, 278 hospitals, 98 hotels, 53 automotive industry buildings and 21 other buildings were analyzed. In 2016, 143 hospitals, 41 auto industry buildings and 17 other buildings were analyzed (Figure 1). After 3–5 days from filtration to cultivation, the plates were checked and the outer morphologies (edges) of colonies were examined under a colony microscope. Colonies suspected of being *Legionella* have a smooth surface and are slightly convex with a gray-white center as well as green, blue, purple, and pink edges with a cut glass appearance.

Identification of *Legionella*

Identification tests were performed for the typing of *Legionella* (Figure 2). According to the typing with the latex agglutination test for 450 samples in 2015, 39 (8.6%) samples tested positive for *Legionella*. The serogroups found were as follows: *L. pneumophila* SG-1, 11 (28.2%); *L. pneumophila* SG-2-14, 25 (64.1%); *Legionella* spp. 3 (7.7%) (Figures 2a, 3a). According to the typing of 201 samples in 2016, 21 (10.4%) samples tested

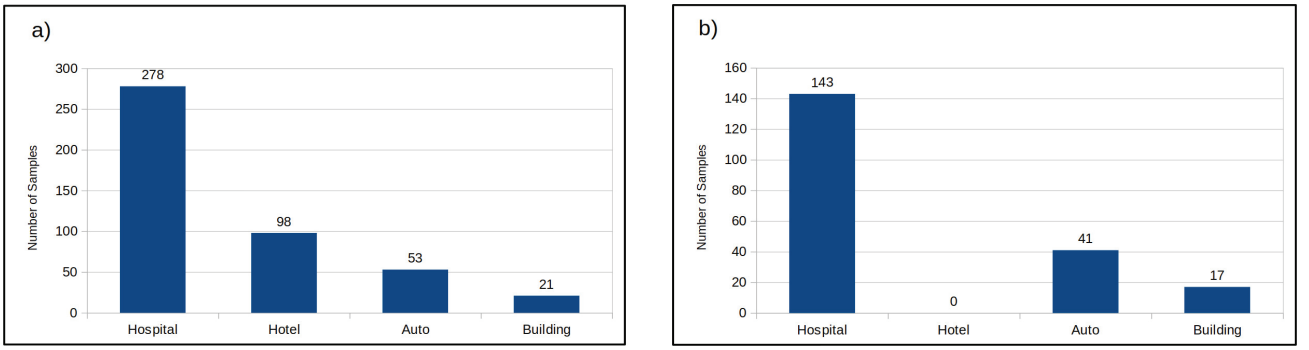

Figure 1. Distribution of water sample sources for the years 2015 (a) and 2016 (b).

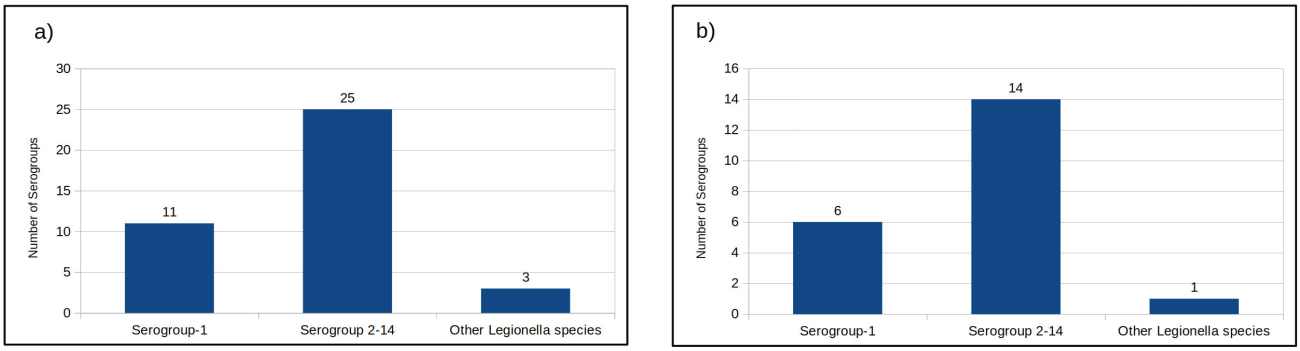

Figure 2. Distribution of serogroups for the years 2015 (a) and 2016 (b).

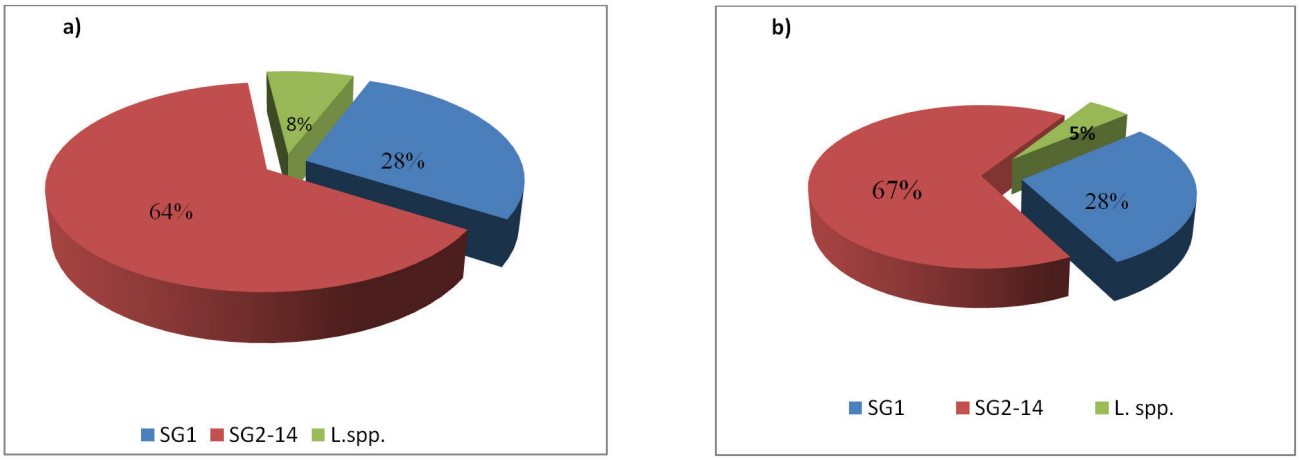

Figure 3. Percent distribution of serogroups for the years 2015 (a) and 2016 (b).

positive for *Legionella*. The serogroups found were as follows: *L. pneumophila* SG-1, six (28.6%); *L. pneumophila* SG-2-14, 14 (66.6%); *Legionella* spp. 1 (4.7%) (Figures 2b, 3b).

Serotyping with DFA and Fluorescence Microscopy

According to the subtyping of samples collected in 2015, the following results were found. Overall, 11 cases of *L. pneumophila* serogroup-1 were found: six as Philadelphia (hotel washstand, automotive industry building shower, hospital room water); four as Olda (hospital collector, heated shower in an automotive industry building); one as Bellingham (intensive care washstand of a hospital) (Figure 4). Overall, 25 cases of *L. pneumophila* serogroup 2-14 were found: 14 were SG-5 (in the rooms, toilets, and showerheads of a hospital, water boiler); 10 were SG-6 (hospital rooms, water boiler); one was SG-10 (hospital room) (Figure 5). Two other *Legionella* species were found (*L. micdadei* and *L. longbeachae*) in automotive industry cooling towers (Figure 6). According to the subtyping of samples collected in 2016, six of them were *L. pneumophila* SG-1—two were Philadelphia and four were Olda subgroups—and they were in the showerheads of automotive industry buildings (Figure 4). Overall, 14 samples with *L. pneumophila* serogroup 2-14 were found (6 were SG-5, in the hot water tank of a hospital, purification tower, and pool

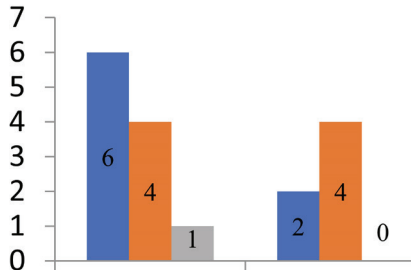

	2015	2016
Philadelphia	6	2
Olda	4	4
Bellingham	1	0

Figure 4. SG-1 Serogroups.

in a chemical industry building). Four of them were SG-6 (from the bathroom tap of a hospital, showerhead of a hospital room, and a hot water boiler). Four of them were SG-2 (from a tap, tap head, and showerhead from a hospital room) (Figure 5). Only one other *Legionella* species was found (*L. micdadei*) in an automotive industry cooling tower (Figure 6).

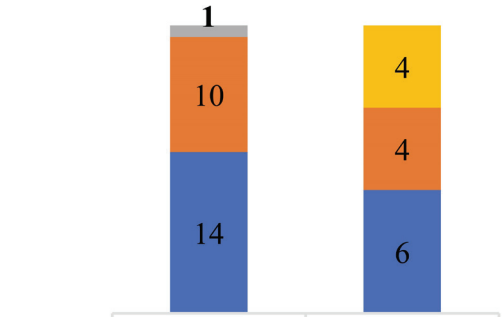

	2015	2016
sg2	0	4
sg10	1	0
sg6	10	4
sg5	14	6

Figure 5. SG-2-14 Distribution.

	2015	2016
L. micdadei	1	1
L. longbeachae	2	0

Figure 6. *Legionella* Species Distribution.

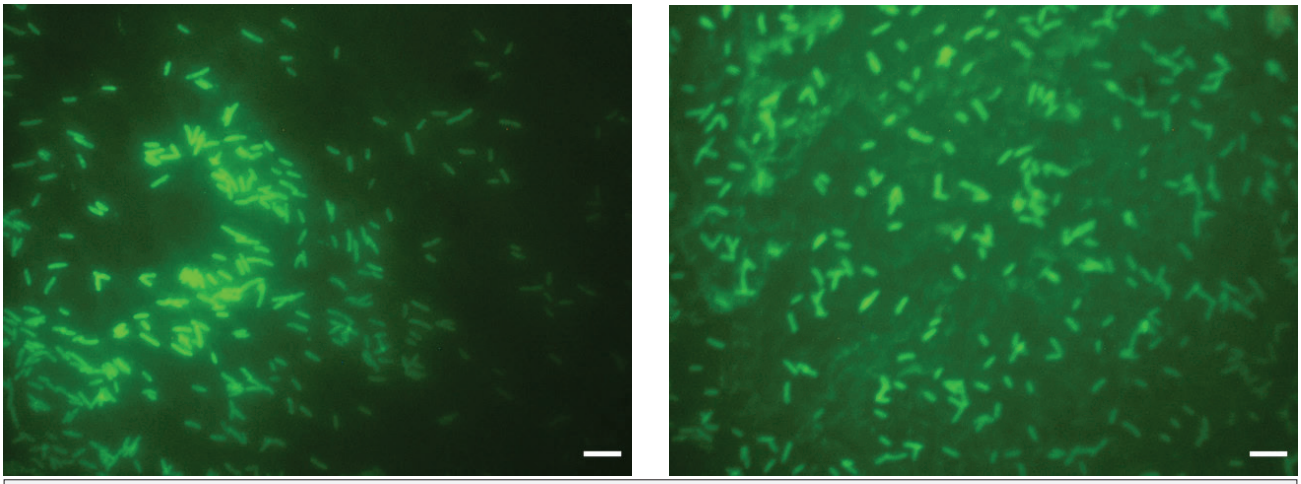

Figure 7. *Legionella* bacteria glowing green under a fluorescence microscope. Scale bar, 20 µm.

According to the DFA method, *Legionella* bacteria glow green in color under a fluorescence microscope (Figure 7).

Locations and numbers of all serogroups and subtypes are shown in Table 1.

DISCUSSION

Legionella bacteria are waterborne pathogens that cause community-acquired Legionnaires' disease, therefore many studies have been conducted to investigate the level of *Legionella* colonization of water systems both in the world and in our country.

Leoni et al. studied 137 hot water samples from apartments, hotels, and hospitals. In apartments, there were 13 samples of *L. pneumophila* (four of them were SG-3 and SG-9, three of them were SG-6, two of them were SG-8), while four of them were other *Legionella* species (one *L. micdadei*, one *L. bozemanii*, and two unidentified *Legionella*). In hotels, there were four positive cases of *Legionella* (three cases of SG-1 and SG-6, one case with both SG-3 and SG-6). In hospitals, seven positive *Legionella* cases were found (five cases of SG-3 and two cases of other *Legionella* species (*L. anisa* and *L. bozemanii* were found at low rates) (20). The *Legionella* serogroups identified in the current study are compatible with the results of Leoni et al.

Afacan et al. assessed water samples collected from touristic hotels in İzmir, Aydın, and Muğla provinces as well as Bodrum. *Legionella* analysis was performed on samples taken from the water systems of hotels (e.g., faucets, cooling towers, Jacuzzis). *Legionella* presence was determined by latex agglutination, while serogroups SG-2–14 were determined by DFA. It was noted that all serogroups (SG-3,-6,-8,-10,-11,-13) were detected in

Table 1. Locations and numbers of all serogroups and subtypes.

2015			2016			
Serogroups Subgroups	**Number**	**Locations**	**Serogroups Subgroups**	**Number**	**Locations**	***L. pneumophila* Serogroups**
Philadelphia	**4**	Hotel washstand	*Philadelphia*	**2**	Automotive industry showerhead	*L. pneumophila* SG-1
	1	Automotive industry shower				
	1	Hospital room tap				
Olda	**2**	Hospital hot water collector	*Olda*	**4**	Automotive industry showerhead	
	1	Automotive industry hot shower				
	1	Residential hot water collector				
Bellingham	**1**	Hospital intensive care washstand				
SG-5	**6**	Hospital hot water tank	**SG- 2**	**2**	Hospital room tap	***L. pneumophila* SG 2-14**
	5	Hospital room showerhead				
	2	Hospital room tap		**1**	Hospital room tap head	
	1	Hospital toilet		**1**	Hospital room showerhead	
SG-6	**4**	Hospital hot water tank	**SG-5**	**2**	Chemical industry purification pool	
	4	Hospital room tap		**2**	Chemical industry purification tower-1	
	1	Hospital room showerhead		**1**	Chemical industry purification tower -2	
	1	Hospital toilet		**1**	Hospital hot water tank	
SG-10	**1**	Hospital room tap	**SG-6**	**2**	Hospital room showerhead	
				1	Hospital hot water tank	
				1	Hospital bathroom tap	
L. micdadei	**1**	Automotive industry cooling tower	***L. micdadei***	**1**	Automotive industry cooling tower	***Legionella* spp.**
L. longbeachae	**2**	Automotive industry cooling tower				

İzmir, while SG-11 was detected in Aydın, SG-6 and SG-8 were detected in Muğla, and only SG-6 was detected in Bodrum. It was emphasized that although SG-1 is the most important cause of *Legionnaires' disease*, other serogroups are also common in tourism regions of Turkey (25).

Tesauro et al. surveyed 271 samples from the hot water systems of two hospitals between 2004 and 2009. *L. pneumophila* prevalence was 37%, SG-2–14 prevalence was 68.3%, and SG-1 prevalence was 18.8%. Moreover, 12.9% of the water samples were positive for both SG-1 and SG-2–14 serogroups. After disinfection with chlorine dioxide five times, *L. pneumophila* concentration reached acceptable limits. This suggests that chlorine dioxide application is effective at keeping *L. pneumophila* concentration within acceptable limits (26). In the current study, due to the high prevalence of SG2-14 in water systems, SG 2-14 incidence was found to be 64% in 2015 and 67% in 2016; these findings are similar to the results of Tesauro et al.

Akkaya et al. analyzed samples taken from various water systems in hospitals, schools, hotels, and residences in Kayseri, Turkey. Serogroups were determined by latex agglutination tests. *Legionella* was detected in eight (6.7%) of 120 water samples, with six of them being *L. pneumophila* SG-1 and two being other *Legionella* species. It was determined that the samples containing other *Legionella* species were taken from the showerheads of hotels, while those containing *L. pneumophila* SG-1 were from a warehouse and the shower systems of hospitals (27). The method used in this study was similar to our study but the distribution of *Legionella* species was different.

In a study conducted by Burak et al., a total of 122 hot water and swab samples were taken from the showerheads of 61 houses that were investigated for the presence of *L. pneumophila* and free-living amoebas in 2009, in Istanbul. According to the results of this study, *L. pneumophila* was isolated from 13 houses (21.3%) and free-living amoebas were isolated from 19 (31%). *L. pneumophila* was isolated from 12 (19.6%) of the water samples and four (6.5%) of the swab samples. Among the isolated *L. pneumophila*, it was reported that 87.5% were *L. pneumophila* serogroup 2-14, while 12.5% were *L. pneumophila* serogroup 1. Although there is no correlation between the presence of *L. pneumophila* and free-living amoebas, it was stated that there was a significant correlation between the presence of *L. pneumophila* and the presence of a central heating system (28). Due to the high SG 2-14 ratio, our results can be considered to be compatible with Burak et al.

İğnak et al. detected *Legionella* colonization in 7% of 100 water samples taken from showerheads, taps, and tank water in different locations within Istanbul University Medical Faculty Hospital. A total of seven *Legionella* strains were isolated. Notably, three SG-1 and three *Legionella* spp. were found in the showerheads and faucets, while only one other *Legionella* species was found in tank water. *Legionella* SG-1 and other *Legionella* species were especially found in pediatric departments. Additionally, *Legionella* spp. were found in the tap water of anesthesiology and reanimation units. *Legionella* growth was not observed in the water systems of clinical units more distant from the water tank where growth was observed (29).

Ulleryd et al. investigated 61 environmental samples from 15 cooling towers and 138 clinical samples. Overall, 84 patients linked to the study were hospitalized in an epidemic that lasted for weeks in the city of Lidköping, Sweden. Overall, two of 32 patients died. Moreover, in an isolated sample, *L. pneumophila* SG-1 Benidorm and Bellingham were found. In three cooling towers, *L. pneumophila* SG-1 Benidorm, Bellingham, Portland, and Olda subgroups were found. Notably, cooling towers effectively spread *Legionella* via aerosols during outbreaks (30). The identification of Bellingham and Olda subgroups in the current study is similar to the findings of these researchers.

In a study by Erdoğan et al., *Legionella* was isolated from 11 out of 13 water samples in a newly opened hotel during a small *Legionella* outbreak in Alanya in 2009. The hotel's water systems and clinical samples were studied together. Water samples taken from 10 different parts of the hotel were examined. Moreover, six patients and 26 suspected cases staying in the same hotel were also examined. *L. pneumophila* SG-1 was found in 11 out of 13 water samples. All six patients were positive for *L. pneumophila* SG-1 in their urine. Moreover, SG-1 antibody positivity was observed in the serum of only one patient. No SG-1 positivity was observed in the urine of patients who applied with complaints of 26 other diseases. Although data could not be adequately collected and detailed tests could not be performed, it was thought that this outbreak was caused by the water systems in hotels, with water systems in newly opened hotels being at higher risk for *Legionnaires' disease* (31).

Sepin Özen et al. studied a total of 1403 water samples from 56 different hotels during January-December 2010 in Antalya, Turkey. *L. pneumophila* was isolated from 37.5% of the hotels and 10.1% of water samples. It was reported that 85% of the samples were positive for *L. pneumophila* serogroup 2–14, while 15% of the samples were positive for *L. pneumophila* serogroup 1 (32).

Quero et al. described and compared 528 isolates collected between 1989 and 2016. Typing studies were carried out using monoclonal antibodies (MAb) and sequence-based typing (SBT) methods. A total of 266 samples (109 clinical samples and 157 environmental samples) were compared to each other. Clinical samples were divided into seven Dresden subgroups. It was indicated that Philadelphia (26.61%), Knoxville (19.27%), Olda (14.68%) and Benidorm (14.68%) were the most frequent subgroups. In typing environmental samples using the Dresden Panel, Olda (33.1%) and non-SG-1 *L. pneumophila* (17.2%) were frequently detected. Although there is a high incidence of *Legionnaires' disease* in Spain, this study was comprised of the Catalan and Valenciana regions. An *L. pneumophila* population was found in clinical and environmental samples in the Valenciana region, while *L. pneumophila* was found only in clinical samples from Catalan. It has been reported that this study is an important term of comparison for *L. pneumophila* typed with MAb and SBT for both clinical and environmental samples in Catalan (33). In our results, Olda subgroup in 2015 was 36%, non-SG-1 *L. pneumophila* was 8%; while in 2016 Olda was 67% and non-SG-1 *L. pneumophila* was 1%.

Zeybek et al. investigated *Legionella* and free-living amoebae in swimming pool samples from Istanbul using different methods. In this study, free-living amoebae were identified/found in four of the water samples and two of the biofilm samples via the culture method. Free-living amoebae were found in three water and three biofilm samples that could not be detected via the culture method. *Legionella* was only found in one biofilm sample via the culture method. By using the fluorescence in situ hybridization (FISH) method, *Legionella* was detected in six water and seven biofilm samples. According to the results of this study, it was stated that the FISH method could be a more effective method for *Legionella* detection. However, it has been expressed that the culture method should be used for the correct isolation of *Legionella* bacteria (34).

Papadakis et al. inspected and tested 3311 water samples from the hot and cold water systems of 132 hotels between 2000 and 2019. The serogroups of *L. pneumophila* were determined via latex polyclonal antisera as SG-1 (27.92%) and SG-3 (17.08%). Moreover, it was found that 25.96% occurred in hot water distribution systems, 16.98% in cold waters, and 13.51% in swab samples. It has been reported that more than 80% of *Legionnaires' disease* cases are caused by *L. pneumophila* serotype 1 (35). The incidence of SG-1 in the current study, 28% in 2015 and 2016, is consistent with the findings of Papadakis et al.

In another study by Yılmaz et al. in Turkey, the presence of *L. pneumophila* was determined in water samples taken from hospitals, hotels, Turkish baths, and shopping centers in Erzurum and nearby provinces. *L. pneumophila* was found in 65 of the 2025 water samples. *L. pneumophila* serogroup 2–14 was detected in 46 (70.8%) of 65 positive samples, while *L. pneumophila* serogroup 1 was detected in 18 samples (27.7%). Additionally, *L. pneumophila* serogroup 2–14 and *L. pneumophila* serogroup 1 were detected (1.5%) in one water sample. It was indicated that the highest positivity rates were in hot water taps (11.6%), hot water tanks (6.1%), and showerheads (4.8%) (36).

Since clinicians need to recognize hospital-acquired *Legionnaires' disease*, the identification of this disease is important. To achieve this, both the phenotypic and genotypic characteristics of the bacterium should be known in greater detail and should be detected more quickly. To understand the pathogenic effect of *Legionella* in humans, mechanisms such as attachment, entry to cells, and avoidance of the host's immune system should be very well known. For these reasons, it is important to define the serogroups, subgroups, and strains of *Legionella* (8). Due to most nosocomial infections originating from water systems, hospitals are risky environments. Thus, *L. pneumophila* infections must be given greater attention in health institutions and organizations (20). All public buildings (including hotels, businesses, schools, apartments, and government buildings) and cooling towers should have water management plans. These plans should establish a program team, identify control measures and where they should be applied to stay within limits, monitor certain parameters to determine whether control measures are working, verify and validate the program, and document everything. It is also important that water entering domestic and public buildings should have a minimum disinfectant residual. In Turkey, the Ministry of Health issues guidelines about legionnaires' disease control programs.

In our study, there are limitations and drawbacks. First of all, the clinical conditions of the people and the patients exposed to *Legionella* positive environments have not been evaluated. Secondly, in other studies, serotyping and subtyping were performed using molecular methods for sequence analysis. Thirdly, the *Legionella* positivity of water samples after disinfection has not been analyzed to demonstrate the success of the disinfection process.

On the other hand, the identification of *Legionella* in our samples indicates that water management plans should be implemented in these locations.

CONCLUSION

Various studies have been carried out in Turkey and abroad for the serological typing of *Legionella* bacteria. It was observed that there was much variation in the distribution of serogroups and subgroups. Since *Legionella* is a waterborne, travel-related, and community-acquired infection, it will be possible to observe different serogroups between countries. Identifying serogroups and subgroups is important for the diagnosis of infections. For this reason, it is important to conduct comprehensive and detailed studies. This study is important because it shows the distribution of serogroups and subtypes of *Legionella* bacteria for at least one region of Turkey. Thus, it should help inform further studies on this subject.

Acknowledgement: We appreciate Selin Nar Otgun, Sinem Bedir and Hakan Hedef from the Public Health National Respiratory Pathogens Legionella Reference Laboratory for their help and support in our DFA experiments.

Peer Review: Externally peer-reviewed.

Author Contributions: Conception/Design of Study- B.G., N.O.E.; Data Acquisition- B.G.; Data Analysis/Interpretation- B.G., N.O.E.; Drafting Manuscript- B.G., N.O.E.; Critical Revision of Manuscript- B.G., N.O.E.; Final Approval and Accountability- B.G., N.O.E.

Conflict of Interest: Authors declared no conflict of interest.

Disclosure Statement: This Research Article was presented in part as a poster at the 24th European Cell Death Organization (ECDO) Conference, "Cell Death in Health and Disease", Barcelona, Spain, September 28-30th, 2016.

Financial Disclosure: This work/research was supported by the Ankara University Coordination of Scientific Research Project Coordination Unit (BAP)[Project number:16L0430010].

REFERENCES

1. Yavuz Cl. Legionnaires'-disease as a waterborne disease and environmental surveillance. Türk Mikrobiyol Cem Derg 2018; 48(4): 211-27.
2. Graham FF, Hales S, White PS, Baker MG. Review Global seroprevalence of legionellosis - a systematic review and meta-analysis. Sci Rep 2020; 10(1): 7337.
3. Xiao-Yong Z, Chao-Hui H, Qing-Yi Z. Comparative study on sampling methods for monitoring *Legionella* species in environmental water. Afr J Microbiol Res 2014; 8(10): 974-85.
4. Felice A, Franchi M, De Martin S, Vitacolonna N, Iacumin L, Civilini M. Environmental surveillance and spatio-temporal analysis of *Legionella spp*. in a region of northeastern Italy (2002–2017). Zhou Z, ed. PLoS ONE 2019; 14(7): e0218687.
5. Fricke C, Xu J, Jiang F, Liu Y, Harms H, Maskow T. Rapid culture-based detection of *Legionella pneumophila* using isothermal microcalorimetry with an improved evaluation method. Microb Biotechnol 2020; 13(4): 1262-72.

6. Yarom R, Sheinman R, Armon R. *Legionella pneumophila* serogroup 3 prevalence in drinking water survey in Israel (2003–2007). Water Supply 2010; 10(5): 746-52.
7. Berjeaud JM, Chevalier S, Schlusselhuber M, et al. *Legionella pneumophila*: the paradox of a highly sensitive opportunistic waterborne pathogen able to persist in the environment. Front Microbiol 2016; 7: 486.
8. Sopena N, Pedro-Botet L, Mateu L, Tolschinsky G, Rey-Joly C, Sabrià M. Community-acquired legionella pneumonia in elderly patients: characteristics and outcome: community legionella pneumonia in elderly patients. J Am Geriatr Soc 2007; 55(1): 114-9.
9. Llewellyn AC, Lucas CE, Roberts SE, Brown EW, Nayak BS, Raphael BH, Winchell JM. Distribution of *Legionella* and bacterial community composition among regionally diverse US cooling towers. PLoS ONE 2017; 12(12): e0189937.
10. Sikora A, Wójtowicz-Bobin M, Kozioł-Montewka M, Magryś A, Gładysz I. Prevalence of *Legionella pneumophila* in water distribution systems in hospitals and public buildings of the Lublin region of eastern Poland. Ann Agric Environ Med 2015; 22(2): 195-201.
11. Scaturro M, Poznanski E, Mupo M, Blasior P, Seeber M, Prast AM, Romanin E, Girolamo A, Rota MC, Bella A, Ricci ML, Stenico A. Evaluation of GVPC and BCYE media for *Legionella* detection and enumeration in water samples by iso 11731: does plating on BCYE medium really improve yield? Pathogens 2020; 9(9): E757.
12. Eisenreich W, Heuner K. The life stage-specific pathometabolism of *Legionella pneumophila.* FEBS Lett 2016; 590(21): 3868-86.
13. Laganà P, Facciolà A, Palermo R, Delia S. Environmental surveillance of legionellosis within an Italian university hospital-Results of 15 years of analysis. Int J Environ Res Public Health 2019; 16(7): 1103.
14. Gruas C, Álvarez I, Lara C, García CB, Savva D, Arruga MV. Identification of *Legionella spp*. in environmental water samples by Scan-VIT-LegionellaTM method in Spain. Indian J Microbiol 2013; 53(2): 142-8.
15. Kirschner AKT. Determination of viable legionellae in engineered water systems: Do we find what we are looking for? Water Research 2016; 93: 276-88.
16. Borges V, Nunes A, Sampaio DA, Vieira L, Machado J, Simões MJ, Gonçalves P, Gomes JP. *Legionella pneumophila* strain associated with the first evidence of person-to-person transmission of Legionnaires' disease: a unique mosaic genetic backbone. Sci Rep 2016; 6(1): 26261.
17. Amemura-Maekawa J, Kura F, Helbig JH, et al. Characterization of Legionella pneumophila isolates from patients in Japan according to serogroups, monoclonal antibody subgroups and sequence types. J Med Microbiol 2010; 59(Pt 6): 653-9.
18. Amemura-Maekawa J, Kikukawa K, Helbig JH, Kaneko S, Suzuki-Hashimoto A, Furuhata K, et al.; Working Group for Legionella in Japan. Distribution of monoclonal antibody subgroups and sequence-based types among *Legionella pneumophila* serogroup 1 isolates derived from cooling tower water, bathwater, and soil in Japan. Appl Environ Microbiol 2012; 78(12): 4263-70.
19. Akbaş E. Basic principles in investigation of *Legionella* in hospital water systems. Türk Mikrobiyol Cem Derg 2013; 43(1): 1-11.
20. Leoni E, De Luca G, Legnani PP, Sacchetti R, Stampi S, Zanetti F. Legionella waterline colonization: detection of *Legionella species* in domestic, hotel and hospital hot water systems. J Appl Microbiol 2005; 98(2): 373-9.
21. Prashar A, Bhatia S, Tabatabaeiyazdi Z, Duncan C, Garduño RA, Tang P, Low DE, Guyard C, Terebiznik MR. Mechanism of invasion of lung epithelial cells by filamentous *Legionella pneumophila*. Cell Microbiol 2012; 14(10): 1632-55.
22. Oliva G, Sahr T, Buchrieser C. The life cycle of *L. Pneumophila*: cellular differentiation is linked to virulence and metabolism. Front Cell Infect Microbiol 2018; 8: 3.
23. Akbaş E, Nar Ötgün S, Turan M. Ulusal mikrobiyoloji standartları, suda *Legionella* türlerinin tanımlanması. 2014. T.C. Sağlık Bakanlığı, Türkiye Halk Sağlığı Kurumu, Sağlık Bakanlığı Yayın No: 965.
24. Winn WC, Cherry WB, Frank RO, Casey CA, Broome CV. Direct immunofluorescent detection of *Legionella pneumophila* in respiratory specimens. J Clin Microbiol 1980; 11(1): 59-64.
25. Afacan G, Yumuk Z, Baskın Y, Balıkcı E. Frequency of *Legionella pneumophila* serogroup 2-14 isolated from water samples at touristic regions. Türk Mikrobiyol Cem Derg 2006; 36(4): 214-8.
26. Tesauro M, Bianchi A, Consonni M, Pregliasco F, Galli MG. Environmental surveillance of *Legionella pneumophila* in two Italian hospitals. Ann Ist Super Sanita 2010; 46(3): 274-8.
27. Akkaya Z, Özbal Y. *Legionella* researching in water depots' of different buildings in Kayseri. Sağlık Bilimleri Dergisi (Journal of Health Sciences); 2011; 20(1): 9-17.
28. Burak DM, Zeybek Z. Investigation of *Legionella pneumophila* and free living amoebas in the domestic hot water systems in Istanbul. Turk J Biol 2011; 35: 679-85.
29. İğnak S. and Gürler B. An investigation of Legionella species in the water system of a university hospital. Türk Mikrobiyol Cem Derg 2012; 42(3): 110-4.
30. Ulleryd P, Hugosson A, Allestam G, Bernander S, Claesson BEB, Eilertz I. Legionnaires' disease from a cooling tower in a community outbreak in Lidköping, Sweden- epidemiological, environmental and microbiological investigation supported by meteorological modelling. BMC Infectious Diseases 2012; 12(1): 313.
31. Erdoğan H, Arslan H. Evaluation of a Legionella outbreak emerged in a recently opening hotel. Mikrobiyol Bul 2013;47(2):240-9.
32. Sepin Özen N, Tuğlu Ataman Ş, Emek M. Exploring the *Legionella pneumophila* positivity rate in hotel water samples from Antalya, Turkey. Environ Sci Pollut Res 2017; 24(13): 12238-42.
33. Quero S, Párraga-Niño N, Barrabeig I, Sala MR, Pedro-Botet ML, Monsó E, et al. Population structure of environmental and clinical *Legionella pneumophila* isolates in Catalonia. Sci Rep 2018; 8(1): 6241.
34. Zeybek Z, Türkmen A. Investigation of the incidence of *legionella* and free-living amoebae in swimming pool waters and biofilm specimens in Istanbul by different methods. Mikrobiyol Bul 2020; 54(1): 50-65.
35. Papadakis A, Keramarou M, Chochlakis D, Sandalakis V, Mouchtouri VA, Psaroulaki A. *Legionella spp*. colonization in water systems of hotels linked with travel-associated legionnaires' disease. *Water* 2021; 13(16): 2243.
36. Yılmaz A, Orhan F. Investigation of the presence of *Legionella pneumophila* in water samples from Erzurum and surrounding provinces in Turkey. Ann Agric Environ Med 2021; 28(2): 255-9.

ISTANBUL UNIVERSITY PRESS

RESEARCH ARTICLE

Eur J Biol 2022; 81(1): 50-57

Yeast Diversity in the Mangrove Sediments of North Kerala, India

Pothayi Vidya[1], Chempakassery Devasia Sebastian[1]

[1]University of Calicut, Division of Molecular Biology, Department of Zoology, Kerala, India

ORCID IDs of the authors: P.V. 0000-0003-0863-1280; C.D.S. 0000-0001-9555-0627

Please cite this article as: Vidya P, Sebastian CD. Yeast Diversity in the Mangrove Sediments of North Kerala, India. Eur J Biol 2022; 81(1): 50-57. DOI: 10.26650/EurJBiol.2022.1027475

ABSTRACT

Objective: Mangrove sediments, due to their unique environment, are considered to be a crucial habitat in identifying yeast strains with potent industrial, biotechnological and bioremediation properties. The goal of the current study was to understand the presence, diversity and hydrolytic enzyme properties of yeasts from the mangrove sediments of North Kerala.

Materials and Methods: Sampling was done during the period 2018-2020 from mangrove sediments of 5 districts along the North Kerala coast. Isolation of yeast was done on yeast glucose peptone agar, and isolates were tested for their potential for the production of extracellular enzymes viz. amylase, cellulase, chitinase, DNase, lipase, ligninase, pectinase, protease and urease, using standard media with specific substrates. Morphological assessment, biochemical characterization and molecular identification of the isolates were performed. The phylogenetic tree of the selected yeast strains was constructed with the Maximum Likelihood method using MEGA X software.

Results: A total of 482 yeast strains belonging to 12 genera were obtained from the mangrove sediment samples, the most dominant genera being Candida (56.3%). *Kluveromyces, Debaromyces, Torulaspora, Trichosporon, pigmented yeast Rhodotorula, Cyberlindnera, Wickerhamiella, Pichia, Trichoderma, Meyerozyma* and *Kodamaea* were the other genera identified. The majority of the yeast present in the mangrove sediment samples were lipolytic (68%), followed by ureolytic (23%), ligninolytic (16%), cellulolytic (9%), DNAlytic (9%), proteolytic (8%), amylolytic (6%), pectinolytic (4%) and chitinolytic (2%) forms. All 12 genera of yeast obtained had positive forms for extracellular lipase.

Conclusion: The yeast strains obtained from mangrove sediments in the study were found to be ecologically important and have great biotechnological potential.

Keywords: Yeast, mangrove sediments, hydrolytic enzymes, phylogeny, North Kerala

INTRODUCTION

Mangroves are a unique ecosystem present in the tropical and subtropical parts of the world, and are considered the most productive coastal ecosystems. The sediments of mangroves harbor a great number of microbial communities composed mainly of bacteria, fungi and actinomycetes, which perform nutrient transformation of the ecosystem (1). The yeasts present in mangrove sediments have gained attention during recent years by virtue of their potential characteristics. Due to their ecological flexibility, they can tolerate extreme conditions like varying salinity, different environmental temperatures, oxygen concentrations and changes in acidity (2). They reproduce and grow quickly on simple substrates, which are decomposed with the help of hydrolytic enzymes they produce (3).

The hydrolytic enzymes that are produced by yeasts have a wide range of applications in industries as well as in bioremediation processes, as they take part in various transformational activities (4). The enzymes produced by yeasts from mangrove sediments are believed to have the capability to withstand extreme climatic

Corresponding Author: Chempakassery Devasia Sebastian E-mail: drcdsebastian@gmail.com

Submitted: 24.11.2021 • **Revision Requested:** 25.03.2022 • **Last Revision Received:** 04.04.2022 • **Accepted:** 05.05.2022 • **Published Online:** 16.05.2022

and cultural conditions, which would help in their large-scale production (5). Moreover, during scale up cultures, they require comparatively cheap substrates, like industrial byproducts and wastes, as nutrient sources (6). Thus, mangrove sediment yeasts can be considered the best for the commercial production of industrially important enzymes due to easier production in terms of genetic and environmental manipulation, cost effectiveness, non-toxic properties and stability (7).

The diversity and identification of yeasts present in mangrove sediments primarily helps in understanding their properties which can be applied in industrial and biotechnological processes and in bioremediation. Assessment of the hydrolytic enzyme potential of the yeasts and analyzing the factors affecting it would be a great advancement in the mass production of commercially important enzymes. Though the Northern part of Kerala, India is bestowed with large mangrove areas, they are not sampled enough to provide any well-vetted information on the yeasts present in the sediments. For these reasons, this work was focused on isolation, identification and evaluation of the enzymatic capability of yeasts present in the sediments of the mangrove ecosystem along the coast of North Kerala.

MATERIALS AND METHODS

Sample Collection

Mangroves of 5 districts along the North Kerala coast were selected for sediment collection. The sampling was done during the period 2018-2020 at 8 sites (Table 1). 10-20 g of sub surface sediment was collected using a hand corer, transferred aseptically into sterile polythene bags, transported in ice boxes and processed within 4 hours of collection. Five sub-samples were collected from each site, which were then homogenized to one composite sample per site.

Isolation of Yeast

Sediment samples were spread plated on Wickerham's agar medium supplemented with 200 mg/l chloramphenicol (8) in duplicates and incubated at 18±2°C for 7 days. The single colonies developed were purified by quadrant streaking. Later they were streaked onto malt extract agar slants for further studies.

Screening for Hydrolytic Enzyme Production

All the isolates were tested for the production of hydrolytic extracellular enzymes, namely protease, amylase, lipase, urease, ligninase, cellulase, DNase, pectinase and chitinase. The detection of extracellular protease, amylase, lipase and chitinase was done in nutrient agar medium containing casein (2%), starch (1%), tributyrin (1%) and colloidal chitin (5%), respectively, as substrates. The detection of DNase, cellulase, pectinase, urease and ligninase activity was tested on DNase agar, Cellulose agar, Pectin agar and Urease agar with 40% urea and Crawford's agar supplemented with 0.5% tannic acid, respectively. The plates were spot inoculated and incubated at 28±2ºC for 7 days. The plates were flooded with 1M HCl, Gram's iodine solution and 1% cetrimonium bromide (CTAB) after incubation for protease amylase and pectinase, respectively. Formation of clearance/ halo zone or brown color around the colonies was considered positive.

Identification of Yeasts

The isolates were identified to the genus level using morphological and biochemical characterization methods. Later, molecular characterization was used for species identification of selected isolates. In morphological characterization, colony characteristics on malt extract agar and microscopic appearance of methyl blue stained smear under 40x and oil immersion (100x) in compound microscope were observed. Biochemical characterization included urea hydrolysis, sugar fermentation (MOF - Microbial Oxidation Fermentation test), fatty acid hydrolysis, nitrate assimilation, starch like substance and citric acid production, Diazonium Blue B reaction and observance of growth at 37°C (9). Isolates showing similar morphological and biochemical characteristics were grouped together. Representative strains from each of these groups were selected for species identification based on their efficiency to produce extracellular enzymes determined qualitatively by screening the

Table 1. Sites of collection of mangrove sediments for the present study.

Sl. No.	Name of the collection site	Site code	Lat-Long coordinates
1	Chandragiri (Kasaragod Dt)	KGD	12°05'32'' N 75°13'39'' E
2	Edat (Kannur Dt)	EDT	12°05'32'' N 75°13'39'' E
3	Pazhayangadi (Kannur Dt)	PYD	12°02'72'' N 75°29'31'' E
4	Valapattanam (Kannur Dt)	VPT	11°93'45'' N 75°35'35'' E
5	Elathur (Kozhikode Dt)	ELR	11°19'43'' N 75°45'20'' E
6	Kadalundi (Kozhikode Dt)	KDI	11°07'43'' N 75°49'48'' E
7	Ponnani (Malappuram Dt)	PON	10°47'10'' N 75°55'30'' E
8	Chettuva (Thrissur Dt)	CTV	10°52'42'' N 76°04'79'' E

hydrolytic activity for respective substrates. The identification of these isolates was performed by sequencing of ITS region as per Harju et al. (10) with Forward ITS1 and Reverse ITS4 primers (11). The amplified fragment of approximately 580 bp, containing the ITS 1, 5.8 S and ITS 2 regions, was used for the sequence similarity search using NCBI BLAST.

Phylogenetic Analysis

Nucleotide sequences of yeasts obtained were statistically analyzed using Molecular Evolutionary Genetic Analysis Version X (MEGA X) software and a phylogenetic tree was constructed using Maximum Likelihood method. Proper outgroup (fungus - *Penicillium chrysogenum*) was selected for the construction of the phylogenetic tree and the nodal support was tested by means of 100 bootstrap pseudo replicates.

RESULTS

After isolation and purification, a total of 482 yeasts strains were obtained from the mangrove sediment samples of 8 sites in North Kerala. Based on their morphological, physiological, biochemical and molecular characterization, it was found that they belonged to 12 genera of yeast. 20 species were identified when selected isolates were sequenced and the sequences were deposited in the GenBank (Table 2). The total number and distribution of different genera of yeast obtained in the study is summarized in Figure 1. 272 of the total isolates (56.31%) belonged to genera *Candida*, in which 7 different species have been identified, among which *Candida tropicalis* was the predominant species found (84.19%). Other genera of yeast obtained from the mangrove sediments were *Kluveromyces* (12.01%), *Debaromyces* (9.52%), *Torulaspora* (9.11%), *Trichosporon* (3.73%), pigmented yeast *Rhodotorula* (3.52%), *Cyberlindnera* (2.07%), *Wickerhamiella* (1.66%), *Pichia* (1.24%), *Trichoderma* (0.62%) and one isolate each of *Meyerozyma* (0.21%) and *Kodamaea* (0.21%) (Table 3).

The majority of the yeast present in the mangrove sediment samples was lipolytic (68%), followed by ureolytic (23%), ligninolytic (16%), cellulolytic (9%), DNAlytic (9%), proteolytic (8%), amylolytic (6%), pectinolytic (4%) and chitinolytic (2%) forms

Table 2. NCBI GenBank accession details of identified yeast strains from mangrove sediments during the present study.

Sl. No.	Isolates	Organism	GenBank Accession
1.	CUMB VP –PN2-03	*Rhodotorula mucilaginosa*	MT 131387
2.	CUMB VP –PN2-10	*Candida pseudolambica*	MT 131389
3.	CUMB VP –KL1-10	*Candida tropicalis*	MT 131391
4.	CUMB VP –KL1-01	*Candida sorboxylosa*	MT 136728
5.	CUMB VP –PN2-12	*Torulaspora globosa*	MT 135124
6.	CUMB VP –ED3-04	*Torulaspora maleeae*	MT 131815
7.	CUMB VP –KG3-05	*Candida dubliniensis*	MT 132376
8.	CUMB VP –KG-4-03	*Pichia kudriavzevii*	MT 138566
9.	CUMB VP –PN4-12	*Trichoderma viride*	MT 138567
10.	CUMB VP –VL-4-03	*Trichosporon asahii*	MT 138568
11.	CUMB VP –CT-1-09	*Debaryomyces nepalensis*	MT 138571
12.	CUMB VP –PZ-4-10	*Kluyveromyces siamensis*	MT 138576
13.	CUMB VP –PZ4-07	*Cyberlindnera saturnus*	MW 617277
14.	CUMB VP –EL4-09	*Wickerhamiella infanticola*	MW 617280
15.	CUMB VP –PN4-08	*Kodamaea ohmeri*	MW 617290
16.	CUMB VP –KL5-01	*Meyerozyma carpophila*	MW 617291
17.	CUMB VP –EL5-01	*Candida membranifaciens*	MW 617296
18.	CUMB VP –VL1-05	*Candida metapsilosis*	MW 617299
19.	CUMB VP –KG4-13	*Candida orthopsilosis*	MW 617302
20.	CUMB VP – KL4-12	*Trichoderma longibrachiatum*	MW 624336

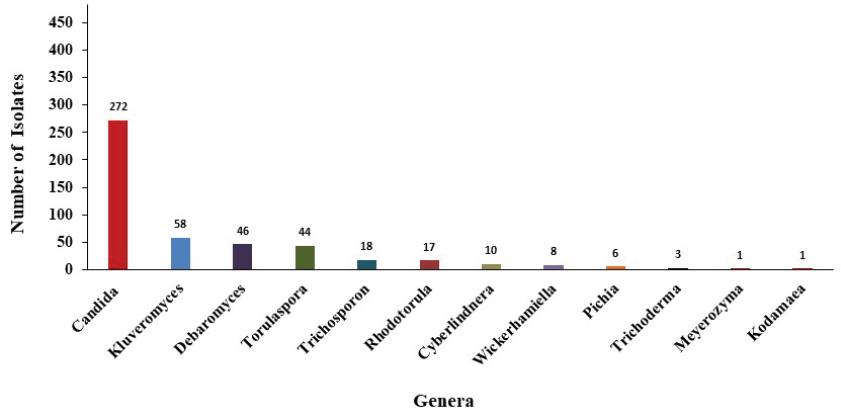

Figure 1. Distribution of different genera of yeast from the mangrove sediments.

Table 3. Taxonomic list of yeast strains obtained and identified from the mangrove sediments.

Identified yeast strains	No. of isolates
Genus: *Candida*	
Candida tropicalis	229
Candida dubliensis	23
Candida matapsilosis	8
Candida pseudolambica	5
Candida sorboxylosa	4
Candida membranifaciens	2
Candida orthopsilosis	1
Genus: *Kluveromyces*	
Kluveromyces siamensis	58
Genus: *Debaromyces*	
Debaromyces napelensis	46
Genus: *Torulaspora*	
Torulaspora maleae	38
Torulaspora globosa	6
Genus: *Trichosporon*	
Trichosporon asahii	18
Genus: *Rhodotorula*	
Rhodotorula mucilaginosa	17
Genus: *Cyberlindnera*	
Cyberlindnera saturnus	10
Genus: *Wickerhamiella*	
Wickerhamiella infanticola	8
Genus: *Pichia*	
Pichia kudriavzevii	6
Genus: *Trichoderma*	
Trichoderma viride	3

(Figures 2 and 3). Generic wise hydrolytic potential for extracellular enzymes of all the isolates is summarized in Figure 4. All 12 genera of yeast obtained had positive forms for extracellular lipase. Isolates belonging to genera *Candida* and *Torulaspora* showed hydrolytic activity for all the enzymes under study, while the representatives belonging to genera *Meyerozyma* and *Kodamaea* showed only lipolytic activity. All the isolates representing genus *Trichosporon*, *Wickerhamiella*, *Trichoderma* and the pigmented red yeast *Rhodotorula* were ureolytic in nature.

Estimates of phylogenetic relatedness among species were determined using the maximum likelihood (ML) in MEGA X software. 52 sequences of yeasts were analyzed and presented as bootstrap consensus tree to illustrate the statistical strength of gene tree (Figure 5). Bootstrap support for the phylogenetic tree was determined from 1,000 replications. The evolutionary history was inferred using the Neighbor Joining method and the tree was drawn to scale, with branch lengths having the same units as those of the evolutionary distances represented and as the number of base substitutions at each site. The positions with missing data and gaps were excluded during tree construction. The fungus *Penicillium chrysogenum* was selected as an outgroup for the phylogenetic tree. The sequences were classified in 5 large clades and subclades.

DISCUSSION

In our study, around 56% of the total isolates belonged to genus *Candida*, making them the most predominant yeast present in the mangrove sediments of Northern Kerala. *C. tropicalis, C. dubliensis, C. matapsilosis, C. pseudolambica, C. sorboxylosa, C. membranifaciens* and *C. orthopsilosis* were the 7 species found under the genus *Candida*, in which *C. tropicalis* (84%) hugely outnumbered others. Reports on the yeasts present in the mangrove sediments from China and different parts of Brazil showed the domination of *Candida* spp. in the ecosystem (12,13). *Candida* is considered the most common genera of yeast present in marine environments and is isolated largely from estuarine and mangrove areas of urban regions that are polluted by human resources (14,15). Due to this reason, they

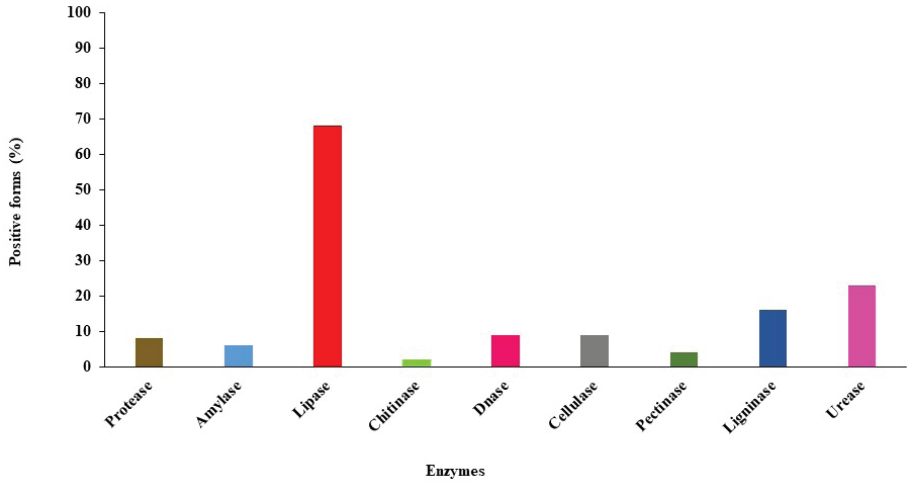

Figure 2. Percentage of yeast isolates (positive forms) showing various enzyme activities.

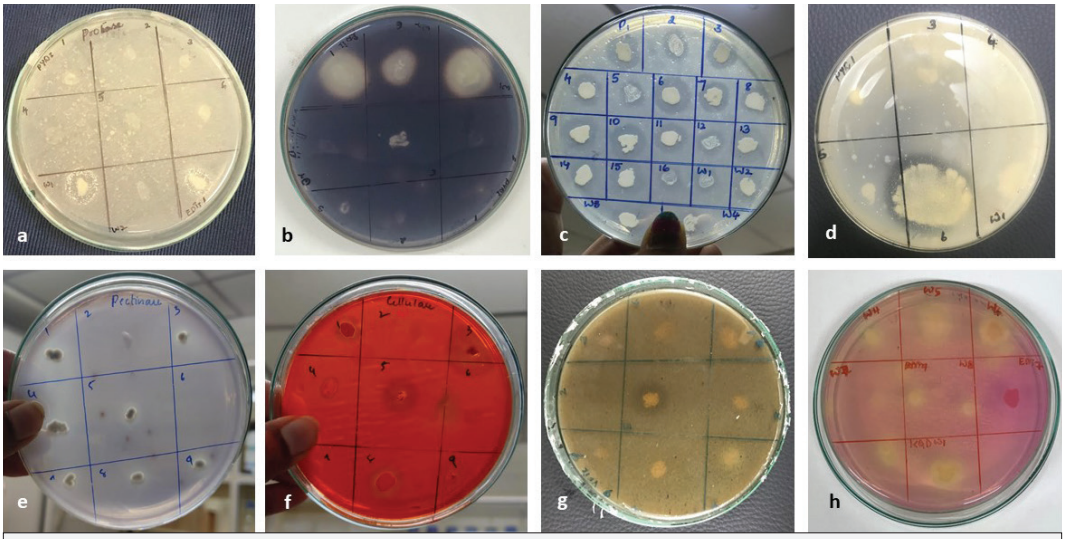

Figure 3. Plates showing various hydrolytic enzyme activities of yeast isolates. Clearance/halo zone or brown/red color around the colonies was considered positive. a) Protease b) Amylase c) Lipase d) DNase e) Pectinase f) Cellulase g) Ligninase h) Urease.

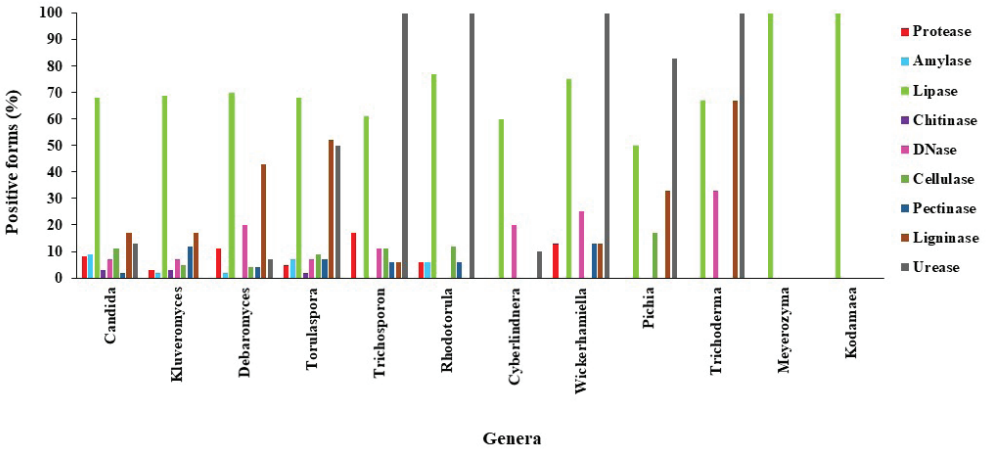

Figure 4. Generic wise distribution of hydrolytic potential of yeast isolates for various extracellular enzymes.

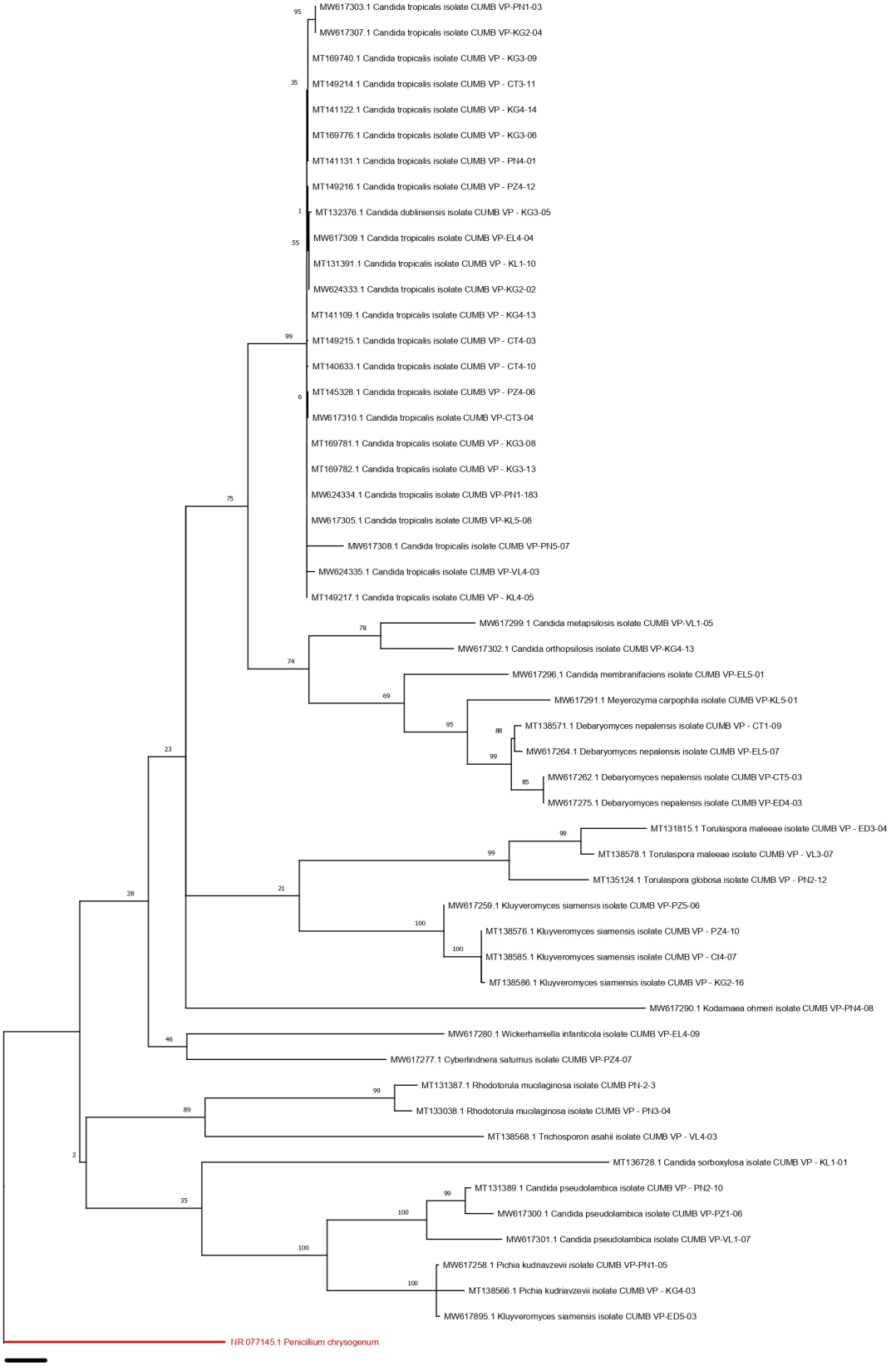

Figure 5. Phylogenetic tree representing relationship between the yeast isolates from the mangrove sediments using Neighbor Joining algorithm.

are considered one of the bio indicators of pollution (16,17). The dominance of *Candida* spp. in the mangrove ecosystem, especially in the sediments, was found to have several ecological significances. It has been found that they are able to withstand the extreme conditions of the mangrove sediments, including fluctuating temperature, high salinity, low oxygen concentration and varying nutrient compositions (3). Most of the yeast belonging to genus *Candida* spp. were found to have a significant role in the process of biodegradation (18). Studies have shown that *C. tropicalis* have the ability to degrade a wide range of pollutants, including crude petroleum, oil while *C. parapsilosis* and *C. intermedia* act efficiently on all kinds of oily pollutants (19,20). Kurtzmann et al. isolated *C. pseudolambica* from the mangrove ecosystem and reported them as a cosmopolitan species in marine environments due to their active role in biodegradation (21). *Candida* spp. were also involved in converting the shell wastes of crustaceans into biomass protein and in the production of silver nano particles (22,23).

Kluveromyces siamensis, *Debaromyces napelensis*, *Torulaspora maleae* and *T. globosa, Trichosporon asahii, Rhodotorula mucilaginosa, Cyberlindnera saturnus, Wickerhamiella infanticola, Pichia kudriavzevii, Trichoderma viride, Meyerozyma carpophila* and *Kodamaea ohmeri* were the other yeast species found in the sediments. Most of the species obtained in our study are not only ecologically important but also have been found to have great biotechnological potential. *Rhodotorula, Torulaspora, Debaryomyces* and *Trichosporon* were considered bioindicators due to their role in the degradation of various pollutants and in controlling algal blooms (24). These species were also found to metabolize aromatic hydrocarbons and heavy metals present in the environment, thereby degrading them to non-toxic products (25). The pigmented yeast *Rhodotorula mucilaginosa* produce carotenoids, which makes them a potential bioindicator and biotechnological candidate. An easy method to assess the quality of sample by the colony count method was developed in which the number of pink colonies of *R. mucilaginosa* indicated the extend of pollution (16). Moreover, the carotenoids extracted from the species are widely used in food and pharmaceutical industries and also in waste water treatment (26).

The extracellular enzymes of yeast are hydrolytic in nature and they take part in a large number of transformation reactions that can be applied in industrial processes and in bioremediation. Lipase is the most common enzyme produced by marine yeast and catalyzes various chemical reactions, including hydrolysis, aminolysis, acidolysis, alcoholysis and esterification. (27,28). The majority of the isolates in our study were lipolytic, those belonging to *Candida* spp. being the highest. Hasan et al have reported that the yeast belonging to genera *Candida, Rhodotorula* and *Pichia* are active lipase producers (29). All the isolates studied belonging to genera *Trichosporon*, *Wickerhamiella*, *Trichoderma* and *Rhodotorula* were able to hydrolyze urea. The nickel containing urease enzyme has tremendous applications in medical and pharmaceutical industries (30,31). Though ligninolytic activity in yeasts is studied least by researchers, our study showed that the yeasts of genera *Debaromyces, Torulaspora* and *Trichoderma* were able to actively break down lignin substrates. The reduced production of other enzymes, including cellulase, DNase, protease, amylase, pectinase and chitinase, by the isolates under study might be due to the absence or low availability of those substrates and their recycling in the sediments of sampling sites (18). Yeast extracellular enzymes from an extreme environment like mangrove sediments should be further explored in order to make them useful in industrial processes and environmental bioremediation.

CONCLUSION

The quest for novel and improved microbial strains that can produce industrially important metabolites is a continuous process. Since, yeasts are one of the most active producers of secondary metabolites and extracellular enzymes that can be fermented using cheap substrates; they have gained massive attention during recent years. In the present study, we investigated the yeasts from mangrove sediments of North Kerala for its diversity and production of extracellular hydrolytic enzymes. The results suggest that yeasts from mangrove sediments are promising candidates for various industrial and biotechnological applications and can be effectively used in the development of strategies for the bioremediation and conservation of the ecosystem.

Informed Consent: Written consent was obtained from the participants.

Peer Review: Externally peer-reviewed.

Author Contributions: Conception/Design of Study- P.V., C.D.S.; Data Acquisition- P.V.; Data Analysis/Interpretation- P.V., C.D.S.; Drafting Manuscript- P.V.; Critical Revision of Manuscript- P.V., C.D.S.; Final Approval and Accountability- P.V., C.D.S.

Conflict of Interest: Authors declared no conflict of interest.

Financial Disclosure: Authors declared no financial support.

REFERENCES

1. Thatoi H, Behera BC, Mishra RR, Dutta SK. Biodiversity and biotechnological potential of microorganisms from mangrove ecosystems: A review. Ann Microbiol 2012; 1-22.
2. Boguslawska-Was E, Dabrowski W. The seasonal variability of yeasts and yeast-like organisms in water and bottom sediment of the Szczecin Lagoon. Int J Hyg Envir Heal 2001; 203: 451-8.
3. Kandasamy K, Alikunhi NM, Subramanian M. Yeasts in marine and estuarine environments. J Yeast Fungal Res 2012; 3: 74-82.
4. Kutty SN, Philip R. Marine yeasts - Areview. Yeast 2008; 25(7): 465-83.
5. Pothayi V, Devasia SC. A study on the distribution and hydrolytic enzyme potential of yeasts in the mangrove sediments of Northern Kerala. Ind J Microbio Res 2020; 7: 161-7.
6. Cheng YT, Yang CF. Using strain *Rhodotorula mucilaginosa* to produce carotenoids using food wastes. J Taiwan Inst Chem Eng 2016; 61: 270-5.

7. Elsanhoty RM, Al-Turki AI, El-Razik MMA. Production of carotenoids from *Rhodotorula mucilaginosa* and their applications as colorant agent in sweet candy. J Food Agr Env 2017; 15: 21-6.
8. Wickerham LJ. Taxonomy of yeasts. U.S. Dept Agricultural Technical Bullettin 1951; 1029: 1-19.
9. Barnett JA, Payne RW, Yarrow D. Yeasts: characteristics and identification, Second ed. Cambridge University Press, Cambridge. 1990.
10. Harju S, Fedosyuk H, Peterson KR. Rapid isolation of yeast genomic DNA. Bust n'Grab. BMC Biotech 2004; 4: 8-12.
11. White TJ, Bruns T, Lee S, Taylor J. Amplification and direct sequencing of fungal ribosomal RNA genes for phylogenetics. Innis MA, Gelfand DH, Sninsky JJ, White TJ, editors. PCR Protocols, A guide to methods and applications. Academic Press: San Diego, CA; 1990.
12. Pagnocca FG, Mendonça-Hagler LC, Hagler AN. Yeasts associated with the white shrimp Penaeus schmitti, sediment, and water of Sepetiba Bay, Rio de Janeiro, Brazil. Yeast 1989; 5: 479-83.
13. Chi ZM, Liu TT, Chi Z, Liu GL, Wang ZP. Occurrence and diversity of yeasts in the mangrove ecosystems in Fujian, Guangdong and Hainan provinces of China. Indian J Microbiol 2012; 52: 346-53.
14. Fell JW, Van Uden N. Yeasts in marine environments. In: Oppenheimer C H, editors. Symposium on Marine Microbiology; Charles C Thomas Publisher, Springfield; 1963. pp. 329-40.
15. Loureiro STA, de Queiroz-Cavalcanti MA, Neves RP, de Oliveira Passavante JZ et al. Yeasts isolated from sand and sea water in beaches of Olinda, Pernambuco state, Brazil. Braz J Microbiol 2005; 36: 1-8.
16. Hagler AN. Yeasts as Indicators of Environmental Quality. Gábor P, Rosa C, editors. Biodiversity and Ecophysiology of Yeasts. Berlin: Springer; 2006. p. 515-32.
17. Silva-Bedoya LM, Ramírez-Castrillón M, Osorio-Cadavid E. Yeast diversity associated to sediments and water from two Colombian artificial lakes. Braz J Microbiol 2014; 45: 135-42.
18. Kutty SN, Damodaran R, Philip R. Yeast isolates from the slope sediments of Arabian Sea and Bay of Bengal: Physiological characterization. Adv App Sci Res 2014; 5: 177-87.
19. Fialova A, Boschke E, Bley T. Rapid monitoring of the biodegradation of phenol-like compounds by the yeast *Candida maltosa* using BOD measurements. Int Biodeterior Biodegrad 2004; 54: 69-76.
20. Farag S, Soliman NA. Biodegradation of crude petroleum oil and environmental pollutants by *Candida tropicalis* strain. Braz Arc Biol Technol 2011; 54: 821-30.
21. Kurtzman CP, Fell JW, Boekhout T, editors. The yeasts: A taxonomic study. USA: Elsevier; 2011. pp 2100.
22. Rishipal R, Philip R. Selection of marine yeasts for the generation of single-cell protein from prawn-shell waste. Biores Technol 1998; 65: 255-6.
23. Manivannan S, Alikunhi NM, Kandasamy K. In vitro Synthesis of Silver Nanoparticles by Marine Yeasts from Coastal Mangrove Sediment. Adv Sci Lett 2010; 3: 1-6.
24. Raspor P, Zupan J. Yeast in extreme environments. Gábor P, Rosa C, editors. Biodiversity and Ecophysiology of Yeasts. Berlin: Springer; 2006. pp 371-417.
25. Botha A. Yeasts in soil. Gábor P, Rosa C, editors. Biodiversity and Ecophysiology of Yeasts. Berlin: Springer; 2006. pp 221-40.
26. Li M L, Chi G L, Chi Z, Chi Z M. Single cell oil production from hydrolysate of cassava starch by marine-derived yeast *Rhodotorula mucilaginosa* TJY15a. Biomass Bioenergy 2010; 34: 101-7.
27. Paskevicius A. Lipase activity of yeasts and yeast-like fungi functioning under natural conditions. Biologija 2001; 4: 16-8.
28. Vakhlu J, Kour A. Yeast lipases: enzyme purification, biochemical properties and gene cloning. Electron J Biotechnol 2006; 9: 69-85.
29. Hasan F, Shah AA, Hameed A. Industrial Applications of Microbial Lipases. Enzyme Microb Technol 2006; 39: 235-51.
30. Bakhtiari MR, Faezi MG, Fallahpour M, Noohi A, Moazami N, Amidi Z. Medium optimization by orthogonal array designs for urease production by Aspergillus niger PTCC5011. Proc Biochem 2006; 41: 547-51.
31. Bharathi N, Meyyappan RM. Production of urease enzyme from ureolytic yeast cell. Int J Eng Res Genl Sci 2015; 3: 643-7.

ISTANBUL UNIVERSITY PRESS

RESEARCH ARTICLE

Eur J Biol 2022; 81(1): 58-67

Effect of Extraction Method on Organoleptic, Physicochemical Properties and Some Biological Activities of Olive Oil from the Algerian *Chemlal* Variety

Sara Messad[1,2], Souhila Bensmail[2], Omar Salhi[3], Djamila Djouahra-Fahem[2]

[1]Akli Mohand Oulhadj University, Faculty of Natural and Life Sciences and Earth Sciences, Laboratory of Management and Valorization of Natural Resources and Quality Assurance (LGVRNAQ), Bouira, Algeria
[2]Akli Mohand Oulhadj University, Faculty of Natural and Life Sciences and Earth Sciences, Department of Biology, Bouira, Algeria
[3]Biotechnology Laboratory of Animal Reproduction, Institute of Veterinary Sciences, Blida, Algeria

ORCID IDs of the authors: S.M. 0000-0002-9815-0327; S.B. 0000-0002-6366-7537; O.S. 0000-0002-0211-1981; D.D.F. 0000-0002-5442-2319

Please cite this article as: Messad S, Bensmail S, Salhi O, Djouahra-Fahem D. Effect of Extraction Method on Organoleptic, Physicochemical Properties and Some Biological Activities of Olive Oil from the Algerian *Chemlal* Variety. Eur J Biol 2022; 81(1): 58-67. DOI: 10.26650/EurJBiol.2022.1109068

ABSTRACT

Objective: The production of olive oil in Algeria is of great importance. The choice of the extraction method is crucial in order to achieve the best yields of high quality oil. This work aims to study the effect of the extraction method on the sensory and physicochemical characteristics and the antioxidant and antimicrobial activities of three types of olive oil derived from the same sample of olive fruits (*Chemlal* variety).

Materials and Methods: Several physicochemical and sensory parameters of olive oil samples were evaluated by referenced methods (ISO, IOC, AFNOR, etc.). The fatty acid composition of oils was determined by gas chromatography. Total phenolic content and antioxidant activity were estimated using the Folin-Ciocalteu assay and FRAP test, respectively. Antimicrobial activity analysis was performed using the agar diffusion technique against five strains.

Results: The analyses revealed that olive oil obtained by manual extraction is classified in the extra virgin category, according to the International Olive Oil Council. The two other oils, traditional and industrial, were of virgin class. Fatty acid composition shows significant differences between the three oils which are characterized by a remarkable richness of phenolic compounds (447-528 mg GAE/kg oil). The best antioxidant activity was noted in the manual olive oil ($PR_{0.5}$=78.60 µg/mL). *Pseudomonas aeruginosa* ATCC 9027 and *Staphylococcus aureus* ATCC 6538 were more sensitive to action of the manual oil compared to other bacterial and fungal strains tested, with inhibition zones of 15.84±0.07 and 15.31±0.20 mm, respectively. This activity was significantly decreased by evaluating antimicrobial effect of the other oils.

Conclusion: The method of extraction significantly affects the properties of olive oil, where the manual method preserves the best quality of oil.

Keywords: Olive oil, extraction process, characterization, antioxidant activity, antimicrobial activity

INTRODUCTION

Olive oil, derived from the fruits of *Olea europaea* L., is one of the most important elements of the Mediterranean diet, not only for its appreciable taste and its usefulness in flavoring of a wide variety of foods, but also for its many beneficial properties due to its chemical composition (1,2). The latter is mainly characterized by a richness in antioxidants, vitamins, phenolic compounds and essential fatty acids for human nutrition, especially polyunsaturated ones. These metabolites are preserved through the consumption of olive oil in crude form, unlike several other common vegetable oils that require a refining step (3-5). For this reason, olive oil production

Corresponding Author: Sara Messad E-mail: s.messad@univ-bouira.dz
Submitted: 27.04.2022 • **Revision Requested:** 12.05.2022 • **Last Revision Received:** 22.05.2022 • **Accepted:** 23.05.2022 • **Published Online:** 16.06.2022

has experienced a remarkable economic increase during the last years (2).

The chemical composition, sensory properties and biological activities of olive oil are highly dependent on several factors: fruit ripening, climate, cultivation procedures, harvesting techniques and extraction method (1,5-7).

The key objective of any extraction method is to obtain the highest possible quantity of oil without altering its original quality (3,7). In order to preserve this, it is essential to proceed with extraction directly from fresh fruits of the olive tree and to use mechanical or physical methods, avoiding chemical and enzymatic reactions that could modify the natural composition of oil and its organoleptic characteristics (3,4,6).

Olive oil extraction involves different processes, such as leaf removal, olive washing, crushing, threshing, and oil separation performed either by pressure or centrifugation (4,8). Olives should be processed as soon as possible after harvest to minimize oxidation and preserve low acidity (4). It is worth mentioning, that extra virgin olive oil is the highest quality olive oil and represents only 10% of the total oil produced (6). For this reason, it is very important to select the extraction process that ensures such quality.

The aim of our study is to determine the influence of the extraction method on the sensory and physicochemical characteristics as well as the antioxidant and antimicrobial activities of three types of olive oil obtained by different extraction methods.

MATERIALS AND METHODS

Collect and Treatment of Samples

The material used consists of three samples of olive oil from the region of Lakhdaria (Wilaya of Bouira, Algeria) (36°33'58.612"N 3°35'29.018"E). The oil extraction was carried out on olive fruits (*Chemlal* variety) harvested during the end of the harvesting season (January, 2017). Choice of olive fruit was focused on fruits with black pigmentation in order to avoid other early stages (semi-black, green or red fruit), having the possibility to affect the oil extraction yield and its conservation. The harvested fruits were mixed and then divided into three groups used for oil extraction according to three processes:

- The first type of oil was the manual olive oil (MOO), which was obtained in a traditional way: the harvested fruits, free of leaves and branches, were washed with running water to eliminate impurities and then dried in open air in a sunny place. The fruits were then crushed by the feet until a smooth blackish paste was obtained. The drained oil was collected in a glass bottle, and the paste was placed in a clean and inclined container.

- The second type of oil was traditional olive oil (TOO), resulting from a press extraction performed at a traditional oil mill.

- The third sample was represented by industrial olive oil (IOO) obtained following a conventional extraction stage, carried out this time at a modern oil mill (industrial), which ensures higher yields of oil.

The three types of oils were stored in hermetically sealed glass bottles and were kept cool and protected from light to avoid polymerization and oxidation.

Sensory Analysis

The organoleptic evaluation is essential to decide on the classification of an olive oil (category virgin, extra virgin or not), because it allows the detection of possible defects not highlighted by the physicochemical analyses. In our study, this evaluation was carried out based on the principles of IOC/T.20/Doc. nº15/Rev.10 (9), by a panel of 20 tasters made up of former previously trained oil mill workers and old olive oil connoisseurs. The oil samples were kept at about 28°C, while the temperature of the analysis room was about 20°C. The analyses were performed in one run. The attributes were quantified on a continuous scale that allowed the tasters to express in a precise way the intensity with which they perceived each attribute. Once the rating sheets were completed, the method used to rank the oils was based on the calculation of the median, considering that the value of the robust coefficient of variation that defines the ranking (defect perceived with the highest intensity and fruitiness) is 20%.

The principle of tasting emphasizes the absence of defects and the intensity of fruitiness. This means that as soon as the slightest trace of a defect is recognized by the majority of tasters on the panel, the oil is no longer entitled to the "extra virgin" designation (IOC/T.15/NC Nº 3/Rev.14 (10).

Physical and Chemical Analysis

Physical indices including refractive index (11), relative density at 20°C, water and volatile content (12), and ultraviolet (UV) absorbance (13) were studied.

For the chemical characterization of oils, different parameters were determined: acid and peroxide indices (EEC N°. 2568) (14), saponification and iodine indices (15). The estimation of chlorophyll content and carotenoids was carried out according to the method described by Minguez-Mosquera et al. (16).

Fatty Acid Composition

Determination of the fatty acid profile of the three oils was carried out with gas chromatography (GPC) of fatty acid methyl esters (17) using a Chrompack CP 9002 type chromatograph equipped with a capillary column Cp Sil 88 CB (5% phenyl + 95% dimethylpolysiloxane) (30 m length, 0.25 µm thick, 0.32 mm inner diameter), a SPLIT 1/100 injector (250°C), a flame ionization detector (FID) (250°C) and an oven (190°C). Nitrogen was used as the carrier gas injected with a flow rate of 1 mL/min. Fatty acids were identified by their retention time in the column in comparison to given standards. The amount of each fatty acid is given in % of total fatty acid.

Evaluation of the Antioxidant Activity

Extraction of Polyphenols

Before proceeding to evaluation of the antioxidant activity, phenolic compounds of the three olive oils were extracted following the protocol described by Pirisi et al. (18). 20 g of each olive oil were introduced into centrifuge tubes. Subsequently 10 mL of n-hexane and 20 mL of 60% methanol were added. After vortex homogenization for 2 min and centrifugation (3000 rpm, 5 min), the supernatants containing polyphenols were recovered separately. The operation was repeated twice to deplete the oil. The resulting supernatants were then combined and evaporated under vacuum at 40°C until a dry residue was obtained, which was re-suspended in 10 mL of 50% methanol. The yield of the extraction (R%) was calculated by the following formula:

$$R(\%) = \frac{m - m_0}{m_T} \times 100$$

m : Mass of the beaker after evaporation.

m_0 : Mass of the beaker before evaporation.

m_T : Total mass of the test sample.

Dosage of Phenolic Compounds

Total polyphenols content of the extracts obtained was determined by the Folin-Ciocalteu method (19). To 200 µL of the methanolic extract, 1 mL of Folin-Ciocalteu reagent (diluted 10 times, v/v) and 800 µL of 7.5% sodium carbonate (w/v) were added. After homogenization and incubation for 30 min in the dark at room temperature, the absorbance was measured at 760 nm using a spectrophotometer against a blank prepared under the same conditions, where the extract was replaced by 50% methanol. Gallic acid (1 mg/mL) was used as a standard. The concentration of polyphenols was reported as mg gallic acid equivalent (GAE)/Kg oil.

FRAP Test (Ferric Reducing Antioxidant Power)

The antioxidant activity of phenolic extracts was determined using the FRAP method (20). 250 µL of each extract prepared at different concentrations (62.5; 125; 250 and 500 µg/mL) were mixed with 250 µL of phosphate buffer (0.2 M, pH 6.6) and 250 µL of 1% (w/v) potassium hexacyanoferrate [$K_3Fe(CN)_6$]. After incubation in a water bath at 50°C for 20 min, 250 µL of 10% (w/v) trichloroacetic acid (TCA) was added. Subsequently, the tubes were centrifuged at 3000 rpm for 10 min. 50 µL of the recovered supernatant was added to 200 µL of distilled water and 10 µL of the 0.1% (w/v) $FeCl_3$ solution. The absorbance was measured at 700 nm against a blank. A higher absorbance of the reaction mixture indicated a higher reducing power.

Evaluation of the Antimicrobial Activity

The antibacterial and antifungal activities of olive oils were performed *in vitro* using the agar diffusion technique described by several authors (21,22). The microbial strains used are known to be pathogenic to humans: two Gram$^+$ bacterial strains (*Staphylococcus aureus* ATCC 6538; *Bacillus subtilis* ATCC 6633); two Gram$^-$ bacterial strains (*Pseudomonas aeruginosa* ATCC 9027, *Escherichia coli* ATCC 8739) and one yeast (*Candida albicans* ATCC 10231). The listed strains were obtained from the collection of the microbiology laboratory "SAIDAL Antibiotical" (Alger, Algeria).

Bacterial inocula were standardized in sterile physiological water, from a pure and fresh culture (18-24 h for bacteria and 48 h for yeast), to obtain an opacity equivalent to 0.5 McFarland (10^7 CFU/mL). Then, a swabbing was performed on the surface of a Muller Hinton Agar. Sterile Whatman paper discs (n°3, 6 mm) were soaked with olive oil (all three types) until impregnation (10 µL), then placed on the surface of the previously inoculated agar and uniformly seeded with the bacterial or fungal suspension to be studied.

Readings were then taken after incubation for 24 h at 37°C for bacterial strains and at 25°C for 48 h in the case of *C. albicans*. Two controls were prepared in parallel: the first did not contain the oil and the second was free of the germ to be tested.

The sensitivity of the target strains towards the different compounds was classified according to the diameters of the inhibition zones obtained: Ø<8 mm: non-sensitive bacteria; 9<Ø<14 mm: sensitive bacteria; 15<Ø<19 mm: highly sensitive bacteria and Ø>20 mm: extremely sensitive bacteria (23,24). The same intervals were respected for the fungal strain.

Statistical Analysis

The variance study was carried out to determine the significant differences (Student's t-test) between the different types of oil by the software "Microsoft Office Excel 2010". Results were represented by the mean with its standard deviation. The differences were considered significant at $p \leq 0.05$ (*), very significant at $p \leq 0.01$ (**) and highly significant if $p \leq 0.001$ (***).

RESULTS

Sensory Analysis

According to the classification made by comparing the value of the median of the majority defect to the reference intervals for each denomination, we concluded that:

- The manual olive oil was in the category "Extra Virgin" (the median of the defects was equal to zero and the median of the fruitiness was greater than zero (m=5) (Figure 1a).
- Traditional olive oil was in the category "Virgin" (the median of defects was equal to: $0 < m \leq 3.5$ (m=1) and the median of fruitiness was greater than zero (m=4) (Figure 1b).
- Industrial olive oil fell into the category "Virgin" (the median of defects was equal to: $0 < m \leq 3.5$ (m=2) and the median of fruitiness was greater than zero (m=3.25) (Figure 1c).

Physicochemical Indices

Acidity is the main criterion of quality and commercial standard of olive oil. However, other criteria of physicochemical and organoleptic quality are also currently associated with these stan-

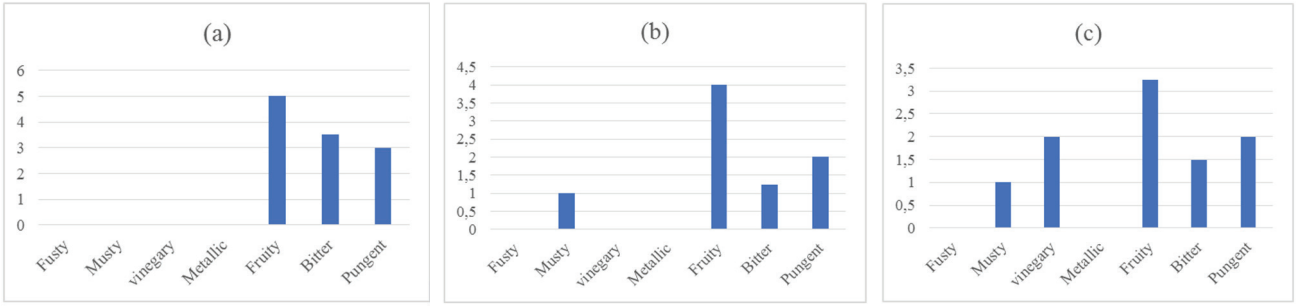

Figure 1. Sensory profile of the studied oil samples: manual (a), traditional (b) and industrial olive oils (c).

Table 1. Physicochemical indices of the three olive oils characterized.

Physicochemical indices - Type of oil	MOO	TOO	IOO
Physical indices			
- Refractive index	1.468±0.00	1.486±0.02	1.468±0.01
- Water and volatile substances content (%)	0.10±0.02	0.095±0.01*	0.067±0.01
- Relative density at 20°C	0.9137±0.01	0.9143±0.00	0.9137±0.00
- $A_{232\ nm}$	2.16±0.02	2.211±0.06	2.211±0.05
- $A_{270\ nm}$	0.158±0.02	0.201±0.03*	0.225±0.03
Chemical indices			
- Acid value (%)	0.80±0.01	0.90±0.01	1.40±0.02
- Peroxide value (meq of O_2/Kg)	15.38±0.03	17.17±0.13	16.66±0.02
- Iodine value	83.93±0.01	83.75±0.04	79.18±0.07
- Saponification index (mg KOH/g oil)	196.7±0.02	192.77±0.09	193.75±0.10
- Chlorophyll content (mg/Kg)	0.24±0.07	0.41±0.02	2.03±0.01
- Carotenoid content (mg/Kg)	7.03±0.05	6.54±0.03	7.62±0.09

MOO: manual olive oil, TOO: traditional olive oil, IOO: industrial olive oil. Significance level: *: p<0.05; Acid index: p<0.001; Peroxide index: p<0.05; Iodine index: p<0.01; Saponification index: p<0.001; Chlorophyll content: p<0.05; Carotenoid content: p<0.001.

dards. The values of the different physical and chemical indices of all samples are listed in Table 1. A significant difference was noted for all chemical indices as well as some physical parameters between the three olive oils.

Fatty Acid Composition

The results of GPC analysis of the fatty acid profile of oils obtained by different extraction processes are summarized in Table 2.

The results obtained indicate a content of fatty acids more or less variable but remaining within the standards of the IOC (10) and Codex Alimentarius (28), except for palmitoleic acid (C16:1ω7), which held a percentage slightly higher than the standard (>3.5%). For all samples, the most intense content was attributed to oleic acid (C18:1ω9), followed by palmitic acid (C16:0), then linoleic acid (C18:2ω6) and palmitoleic acid. Stearic

Table 2. Fatty acid composition (%) of the studied oil samples.

Fatty acid	Name	MOO	TOO	IOO
C16:0	Palmitic acid	16.87	17.61	17.68
C16:1ω7	Palmitoleic acid	4.26	3.64	3.80
C17:0	Margaric acid	Trace	0.42	0.33
C18:0	Stearic acid	1.67	2.10	2.11
C18:1ω9	Oleic acid	62.39	61.89	60.87
C18:2ω6	Linoleic acid	14.11	13.43	13.33
C18:3ω3	Linolenic acid	0.20	0.28	0.98
C20:0	Arachidic acid	0.25	0.20	0.20
C20:1ω9	Gondolic acid	0.21	Trace	Trace

MOO: manual olive oil, TOO: traditional olive oil, IOO: industrial olive oil.

acid (C18:0), arachidic acid (C20:0) and linolenic acid (C18:3ω3) represented more or less small amounts.

Yield and Total Polyphenols Content

According to the results shown in Table 3, the best yield of total polyphenols was noted for the olive oil obtained by the manual method. The yields noted for the other two oils were quite close and lower compared to the first type. Total polyphenols content of the three olive oils varied from 447 to 528.45 mg GAE/Kg oil.

Table 3. Yield and polyphenols content of the three olive oil samples.

Type of oil	MOO	TOO	IOO
Yield (%)	11.55	6.45	6.55
Polyphenols content (mg GAE/Kg oil)	528±12.40	496±11.80	447±10.70

MOO: manual olive oil, TOO: traditional olive oil, IOO: industrial olive oil.

Antioxidant Activity

From Figure 2, we can note that polyphenols of the manual olive oil and traditional oil mill had a much higher antioxidant power compared to industrial oil mill.

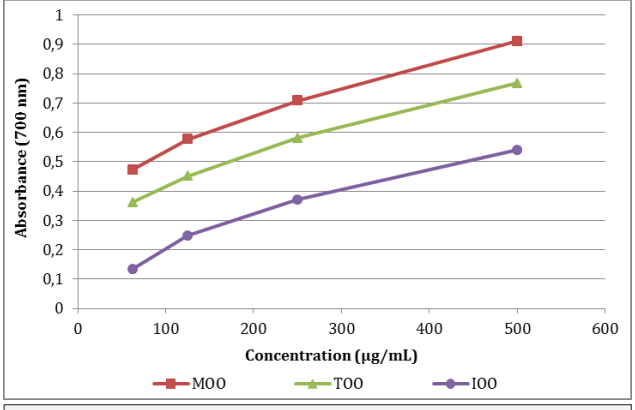

Figure 2. Reducing power of phenolic extracts obtained at different concentrations.

MOO: manual olive oil, TOO: traditional olive oil, IOO: industrial olive oil.

The parameter $PR_{0.5}$ was determined in order to further compare the reducing power. It corresponds to the concentration for which the reduction product gives an absorbance of 0.5 at 700 nm. The OriginPro 8.5 SRI software was used to determine the $PR_{0.5}$ values for each extract with greater accuracy. The values obtained are represented in Table 4.

Table 4. Phenolic extract concentration (µg/mL) of the different oils at A_{700nm}=0.5

Sample	MOO	TOO	IOO
Concentration corresponds to $PR_{0.5}$	78.60	170.00	439.05

MOO: manual olive oil, TOO: traditional olive oil, IOO: industrial olive oil.

Antimicrobial Activity

The results of the inhibition zone diameters of the different olive oils tested on a range of pathogenic bacteria are represented in Table 5. All 3 types of olive oil showed antimicrobial activity on all strains studied with inhibition zones ranging from 12.07 to 15.84 mm. However, modern mill olive oil was found to be inactive against *S. aureus* ATCC 6538 and exhibited lower antimicrobial activity than the traditional olive oil, but without a significant difference only in the case of *C. albicans* ATCC 10231. Activity of the two oils was significantly lowest compared to that provided by the manual extraction.

DISCUSSION

The sensory analysis shows that the three samples of olive oil were of a superior category, which would be due not only to the variety, degree of ripening, climate, cultivation techniques (mainly irrigation) (25), but also because these oils were obtained only by mechanical processes, under conditions that prevented alteration of oil, and which had not undergone any treatment other than washing, decanting, centrifugation and filtration (26). Traditional manual olive oil was extracted from the paste only, without crushing the pit and according to Amirante et al., (27), oils obtained from pitted fruit are more resistant to oxidation than oils obtained by crushing the whole fruit by about 20-25%. The pitting of the olive induces an increase in

Table 5. Diameter (mm) of the inhibition zones obtained with the three olive oils.

Germs - Type of oil	MOO	TOO	IOO
S. aureus ATCC 6538	15.31±0.20	13.59±0.19***	-
B. subtilis ATCC 6633	14.04±0.13	13.00±0.00**	12.07±1.02*
P. aeruginosa ATCC 9027	15.84±0.07	12.81±1.10*	13.07±0.33**
E. coli ATCC 8739	14.23±0.45	13.92±0.26	13.84±0.12
C. albicans ATCC 10231	14.52±0.13	13.37±0.19**	12.42±0.30***

MOO: manual olive oil, TOO: traditional olive oil, IOO: industrial olive oil. -: Absence of inhibition zone. Significance level: *: p<0.05, **: p<0.01, ***: p<0.001.

pleasant aromatic compounds and seems to be responsible for the pronounced fruity aroma.

The results of physicochemical indices indicate that for refractive index, the MOO and IOO samples complied with the Codex Alimentarius (28) standards (1.4677-1.4705) except for the traditional olive oil which slightly exceeded the standards. Its value was influenced by different factors such as free fatty acid content, oxidation level and heat treatment (29).

The values obtained for density were in accordance with the Codex Alimentarius (28) standards (0.910-0.916). This parameter is a function of unsaturation, but also of the state of their oxidation, the more it increases, the more oxidized the oil is (30).

Water and volatile content values were below the maximum limits of IOC (10) (≤0.2%). Cultivar, geographical region, fruit ripening and processing methods are the parameters that influence the volatile composition of olive oil (31).

Regarding the specific extinction coefficients at 232 nm and 270 nm of our samples, they were lower than the maximum limits of IOC (10) (≤2.60 and 0.25, respectively), and confirm the low oxidation and stability of the three oils, especially the MOO sample, which showed the lowest extinction values. Oxidative stability is an important parameter for olive oil quality assessment (32). The specific extinction of a fat is considered a picture of its oxidation state. The higher its extinction at 232 nm, the more peroxidized it is; the higher it is at 270 nm, the richer it is in oxidation by-products (33). Vidal et al. (34) have previously reported the influence of extraction time and temperature on the two extinction coefficients K_{232} and K_{270}.

Free acidity is the main quality factor of olive oil. The values obtained are in accordance with the IOC (10) standards (≤2%). High acidity induces oxidation resulting in rancidity of the oil due to the degradation of unsaturated fatty acids (oleic, linoleic acid) and the production of secondary oxidation compounds (35).

The peroxide value determines the initial oxidation of olive oil, which oxidizes when it enters into contact with air, light, and heat. The values of this index regarding our samples are in accordance with IOC (10) standards (≤20 meq O_2/Kg).

The values of iodine index recorded for the three olive oil samples are in accordance with the Codex Alimentarius (28) standards (75-94).

Determination of the saponification index allows characterization of the molecular weight and the average length of the fatty chain to which it is inversely proportional. The values obtained were in accordance with Codex Alimentarius (28) standards (184-196 mg KOH/g oil).

For chlorophyll and carotenoid contents, a significant difference was noted for the values obtained, as in the case of the other chemical indices. These results would be due to the extraction conditions applied for each type of oil, as demonstrated by the work of Salvador et al. (36) and Psomiadou and Tsimidou (37).

The low levels of chlorophyll obtained during our work (0.24-2.03 mg/Kg) allowed a reduction in the risk of oil oxidation, since chlorophylls are pro-oxidants in the presence of light (38,39). According to the last reference, the chlorophyll concentration can exceed 80 mg/kg for oils obtained from olives in the early stage of ripening and dropping to values of about 2 mg/kg when the fruit is fully ripe. Higher levels of chlorophylls were determined by Baccouri et al. (40) and Sait (41).

The carotenoid contents recorded for our samples were higher compared to those noted by Baccouri et al., (42), Hashempour et al. (43) and Sait (41), who analyzed oils of different varieties (*Chemlal* and *Oleaster*). This difference can be attributed to several factors such as: degree of ripeness of olives, production area, nature of soil, climatic conditions, olive variety and storage time (44,45). These compounds act favorably on oil stability and help protect against oxidative stress, which contributes to make olive oil a healthier product (2,46).

The values of free acidity, peroxide value, specific extinction at 232 nm and 270 nm of our samples, as well as the values of water and volatile matter content, which represent quality criteria according to the IOC and suggest that the manual olive oil is extra virgin olive oil, while traditional oil and industrial one are virgin olive oils. Thus, we can deduce that extraction method also affects several physicochemical properties of olive oil and it is possible de significantly reduce its quality.

Compared to the oils of other oilseeds, olive oil is distinguished by a significant content of monounsaturated oleic acid (more than 60%) and palmitic acid, while linoleic acid is less represented compared to other oilseeds (47). For oleic acid, our results are close to those obtained by Faci et al. (48) who worked on two olive varieties (*Chemlal* and *Azeradj*) from three regions of the wilaya of Tizi-Ouzou (Algeria). They reported contents varying from 61.14% to 67.67% in the *Chemlal* variety crop. Oleic acid behaves differently depending on the stage of maturity. According to Zaringhalami et al. (49), the highest level of oleic acid is observed at early harvest dates and then it gradually decreases as the olives ripen. This behavior is related to changes in the activity of the enzyme oleate desaturase during olive ripening, which converts oleic acid to linoleic acid during ripening (50,51). For palmitic acid and linoleic acid, our results are also comparable to those reported by Faci et al. (48), which vary between 13.12-17.92% for the first fatty acid and 9.12-15.12% for the second. If we consider the percentage of oleic acid (C18:1ω9) alone without taking into account the other quality criteria, our samples can fit into the extra virgin category (55-83%). The ratio of oleic acid/linoleic acid varies according to the degree of maturity. It is used as a stability parameter and several studies have shown that a high ratio indicates a high oxidative stability (52). Our results are close to those reported recently by Douzane et al. (53) and Faci et al. (48) for several olive varieties from central and western Algeria.

The number of phenolic compounds in olive oil is an important factor when evaluating its quality, since natural polyphenols

improve its resistance to oxidation and, in some cases, are responsible for its pronounced bitter taste (51). Yield and total polyphenols content reflect the influence of the treatments applied for each extraction method. These conclusions were confirmed by the determination of phenolic compounds.

Our results are superior to those found by Douzane et al. (54) and Laincer et al. (55), who reported that concentration of polyphenols in the different extra virgin olive oil samples analyzed varies between 109.45-322.18 and 115-420 mg GAE/Kg oil, respectively. Similarly, according to Douzane et al. (53), the concentration of total polyphenols in the different types of virgin olive oil harvested from several regions in Algeria ranges from 46.29-351.45 mg GAE/Kg oil. On the other hand, the levels found in the present study were lower compared to those reported by Medjkouh et al. (56) (710.44-1139.62 mg GAE/Kg oil). According to Marouane et al. (57), the *Chemlal* variety is characterized by moderate polyphenols richness compared to other olive varieties. Therefore, it can be concluded that variation in the phenolic content of olive oil can be attributed to several factors: the influence of climatic and geographical factors, the intra-varietal diversity of olive tree and the stage of maturity, the harvesting period, as well as the conditions of oil extraction (57,58).

Statistical analysis of the polyphenols contents obtained by the Student's t-test did not show a significant difference ($p>0.05$) between the three oils, which reflects that extraction method does not have an effect on the content of these metabolites.

For the antioxidant activity, manual olive oil exhibited the highest $PR_{0.5}$ provided by the lowest polyphenols concentration which was about 78.60 µg/mL, whereas, it was twice to five times higher in the case of the methanolic extract from the traditional (170 µg/mL) and industrial olive oil (439.05 µg/mL), respectively. This reflects a decrease of the antioxidant power of oil induced by the extraction method used.

Taking into account that the content of total polyphenols did not vary significantly between the three oils, it can be deduced that there are some kind of phytochemical (flavonoids, tannins,...) or other metabolites (responsible or participated in the antioxidant activity) which are affected during the extraction process and require specific and additional assays to be identified.

Iron reduction is a rapid, reproducible, and easy to perform antioxidant activity assay. The reducing power is probably due to the presence of hydroxyl groups in the phenolic compounds which can serve as electron donors. Several works have proved the presence of high antioxidant activity exerted by phenolic extracts from different olive oil samples, comparable to reference antioxidants such as BHT, using different assay methods (DPPH Test, β-carotene bleaching test, ABTS test, ...) (55-57). Virgin olive oil is a rich source of natural antioxidants (carotenoids, tocopherols, phenolic compounds) that can act, through different mechanisms, to confer an effective defense system against free radical attack (59). The phenolic compounds participate with about 30% in the oxidative stability of olive oil among other constituents (α-tocopherol, fatty acids, and carotenoids). They are able to give a hydrogen atom to the lipid radical formed during the propagation phase of lipid oxidation (59,60). While the interest of phenolic compounds is mainly related to their antioxidant activity that can last up to 6 days, they also present several other important biological activities *in vivo* and that can be beneficial in the fight against several diseases related to excessive free radical formation (59,61).

Several studies have demonstrated the presence of antibacterial activity of olive oil (21,62,63). In this study, a significant difference was observed in the sensitivity of the tested strains towards the antimicrobial effect of the studied oil samples. Our results clearly illustrate the influence of the extraction method on the antimicrobial activity of olive oil samples. Practices followed during large-scale extraction processes of olive oil reduce such activity compared to the manual one, closely related to their composition.

Comparing our work to those reported by Djedioui (64), who worked on oil of the variety *Rougette de la Mitidja*, the diameters of inhibition were higher with respect to Gram-positive bacteria. However, Laribi (65) reported that *E. coli, P. aeruginosa* and *K. pneumoniae* were the least sensitive species towards the different olive oil extracts. This was in contrast to *S. aureus* species which was sensitive to all the extracts tested. The antibacterial activity may be related to the presence of phenolic compounds such as tannins and flavonoids, which are important antibacterial substances (21,66-68). Olive oil is mainly composed of monounsaturated oleic acid and linoleic acid. Carvalho and Caramujo (69) and Dilika et al. (70) observed a high antibacterial activity of oleic and linoleic acids especially towards Gram-positive strains compared to Gram-negative ones. Bisignano et al. (71), Tuck and Hayball (72) and Cicerale et al. (73) have confirmed the inhibitory effect of hydroxytyrosol towards both Gram-positive and Gram-negative strains. Aldehydes present in olive oil also show antibacterial activity. A study by Carvalho and Caramujo (69) showed that saturated and unsaturated aldehydes in olive oil are effective against both Gram strains. The antibacterial activities tested may also result from a synergy between the compounds present in oil. It is likely that the decrease in activity is due to a change in the properties of the substance responsible for the activity in the presence of other oil compounds, resulting in a combination of two active components (major or minor) acting in synergy, or minor oil components that are also active at low concentrations (52).

CONCLUSION

In the present study, the effect of three extraction methods (manual, traditional and industrial) on the quality and biological properties of olive oil (*Chemlal* variety) was investigated. According to findings related to the sensory and physicochemical parameters, and fatty acid content, oils were classified into two groups-extra virgin and virgin category. The oleic acid content of the manual oil (62.39%) remained higher than the others, which affirms that the oils obtained from pitted fruits and with-

out addition of ingredients have the best quality criteria. Analysis of the polyphenols composition of olive oil samples revealed a higher content (528±12.40 mg GAE/Kg oil) for oil obtained by the manual extraction than the other types, which is characterized also by the best $PR_{0.5}$ provided by the lowest concentration of polyphenols (78.60 µg/mL). In addition, the manual olive oil showed more significant antimicrobial activity on all bacterial and fungal strains studied with inhibition zones greater than 14.04 mm, mainly against *S. aureus* ATCC 6538, *P. aeruginosa* ATCC 9027 and *C. albicans* ATCC 10231. All the properties of the other olive oils studied, and which were obtained using modern extraction processes, were reduced when compared to the manual oil.

As a conclusion, the manual method of extraction preserves the best quality of oil on the sensory and physicochemical level with more interesting nutritional and biological effects.

Peer Review: Externally peer-reviewed.

Author Contributions: Conception/Design of Study- S.M., S.B.; Data Acquisition- S.M.; Data Analysis/Interpretation- S.M., S.B., D.D.F.; Drafting Manuscript- S.M., S.B., D.D.F.; Critical Revision of Manuscript- S.M., S.B., O.S.; Final Approval and Accountability- S.M., S.B., O.S., D.D.F.

Conflict of Interest: Authors declared no conflict of interest.

Financial Disclosure: Authors declared no financial support.

REFERENCES

1. Serreli G, Deiana M. Biological relevance of extra virgin olive oil polyphenols metabolites. Antioxidants 2018; 7(12): 170.
2. Otero P, Garcia-Oliveira P, Carpena M, Barral-Martinez M, Chamorro F, Echave J, et al. Applications of by-products from the olive oil processing: Revalorization strategies based on target molecules and green extraction technologies. Trends Food Sci Technol 2021; 116: 1084-104.
3. Petrakis C. Olive oil extraction. Boskou D, editor. Olive Oil: Chemistry and Technology. 2nd ed. AOCS Press; 2006.p.191-23.
4. Souilem S, El-Abbassi A, Kiai H, Hafidi A, Sayadi S, Galanakis, CM. Olive oil production sector: Environmental effects and sustainability challenges. Galanakis CM, editor. Olive mill waste. Academic Press; 2017.p.1-28.
5. Saffar Taluri S, Jafari SM, Bahrami A. Evaluation of changes in the quality of extracted oil from olive fruits stored under different temperatures and time intervals. Sci Rep 2019; 9(1): 19688.
6. Huang CL, Sumpio BE. Olive Oil, the Mediterranean Diet, and Cardiovascular Health. J. Am. Coll. Surg 2008; 207(3): 407-16.
7. Titouh K, Mazari A, Aït Meziane MZ. Contribution to improvement of the traditional extraction of olive oil by pressure from whole and stoned olives by addition of a co-adjuvant (talc). OCL 2020; 27, 23.
8. Acar A, Arslan D. Some technological pretreatments applied during olive oil extraction: Impacts on quality parameters and minor constituents. Glob J Agric Innov Res Dev 2017; 4: 47-7.
9. International Olive Oil Council (IOC). Sensory analysis of olive oil: method of organoleptic evaluation of virgin olive oil. COI/T.20/ Doc. /Rév.10: 2018. Report N° 15.
10. International Olive Oil Council (IOC). Trade standard applicable to olive oils and olive-pomace oils. COI/T.15/NC /Rév.14: 2019. Report N° 3.
11. International Organization for Standardization (ISO). Animal and vegetable fats and oils - Determination of refractive index. Ref. N°.EN ISO 6320:2000/AC: 2006 D/E/F.
12. Journal officiel de la république algérienne (JORA). Méthodes officielles d'analyses physico-chimiques relatives aux corps gras d'origine animales et végétales (*Official Journal of the Algerian Republic (JORA). Official methods of physico-chemical analysis relating to fatty substances of animal and vegetable origin*): 2011. Report N° 64.
13. International Olive Oil Council (IOC). Spectrophotometer investigation in the ultraviolet, COI/T.20/ Doc./Rev.3: 2015. Report N° 19.
14. Règlement relatif aux caractéristiques des huiles d'olive et des huiles de grignons d'olive ainsi qu'aux méthodes d'analyse y afférentes (JOL 248 du 5.9.1991, p : 114): 1991. Report N° 2568/91.
15. French Association for Standardization (AFNOR). Fats – oilseeds – derived products, 4th ed, Paris: 1984. p: 459.
16. Minguez-Mosquera IM, Rejano-Navarro L, Gandul-Rojas B, Sanchez Gomez AH, Garrido-Fernandez J. Color-pigment correlation in virgin olive oil. J Am Oil Chem Soc 1991; 68(5): 33-6.
17. International Olive Oil Council (IOC). Préparation des esters méthyliques d'acides gras de l'huile d'olive et de l'huile de grignons d'olive. Conseil Oléicole International. COI/T.20/Doc.: 2001. Report No 24.
18. Pirisi FM, Cabras P, Cao CF, Migliorini M, Muggelli M. Phenolic compounds in virgin olive oil. 2. Reappraisal of the extraction, HPLC separation, and quantification procedures. J Agric Food Chem 2000; 48(4): 1191-916.
19. Singleton VL, Rossi JA. Colorimetry of total phenolics with phosphomolybdic-phosphotungstic acid reagents. Am. J. Enol. Vitic 1965; 16(3): 144-58.
20. Topçu G, Ay M, Bilici A, Sarıkürkcü C, Öztürk M, Ulubelen A. A new flavone from antioxidant extracts of *Pistacia terebinthus*. Food Chem 2007; 103(3): 816-22.
21. Medina E, de Castro A, Romero C, Brenes M. Comparison of the concentrations of phenolic compounds in olive oils and other plant oils: Correlation with antimicrobial activity. J Agric Food Chem 2006; 54(14): 4954-961.
22. Bouzid W, Yahia M., Abdeddaim M., Aberkane MC, Ayachi A. Évaluation de l'activité antioxydante et antimicrobienne des extraits de l'aubépine monogyne. Leban Sci J 2011; 12(1): 59-69.
23. Ponce AG, Fritz R, del Valle C, Roura SI. Antimicrobial activity of essential oils on the native microflora of organic Swiss chard. LWT. Food Sci. Technol. J 2003; 36(7): 679-84.
24. Ouelhadj A, Salem LA, Djenane D. Activité antibactérienne de l'huile essentielle de *Pelargonium x asperum* et son potentiel synergique avec la nisine. Phytothérapie 2019; 17(3): 140-8.
25. Bianchi G. Extraction systems and olive oil. OCL 1999; 6(1): 49-55.
26. Pouyet B, Ollivier V. Réglementations sur l'étiquetage et la présentation des huiles d'olive. OCL 2014; 21(5): D508.
27. Amirante P, Clodoveo ML, Dugo G, Leone A, Tamborrino A. Advance technology in virgin olive oil production from traditional and de-stoned pastes: Influence of the introduction of a heat exchanger on oil quality. Food Chem 2006; 98(4): 797-05.
28. Codex Alimentarius. Norme pour les huiles d'olive et les huiles de grignons d'olive. CODEX STAN 33-1981 Adoptée en 1981. Révisée en 1989, 2003, 2015, 2017. Amendée en 2009, 2013. Codex STAN 33-1981. Rév 2017.
29. Santos OV, Corrêa NCF, Soares FASM, Gioielli LA, Costa CEF, Lannes SCS. Chemical evaluation and thermal behavior of Brazil nut oil obtained by different extraction processes. Food Res Int 2012; 47(2): 253-8.
30. Sekour B. Phyto-protection de l'huile d'olive vierge par ajout des plantes végétales (thym, ail, romarin) (*Phyto-protection of virgin olive oil by adding vegetable plants (thyme, garlic, rosemary*). University of Boumerdes, Magister thesis. 2012.

31. Benincasa C, De Nino A, Lombardo N, Perri E, Sindona G, Tagarelli A. Assay of aroma active components of virgin olive oils from Southern Italian Regions by SPME-GC/Ion Trap Mass Spectrometry. J Agric Food Chem 2003; 51(3):733-41.
32. Essiari M, Zouhair R, Chimi H. Contribution à l'étude de la typicité des huiles d'olives vierges produites dans la région de Sais (Maroc). Olivae 2014; 119: 8-22.
33. Abdullah F, Mohammed E. Modélisation de la répartition du transfert des métaux lourds et des oligoéléments dans les sols forestiers, l'huile d'argan et dans les différentes parties d'arganier (*Modeling of the distribution of the transfer of heavy metals and trace elements in forest soils, argan oil and in the different parts of the argan tree*). Mohammed V-Agdal University, Doctoral thesis. 2012.
34. Vidal AM, Alcalá S, de Torres A, Moya M, Espínola F. Industrial production of a balanced virgin olive oil. LWT. 2018;97:588–96.
35. Meftah H, Latrache H, Hamadi F, Hanine H, Zahir H,. El louali M. Comparaison des caractéristiques physicochimiques des huiles d'olives issus de différentes zones de la région Tadla Azilal (Maroc) (*Comparison of the physico-chemical characteristics of the olive oil coming from different zones in Tadla Azilal area (Morocco*). J Mater Environ Sci 2014; 5(2): 641-6.
36. Salvador MD, Aranda F, Gómez-Alonso S, Fregapane G. Cornicabra virgin olive oil: a study of five crop seasons. Composition, quality and oxidative stability. Food Chem 2001; 74(3): 267-74.
37. Psomiadou E, Tsimidou M. Pigments in Greek virgin olive oils: occurrence and levels. J Sci Food Agric 2001; 81(7): 640-7.
38. Giuffrida D, Salvo F, Salvo A, Pera LL, Dugo G. Pigments composition in monovarietal virgin olive oils from various sicilian olive varieties. Food Chem 2007; 101(2): 833-7.
39. Tanouti K, Elamrani A, Serghini-Caid H, khalid A, Bahetta Y, Benali A, et al. Caractérisation d'huiles d'olive produites dans des coopératives pilotes (Lakrarma et Kenine) au niveau du Maroc Oriental. Les Technologies De Laboratoire 2010; 5(18): 18-26.
40. Baccouri B, Guerfel M, Zarrouk W, Taamalli W, Daoud D, Zarrouk M. Wild olive (*Olea europaea* L.) selection for quality oil production. J. Food Biochem 2011; 35(1): 161-76.
41. Sait S. Activités antioxydante et antibactérienne des huiles d'oléastres (*Olea europaea* var. *oleaster*) de la région de Béjaïa (*Antioxidant and antibacterial activities of oleaster oils (Olea europaea var. oleaster) from the Béjaïa region*). University of Bejaia, Magister thesis. 2012.
42. Baccouri B, Temime SB, Taamalli W, Daoud D, M'Sallem M, Zarrouk M. Analytical characteristics of virgin olive oils from two new varieties obtained by controlled crossing on *Meski* variety. J Food Lipids 2007; 14(1): 19-34.
43. Hashempour A, Ghazvini RF, Bakhshi D, Sanam SA. Fatty acids composition and pigments changing of virgin olive oil (*Olea europea L.*) in five cultivars grown in Iran. Aust J Crop Sci 2010; 4(4): 258-63.
44. Allalout A, Krichène D, Methenni K, Taamalli A, Oueslati I, Daoud D, et al. Characterization of virgin olive oil from Super Intensive Spanish and Greek varieties grown in northern Tunisia. Scientia Horticulturae 2009;120(1): 77-83.
45. Tanouti K, Serghini-Caid H, Chaieb E, Benali A, Harkous M, Elamrani A. Amélioration qualitative d'huiles d'olive produites dans le Maroc oriental. Les Technologies de Laboratoire. 2011; 6(22): 1-12.
46. Viljanen K, Sundberg S, Ohshima T, Heinonen M. Carotenoids as antioxidants to prevent photooxidation. Eur J Lipid Sci Technol 2002; 104(6): 353-9.
47. Hadj Sadok T, Rebiha K, Teriki D. Caractérisation physico-chimique et organoleptique des huiles d'olive vièrges de quelques variétés algériennes. Agrobiologia 2018; 8(1): 706-18.
48. Faci M, Hedjal M, Douzane M, Sevim D, Köseoğlu O, Tamendjari A. Locations effects on the quality of *Chemlal* and *Azeradj* olives grown in Algeria. J Am Oil Chem Soc 2021; 98(5): 551-66.
49. Zaringhalami S, Ebrahimi M, Piravi Vanak Z, Ganjloo A. Effects of cultivar and ripening stage of Iranian olive fruit on bioactive compounds and antioxidant activity of its virgin oil. Int. Food Res. J 2015; 22(5): 1961-7.
50. Gutiérrez F, Jímenez B, Ruíz A, Albi MA. Effect of olive ripeness on the oxidative stability of virgin olive oil extracted from the varieties *Picual* and *Hojiblanca* and on the different components involved. J Agric Food Chem 1999; 47(1): 121-7.
51. Baccouri O, Guerfel M, Baccouri B, Cerretani L, Bendini A, Lercker G, et al. Chemical composition and oxidative stability of Tunisian monovarietal virgin olive oils with regard to fruit ripening. Food Chem 2008; 109(4): 743-54.
52. Matos L, Pereira J, Andrade P, Seabra R, Oliveira M. Evaluation of a numerical method to predict the polyphenols content in monovarietal olive oils. Food Chem 2007; 102(3): 976-83.
53. Douzane M, Daas MS, Meribai A, Guezil AH, Abdi A, Tamendjari A. Physico-chemical and sensory evaluation of virgin olive oils from several Algerian olive-growing regions. OCL 2021; 28: 55.
54. Douzane M, Tamendjari A, Abdi AK, Daas MS, Mehdid F, Bellal MM. Phenolic compounds in mono-cultivar extra virgin olive oils from Algeria. Grasas y Aceites 2013; 64(3): 285-94.
55. Laincer F, Laribi R, Tamendjari A, Arrar L, Rovellini P, Venturini S. Olive oils from Algeria: Phenolic compounds, antioxidant and antibacterial activities. Grasas y Aceites 2014; 65(1): e001.
56. Medjkouh L, Tamendjari A, Keciri S, Santos J, Nunes MA, Oliveira MBPP. The effect of the olive fruit fly (*Bactrocera oleae*) on quality parameters, and antioxidant and antibacterial activities of olive oil. Food Funct 2016; 7(6): 2780-8.
57. Merouane A, Noui A, Medjahed H, Nedjari Benhadj Ali K, Saadi A. Activité antioxydante des composés phénoliques d'huile d'olive extraite par méthode traditionnelle. Int J Bio Chem Sci 2015; 8(4): 1865-70.
58. Ranalli A, Ferrante ML, De Mattia G, Costantini N. Analytical evaluation of virgin olive oil of first and second extraction. J Agric Food Chem 1999; 47(2): 417-24.
59. Morelló JR, Motilva MJ, Tovar MJ, Romero MP. Changes in commercial virgin olive oil (cv *Arbequina*) during storage, with special emphasis on the phenolic fraction. Food Chem 2004; 85(3): 357-64.
60. Aparicio R, Roda L, Albi MA, Gutiérrez F. Effect of various compounds on virgin olive oil stability measured by Rancimat. J Agric Food Chem 1999; 47(10): 4150-5.
61. Benlemlih M, Ghanam J, Joyeux H. Polyphénols d'huile d'olive, trésors santé!: polyphénols aux actions antioxydantes, anti-inflammatoires, anticancéreuses, anti-vieillissement et protectrices cardio-vasculaires. 2nd ed, Medicatrix, France; 2016. p.208.
62. Tunçel G, Nergiz C. Antimicrobial effect of some olive phenols in a laboratory medium. Lett Appl Microbiol 1993; 17(6): 300-12.
63. Melguizo-Rodríguez L, Illescas-Montes R, Costela-Ruiz VJ, Ramos-Torrecillas J, de Luna-Bertos E, García-Martínez O, et al. Antimicrobial properties of olive oil phenolic compounds and their regenerative capacity towards fibroblast cells. J Tissue Viability 2021; 30(3): 372-78.
64. Djedioui A. Caractérisation d'une huile d'olive vierge algérienne d'une variété cultivée dans la région de Skikda (*Characterization of an Algerian virgin olive oil of a variety grown in the Skikda region*). University of Annaba, Doctoral thesis. 2018.
65. Laribi R. Les composés phénoliques de quelques variétés de l'huile algériennes: identification et propriétés (*The phenolic compounds of some varieties of Algerian oil: identification and properties*). University of Setif, Doctoral thesis. 2015.

66. Romero C, Medina E, Vargas J, Brenes M, De Castro A. *In vitro* activity of olive oil polyphenols against *Helicobacter pylori*. J Agric Food Chem 2007; 55(3): 680-6.
67. Karaosmanoglu H, Soyer F, Ozen B, Tokatli F. Antimicrobial and antioxidant activities of Turkish extra virgin olive oils. J Agric Food Chem 2010; 58(14): 8238-45.
68. Toty AA, Guessennd N, Bahi C, Kra AK, Tokore DA, Dosso M. Évaluation *in-vitro* de l'activité antibactérienne de l'extrait aqueux de l'écorce de tronc de *Harungana madagascariensis* sur la croissance de souches multi-résistantes. Bulletin de la société royale des sciences de Liège 2013; 82: 12-21.
69. Carvalho CCCR, Caramujo MJ. Ancient procedures for the High-Tech World: Health benefits and antimicrobial compounds from the Mediterranean Empires. TOBIOTJ 2008; 2(1): 235-46.
70. Dilika F, Bremner PD, Meyer JJM. Antibacterial activity of linoleic and oleic acids isolated from *Helichrysum pedunculatum*: a plant used during circumcision rites. Fitoterapia 2000; 71(4): 450-2.
71. Bisignano G, Tomaino A, Cascio RL, Crisafi G, Uccella N, Saija A. On the *in-vitro* antimicrobial activity of oleuropein and hydroxytyrosol. J. Pharm. Pharmacol 2010; 51(8): 971-74.
72. Tuck KL, Hayball PJ. Major phenolic compounds in olive oil: metabolism and health effects. J. Nutr. Biochem 2002; 13(11): 636-44.
73. Cicerale S, Conlan XA, Barnett NW, Keast RSJ. The concentration of oleocanthal in olive oil waste. Nat. Prod. Res 2011; 25(5): 542-8.

ISTANBUL UNIVERSITY PRESS

RESEARCH ARTICLE

Eur J Biol 2022; 81(1): 68-84

Floristic, Ecological and Phytogeographic Study of the Wamba Valley Massif Forest in Kwango in DRC

Ntalakwa Makolo Théophane, Mayanu Pemba Bibiche, Kidikwadi Tango Eustache, Azangidi Mapwama Jean-Pierre, Belesi Katula Honoré, Lubini Ayingweu Constantin

University of Kinshasa, Department of Environmental Sciences, Faculty of Sciences, Laboratory of Systemics, Biodiversity, Nature Conservation and Endogenous Knowledge (LSBCSE), DR Congo

ORCID IDs of the authors: N.M.T. 0000-0001-2345-6991; M.P.B. 0000-0002-2345-6992; K.T.E. 0000-0003-2345-6993; A.M.J.P. 0000-0004-2345-6994; B.K.H. 0000-0005-2345-6995; L.A.C. 0000-0006-2345-6996

Please cite this article as: Théophane NM, Bibiche MP, Eustache KT, Jean-Pierre AM, Honoré BK, Constantin LA. Floristic, Ecological and Phytogeographic Study of the Wamba Valley Massif Forest in Kwango in DRC. Eur J Biol 2022; 81(1): 68-84. DOI: 10.26650/EurJBiol.2022.1073708

ABSTRACT

Objective: The Wamba valley is one of the rare forest areas of Kwango and Bagata. This research aims to understand the phytodiversity of this area in order to have a database necessary for the rational management of this area's natural resources. It means also to characterize the floristic, ecological, and phytogeiographic parameters of the study area.

Materials and Methods: The botanical samples collected in the study area represent the biological material that was used for identification species of the forest under study. To achieve the objectives pursued, we carried out floristic inventories, supported by the systematic sampling technique. The progress of this study is as follows: field visits and choice of study sites; collection of samples and identification of the material collected; ecological study and phytogeographic spectra of the identified species.

Results: The floristic inventory noted the presence of 192 species grouped into 160 genera and 58 families. This flora is rich and diverse. The recognized species of this forest area belong more to the family of *Fabaceae*, and *Rubiaceae*. The morphological structure of the species reveals the abundance of phanerophyte species while the chorological aspect remains dominated by Guinean-Congolese elements.

Conclusion: The study environment is part of the Guinean-Congolese-Zambézian transition zone. This area is characterized by the mixture of species from the Guineo-Congolese regional center of endemism and Zambezian species. This study contributed to the knowledge of the phytodiversity of the area.

Keywords: Flora, ecology, phytogeography, massif forest, Wamba valley

INTRODUCTION

Forests and wooded herbaceous formations represent in most of the humid and subhumid regions of the tropical world a type of natural vegetation. Their importance is great for a variety of reasons, not the least of which is meeting wood and food needs; they also play an essential role on the ecological, economic, and socio-cultural level. Forests contribute to the decrease in the concentration of atmospheric carbon dioxide, necessary for fighting against climate change. For developing countries, the rational use of the resources offered by tropical forests and the development of the rural areas to which they correspond are at the heart of development policy planning (1,2).

Local and regional forest cover dynamics influence climate, biodiversity, and environmental services. National and international decision-makers must be able to rely on reliable, up-to-date, and verifiable data

Corresponding Author: Ntalakwa Makolo Théophane E-mail: ntalakwakrios@gmail.com
Submitted: 15.02.2022 • **Revision Requested:** 25.04.2022 • **Last Revision Received:** 11.05.2022 • **Accepted:** 01.06.2022 • **Published Online:** 29.06.2022

to develop and monitor the implementation of forest policies as well as to provide the relevant information required at the level of international conventions (3).

Indeed, the Wamba Valley presents an ecosystems diversity linked to its ecological diversity conditions. Its vegetation includes gallery forests, generally degraded, and shrubby savannahs, sometimes low grassy savannahs. The flora of the study area remains little known. This region of the DRC is experiencing significant demographic growth; the population is generally poor. There are not enough social opportunities, and the population only has logging as their main activity. This exclusive dependence on the forest is likely to have negative impacts on it. This is why, as part of our research, we are committed to the study of the flora, ecology, and phytogeography of the Wamba Valley massif forest in Kwango in the DRC, more precisely the gallery forests around the city of Kenge 2.

MATERIALS AND METHODS

Study Environment

Our research was carried out in the massif forest around Kenge 2 located on the left bank of the Wamba River. It is located at 04° 51'14.5" south latitude and 016°57'0.3" east longitude at an altitude of 450 m. The following map locates the area under study (Figure 1).

Climatic Aspects of the Area

The Wamba Valley enjoys a climate that belongs to the AW4 type according to the Koppen classification criteria. The main parameters of this climate type can be summarized as follows: the annual balance of total radiation is 70 to 75 kcal/cm^2, the relative insolation is around 40% during the rainy season and 70% during the months of June, July, and August (i.e., the dry season). The average annual rainfall is more or less 1600 mm. It reaches 1700mm in the center-east of the region and 1500mm in the southern part. The average temperature of the coldest month is above 18°C (4).

Material

The collections of botanical samples in the gallery forests of the Wamba Valley were carried out in order to carry out scientific identifications and constitute a reference herbarium.

This material was collected and deposited at the INERA herbarium at the Faculty of Sciences, University of Kinshasa, an extension of the national herbarium based in Yangambi. The internationally recognized code: IUK (INERA, University of Kinshasa). The following equipment was used: 1 GPS, 1 clinometer or a graduated pole, 1 magnifying glass and binoculars, 1 tape of 50 m and 1 tape of 30 m, stakes or milestones (markers), inventory sheets and pencils, and a field notebook.

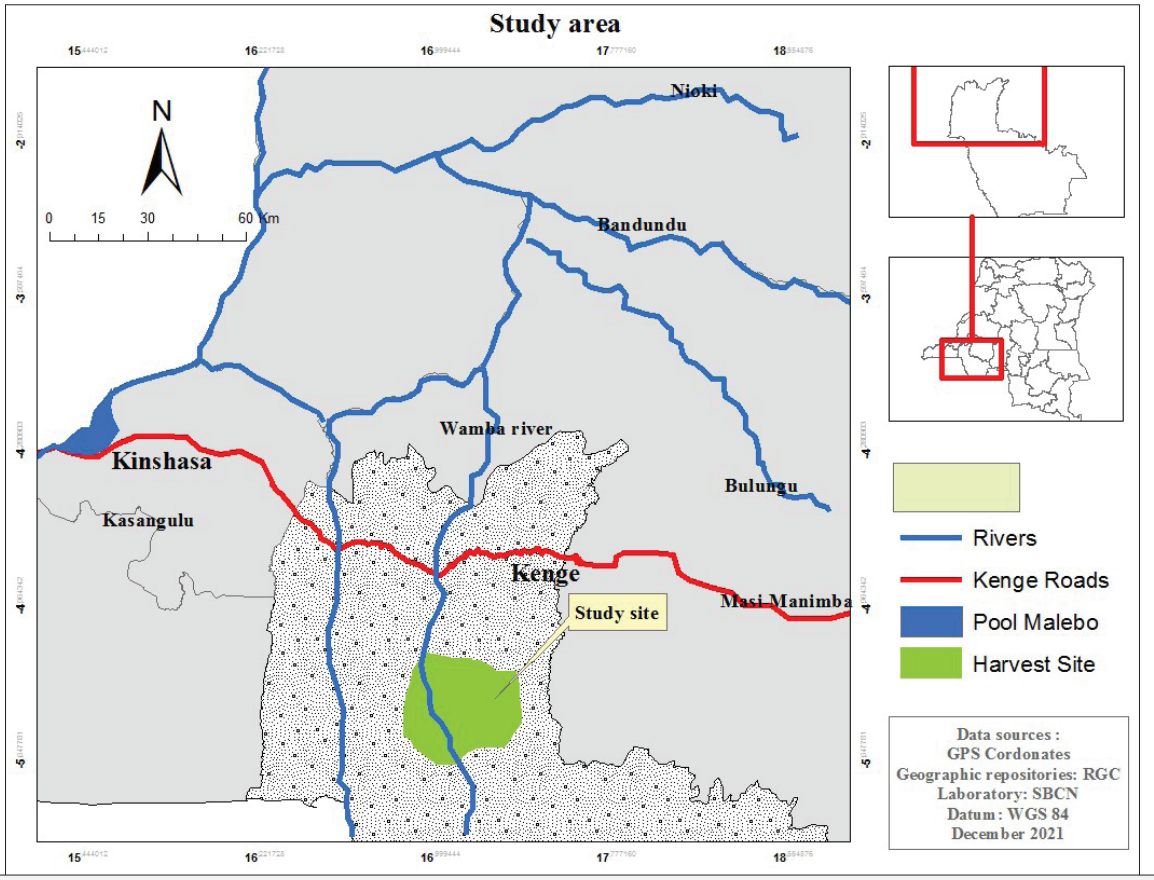

Figure 1. Presentation of the study area.

Methods

We used the observation method and floristic inventories. Our study concerns the floristic, ecological, and phytogeographical aspects of Wamba vegetation. Several research works on the floristic, ecological, and phytogeographical study have been carried out by several authors (5-8).

More specifically, it is the complete or foot-by-foot inventory method using the systematic sampling technique. The principle of this inventory type is to cover the entire forest (9). In practice, the progress of the methodological approach is presented as follows: field visits and choice of study sites; collection of samples and identification of the material collected; and study of the ecological and phytogeographic spectra of the identified species.

Field Visits and Selection of Study Sites

To make the choice on the site and the options to be raised for the type of study to be carried out in this area, a preliminary visit to the field was carried out. Surveys were also carried out in most of the Wamba valley, Kenge 2 site, and Fayala, which still contains some massif forests which include several species of local flora. To another extent, field surveys were also done using the Google Earth remote sensing tool.

Samples and Inventory Devices

This work relates to the floristic, ecological, and phytogeographical study, foresters use standard surfaces of one hectare or 10,000 m^2 as the minimum area for forest inventory (10-12). The Wamba gallery forest has an area of 2000 hectares, we drew a sample of 0.001% (9,11,13). Observations and inventories of species were carried out in an area of 20,000 m^2 or 2 hectares. Each hectare was subdivided into four sampled forest plots of 2500 m^2 with each more than 100m apart. We proceeded to the random establishment in the forest's one hectare plot playing the role of the study field experimental device. Thus, we first proceeded to measure and open four peripheral paths delimiting this hectare; then inside it, we measured and opened two main paths of more or less 0.5 m wide and 100 m long which intersect at 50 m, thus forming 4 sub plots of 2500 m^2 each, i.e. 50 m x 50 m. Figure 2 represents the inventory device installed in the study area.

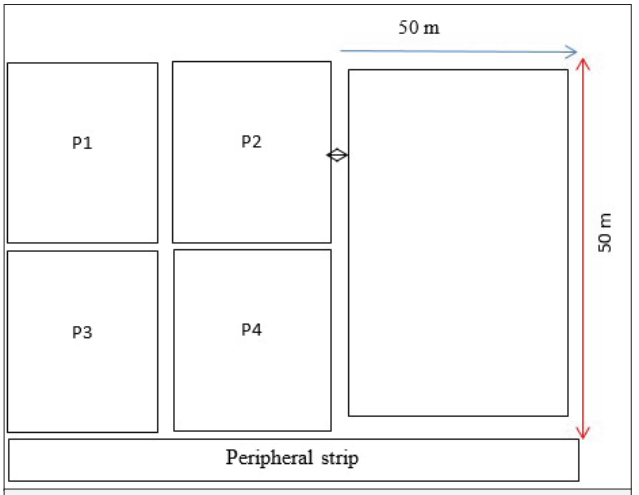

Figure 2. Presentation of inventory system in the study area.

Identification of Harvested Material

The herbarium specimens gathered during the prospecting on the ground were the subject of scientific identification using the flora of central Africa (vol. 1 to 10 and fascicles) and Flora of West Tropical Africa (vol. 1 to 10 and booklets) (14,15). Other samples have been identified by comparison with the herbarium of references to the herbarium of the INERA, Code: IUK (Inera, University of Kinshasa). This identification was made according to the current classification of the APG II, III, and IV (1998, 2003). Exudates and tree slices were also considered for species identifications. If other botanical materials that can be used for identifications are not available, you can use exudats, slices, etc. (16).

Analysis of Ecological Aspects

Ecological Groups of Species

The ecological requirements of the groups (i.e., of an ecosystem's species) can be detected by the ecological characteristics of the station (temperature, atmospheric humidity, substrate, light) (5). The ecological group brings together all the species which approximately agree in their ecological constitution and therefore in their behaviour vis-à-vis the main factors of the station.

Light and shade are essential to the development of a plant, and the competition for these resources is permanent during its life. The classification of different ecological groups of the stations studied was mainly based on mesological factors: habitat, substrate, light, and atmospheric humidity; according to the aspirations of Lubini (6). We also talk about the temperament of the species. To do this, several categories of ecological group of species have been retained. These are: helophilic species (Helio), nitrophilous species (Nit), hygro-helio-nitrophilic species (Hygr-Nit-Helio), hemi-sciaphilic species (Hémi-Scia), hygro-heliophilic species (Hygr-Helio), psammophiles (Psa), hygro-sciaphile group (Hygr-Scia), meso-hygrophile (Més-Hygro), mesophiles (Més), and sciaphile (Scia).

Bioclimatic Characteristics

Precipitation and temperature are the ecological factors. The climatic factors of a station are more decisive and influence the evolution of a type of vegetation in a given territory (5, 17-19). Climatic data for the study area were collected and recorded at the Kenge metrological station. These data made it possible to establish the ombrothermic diagram using the BecyClimate software.

Soil Analysis

Soil analysis methods have been tested by several researchers (20). As far as we are concerned, we have set up a soil pit of 1.5 m^3. Soil samples were taken from different horizons. The soils sampled were dried in the open air for 10 days and sieved with a 2 mm sieve to remove coarse particles. The analyzes focused more on the particle size, the hydrogen potential and the cation exchange capacity. These analyzes were carried out at sciences faculty's pedology laboratory, University of Kinshasa.

Ecological Spectra

Biological Types

The biological spectra of a grouping constitute a relative representation of the biological types. The biologicaltypes spectra analysis provides valuable information on the structure, physiognomy and adaptive strategies of the community (19,21-23).

To do this, the biological types considered in this research are mainly those defined according to the classification of Raunkiaer (24), extendable to tropical regions (5,19,25-35).

Types of Diaspores

The spectra diaspores types provide information on the nature of the diaspores of the species, the mode of dissemination, and the possible disseminating agents. In this research we consider two diaspores classification types: the morphological classification of Dansereau and Lems (30), commonly used by Lubini (5), and Masens (36), Evrad (37), and the ecomorphological classification of Molinier and Muller (35), which focuses more on the possible disseminating agent. In autochorus species of the ecomorphological classification, diaspores do not show obvious adaptations to any external dispersal agent (10, 38).

Types of Leaf Sizes

The leaf sizes type spectra were inspired by the system of Raunkiaer (5,19,24,36). This classification takes leaf dimensions into account. These are therefore the following types: leptophylls (lepto), nanophylls (Nano), microphylls (Micro), mesophylls (Meso), and macrophylls (Macro) or even megaphylls.

Phytogeographic Analysis of the Flora

Harari (19) specifies that the chorological spectra make it possible to give valuable indications on the origin and on the area of different species group distribution. This information in turn makes it possible to define chorological affinities at the local, sub-regional, regional, etc. scale. To do so, the following categories are recognized:

Species with a very wide distribution that are widespread in several parts of the world, namely: cosmopolitan species (Cos), pantropical species (Pan), Afroneotropical species (Ant), and paleo-tropical species (Pal).

African species with wide distribution other than the regional species. They are widespread in several phytogeographical regions of the continent; they are precisely continental Afro-tropical (AT) species.

1. Regional species confined to a single phytogeographical entity

These include Guineo-Congolese species and species from the former Sudano-Zambezi region, which White (39-41) split into two regional centers of endemism Sudanese and Zambezian. As a result, we then distinguish: species from the regional center of Guinea-Congolese endemism. e.g.: *Fillaeopsis discophora*; omni-Guineo-Congolese species (GC): observed throughout the Guinea-Congolese region, e.g.: *Pterygota macrocarpa*; Lower Guinean species (BG) e.g.: *Pseudospondias microcarpa*; Bas-Guineo-Congolese species (BGC): present in the Lower Guinean and Congolese sub-centres, e.g.: *Afrocalanthea rhizantha*; and species from the Congolese sub-center (C) as defined by White (40) and Lubini (42). e.g.: *Anthocleista schweinfurthii*.

2. Species of regional transition zones

Guinean-Congolese-Zambézian species: species found in the Guinean-Congolese-Zambézian transition zone. e.g.: *Rothmania whitfieldii*.

RESULTS

In this section, we present the results of the floristic, ecological and phytogeographical study of the Wamba Valley massif forest in Kwango in the DRC. These results relate to observations made in the forest massif around the Kinsanga River and in the Wamba River basin in Kenge city vicinity. Kinsanga is a tributary of the Wamba River. The study site is part of the Guineo-Congolese-Zambézi transition zone.

Floristic Composition of the Wamba Valley Forest Flora (Kenge 2) in the DRC

The forest flora of this area is rich and diversified. Examination of the whole flora reveals the presence of 192 species, subspecies, and varieties divided into 160 genera and 58 families. The detailed analysis of the inventoried species systematic groups appears in Table 1.

Table 1. Analysis of systematic groups of species.

Systematic groups	Number of families	Number of genera	Number of species	%
1. Ptéridophytes	3	3	3	1.5
2. Spermatophytes				
Pynophyta (Gymnosperm)	1	1	1	0.5
Magnolophyta (Angiosperm)				
Magnoliopsida (Dicotyledonous)	43	130	157	81.7
Liliopsida (Monocotyledon)	11	26	31	16.1
Total	58	160	192	100

The Table 1 above on the analysis of the species systematic groups shows the abundance of spermatophytes magnolophyta (angiosperms) magnoliopsida (dicots) (i.e., 81.7% of species), followed by angiosperms monocotyledons spermatophytes (i.e., 16.1%) with the others groups being less represented.

Pteridophytes

In total, 3 species of pteridophytes were identified in the study environment. This taxonomic group forms 1.5% of the species that constitute the phytodiversity of this massif forest. They are cosmopolitan perennial herbs, edible by local people. Among these species, *Pteridium aquilinum* represents food and economic values insofar as its young shoots are consumed as a vegetable and can be the subject of small trade in both rural and urban areas.

Spermatophytes

Two systematic groups characterize the spermatophyte flora in this massif forest. These represent 98.5% of the species inventoried.

The pynophyta (or gymnosperms)

In this category, only one species (*Gnetum africanum*) was inventoried and this constitutes 0.5% of the species of the study area massif forest. This species is subject to strong human pressure because of its nutritional and economic values. The leaves of this species are found everywhere in the various markets of the DRC, in rural and urban areas. This strong pressure on the resource represents a threat to the survival of the species in the study area.

Magnolophyta (or angiosperms)

This group characterizes the majority of the species identified and represents 98% of the forest flora species in the study area. In this group; magnoliopsida (or dicotyledons) represent 81.7% of species while liliopsida (or monocotyledons) constitute 16.1% of the studied flora species.

Specific Diversity

Species richness gives an idea of the inventoried species diversity in a given environment. Thus, the inventory carried out in the Wamba Valley massif forest (Kenge 2) shows that this massif is rich and contains within it an important diversity. Of all these species, we note the dominance of species of the Fabaceae family with 30 species, followed by the Rubiaceae family with 18 species, the Euphorbiaceae family, Malvaceae and Apocynaceae with 9 species for each of the families, and the Marantaceae family with 8 species. The other families are less represented. The complete floristic list is given in the Table 2.

Table 2. Floristic composition of the forest massif studied (final list of all species inventoried and their ecological spectra).

Family	Genus and species	DP	TB	TD	TF	Ecol.g
Acanthaceae	*Anonidium mannii Diels.*	*BGC*	*MgPh*	*Sar*	*Meso*	*Scia*
Adianthaceae	*Antrocaryon nannanii De wild.*	*BG*	*MsPh*	*Sar*	*Meso*	*Helio*
Anacardiaceae	*Greenwayodendron swaviolens Verdc.*	*BG*	*MgPh*	*Sar*	*Meso*	*Helio*
Anacardiaceae	*Pseudospondias microcarpa Engl.*	*AT*	*MsPh*	*Sar*	*Meso*	*Helio*
Annonaceae	*Pteris similis Kuhn.*	*GC*	*Grh*	*Scl*	*Meso*	*Hemi-Helio*
Annonaceae	*Thomandersia butayei De Wild.*	*BGC*	*NPh*	*Bal*	*Meso*	*Hgr-Scia*
Annonaceae	*Uvariospis congensis Robyns et Ghesp.*	*CGC*	*MsPh*	*Sar*	*Meso*	*Hgr-Scia*
Annonaceae	*Xylopia aethiopica (Dunal) A. Rich.*	*AT*	*MsPh*	*Sar*	*Micro*	*Hemi-Helio*
Apocynaceae/Apocynioideae	*Alstonia congolensis. Engl.*	*GC*	*MgPh*	*Pog*	*Meso*	*Helio*
Apocynaceae/Apocynioideae	*Dewevrella cochliostema De wild.*	*CGC*	*Lph*	*Sar*	*Micro*	*Hgr-H-Scia*
Apocynaceae/Apocynioideae	*Funtumia africana (Benth.) Stapf.*	*GC*	*MsPh*	*Sar*	*Meso*	*Hemi-Scia*
Apocynaceae/Apocynioideae	*Landolphia jumullei Pichon*	*BGC*	*Lph*	*Sar*	*Meso*	*Scia*
Apocynaceae/Apocynioideae	*Landolphia owariensis P.Beauv.*	*GC*	*Lph*	*Sar*	*Meso*	*Helio*
Apocynaceae/Apocynioideae	*Pycnobotrya nitida Benth.*	*AT*	*Lph*	*Sar*	*Meso*	*Hemi-Scia*
Apocynaceae/Apocynioideae	*Rauvolfia vomitoria Afzel.*	*GC*	*McPh*	*Sar*	*Meso*	*Helio*
Apocynaceae/Apocynioideae	*Strophanthus hipidus DC.*	*GC*	*Lph*	*Pog*	*Meso*	*Helio*
Apocynaceae/Apocynioideae	*Tabernaemontana crassa Benth.*	*GC*	*MsPh*	*Sar*	*Mega*	*Helio*

Table 2. Floristic composition of the forest massif studied (final list of all species inventoried and their ecological spectra). **(continued)**

Family	Genus and species	DP	TB	TD	TF	Ecol.g
Araceae	*Anchomanes difformis (BL.)Engl.*	*GC*	*meG*	*Sar*	*Mega*	*Scia*
Araceae	*Anchomanes giganteus Engl.*	*GC*	*meG*	*Sar*	*Mega*	*Scia*
Araceae	*Culcasia angolensis Welw.Ex. Schott.*	*GC*	*Phgr*	*Sar*	*Mega*	*Hemi-Helio*
Araceae	*Lasimorpha senegalense Schott.*	*AT*	*Gt*	*Sar*	*Mega*	*Helio*
Asparagaceae	*Draceana mannii Baker.*	*AT*	*MsPh*	*Sar*	*Micro*	*Hemi*
Balsaminaceae	*Impatiens niamniamensis Gilg.*	*AT*	*Thd*	*Bal*	*Meso*	*Hgr-Helio*
Bignoniaceae	*Kigella africana (Lam.)Benth.*	*AT*	*MsPh*	*Bal*	*Meso*	*Hgr-H-Scia*
Bignoniaceae	*Markhamia tomentosa K.Schum.*	*GC*	*MsPh*	*Ptér*	*Meso*	*Helio*
Bignoniaceae	*Spathodea campanulata P. Beauv.*	*AT*	*MsPh*	*Sar*	*Meso*	*Hgr-Nit-Helio*
Burceraceae	*Canarium schweimfurthii Engl.*	*GC*	*MgPh*	*Sar*	*Mega*	*Scia*
Burceraceae	*Dacryodes edulis H.J.Lam*	*GC*	*MsPh*	*Sar*	*Meso*	*Hemi-Scia*
Cannabaceae	*Celtis tessmannii Rendle.*	*GC*	*MgPh*	*Sar*	*Micro*	*Scia*
Cannabaceae	*Trema orientalis L.Blume*	*Pal*	*McPh*	*Sar*	*Meso*	*Helio*
Cealastraceae	*Salacia debilis (G.Don) Walp.*	*GC*	*Lph*	*Sar*	*Meso*	*Scia*
Chrysobalanaceae	*Parinari excelsa Sabine.*	*BGC*	*MgPh*	*Sar*	*Meso*	*Hygr-Scia*
Clusiaceae	*Garcinia kola Haeckel*	*GC*	*MsPh*	*Sar*	*Meso*	*Helio*
Clusiaceae	*Harungana madagascariense Lam. ex Poir*	*Ant*	*MsPh*	*Sar*	*Meso*	*Helio*
Commelinaceae	*Palisota ambigua (P.Beauv.) C.BCl.*	*GC*	*Grh*	*Sar*	*Meso*	*Hemi-Scia*
Connaraceae	*Agelaea dewevrei De Wild.*	*BGC*	*Lph*	*Sar*	*Meso*	*Hgr-H-Scia*
Connaraceae	*Agelaea pentagyna (Lam.) Bail.*	*BGC*	*Lph*	*Sar*	*Meso*	*Hgr-H-Scia*
Connaraceae	*Cnestis ferrugineus Dc.*	*GC*	*Lph*	*Sar*	*Micro*	*Helio*
Costaceae	*costus afer Ker-Gawl.*	*BGC*	*Grh*	*Sar*	*Mega*	*Helio*
Cyperaceae	*Scleria boivinii Steud.*	*GC*	*Grh*	*Scl*	*Micro*	*Helio*
Dennstaedtiaceae	*Ptéridium aquilinum L.Kuhn*	*Cos*	*Grh*	*Scl*	*Micro*	*Helio*
Dichapetalaceae	*Dichapetalum brazzae Pellegr.*	*BG*	*Lph*	*Sar*	*Meso*	*Hygr-Scia*
Dichapetalaceae	*Dichapetalum germainii Hauman.*	*BG*	*Lph*	*Sar*	*Meso*	*Hgr-Scia*
Dichapetalaceae	*Dichapetalum pedicellatum Krause.*	*BGC*	*Lph*	*Sar*	*Meso*	*Hygr-Scia*
Dilleniaceae	*Tetracera poggei Gilg.*	*GC*	*Lph*	*Bal*	*Meso*	*Psa*
Dioscoreaceae	*Dioscorea similasiphonia De wild.*	*GC*	*Gt*	*Ptér*	*Meso*	*Hemi-Helio*
Ebenaceae	*Diospyros crassiflora Hiern.*	*BGC*	*MsPh*	*Sar*	*Meso*	*Hygr-H-Scia*
Ebenaceae	*Diospyros gilletii De wild.*	*C*	*McPh*	*Sar*	*Meso*	*Hemi-Helio*

Table 2. Floristic composition of the forest massif studied (final list of all species inventoried and their ecological spectra). **(continued)**

Family	Genus and species	DP	TB	TD	TF	Ecol.g
Ebenaceae	*Diospyros pseudomespilus Muld.br*	*BG*	*McPh*	*Sar*	*Meso*	*Hemi-Helio*
Euphorbiaceae	*Alchornea cordifolia Arg.*	*AT*	*MsPh*	*Sar*	*Meso*	*Helio*
Euphorbiaceae	*Chaetocarpus africanus Pax*	*BGC*	*MsPh*	*Bal*	*Meso*	*Scia*
Euphorbiaceae	*Croton mubango Mull. Arg.*	*BGC*	*MsPh*	*Bal*	*Meso*	*Psa*
Euphorbiaceae	*Croton sylvaticus Hochst.*	*AT*	*MsPh*	*Sar*	*Meso*	*Hygr-Helio*
Euphorbiaceae	*Macaranga monandra Mull.Arg.*	*BGC*	*MsPh*	*Sar*	*Meso*	*Helio*
Euphorbiaceae	*Macaranga spinosa Mull. Arg.*	*GC*	*MsPh*	*Sar*	*Meso*	*Helio*
Euphorbiaceae	*Necepsia zairensis Bouchat & J.Léonard.*	*C*	*McPh*	*Bal*	*Meso*	*Helio*
Euphorbiaceae	*Sclerocroton cornitus Pax.*	*BGC*	*MsPh*	*Bal*	*Micro*	*Helio*
Euphorbiaceae	*Sclerocroton oblongifolium Pax.*	*BGC*	*MsPh*	*Bal*	*Micro*	*Helio*
Fabaceae/Caesalpinioideae	*Cassia absus L.*	*Pan*	*Thd*	*Bal*	*Meso*	*Nit*
Fabaceae/Caesalpinioideae	*Cassia mimosoides L.*	*Pal*	*Chd*	*Bal*	*Meso*	*Hygr-Helio*
Fabaceae/Caesalpinioideae	*Cassia siamea Lam.*	*BGC*	*MgPh*	*Sar*	*Meso*	*Nit*
Fabaceae/Caesalpinioideae	*Copaifera religiosa J. Léonard*	*BGC*	*MgPh*	*Bar*	*Micro*	*Hygr-H-Scia*
Fabaceae/Caesalpinioideae	*Dialum pachyphyllum Harms. Engl.*	*BGC*	*MgPh*	*Sar*	*Micro*	*Scia*
Fabaceae/Caesalpinioideae	*Griffonia physiocarpa Baill.*	*GC*	*Phgr*	*Bar*	*Meso*	*Hemi-Scia*
Fabaceae/Caesalpinioideae	*Griffonia speciosa Comper.*	*CGC*	*Lph*	*Bal*	*Meso*	*Hygr-Helio*
Fabaceae/Caesalpinioideae	*Guibourtia demeusei J.Léonard.*	*CGC*	*MgPh*	*Sar*	*Meso*	*Helio*
Fabaceae/Caesalpinioideae	*Hymenostegia mundungu Harms.*	*BG*	*MgPh*	*Bal*	*Lepto*	*Scia*
Fabaceae/Caesalpinioideae	*Paramacrolobium coeruleum J.Léonard.*	*AT*	*MgPh*	*Bal*	*Meso*	*Hemi-Scia*
Fabaceae/Caesalpinioideae	*Prioria balsamifera (Harms) Breteler.*	*BGC*	*MgPh*	*Ptér*	*Meso*	*Hemi-Helio*
Fabaceae/Caesalpinioideae	*Prioria oxyphila Breteler.*	*BGC*	*MgPh*	*Pog*	*Meso*	*Helio*
Fabaceae/Caesalpinioideae	*Scorodophloeus zenkeri Harms.*	*BGC*	*MgPh*	*Bar*	*Lepto*	*Scia*
Fabaceae/Caesalpinioideae	*Tessmania africana. Engl.*	*CGC*	*MgPh*	*Bar*	*Meso*	*Hygr-Helio*
Fabaceae/Faboideae	*Amphirmas feruginea Pierre.*	*GC*	*MgPh*	*Sar*	*Meso*	*Helio*
Fabaceae/Faboideae	*Centrosema pubescens Benth*	*Ant*	*Chgr*	*Bar*	*Micro*	*Helio*
Fabaceae/Faboideae	*Dalhousea africana S. Moore.*	*BGC*	*Lph*	*Bal*	*Meso*	*Helio*
Fabaceae/Faboideae	*Dewevrea bilabiata Midreli.*	*CGC*	*Lph*	*Bal*	*Meso*	*Hygr-Helio*
Fabaceae/Faboideae	*Leptoderris nobilis Dunn.*	*BGC*	*Lph*	*Bal*	*Meso*	*Hygr-Helio*
Fabaceae/Faboideae	*Milletia laurentii De wild.*	*BGC*	*MgPh*	*Bal*	*Meso*	*Helio*
Fabaceae/Faboideae	*Milletia versicolor Welw. Ex. Bak.*	*AT*	*MsPh*	*Bal*	*Meso*	*Helio*
Fabaceae/Faboideae	*Pterocarpus angolensis DC.*	*AT*	*MsPh*	*Ptér*	*Lepto*	*Helio*

Table 2. Floristic composition of the forest massif studied (final list of all species inventoried and their ecological spectra). **(continued)**

Family	Genus and species	DP	TB	TD	TF	Ecol.g
Fabaceae/Mimosoideae	*Acasia pentagona Gilbert et Boutique.*	*AT*	*Lph*	*Bal*	*Lepto*	*Hygr-Helio*
Fabaceae/Mimosoideae	*Dalbergia ealaensis De wild.*	*CGC*	*Lph*	*Ptér*	*Meso*	*Mes-Hygr*
Fabaceae/Mimosoideae	*Fillaeopsis discophora Harms.*	*CGC*	*MgPh*	*Bar*	*Micro*	*Helio*
Fabaceae/Mimosoideae	*Pentaclethra eetveldeana De wild. & Th. Dur.*	*BGC*	*MgPh*	*Bal*	*Lepto*	*Helio*
Fabaceae/Mimosoideae	*Pentaclethra macrophylla Benth.*	*GC*	*MgPh*	*Bal*	*Micro*	*Helio*
Fabaceae/Mimosoideae	*Piptadeniastrum africanum (Hook.F.) Brenan.*	*GC*	*MgPh*	*Bal*	*Lepto*	*Helio*
Fabaceae/Mimosoideae	*Pseudoprosopus claessensii (De wild) Gilbert et Boutique.*	*GC*	*Lph*	*Bal*	*Micro*	*Hygr-H-Scia*
Fabaceae/Mimosoideae	*Tetrapleura tetraptera Taub.*	*GC*	*MsPh*	*Bal*	*Lepto*	*Helio*
Gentianaceae	*Anthocleista schweinfurthii Gilg.*	*C*	*MsPh*	*Scl*	*Mega*	*Helio*
Gleicheniaceae	*Gleichenia linearis Cl.*	*Pal*	*Grh*	*Scl*	*Meso*	*Helio*
Gnetaceae	*Gnetum africanum Welw.*	*BGC*	*Phgr*	*Sar*	*Micro*	*Hélio*
Huaceae	*Afrotirax lepidophyllus Mildbr.*	*CGC*	*MgPh*	*Sar*	*Meso*	*Hemi-Scia*
Huaceae	*Hua gaboni Pierre.*	*BGC*	*MsPh*	*Sar*	*Meso*	*Scia*
Irvingiaceae	*Irvingia gabonensis Baill.*	*GC*	*MsPh*	*Bar*	*Meso*	*Helio*
Irvingiaceae	*Irvingia grandifolia Engl.*	*BGC*	*MgPh*	*Bar*	*Meso*	*Helio*
Irvingiaceae	*Irvingia smithii Mildbr.*	*BGC*	*MsPh*	*Bar*	*Meso*	*Helio*
Irvingiaceae	*Klainedoxa gabonensis Pierre ex. Engl. K.*	*GC*	*MgPh*	*Bar*	*Meso*	*Helio*
Lamiaceae	*Vitex congolensis De Wild.& Th. Dur.*	*GC*	*MsPh*	*Sar*	*Meso*	*Helio*
Lamiaceae	*Vitex ferruginea Schumach et Thonn.*	*GC*	*MsPh*	*Sar*	*Meso*	*Helio*
Lamiaceae	*Vitex madiensis Oliv*	*AT*	*MsPh*	*Sar*	*Meso*	*Helio*
Lecythidaceae	*Petersianthus macrocarpus (P. Beauv.) K.Schum.*	*GC*	*MsPh*	*Ptér*	*Meso*	*Helio*
Logoniaceae	*Mostuea hursuta Bak.*	*GC*	*NPh*	*Scl*	*Micro*	*Scia*
Malvaceae/Bombacoideae	*Ceiba pentadra (L.)Gaertn.*	*Pan*	*MsPh*	*Pog*	*Meso*	*Helio*
Malvaceae/Malvoideae	*Urena lobata (L.)ASA-SP-C*	*Pan*	*Nph*	*Desm*	*Meso*	*Helio*
Malvaceae/sterculioideae	*Cola acumunata Schott & Endl.*	*GC*	*MsPh*	*Sar*	*Meso*	*Scia*
Malvaceae/sterculioideae	*Cola altissina Engl.*	*GC*	*MsPh*	*Sar*	*Meso*	*Scia*
Malvaceae/sterculioideae	*cola marsupium K. Schum.*	*GC*	*McPh*	*Sar*	*Meso*	*Scia*
Malvaceae/sterculioideae	*Pterygota bequaertii De wild.*	*GC*	*MsPh*	*Sar*	*Meso*	*Helio*
Malvaceae/sterculioideae	*Pterygota macrocarpa K. Schum.*	*GC*	*MsPh*	*Ptér*	*Meso*	*Helio*
Malvaceae/sterculioideae	*Sterculia bequaertii De wild.*	*BGC*	*MsPh*	*Bal*	*Meso*	*Helio*

Table 2. Floristic composition of the forest massif studied (final list of all species inventoried and their ecological spectra). **(continued)**

Family	Genus and species	DP	TB	TD	TF	Ecol.g
Malvaceae/sterculioideae	*Sterculia tragacantha Lindi.*	*AT*	*MgPh*	*Bal*	*Meso*	*Hemi-helio*
Marantaceae	*Afrocalanthea rhizantha K. Schum.*	*BGC*	*Thd*	*Sar*	*Meso*	*Hemi-Scia*
Marantaceae	*Halopegia azurea K. Schum.*	*GC*	*Thd*	*Sar*	*Meso*	*Hemi-Scia*
Marantaceae	*Haumania liebrechtsiana J.Léonard.*	*GCZ*	*Thd*	*Sar*	*Mega*	*Helio*
Marantaceae	*Hypcelodelphys scandes Louis & Mullend.*	*GC*	*mGrh*	*Sar*	*Meso*	*Helio*
Marantaceae	*Hypselodelphys poggeana (K. Schum.) Milne-Redh.*	*GC*	*mGrh*	*Sar*	*Meso*	*Helio*
Marantaceae	*Marantochloa purpurea (Ridl.)Milne-Redh.*	*GC*	*Thd*	*Sar*	*Meso*	*Hemi-Scia*
Marantaceae	*Sarcophrynium brachystachys (Benth.) K. Schum.*	*GC*	*mGrh*	*Sar*	*Meso*	*Hemi-Scia*
Marantaceae	*Thaumatococcus daniellii (Benn) Benth. & Hook. F.*	*GC*	*Grh*	*Sar*	*Meso*	*Helio*
Melastomataceae	*Memecylon buchananii Gilg.*	*GC*	*McPh*	*Sar*	*Meso*	*Scia*
Melastomataceae	*Dichaetanthera corymbosa Jacq.- Fél.*	*AT*	*MsPh*	*Sar*	*Meso*	*Hemi-Scia*
Meliaceae	*Entandrophragma angolense (Welw) C.DC.*	*GC*	*MgPh*	*Bal*	*Meso*	*Hemi-Scia*
Meliaceae	*Entandrophragma candollei Harms.*	*GC*	*MgPh*	*Bal*	*Meso*	*Hemi-Scia*
Meliaceae	*Entandrophragma cylindicum Sprague.*	*GC*	*MgPh*	*Bal*	*Meso*	*Hemi-Scia*
Meliaceae	*Entandrophragma utile Dawe & Sprague,*	*GC*	*MgPh*	*Bal*	*Meso*	*Hemi-Scia*
Meliaceae	*Lovoa trichilioides Harms.*	*GC*	*MgPh*	*Bal*	*Meso*	*Helio*
Menispermaceae	*Triclisia gilletii Staner.*	*GC*	*Lph*	*Sar*	*Meso*	*Helio*
Moraceae	*Dorstenia bequaertii De wild.*	*GC*	*Chd*	*Bal*	*Meso*	*Scia*
Moraceae	*Ficus exasperata Vahl.*	*BGC*	*MgPh*	*Sar*	*Meso*	*Helio*
Moraceae	*Ficus mucuso Welw.*	*AT*	*MsPh*	*Sar*	*Meso*	*Helio*
Moraceae	*Milisia excelsa Berg.*	*GC*	*MsPh*	*Sar*	*Meso*	*Helio*
Moraceae	*Trilepisium madagascariense D.C.*	*AT*	*MgPh*	*Sar*	*Meso*	*Helio*
Myristicaceae	*Embelia guineensis Bak.*	*Ant*	*Lph*	*Sar*	*Micro*	*Helio*
Myristicaceae	*Pycnanthus angolens Gilbert.*	*GC*	*MgPh*	*Bal*	*Meso*	*Scia*
Myristicaceae	*Pycnanthus marchalianus Ghesq.*	*BGC*	*MgPh*	*Bal*	*Meso*	*Scia*
Myristicaceae	*Staudia kamerunensis Warb.*	*GC*	*MgPh*	*Bal*	*Meso*	*Scia*
Ochnaceae	*Rhabdophyllum arnoldiunum Tiegh.*	*BGC*	*McPh*	*Sar*	*Meso*	*Scia*
Olacaceae	*Olax gambecola Baill.*	*GC*	*NPh*	*Sar*	*Meso*	*Scia*

Table 2. Floristic composition of the forest massif studied (final list of all species inventoried and their ecological spectra). **(continued)**

Family	Genus and species	DP	TB	TD	TF	Ecol.g
Olacaceae	*Olax latifolia Engl.*	*BGC*	*MsPh*	*Sar*	*Meso*	*Scia*
Olacaceae	*Olax subscorpioides Oliv.*	*BGC*	*MsPh*	*Sar*	*Meso*	*Hemi-Scia*
Olacaceae	*Olax wildemanii Engl.*	*BGC*	*McPh*	*Sar*	*Meso*	*Scia*
Olacaceae	*Ongokea gore Pierre.*	*GC*	*MgPh*	*Bal*	*Meso*	*Scia*
Palmae (Arecaceae	*Elaeis guineensis Jacq.*	*Pan*	*MsPh*	*Sar*	*Meso*	*Helio*
Palmae (Arecaceae)	*Eremospatha haullevilleana De wild.*	*BGC*	*Lph*	*Sar*	*Meso*	*Hemi-Scia*
Palmae (Arecaceae)	*Laccosperma secundiflorum (P.Beauv.) Wendl.*	*GCZ*	*Phgr*	*Sar*	*Meso*	*Helio*
Palmae (Arecaceae)	*Raphia regalis Becc.*	*BGC*	*MsPh*	*Sar*	*Meso*	*Helio*
Palmae (Arecaceae)	*Raphia sese De wild.*	*BGC*	*MsPh*	*Sar*	*Meso*	*Helio*
Palmae (Arecaceae)	*Rhektophyllum mirabile De wild.*	*BGC*	*Lph*	*Sar*	*Meso*	*Helio*
Passifloraceae	*Barteria fistulosa Sleumer*	*BGC*	*MsPh*	*Sar*	*Meso*	*Helio*
Phyllantaceae (Pandaceae)	*Microdesmis haumaniana J. Léonard.*	*GC*	*MsPh*	*Sar*	*Meso*	*Helio*
Phytolaccaceae	*Hilleria latifolia Walter.*	*AT*	*McPh*	*Sar*	*Meso*	*Hygr-scia*
Piperaceae	*Piper guineense Schumach.*	*C*	*Phgr*	*Sar*	*Meso*	*Hemi-Scia*
Poaceae	*Leptaspis cochleata Thwait.*	*Pal*	*Chp*	*Scl*	*Micro*	*Hemi-Scia*
Poaceae	*Olyra latifolia L.*	*Pan*	*Chp*	*Scl*	*Meso*	*Hemi-Scia*
Putranjivaceae	*Drypetes gossweileri S.Moore*	*BGC*	*MsPh*	*Sar*	*Meso*	*Helio*
Rubiaceae	*Bertiera letouzeyi N. Hallé.*	*GC*	*McPh*	*Sar*	*Meso*	*Hemi-helio*
Rubiaceae	*Craterispermum laurinum Benth.*	*AT*	*McPh*	*Sar*	*Meso*	*Helio*
Rubiaceae	*Cremaspora triflora Thonn.*	*GC*	*Lph*	*Sar*	*Micro*	*Helio*
Rubiaceae	*Crossopteryx febrifuga Benth.*	*BGC*	*MsPh*	*Sar*	*Micro*	*Helio*
Rubiaceae	*Gaertnera bracteata Petit.*	*GC*	*MsPh*	*Sar*	*Meso*	*Helio*
Rubiaceae	*Gaertnera paniculata Benth.*	*GC*	*MsPh*	*Sar*	*Meso*	*Helio*
Rubiaceae	*Gardenia imperialis Schum.*	*AT*	*MsPh*	*Sar*	*Meso*	*Helio*
Rubiaceae	*Leptactina leopoldi At.Buttner*	*BGC*	*MsPh*	*Sar*	*Meso*	*Helio*
Rubiaceae	*Mittragyna stipulosa (D.c) O. Kunttze.*	*AT*	*MsPh*	*Ptér*	*Mega*	*Hemi-Scia*
Rubiaceae	*Morinda lucida Benth.*	*GC*	*MsPh*	*Sar*	*Mega*	*Helio*
Rubiaceae	*Morinda morindoides Milne-Redh.*	*GC*	*Lph*	*Sar*	*Meso*	*Helio*
Rubiaceae	*Nauclea diderrichii Merr.*	*GC*	*MsPh*	*Sar*	*Meso*	*Helio*
Rubiaceae	*Pausinystalia johimbe Pierre.*	*BG*	*MsPh*	*Sar*	*Mega*	*scia*
Rubiaceae	*Psydrax palma K. Schum.*	*C*	*McPh*	*Sar*	*Nano*	*Hemi-Scia*
Rubiaceae	*Rothmania whitfieldii (Lindl.)Dandy.*	*GCZ*	*MsPh*	*Sar*	*Meso*	*Scia*

Table 2. Floristic composition of the forest massif studied (final list of all species inventoried and their ecological spectra). **(continued)**

Family	Genus and species	DP	TB	TD	TF	Ecol.g
Rubiaceae	*Sabicea dinklagei K. Schum.*	*BGC*	*Lph*	*Sar*	*Meso*	*Hemi-Scia*
Rubiaceae	*Sareocephalus latifolius E.A Bruce.*	*AT*	*MsPh*	*Sar*	Méso	*Helio*
Rubiaceae	*Spermacoce latifolia Aubl*	*GC*	*Thpr*	*Scl*	*Micro*	*Helio*
Rutaceae	*Zanthoxylum gilletii (De wild.) Waternan.*	*GC*	*MsPh*	*Bal*	*Mega*	*Helio*
Salicaceae	*Homalium africanum (Hook. F.)Benth.*	*AT*	*MsPh*	*Sar*	*Meso*	*Helio*
Salicaceae	*Oncoba welwetschii.Oliv.*	*AT*	*McPh*	*Sar*	*Meso*	*Helio*
Salicaceae	*Paropsia guineensis. Oliv.*	*BGC*	*MsPh*	*Bal*	Meso	*Helio*
Sapindaceae	*Allophylus lastourvillensis Pellerg.*	*CGC*	*MsPh*	*Sar*	*Méso*	*Helio*
Sapindaceae	*Blighia welwitschii Engl.*	*GC*	*MsPh*	*Bal*	*Meso*	*Scia*
Sapindaceae	*Chytranthus gilletii De wild.*	*GC*	*MsPh*	*Sar*	*Meso*	*Scia*
Sapotaceae	*Manilkara argentéa P.ex Dubard.*	*GC*	*MsPh*	*Sar*	*Meso*	*Helio*
Sapotaceae	*Chrysophyllum lacourtianum De wild.*	*BGC*	*MsPh*	*Sar*	*Meso*	*Hemi-Scia*
Sapotaceae	*Donella ubangiensis (De wild.). Aubr.*	*CGC*	*MsPh*	*Sar*	*Meso*	*Hygr-Helio*
Sapotaceae	*Manilkara obovata J.H*	*GC*	*MsPh*	*Sar*	*Meso*	*Helio*
Similacaceae	*Smilax anceps Willd.*	*AT*	*Lph*	*Sar*	*Meso*	*Helio*
Strychnaceae	*Strychnos variabilis De.wild*	*GC*	*MsPh*	*Sar*	*Micro*	*Hemi-Scia*
Thelipteridaceae	*Cyclosorus striatus (Schum.) Ching.*	*AT*	*Grh*	*Scl*	*Nano*	*Helio*
Urticaceae	*Musanga cecropioides R. Br.*	*GC*	*MgPh*	*Sar*	*Mega*	*Helio*
Urticaceae	*Myrianthus arborea P. Beauv.*	*GC*	*MsPh*	*Sar*	*Mega*	*Hygr-Helio*
Zingiberaceae	*Afromomum angustifolium K. Schum.*	*BGC*	*mGrh*	*Sar*	*Mega*	*Helio*
Zingiberaceae	*Afromomum giganteum K.Schum.*	*BGC*	*mGrh*	*Sar*	*Mega*	*Helio*
Zingiberaceae	*Aframomum melegueta K.Schum.*	*GC*	*mGrh*	*Sar*	*Mega*	*Hemi-Scia*

TB: biological type; DP: phytogeographical distribution; TD: type of diaspore; TF: Type of leaf size; Ecol.g: ecological group; BGC: Lower Guinean-Congolese; BG: Lower Guinean; AT: afrotropical; GC: Guinean-Congolese; CGC: Guinean-Congolese center; C: central Congolese species; Pal: paleotropical; Ant: afroneotropical; Cos: cosmopolitan; Pan: pan-tropical; MgPh: megaphanerophytes; MsPh: mesophanerophytes; McPh: microphanerophytes; LPh: woody phanerophytes; Grh: rhizomatous geophytes; mGrh: rhizomatous megaphanerophytes; Gt: geophytes; Chgr: climbing chamaephytes; Thd: erect therophytes; Chp: prostrate chamaephytes; Sar: sarcochores; Pog: pogonochores; Scl: sclerochores; Pter: pterochores; Desm: desmochores; Bar: barochores; Meso: mesophylls; Micro: microphyll, Mega: megaphyll; Lepto: leptophyll; Scia: sciophilous; Helio: heliophile; Hemi-Helio: hemi-heliophile; Hgr-scia: hygro-sciaphilic; Hgr-H-Scia: hygro-hemi-sciaphilic; Hemi-Scia: hemi-sciaphilous; Hygr-Helio: hygro-heliophilic; Hygr-Nit-Helio: hygro-nitro-heliophilic; Psa: spamophile; Nit: nitrophile.

Studies of the Ecological Spectra of Species

Biological types

The analysis of spectra of biological types of species shows that the forest massif of the study area is characterized by the majority of phanerophyte species. The other categories are poorly represented (Figure 3).

Diaspore Type

It should be remembered that the type spectra of the diaspores provide information on the nature of the diaspores of the species and give indications as to their mode of dissemination and their possible disseminating agents. Analysis of the results in the following Figure 4 shows the presence of several types of diaspores. Of all these different categories of types of diaspores identified in the study area, we note the strong presence of

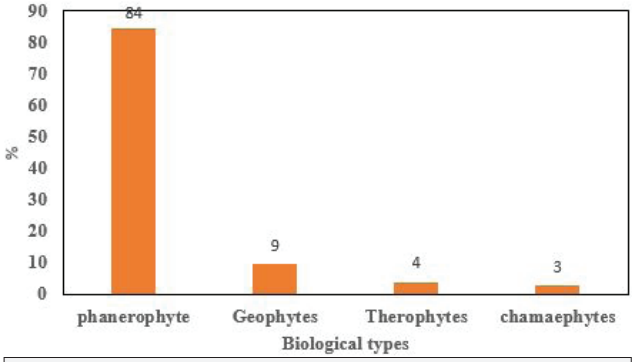

Figure 3. Analysis of the biological types of the inventoried and identified species.

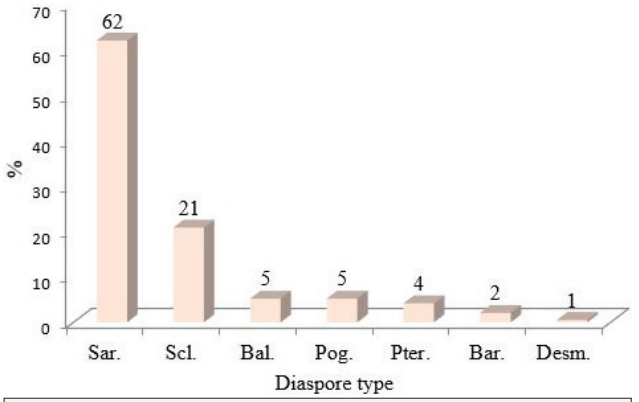

Figure 4. Analysis of diaspores types according to the dissemination of each species.

Sar: sarcochores; Pog: pogonochores; Scl: sclerochores; Pter: pterochores; Desm: desmochores; Bar: barochores.

sarcochores followed by ballochores and sclerochores. Pterochores, desmochores, pogonochores, and barochores remain weakly represented.

Phytogeographic Distribution

The chorological study of a plant group is the representation of species according to the area of geographical distribution in the surface of the terrestrial globe. Indeed, Figure 5 shows the phytogeographical distribution of species. It appears from the results obtained that the Guinean-Congolese species predominate, followed by the Bas-Guinean-Congolese, Afrotopical species, and the elements of the Guinean-Congolese center.

Type of Leaf Size

The type spectra of the leaf sizes of the species inventoried in the study area are shown in Figure 6.

Ecological Group

The ecological group gives precious indications on the temperament of the species at the young stage. It also provides information on the substrate and the possible habitat of the species (Figure 7). The analysis of the observations made on the eco-

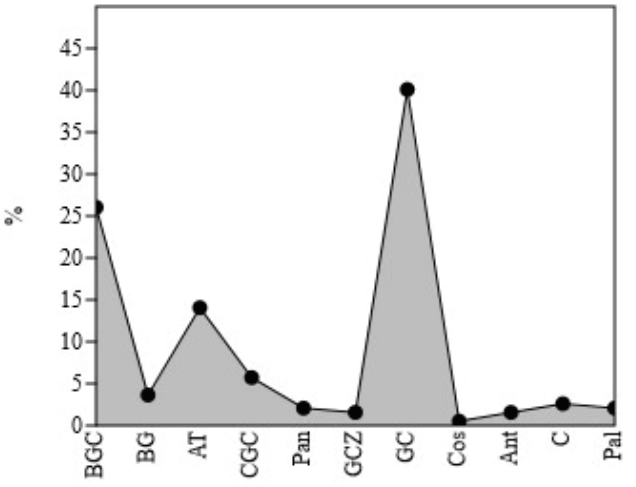

Figure 5. Phytogeographic distribution of species.

BGC: Bas Guineo-Congolais; BG: Guinean stockings; AT: Afrotropical; GC: Guineo-Congolais; CGC: Guineo-Congolese center; C: species of the Congolese center; Pal: paleotropical; Ant: Afroneotropical; Cos: Cosmopolite; Pan: Pan-Tropical.

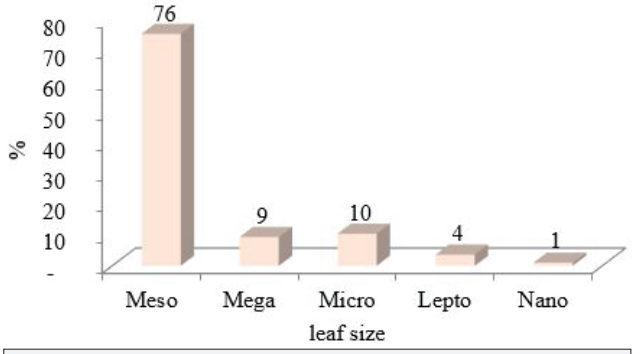

Figure 6. Analysis of leaf quantities of species identified. Examination of this figure provides information on the abundance of mesophyll (Meso) species, followed by microphylls (Micro) and megaphylls (Mega), while nanophylls (Nano) and leptophylls (Lepto) are poorly represented.

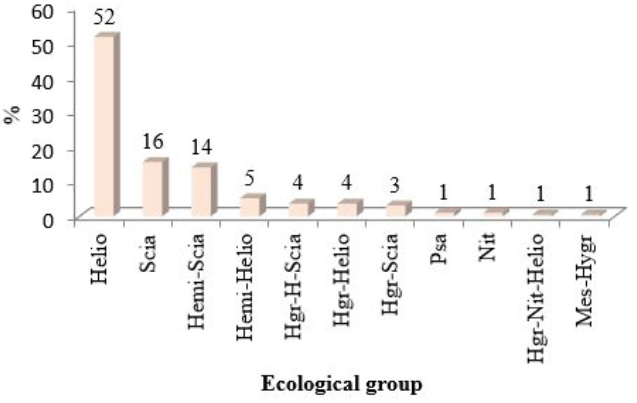

Figure 7. Ecological affinity of species in the study area.

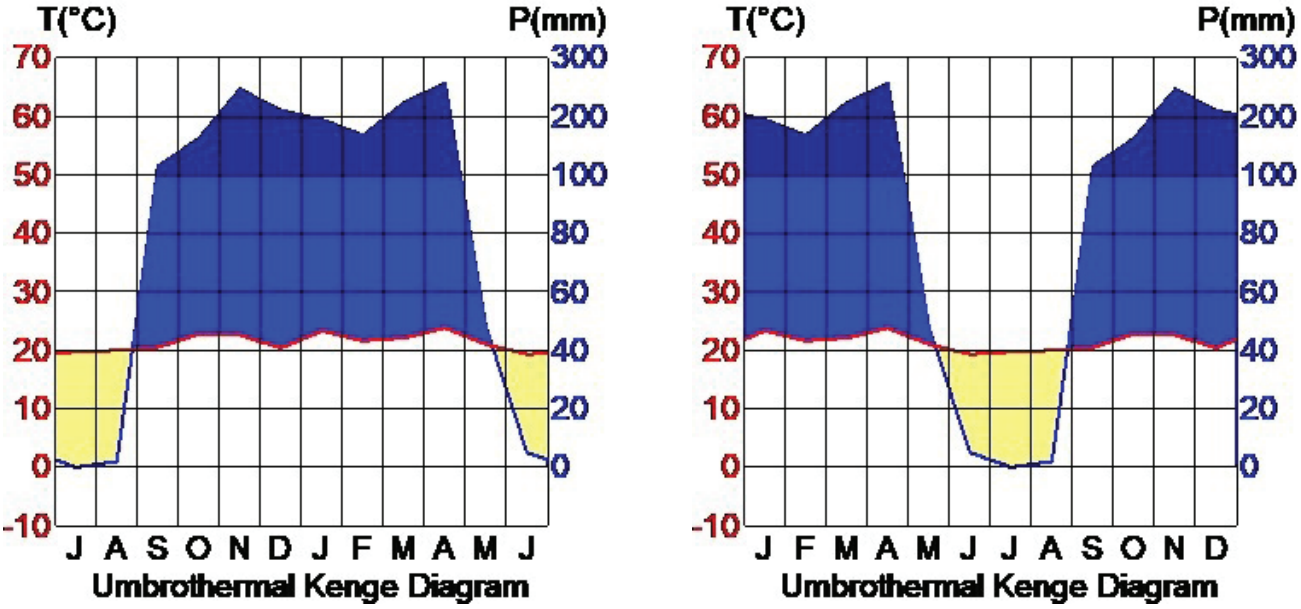

Figure 8. Ombrothermic diagram in hydrological and civil year.

logical group of species highlights the observation that, in the forest massif visited, there are more heliophilous species. The other groups are poorly represented.

Analysis of Climatic Aspects

Climatic factors play a decisive role in the evolution of vegetation. Temperatures and precipitation characterize the climatic elements that influence the distribution of living beings in a given territory. The climatic data collected in the field (Kenge station) enabled us to establish the ombrothermic diagram of the area in order to characterize the type of vegetation relating thereto (Figure 8). The analysis of the climatic data reveals that the study area is characterized by a humid tropical climate, with an average monthly temperature of 22°C while the cumulative monthly rainfall is around 231 mm. These factors are favorable to the evolution of a vegetation of the Guineo-Congolese type.

Soil Test Result

The soil analyses show that the study site is characterized by a type of clayey-sandy soil. This type of soil is favorable to the evolution of vegetation of the Guineo-Congolese type. The results indicate the presence of exchangeable cations. Table 3 below presents the particle size composition of the soil in the study area. The particle size analysis of the studied soil gives as results 58.7% for sands, 32.4% for clays, and 8.9% for silts

Table 3. Particle size composition of the soil studied.

Components	Particle size composition in %
Coarse sands	48.1
Fine sands	10.6
Clays	32.4
Fine silts	5.3
Coarse silts	3.6

Threatened or Rare Species

In the study area, these different species are threatened and have become rare in the region due to overexploitation and the fragmentation or degradation of their habitats. These different species have food, medicinal, and socio-cultural values, and others are highly coveted species for timber and construction timber while the fibers of the Palmae are used to make craft tools (furniture, shelves, bags, sandals, clothes, etc.). Table 4 presents the threatened species.

Environment Study

This research was carried out in the Wamba Valley. The Wamba is a river in the DRC that has its source in Angola, and forms the hydrographic network of the basin of the Kasai River, the main tributary of the Congo River. The following image (Figure 9) shows the Wamba River, the studied forest and a few plants of *Elaeis guineensis* Jacq. (Oil palm tree).

DISCUSSION

This ecological and phytogeographic floristic study of the Wamba Valley massif forest is part of the inventory and knowledge of natural resources for sustainable management. The study environment is part of the Guinean-Congolese-Zambézian transition zone. This area is characterized by the mixture of species from the Guineo-Congolese regional center of endemism and Zambezian species (42). Despite an important anthropogenic pressure to which the massif forest concerned by our study is subjected, the floristic inventory has noted the existence of 192 species, subspecies, and varieties divided into 160 genera and 58 families. This flora is rich and diverse. More a

Table 4. Threatened or rare species. The analysis of this table shows that a whole diversity of species in the area undergo enormous pressures and are carried out from their local disappearance. A total of 26 species were identified.

Family	Species
Annonaceae	*Xylopia aethiopica (Dunal) A. Rich.*
Burceraceae	*Canarium schweimfurthii Engl.*
Cannabaceae	*Celtis tessmannii Rendle.*
Clusiaceae	*Garcinia kola Haeckel*
Fabaceae/Caesalpinioideae	*Paramacrolobium coeruleum J.Léonard.*
Fabaceae/Caesalpinioideae	*Prioria balsamifera (Harms) Breteler.*
Fabaceae/Caesalpinioideae	*Prioria oxyphila Breteler.*
Fabaceae/Caesalpinioideae	*Scorodophloeus zenkeri Harms.*
Fabaceae/Faboideae	*Milletia laurentii De wild.*
Fabaceae/Faboideae	*Pterocarpus angolensis DC.*
Gnetaceae	*Gnetum africanum Welw.*
Huaceae	*Afrotirax lepidophyllus Mildbr.*
Huaceae	*Hua gaboni Pierre.*
Malvaceae/sterculioideae	*Cola acumunata Schott & Endl.*
Marantaceae	*Sarcophrynium brachystachys (Benth.)K. Schum.*
Meliaceae	*Entandrophragma angolense (Welw) C.DC.*
Meliaceae	*Entandrophragma candollei Harms.*
Meliaceae	*Entandrophragma cylindicum Sprague.*
Meliaceae	*Entandrophragma utile Dawe & Sprague,*
Moraceae	*Milisia excelsa Berg.*
Moraceae	*Trilepisium madagascariense D.C.*
Palmae (Arecaceae)	*Eremospatha haullevilleana De wild.*
Palmae (Arecaceae)	*Raphia regalis Becc.*
Palmae (Arecaceae)	*Raphia sese De wild.*
Rubiaceae	*Mittragyna stipulosa (D.c) O. Kunttze.*
Zingiberaceae	*Aframomum melegueta K.Schum.*

Figure 9. The presentation of the Wamba River and gallery forest studied with a few visible plants of *Elaeis guineensis* Jacq. (Oil palm tree).

stand is floristically rich in cash, less than homogeneous (6,41). The heterogeneity of flora is the result of geological, climatic, and edaphic factors. Of all the families of the inventoried species, that of Fabaceae predominates with 30 species, followed by that of Rubiaceae with 18 species, while the other families are weakly represented. The analysis of these results shows that this zone is rich in biodiversity and deserves rational conservation. These results corroborate those of Belesi (7) in the bottom Kasai, which also reports the dominance of the species of the Fabaceae family; Former family of the flora of the intertropical area in general and from Central Africa in particular. This same observation is also done in the N'djili River Basin in Kinshasa, and Habari (19) in this area of study, the abundance of the old families of the local flora characterized by the Fabaceae, Rubiaceae, and Euphorbiaceae, which are often more dominant than other families. Dewasseige et. al. (3), Lebrun (25,26), and Menga (43) confirm that in Congolese forests, the Fabaceae family (Caesalpinioideae) often remain dominant and rich in genre and species. This great diversity is justified by the fact that several factors influence the diversity of a given territory. This is particularly the case of the diversity of ecological sites since this massif is evolving in a relief consisting of the slopes and valley, without forgetting the hydromorphic substrate. Ntalakwa and al. (23) confirm that the diversity of ecological sites promotes isolation, that is to say an adaptation to the particular ecological conditions. These conditions may induce or introduce morphological and physiological modifications and create new features within the species (44). The more geologically and climately a variety of, the more species it will have more species than another bit diversified (10,36). In total, 3 species of pteridophytes were identified in the study environment. This taxonomic group forms 1.5% of the species that constitute the phytodiversity of this massif forest. Two systematic groups characterize the spermatophyte flora in this area. These represent 98.5% of the species inventoried. These results corroborate those of research carried out on the flora of the Luki Forest Reserve (45). The observations made on the biological species type show that in this area, there is an abundance of phanerophytes. The abundance of phanerophytes proves the forest character of the study site. The structure of this massif forest presents 4 strata, that is to say the herbaceous stratum and under shrubs, the shrubby stratum, the middle tree stratum, and the upper tree stratum. The upper tree stratum is characterized by large trees that we call Megaphanerophytes (MgPh). The same observations were made by Lubini (17) in his study on the stratification and phytosociological classification of secondary forests in Central Africa. Examination of the diaspore type spectra shows the dominance of sarcochore species. This result reflects a general fact observed in the forest. Very often in the forest, species with fleshy fruits are observed. These fruits are eaten more by animals, and it is considered that the species with fleshy fruits are older than those with dried fruits. Dissemination of these types of diaspores is ensured by animals (Zoochoria) (5,16). The phytogeographical distribution of species shows the abundance of Guinean-Congolese species, followed by Bas-Guinean-Congolese and Afrotropical species. This observation confirms the forest character of the study area and its phytogeographical belonging to the Guinean-Congolese-Zambézian transition zone. White (40) confirms that the ecosystems of the Kwango high plateau are characterized by mixtures of Guineo-Congolese and Zambezian species. The author qualifies this environment as a state of a Guineo-Congolese-Zambézian transition zone. The leaf size type analysis highlights the dominance of mesophilic species. This abundance of mesophiles confirms the morphological structure of the species of this massif forest. Regarding the ecological group, the result obtained shows the abundance of heliophilous species, followed by sciaphilous and hemi-sciaphilous species (46).

This result confirms the physiological characteristics of the species of this forest massif, the capacity and the light needs of the species at the young stage (the temperament of the species). Our results corroborate those of Miabangana (8), who makes the same observation in his study on the floristic, phytogeographical, and phytosociological analysis of island and riparian vegetation of the Congo River in the Cataract Plateau (Republic of Congo). Environmental conditions can influence the adaptation or disappearance of a species or species (47). The characteristics of the soil studied favor the evolution of a vegetation rich in plant species. It is therefore important to continue future studies on the possibilities of conserving the biodiversity of the area, which adapts to the pedoclimatic conditions of the environment.

CONCLUSION

The floristic, ecological, and phytogeographical study was carried out in the Wamba valley massif forest, more precisely in Kenge 2. The objective of this research consists of the floristic inventory and analysis of the biodiversity in this study area, which remains little known on the botanical level. This inventory noted the presence of 192 species, subspecies, and varieties divided into 160 genera and 58 families. Of all these families that of Fabaceae predominates with 30 species followed by that of Rubiaceae with 18 species. The studied massif forest is part of the Guinean-Congolese-Zambézian transition zone. This region is characterized by strong demographic pressure which constitutes a threat to the sustainable conservation of the resources of this massif forest. Given the significant biological diversity contained in this forest, we suggest that it be created as a protected area for the sustainable management of resources in the study area.

Peer Review: Externally peer-reviewed.

Author Contributions: Conception/Design of Study- L.A.C., N.M.T.; Data Acquisition- N.M.T., M.P.B.; Data Analysis/Interpretation- N.M.T., A.M.J.P., M.P.B.; Drafting Manuscript- N.M.T., M.P.B.; Critical Revision of Manuscript- L.A.C., K.T.E., B.K.H.; Final Approval and Accountability- N.M.T., M.P.B., K.T.E., A.M.J.P., B.K.H., L.A.C.

Conflict of Interest: Authors declared no conflict of interest.

Financial Disclosure: Authors declared no financial support.

REFERENCES

1. Sébastien LK and Kiyulu N'yanga-Nzo J. Integrating biodiversity into national forest planning programmes. Ed. Center for International Forestry Research Indonesia. 2001; 33.
2. FAO. Regional workshop on the management of secondary tropical forests in French-speaking Africa: realities and perspectives, Rome, 2004; p.280.
3. De Wasseige C, De Marcken P, Bayol N, Hiol Hiol F. et al., editors. Congo Basin forests. State of the Forests 2010, ISBN 978-92-79-22717-2, Publication Office of the European Union; Ed. 2012.
4. Zenga KJ, Omasombo TJ, Guillaume L, M'pene NZ, Zana EM, Simons E. et al. Kwango, country of Lunda citizen, MRAC, Brussels: cri-edition, 2012.
5. Lubini A. Vegetation of the Luki Biosphere Reserve in Mayombe (Zaire) Meise;1997; p.155.
6. Lubini A. Messicole and post-cultural vegetation of the Kisangani and Tshopo sub-regions (Haut-Zaire). University of Kisangani Faculty of Science. Doctoral thesis, 1982.
7. Belesi KH. Floristic, phytogeographical and phytosociological study of the vegetation of Bas-Kasai in the Democratic Republic of Congo. Faculty of Science, University of Kinshasa. Doctoral thesis. 2009.
8. Miabangana ES. Floristic, phytogeographical and phytosociological analysis of island and riparian vegetation of the Congo River in the Cataracts Plateau (Republic of Congo). Faculty of Science, University of Kinshasa. Doctoral thesis. 2019.
9. Rondeux J. The measurement of trees and forest stands. The agricultural presses of Gembloux; Duculot, B-6060 Gilly: 1999; p.521.
10. Doucet JL. The delicate alliance of management and biodiversity in the forests of Gabon. University Faculty of Agronomic Sciences Gembloux. Doctoral thesis. 2003.
11. Dupuy B. Basis for silviculture in dense African humid tropical forest. 4th ed. France; CIRAD-Forêt; 1998.
12. Kidikwadi ET. Ecological and phytogeographical study of the natural populations of priora balsamifera (harms) breteler in lower Guinea-Congo. Faculty of Sciences University of Kinshasa. Doctoral thesis. 2018.
13. Mandango MA. Flora and vegetation of the islands of the Zaire River in the Tshopo Sub-Region (Upper Zaire), T. 1 and 2. Faculty of Sciences University of Kisangani. Doctoral thesis. 1982.
14. Germain R. Grassy alluvial biotopes and intercalated savannahs of the equatorial Congo. More planks. Overseas Academy of Sciences, Brussels, 1964.
15. INEAC. Flora of the Belgian Congo and Ruanda-Urundi. Volumes 3-10. Belgian Congo and Ruanda-Urundi Information and Public Relation Office Brussels; 1952, 1953, 1954.
16. Quentin M, Moumbogou C, Doucet JL, Ondimba AB. The useful trees of Gabon. 1st Ed. The agricultural presses of Gembloux, 2008.
17. Lubini A. Stratification and phytosociological classification of secondary forests in Central Africa. Int J Innov Appl Stud, 2013;14:549-80.
18. Lubini A. Phytogeographical analysis of the forest flora of the Kasaï sector in Congo Kinshasa, in minutes of the XVth plenary meeting of AETFAT. Flight. 72 No. 2, Brussels, Bot G B Nat; 2003; p.859-72.
19. Habari M. Floristic, phytosociological and phytogeographical study of the vegetation of Kinshasa and its middle basins of the N'djili and N'sele rivers in the DRC. Faculties of Sciences University of Kinshasa. Doctoral thesis. 2009.
20. Ndiaye O. Soil characteristics of the flora and vegetation of Ferlo, Senegal. FST-UCAD Ecology and Agroforestry. Doctoral thesis. 2013.
21. Gillet JF, Ngaloua B, Missamba-Lola A. Analysis report-Forest dynamic component. CIB-FFEM project "Monitoring of the dynamic forest-agroforestry-wildlife inventory program". 2008; p.99.
22. Ngok Banak L. Plant diversity of inselbergs and rock slabs in northern Gabon. ULB Doctoral thesis. 2005.
23. Ntalakwa MT, Lubini C, Kidikwadi E, Bamvingana C, Mayanu P, Kwambanda J. Floristic, ecological, and phytogeographical study of the forest islet of the Father Eyimard Eucharistic center in Mont-Ngafula/Kinshasa. Int J Latest Res in Humanit Soc Sci, 2019; 2:7-16.
24. Raunkiaer C, Gilbert-Carter H, Fausboll A, Tansley AG. The life forms of plants and statistical plant geography. London: Oxford University Press; 1934.
25. Lebrun J. The vegetation of the alluvial plain south of Lake Edward. Expl. Park. Nat. Albert, Mission J. Lebrun (1937-1938), Fasc.1, Brussels, Inst. Belgian Congo National Parks. 1947; p.467.
26. Lebrun J and Gilbert G. Ecological classification of the forests of the Congo. INEAC 1954; p.89.
27. Mullenders W. The vegetation of Kaniama (between Lubishi-Lubilash, Belgian Congo). INEAC, editors. France, 1954; p.499.
28. Koechlin J. Savannah vegetation in the south of the Republic of Congo Brazzaville. Montpellier editors. Paris, France, 1961; p.310.
29. Leonard A. The grassy savannahs of Kivu, INEAC editors. S2R. SCI. 1962, 95:1-87.
30. Dansereau P, Lems K. The grading of dispersal types in plant communities and their significance. Contribution Inst Bot Montreal 1957: N°71, p.52.
31. Germain R. Grassy alluvial biotopes and intercalated savannahs of the equatorial Congo, More planks. Overseas Academy of Sciences, Brussels 1964; p.399.
32. Schmitz A. The vegetation of the plain of Lubumbashi (Haut-Katanga). INEAC, editors. Brussels, 1971; p.113.
33. Schnell R. Flora and vegetation of tropical Africa; Volume 1. C. BORDAS, Paris. 1976; p.468.
34. Trochain JL. Plant ecology of the non-desert intertropical zone Univ. Paul Sabatier Toulouse, France, 1980; p.468.
35. Troupin G. Phycoenological study of the Akagera National Park and eastern Rwanda: Search for an analysis method appropriate to the vegetation of intertropical Africa. Butare-Rep. Rwandan. Brussels, 1966.
36. Masens DMY. Phytosociological study of the Kikwit region (Bandundu, DRC). ULB-Belgium. Doctoral thesis. 1997.
37. Evrard C. Ecological research on the forest population of hydromorphic soils in the central Congolese basin. INEAC editors. Brussels, 1968; p. 295.
38. Mollinier R and Muller P. The dissemination of plant species, Passim; RGBL, 1938; 53-67.
39. White F. The vegetation of Africa: A descriptive memoir to accompany the Unesco/AETFAT/UNSO Vegetation map of Africa. Nat Resour Res (UNESCO). 1983; 20:1-356.
40. White F. The Guineo-Congolian Region and its relationships to other phytochoria. Bull Jard Bot Belg 1979; 49: 11-55.
41. White F. The vegetation of Africa: memorandum accompanying the map of the vegetation of Africa (new edition). ORSTOM-UNESCO editors. Paris; 1986; p.384.
42. Lubini A. The resources of secondary forests in French-speaking central and western Africa. French-speaking Africa, realities and prospects; Douala. Proceedings of the regional workshop on the management of secondary tropical forests in, Cameroon. 2003; 17-21.
43. Menga MP. Ecology of natural stands of *Millettia laurentii* in region of Lake Maï-Ndombe in DRC: Implications for the sustainable management of an exploited species. University of Kinshasa, Kinshasa/DRC, Doctoral thesis. 2012.

44. Ernst M. Populations, Species and Evolution. Paris.1974, p.495.
45. Lubini A. The flora of the Luki Forest Reserve (Bas-Zaire) In Minutes of the XIIth Plenary Meeting of AETFAT, Mitt Allg Bot Hamburg, 1990; p.135–54.
46. Devred R. Soil and vegetation maps of the Belgian Congo and Ruanda-Urundi, n°10, Kwango A and B, Vegetation notice. INEAC, Brussels, Ser. Sc, 1958; p.44.
47. Kayabas A and Yildirim E. Chemical Profiling and Wetting Behaviors of Endemic *Salvia absconditiflora* Greuter & Burdet (Lamiaceae) Collected from Gypsum Areas. Eur J Biol 2022; 81(1): 1-10.|

ISTANBUL UNIVERSITY PRESS

REVIEW ARTICLE

Eur J Biol 2022; 81(1): 85-95

Enigmatic Entities of the Acellular World: Viruses, Viroids, and Virusoids

Sidhant Jain[1,2], Soumen Das[3]

[1]University of Delhi, Department of Zoology, Delhi, India
[2]Institute for Globally Distributed Open Research and Education (IGDORE), India
[3]Indian Institute of Science, Centre for Neurosciences, Karnataka, India

ORCID IDs of the authors: S.J. 0000-0003-2596-9566; S.D. 0000-0001-6422-0238

Please cite this article as: Jain S, Das S. Enigmatic Entities of the Acellular World: Viruses, Viroids, and Virusoids. Eur J Biol 2022; 81(1): 85-95. DOI: 10.26650/EurJBiol.2022.1079841

ABSTRACT

Genetic material confined within the lipid based cellular boundaries was earlier considered synonymous with life. However, with the discovery of viruses in late 19th century, the existence of acellular biological entities was established. Viruses, viroids, and virusoids are unique entities which have different relationships with different life forms ranging from mutualistic to parasitic ones. These entities provide evidence in support of the idea of 'RNA world' in the origin of life on Earth. In the present time, viruses are relatively well studied but the same cannot be said for viroids and virusoids. There has been a growing focus on the impact of these entities, in terms of human welfare as well as their impact on susceptible varieties of plants. As a result, studying their origin, evolution and pathogenicity has become a subject of the uttermost importance. In this review, we have discussed different facets of viruses, viroids and virusoids like their historical background, classification and mode of entry and replication in the host. We have also summarized various possible theories on their origin and evolution and have provided our take on it. This work indicates the possibility that different viruses originated distinctly by utilizing different strategies and evolved further. Clues like small size and high GC content in genomes indicate that viroids must be an important component of the pre-cellular world and it is possible that they might have originated before viruses. Furthermore, as viroids and virusoids show certain conserved properties, it suggests a probable link between them.

Keywords: Viruses, Viroids, Virusoids, Origin, Evolution, Infection

INTRODUCTION

Viruses are a type of mobile genetic element (MGE) that consist of a genome enclosed by a protein capsid with some of them having an external lipid envelope (1,2). Viruses encode at least one protein which is a major component of the virion (1). Viroids are small (approx. 250-400 nucleotides), non-coding, non-translatable, non-encapsidated, single-stranded, circular RNAs that replicate by rolling circle mechanism utilizing the host enzymes (1,3-5) whereas virusoids are small RNAs (with a circular genome of 400 nucleotides or less) which depend upon helper viruses (HV) for their replication, encapsidation and transmission (6-8). Virusoid genomes do not generally code for proteins but a virusoid associated with the rice yellow mottle virus is known to code for a 16 kDa, highly basic protein (9).

Virusoids come under a larger group of satellite RNAs (satRNAs). SatRNAs and satellite viruses are associated with several viruses. SatRNAs are small RNA molecules (up to 1500 nucleotides in length), which depend on a HV to replicate, encapsidate and to transmit but rarely have any nucleotide sequence homology with HV (6). Satellite viruses, on the other hand, encode their own capsid protein and are not dependent on a HV, at least for encapsidation. For

Corresponding Author: Sidhant Jain E-mail: jain.sidhant482@gmail.com
Submitted: 04.03.2022 • **Revision Requested:** 17.04.2022 • **Last Revision Received:** 22.04.2022 • **Accepted:** 25.04.2022 • **Published Online:** 16.05.2022

example, the satellite tobacco necrosis virus encodes its icosahedral capsid that accommodates its 1260 nucleotide long RNA, however, it depends upon its HV i.e., tobacco necrosis virus, for RNA polymerase which replicates the genomes of both the entities (10).

SatRNAs and satellite viruses are small molecular parasites. SatRNAs are mostly parasitic, but commensal or beneficial associations are also reported (6). SatRNAs have been subdivided into three subgroups (7), namely Small linear satRNAs (satRNA of less than 700 nucleotides), Large linear satRNAs (satRNA of 0.7-1.5 kb encoding a minimum of one non-structural protein) and Small circular satRNAs or Virusoids (circular RNA shorter than 400 nucleotides). In this work, only the third sub-group of satRNAs, i.e., small circular satRNAs, which is traditionally labelled as virusoids, is discussed. Viruses, viroids, and satellites (along with viriforms) are selfish MGEs which move between different hosts and can change their integration sites in the genomes of hosts. The relationship between hosts and MGEs vary from mutualism to parasitism (1).

Since the late 19th century, the world of acellular biological entities has been extensively studied. The discovery of the tobacco mosaic virus (TMV) provided a foundation for future research on other viruses as well as other acellular entities like viroids and virusoids. In the field of molecular biology, initially, the widely accepted idea was the "Central Dogma" which believed in unidirectional flow of genetic information from DNA to RNA to protein. This flow was presumed to be irreversible (11). However, with the discovery of viruses, the existence of acellular organisms was established, a fact which was further strengthened by subsequent discoveries of viroids and virusoids in the 20th century. These discoveries also challenged the widely accepted Central dogma, as certain viruses have RNA as their genome, which is reverse transcribed to produce DNA (12), whereas viroids and virusoids lack DNA altogether.

These acellular units are the smallest known biological entities. While the prevalence of viral infections is considerably high, the same cannot be said about viroids and virusoids. The latter two are known to infect plants. It is interesting to note that the very existence of these acellular entities supports the possibility of the 'RNA world'. This theory was proposed in 1986 and advocated for a living system which was entirely composed of RNA in the early evolutionary stages of these living systems (13). The existence of viroids and virusoids as RNAs and the use of RNA by some viruses as their genetic material hint towards a plausible RNA world stage in the initial stages of the origin of life on Earth (14).

In this review, we discuss some of the historical milestones achieved since the discovery of these acellular entities with a description of the different mechanisms by which these entities infect and replicate. We also elaborate upon the various theories which have been proposed for their origin and possible evolution in nature.

HISTORICAL BACKGROUND

Viruses

Viruses were first discovered around the end of the 19th century as small entities which were initially identified as unusual pathogens capable of passing through filters which bacteria couldn't cross (15). The first virus, TMV, was discovered in 1892 as a plant pathogen (16). In 1898, the foot-and-mouth disease virus (FMDV) was the second virus to be discovered which is now known to infect farm animals (17). It was also the first animal virus to be discovered followed by the discovery of the first human infecting virus, the Yellow fever virus.

An important breakthrough in the field of virology and molecular biology came with the discovery of bacteriophages i.e., viruses that infect bacteria. Bacteriophages were independently discovered by two notable scientists, namely Twort and d'Herelle (18,19). Bacteriophages are currently being used in the field of molecular biology as vehicles for gene deliveries, phage display, bacterial bio-sensing devices and even biofilm growth control (20). In the field of human clinical biology, phages are being used for the treatment of skin infections caused by bacteria, otitis externa, cholera, and certain lung infections (21). Currently, viruses are also being researched in terms of their development as effective therapeutics. For example, Oncolytic viruses specifically infect and damage tumor cells and are minimally toxic to other cells. Zika virus has demonstrated a unique oncolytic potential against aggressive glioblastoma stem cells and may become a possible therapy against brain tumors in the future (22). There are many clinically important viruses that were discovered between the 1920s and 1960s including the mumps virus, poliovirus, influenza virus, dengue virus and many others.

Another revolution was attained in the field of virology when a new class of viruses, the retrovirus, was discovered in the 1960s. Retroviruses possess RNA as their genetic material and employ an enzyme called reverse transcriptase to synthesize DNA copies from their RNA genome (12). Retroviruses are responsible for a huge disease load in humans. Several cancers are caused due to infection by retroviruses like the Rous sarcoma virus or human T-lymphotropic virus type 1 (HTLV-I). Another major disease linked to retroviruses is Acquired Immunodeficiency Syndrome (AIDS), caused by the human immunodeficiency virus (HIV). Retroviruses are responsible for many diseases in humans, but they have been utilized in many clinical applications. For example, retrovirus vectors have been in use for many years now to attain stable gene transfer— a molecular technique which is widely utilized in gene therapy (23).

Certain viruses identified over the course of time were the root cause of many epidemics. For example, in 1932, the influenza virus was first isolated in a laboratory (24). Several members of this influenza group of viruses have been noted to be responsible for many epidemics and pandemics throughout the course of history. It is generally agreed that the first influenza pandemic outbreak happened in 1580, however, some researchers

place the first outbreak in 1510. The 1580 pandemic originated in Asia and then reached Africa and Europe, subsequently spreading to America (25,26). Since 1700, influenza pandemics have caused a huge number of human fatalities, where three pandemics, namely the 1918 influenza flu, Hong Kong flu and Asian flu, claimed millions of lives (25). Other major diseases like smallpox, measles, poliomyelitis, and AIDS have claimed many millions of human lives in the past. Similarly, pandemics of 21st century like SARS, MERS (27) and COVID-19 were caused by different members of the coronavirus family.

Viroids

In 1971, Theodor O. Diener discovered a type of sub-viral pathogen which causes a devastating disease in potato plants known as potato spindle tuber disease. He later coined the name 'Viroids' for such an infectious agent (3). It was initially believed that the underlying causative agent of the potato spindle tuber disease was a virus, however, further experimentation with the extracts from the infected plants proved that the agent was a free RNA and not a virion, as previously expected (3, 28). The infected plant extracts when treated with ribonuclease, destroyed the infectivity of the infectious agent, whereas incubation with deoxyribonucleases or proteases did not affect its infectivity.

In 1974, it was established that the viroid RNA doesn't code for any proteins (29) however it was only in 1978 that the nucleotide sequence and secondary structures of the potato spindle tuber viroid were decoded (4). Viroids are pathogenic to plants. The viroid genome doesn't code for any protein and its pathogenicity is attributed to the host RNA silencing pathways (30). Current knowledge about viroid structure and its pathogenicity was dealt with tactfully in a recent review article (31).

Virusoids

Randles and group reported the first virusoid in 1981, associated with the Velvet tobacco mottle virus. They isolated it from the Australian tobacco plant (*Nicotiana velutina)* and called it a 'viroid like RNA' (32). Virusoids are known to infect plants. Like viroids, the pathogenicity of virusoids is attributed to host RNA silencing mechanisms (6).

CLASSIFICATION

The International Committee on Taxonomy of Viruses (ICTV) is the sole body which is now responsible for taxonomic classification of viruses, viroids and satRNAs along with other sub-viral agents like prions.

Viruses

Viruses have been conventionally classified by various criteria. For example, viruses have been classified based on their capsid structure, presence of an outer envelope, genetic material, disease caused, host species etc. One of the initial methods involved classifying them by their genetic material. This method was developed in the 1970s by David Baltimore (15,33) and is summarized in Table 1.

Viruses with double stranded (ds) DNA genomes parasitize a great majority of prokaryotes, followed by a significant number of single stranded (ss) DNA viruses. Most of the viruses which infect eukaryotes possess the RNA genome, however, relatively few viruses with RNA genomes are known to infect prokaryotes (34).

The ICTV has been classifying viruses since 1966. It uses an array of characteristics like type of nucleic acids, number of proteins coded, virion size, presence or absence of capsid and many more parameters to classify viruses. (35).

The ICTV has recently recognized that the taxonomy which it developed can be extended in order to project the evolutionary relationships between viruses which are distantly related. Hence, the ICTV has now changed its code in order to allow a 15 rank hierarchy, which is very similar to the Linnaean taxonomic system. 8 primary and 7 derivative ranks are used in this system. The eight principal ranks include four ranks which were already being used as described above (order, family, genus, and species) and four are new, i.e., realm, kingdom, phylum and class. The seven derivative ranks are derived from principal ranks, of which 'subfamily' was already in use in the previous ICTV system. Only primary rank, which doesn't have a derivative rank, is 'species' as no conclusive definition of 'subspecies' could be reached (36). The viruses are currently classified in six

Table 1. Baltimore classification of viruses. ss: single stranded; ds: double stranded; RT: Reverse transcriptase.

Group	Group Name	mRNA generation mechanism
I	dsDNA	Transcription takes place directly from ds DNA.
II	ssDNA	DNA is made ds by replication before the transcription.
III	dsRNA	mRNA is produced from genomic RNA
IV	ssRNA (+)	Replication to generate the negative strand from positive strand. Negative strand is transcribed.
V	ssRNA (-)	Negative strand is directly transcribed.
VI	RT ssRNA	RT is used to generate DNA from genomic RNA. This DNA is used for transcription.
VII	RT dsDNA	DNA is transcribed to generate mRNA. This mRNA is reverse transcribed to generate DNA.

realms and the complete taxonomic details can be accessed through the ICTV master list (https://talk.ictvonline.org/files/master-species-lists/m/msl/12314).

Viroids

The potato spindle tuber viroid (PSTVd) was the first viroid identified by Diener in the early 1970s (3). Another viroid, the Avocado sun blotch viroid (ASBVd), showed remarkable self-cleaving properties through hammerhead ribozymes, thus behaving like catalytic RNAs. Based on all the evidence procured from the studies on PSTVd and ASBVd, two viroid families, *Pospiviroidae* and *Avsunviroidae*, were proposed (28,37,38). The use of next generation sequencing technologies has enabled the researchers to identify new viroids (39,40). As per the ICTV, 33 viroid species are officially recognized (41,42).

Until today, 5 viroid species have been grouped in 3 genera under family *Avsunviroidae* (41) whereas 28 viroid species have been grouped in 5 genera under family *Pospiviroidae* (42). The members of *Avsunviroidae* exclusively infect dicots, whereas the members of *Pospiviroidae* infects dicots and some monocots (41,42).

In *Pospiviroidae*, the viroid replication is localized to the nucleus and is facilitated by a Class-III RNase mediated cleavage of the dsRNA structure, whereas in *Avsunviroidae*, replication takes place in the plastids, mainly the chloroplasts, using the self-cleaving properties of the hammerhead ribozyme RNA motif. The members of *Pospiviroidae* exhibit relatively low sequence diversity among themselves whereas in *Avsunviroidae*, high mutation rates have led to a complex array of sequence diversity (38,43).

Virusoids

As per the 9th ICTV report (44), a total of nine small circular satRNAs or virusoids are known and a possible member i.e. Cherry small circular viroid-like RNA is proposed. These nine officially recognized virusoids have been placed in three groups. The first of these groups concerns circular satRNAs associated with viruses belonging to the *Secoviridae* family having 3 virusoid members, whereas the second group involves one virusoid associated with viruses belonging to the *Luteoviridae* family. The last group involves virusoids associated with viruses belonging to the genus *Sobemovirus* and has 5 virusoids.

Most virusoids infect plants but the Hepatitis Delta Virus (HDV), which infect humans was previously labelled as a virusoid by some researchers. HDV has a circular RNA genome and uses Hepatitis B virus as a HV but as its genome size is relatively large (~1700 nucleotides), it doesn't strictly fulfil the requirements to be a virusoid (45). Moreover, the ICTV has classified HDV as a bona fide virus (44).

ORIGIN AND EVOLUTION

Viruses

Viruses can neither multiply nor carry out essential metabolic processes outside living cells, hence their origin still poses a dilemma to virologists. As viruses are entirely dependent on living cells, the origin and evolution of both viruses and cells seems to be intertwined (46).

Three hypotheses (namely the Virus-first hypothesis, Escape hypothesis and Reduction hypothesis) have been put forward to explain the origin of viruses:

Virus-first hypothesis

d'Herelle first claimed that viruses appeared before cells (47). Others claimed that most viruses (apart from dsRNA and negative-strand RNA viruses) originated within the primordial pool (15). As per this study, positive-strand RNA viruses descended directly from the primordial RNA-protein world and reverse-transcribing elements provided a means for transition to the DNA world.

This hypothesis is strengthened by two observations. First, RNA is currently considered as the first replicating molecule by many biologists rather than DNA. Second, ribozymes i.e., RNA molecules having enzymatic properties of catalyzing chemical reactions, are reported in the literature. These two observations point towards a possibility that these self-replicating RNA molecules originated first, even before the first cells, and then developed the ability to infect the cells, which originated later (48).

Further, a considerable portion of all viral genomes is made up of genetic sequences that lack cellular homologues and hence point towards an exclusive origin of viruses (49). However, as of today, all viruses need a cellular machinery to replicate which necessitates the presence of cells and hence this hypothesis is widely questioned.

Escape hypothesis

According to this hypothesis, viruses were initially a part of cell and are derived from fragments of cellular RNA or DNA or both, such as plasmids. These fragments escaped cellular control, acquired a protein coat and became independent structures which were capable of infecting other cells. These viruses further evolved by robbing the genes from other cells by the horizontal gene transfer mechanism (46,50).

Reduction hypothesis

This hypothesis labels viruses as 'reduced' parasitic organisms. Initially, two autonomous organisms might have entered into a symbiotic relationship with each other but over time the dependence of one might have grown more and more such that it became parasitic in nature. This parasitic organism then lost its genes which were once considered essential. As a result, they lost their ability to replicate and became obligatory intracellular parasites or 'viruses' (48,50).

Both the escape and the reduction hypothesis can be considered as 'cell-first' hypothesis as they advocate for the presence of a free-living cell before the origin of viruses. However, these Cell-first hypotheses cannot explain the presence of genetic sequences in viral genomes which lack the cellular homologues (49).

It is not possible to select any of these hypotheses as the exact mechanism. The 'Virus-first' hypothesis explains the lack of clear cellular homologues. However, ribozymes in HDV are related to the human ribozyme CPEB3, both structurally and biochemically. This observation points towards a possible origin of HDV from human transcriptome, hence advocating for the escape hypothesis (51).

Nucleocytoplasmic large DNA viruses (NCDLVs) support the reduction hypothesis. Members of this group, especially the mimivirus and poxvirus, are relatively more complex and hence they depend less on their hosts. The Mimivirus has a huge genome of 1.2 million base pairs as compared to other viruses. Similarly, the poxvirus carries many viral enzymes which allows it to produce functional mRNAs in the cytoplasm of the host cell (48,52).

In our view, strong evidence exists in favor of all three hypotheses. It is possible that different viruses must have originated distinctly using different strategies and evolved further. This conclusion is further backed by a recent study (53) which showed that major virion proteins evolved at 20 independent occasions. In some of these cases, the ancestry could be traced to the cellular proteins. Krupovic and Koonin hence inferred that some viruses could have descended from the primordial RNA world and most others evolved on multiple occasions by recruiting diverse proteins of the host cell which later became major components of the virion.

Viruses evolve just like cellular life. They undergo genetic recombination (insertion of gene fragments), genome re-assortment (replacement of genetic segments from a related virus) and point mutations where the 'fittest' mutants quickly outnumber the others (54). Viral mutation rates depend upon an array of factors involving genome type, intrinsic polymerase fidelity, presence or absence of fidelity mechanisms, editing by deaminases encoded by hosts, other host dependent factors that include an unbalanced nucleotide pool or levels of reactive oxygen species (55).

As the number of viruses is extremely large, it is beyond the scope of the current work to enumerate most of the evolutionary phenomena and other mechanisms observed among distinct classes of viruses. Therefore, influenza viruses are used as a model example to demonstrate the three mechanisms of viral evolution.

Influenza viruses are among the most notorious viruses when it comes to causing epidemics and pandemics in the history of the human race. Since 1510, 14 pandemics have been directly linked to influenza viruses, with the 1918 pandemic being the deadliest which claimed about 50 million lives worldwide (26,56). However, a recent re-assessment study of 1918 pandemic placed the number of global deaths at around 15 million (57).

The Influenza A virus (IAV) contains three proteins in its membranes, namely, hemagglutinin (HA), neuraminidase (NA) and a proton channel (M2). HA helps in the binding of the virus to the sialic acid receptor on the host cell membrane and fusion of the cell membrane with the virus. The NA cleaves the sialic acid residues and other conjugates from the newly assembled virus, facilitating its spread to other cells. As HA and NA facilitate the binding and cleaving of viruses, they play an extremely crucial role in the determination of host specificity (58). There are 16 HA subtypes which are sorted in two major groups (59). Similarly, there are 9 major subtypes of NA which are sorted in 3 groups. Two new subtypes have been recently described in bats for both HA and NA, i.e., H17, H18 and N10, N11 respectively (60).

The best strategy for IAVs (or any other parasite) to thrive is to evade the immune system of the host but at the same time preserving its ability to interact and infect host cells. Like other viruses, IAVs also employ all the 3 mechanisms to evolve and evade the immune system (58). Point mutations that change the amino acids in the antigenic portions of HA and NA can provide selective advantage to the virus (e.g., by helping the virus to better evade the immune system) and this has been labelled as antigenic drift. When re-assortment occurs in genes coding for HA and/or NA between two or more viruses in a host cell, it leads to the emergence of new progeny viruses, and this is called antigenic shift (Figure 1) (56,61).

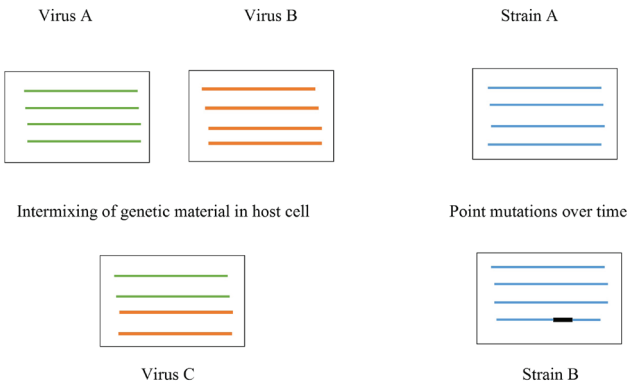

Figure 1. Antigenic shift (leading to the generation of Virus C) vs Antigenic drift (leading to the formation of a new strain of the virus).

Antigenic drift can occur in any subtype of influenza virus, however it often occurs in human IAVs due to which the IAV vaccination has a limited effect on human population, hence necessitating flu shots in every flu season. As a consequence, it kills tens of thousands of humans and adds an economic burden of USD 50 billion in the USA alone (62). If an amino acid substitution in HA or NA helps a virus escape the host immune system, it provides a fitness benefit, as a result of which, it might replace the circulating strain and emerge as a novel epidemic strain which can even lead to an epidemic or pandemic (63). It has been proposed that the surface proteins of influenza virus responsible for the 1918 pandemic drifted more rapidly which made it more lethal when compared to other viruses (64).

There are eight RNA segments in the genome of IAVs. When two related IAVs co-infect one host, there is a possibility of 256 combinations for shuffling and re-assortment. When HA or NA or both are exchanged, antigenic shift takes place leading to the emergence of a new IAV altogether, which can allow the virus to spill between the species, having the potential to cause pandemics (56). Most IAV associated pandemics are a result of re-assortment including the H2N2 virus of 1957, H3N2 of 1968 and the somewhat recent pandemic of 2009 involving the H1N1 virus (65).

The 2009 pandemic comprehensively explains the kind of evolution IAVs go through. The emergence of the H1N1 virus of 2009 involved multiple re-assortment events. A triple re-assortment event, involving three influenza viruses namely, 'classical swine' H1N1, 'human seasonal' H3N2 and North American avian influenza virus, led to the emergence of the North American 'triple reassortant' H1N2 virus in swine, which again re-assorted with the 'Eurasian-avian like' swine H1N1 influenza virus leading to the generation of the 2009 H1N1 virus which spilled over to humans causing the pandemic (66,67).

Though a rare event, recombination in IAVs occurs by two mechanisms. Non-homologous recombination (occurs between two different RNA fragments) and by the extremely rare homologous recombination which causes template switching when RNA is being replicated by the polymerase (58). The A/seal/Mass/1/80 influenza virus (H7N7) mutants contains an insertion in HA genes which is 60 nucleotides long in length and is most probably a result of a non-homologous recombination event between nucleoprotein gene and the HA gene of the same virus. This evolutionary event led to increased pathogenicity in chickens and broadened the range of host cells that the virus can infect (68). Although rare in influenza viruses, recombination is commonly encountered in natural evolution of poliovirus strains (69).

Viroids

Earlier propositions suggested that viroids might be introns that somehow escaped from the host RNAs. Such propositions were based on their shared similarities with the introns. The way viroids self-replicate resembles the process of self-splicing in introns (70). Viroids like PSTVd share nucleotide sequence similarities with the group I and group II introns (although the new bioinformatics tools put a question mark on the significance of this sequence similarity). Another theory suggested their possible origin from transposable elements, but the evidence is scarce (71,72). Moreover, many other viroids like ASBVd did not fit into this theory (38,73).

There are several features that make viroids suitable as reminiscent of the pre-cellular world. Their small size could have been a way to survive and escape their extinction due to the error-prone process of replication (74-77). Most of them possess GC rich sequences which is suggestive of relatively higher replication fidelity as GC pairs exhibit greater thermodynamic stability relative to AU pairs (78).

Their circular nature aided by the rolling circle mode of replication would have ensured complete end to end replication without loss of genetic information. It is interesting to note that there are repeating units of different lengths in the viroid genome which provides structural periodicity. The presence of ribozymes and lack of protein coding ability is suggestive of their appearance before ribosomes in an 'RNA world'. All these characteristics together with the appearance of catalytic activity (to catalyze cleavage and ligation) mediated by simple hairpin and hammerhead ribozymes would have enabled viroid replication in a pre-protein world (38). Most of the evidence points towards a monophyletic origin for the viroids and all these comparisons are deduced based on phylogenetic reconstructions. However, the possibility of viroids having a polyphyletic origin cannot be dismissed entirely, as members of the family *Avsunviroidae* show nucleotide base composition different from other viroids (38).

Virusoids

Even today our knowledge about virusoids remains limited. Hence, our knowledge about their origin and evolution still remains somewhat elusive. One reason for this information scarcity may be attributed to the low number of virusoids which have been discovered to date and their recent discovery relative to the viruses.

One study has linked virusoids to Group 1 introns. As per this study (79), Group 1 introns, which are found in the genes of nuclear and mitochondrial rRNA and chloroplastic tRNA, have a 16-nucleotide consensus sequence along with three sets of complementary sequences. These hallmarks of group 1 introns are also present in virusoids (79).

It is possible that both viroids and virusoids may have a similar history of origin despite being different in aspects of encapsidation and dependence on HVs. Both share certain features like having a small nucleotide sequence of less than 400 nucleotides and presence of hammerhead ribozymes. In our view, an elaborate mechanism for their origin cannot be predicted as of now, however the possibility of origin of these virusoids from their HVs can be out rightly rejected as most of them lack any nucleotide sequence similarities with their HV.

MODE of ENTRY and REPLICATION

Viruses

Most viruses have their genetic material encased in a protein covering which is covered by a lipid bilayer in case of enveloped viruses (80). Depending upon the virus type, they either fuse directly with the plasma membranes of the cells by receptor mediated fusion or are engulfed into an endosome.

In some cases, like HIV and poliovirus, conventional understanding advocated for a direct penetration into the host cell membrane, however, development of newer techniques, like the use of specific drugs and siRNA, which selectively prevented virus entries through specific pathways, have challenged this understanding (81). For example, in the case of the poliovirus,

a drug (ionophore monensin) was used to dissipate the cellular protein gradients which suggested a pH dependent route of virus entry and challenged the traditional understanding (81,82).

In the case of enveloped viruses, the host cell surface proteins act as receptors for viruses. For example, viruses like SARS-CoV and SARS-CoV-2, have been shown to exploit the Angiotensin-converting enzyme 2 (ACE2) receptor (83). ACE2 is widely expressed in the human respiratory tract epithelium and alveolar monocytes along with other locations like the venous endothelium, small intestine cells and in renal tubule epithelial cells (83-85).

These viruses then tend to fuse their membrane with that of the cell. The fusion process is energy driven (as lipid membranes do not fuse spontaneously) and is mediated by viral envelope glycoproteins. Three classes of these proteins have been defined according to the mechanical and structural dynamics of the viral fusion proteins, but the fundamental process of viral membrane fusion remains the same for all the classes. This process involves the simultaneous engagement of viral and target membrane which is followed by hairpin formation, ultimately leading to fusion (86). The viral genome enters the cytosol through a fusion pore which then initiates the infection (86,87).

In case of non-enveloped viruses like the simian virus 40 (SV40), the exact biophysical and molecular mechanism for cytosol entry is still poorly understood, however it is clear that the endocytic pathway plays a major role. As a result of the use of endocytic pathway, membranes of many cell organelles like Golgi and endoplasmic reticulum are also penetrated by certain non-enveloped viruses (81). Interestingly, many enveloped viruses like influenza viruses, the vesicular stomatitis virus and some others use the endocytic pathway for internalization (88).

Once inside the cell, the virus hijacks the cellular machinery. Viruses completely rely on a host's protein synthesis machinery and recruit cellular ribosomes to translate viral mRNAs (89). Depending upon the genomic constitution of the viruses, newly translated structural and non-structural or catalytic proteins are then used in the assembly of virion and to replicate the genetic material of the virus (like RNA-dependent RNA polymerases or RdRps of RNA viruses) respectively. Viruses, depending upon their genomic constitution, invoke different replication mechanisms, like rolling circle replication, rolling hairpin replication, and dsDNA bidirectional replication, among others. New viral particles are produced with the viral genetic material which are now ready for a new round of infection (87,90).

In case of viruses like bacteriophages, two types of replication cycles are reported—the lytic cycle and the lysogenic cycle. The lytic cycle involves immediate transcription, replication, and release of mature phage particles soon after infection of the bacterial cells, whereas the lysogenic cycle involves the integration of the phage genome into the bacterial genome where the phage survives as a prophage till it is induced by a stimulus to replicate and get released (91).

Few viruses have evolved this ability to integrate their genomes into the host genomes, which can have multiple consequences for the host cell involving oncogenesis, gene disruption, premature cell death and even species evolution through genome inclusions of a heritable nature. In DNA viruses like the Adenovirus, SV40 and others, viral genome integration is rarely reported, whereas it is necessary for retroviruses. Incidental integration by has been reported in the measles virus, Ebola virus, rabies virus and others (92).

Viroids

After mechanical damage to the plant cell wall, viroids enter the host through the leaf epidermis and are transported to neighboring cells (43). In some cases of an infected plant, they can enter the pollen or ovule from where they get transmitted to the seed (93). If and when the seed germinates, it gives rise to an infected plant. In the case of plants infested by the members of the *Pospiviroidae*, viroid RNA is imported into the nucleus, and is copied by plant DNA-dependent RNA polymerase II, whereas in cases of plants infected by *Avsunviroidae members*, viroid RNA is imported into the chloroplast, and RNA replication is carried out by chloroplast DNA-dependent RNA polymerase (94).

In order to systemically infect the host, viroids show three types of movements. Intracellular movement is essential for import in nucleus or chloroplast for replication. Within the cell, viroid movement is independent of the cytoskeleton and seems to be receptor-mediated, specific to certain conserved sequences and/or structural motifs. After replication, the viroid exits to the cytoplasm and utilizes cell-to-cell movement to reach neighboring cells. In order to reach the neighboring cells, viroids have been shown to exploit specialized connections between plant cells called plasmodesmata which allow them to avoid crossing the plasma membrane. Long distance movement is then utilized to reach the vasculature (e.g., phloem) and invade the most distal parts of the plants (43,95).

Viroids (*Avsunviroidae*) bear self-cleaving ribozyme structures in their RNA genomes. Viroids are not encapsidated and replicate via a 'rolling-circle' mechanism in plant hosts (96). Replication involves RNA-RNA transcription which is aided by host coded DNA-dependent RNA polymerase and are often considered as parasites of the subcellular transcriptional machinery in the nucleus and chloroplasts in plants (43).

The entire process of viroid replication occurs through two different pathways: (1) In the asymmetric pathway (family *Pospiviroidae*), the monomeric circular (+) strand is repeatedly transcribed into oligomeric (-) strands. These (-) strands are transcribed to the oligomeric (+) strand by RNA polymerase. This is followed by site-specific cleavage of the (+) strand by the RNae III-like enzyme, to produce a linear monomer that is circularized by DNA ligase (97).

(2) In the symmetric pathway (family *Avsunviroidae)*, the oligomeric (-) strand, generated in the first rolling circle generated from the monomeric circular (+) strand, is cleaved and ligated in the monomeric circular (-) strand which serves as a template

for the second rolling circle producing the oligomeric (+) strand which is processed to generate monomeric (+) strands (38,97).

Virusoids

Like other satRNAs, virusoids depend upon a HV to move, transmit and infect cells (6). Once inside the cell, a complex interaction occurs between the virusoid, HV and the host cell for the virusoid's replication. These interactions occur as a result of the dependence of the virusoid on the HV for replication and the dependence of the HV on the host cell for replication (98). Virusoids replicate in the cytoplasm of the host cell and use transcription and processing machinery, which is in part encoded by the host cells and in part by the HV (94). Structural and sequence motifs in RNA are used by virusoids to signal the HV and host cell to replicate and encapsidate it (99). Owing to the circular genome, the rolling circle mechanism is used for RNA replication. A hammerhead self-cleavage reaction is involved in the production of positive and negative monomeric RNA strands as a part of the rolling circle mechanism (100). Once replicated, the HV encapsidates the virusoid 'genome'.

The three entities show very different modes of infection. On one hand, where viruses utilize either endocytosis or receptor mediated fusion, viroids enter a host either through a damaged cell wall, infected pollen or through an infected ovule which becomes seed upon fertilization. However, the transmission from pollen to seeds is not observed in all the viroids (101). Utilizing the three different movements, viroids then infect the entire host. Virusoids movements are dependent upon HVs, and they invade the cell which is being infected by the HV. Once in the cytoplasm, virusoids show the ribozyme activity for replication. This is in contrast to viroids, which replicate either in nucleus or chloroplast.

DISCUSSION

Viruses and other sub-viral particles seem to have been with their cellular counterparts since the very beginning. Owing to the discovery of viruses before other sub-viral particles and a relatively higher impact on humans, a lot more is known about them as compared to others. In-spite of this, we still do not have a clear mechanism for the origin of viruses. It is possible that different viruses originated separately by utilizing different strategies (as explained by the Virus-first hypothesis, Escape hypothesis and Reduction hypothesis) and evolved further. It can also be speculated that all viruses originated through a mechanism which still needs to be discovered. The presence of different kinds of genomes and the ability to infect almost all cellular forms (15) point towards the intricate evolution that viruses must have undergone to achieve these extensive capabilities

The current case of the COVID-19 pandemic shows how mutations in the genome of related viruses can have huge repercussions for humanity. In spite of using the same ACE2 receptor (83), three different coronaviruses, i.e., HCoV-NL63, SARS-CoV and SARS-CoV-2 have very different infectivity and mortality rates. This shows that sharing common receptors by related viruses need not have similar outcomes. This capability would have been achieved through evolution at different levels which involves complex dynamics between primary and intermediary hosts as well as the environmental conditions alongside opportunistic infection probabilities. Epidemics and pandemics from recent history and the present show that in spite of knowing much about viruses, we are not fully capable of controlling pandemics, and hence a greater amount of support is needed for research as well as for the healthcare sector.

Owing to a much simpler structure of viroids than viruses, it is possible that they originated before viruses. There are other clues like small size, high GC content in genome and others which show that viroids must be an important component of a pre-cellular world (74).

Virusoids totally depend upon HVs to infect cells and move among them, and two scenarios are possible. Either virusoids were always dependent on HVs and originated only after the origin of viruses or it is possible that these are two independently evolved entities. It is possible that through opportunistic co-infection of similar cells, virusoids started depending upon HVs, lost their protein coding abilities and became totally dependent on viruses. The latter observation is supported by the fact that viruses and virusoids don't have nucleotide sequence homology. Furthermore, discovery of a virusoid associated with the rice yellow mottle virus, which codes for a 16 kDa protein, also supports the latter scenario (9).

Both virusoids and viroids infect plants, have similar genome size, both use the rolling circle mechanism for replication and exhibit hammerhead cleavage reaction (14,96,100). These properties suggest a probable relation between them which calls for further study.

It is of utmost importance to understand the pathogenicity of viroids and virusoids better. Since there is limited to no natural resistance in plants against the viroid infections, it has become a necessity to try and develop resistant varieties of susceptible plants. Over the years, though scientists have achieved considerable success in generating plants that show delayed occurrence of symptoms and the severity of the symptoms has also been reduced significantly (102), there is a long way to go.

Peer Review: Externally peer-reviewed.

Author Contributions: Conception/Design of Study- S.J.; Data Acquisition- S.J., S.D.; Data Analysis/Interpretation- S.J., S.D. ; Drafting Manuscript- S.J., S.D.; Critical Revision of Manuscript- S.J., S.D.; Final Approval and Accountability- S.J., S.D.

Conflict of Interest: Authors declared no conflict of interest.

Financial Disclosure: Authors declared no financial support.

REFERENCES

1. ICVCN (2021). The international code of virus classification and nomenclature. (https://talk.ictvonline.org/information/w/ictv-information/383/ictv-code)

2. Agut H, Fillet AM and Calvez V. Qu'est-ce qu'un virus? [What is a virus?]. La Revue du praticien 1997; 47(6): 602-7.
3. Diener TO. Potato spindle tuber "virus". IV. A replicating, low molecular weight RNA. Virology 1971; 45(2): 411-28.
4. Gross HJ, Domdey H, Lossow C, Jank P, Raba M, Alberty H, et al. Nucleotide sequence and secondary structure of potato spindle tuber viroid. Nature 1978; 273(5659): 203-8.
5. Sanger HL, Klotz G, Riesner D, Gross HJ and Kleinschmidt AK. Viroids are single-stranded covalently closed circular RNA molecules existing as highly base-paired rod-like structures. Proc Natl Acad Sci U S A 1976; 73(11): 3852-6.
6. Hu CC, Hsu YH and Lin NS. Satellite RNAs and Satellite Viruses of Plants. Viruses 2009; 1(3): 1325-50.
7. Palukaitis P. Satellite RNAs and Satellite Viruses. Mol Plant Microbe Interact 2016; 29(3): 181-6.
8. Palukaitis P. What has been happening with viroids? Virus Genes 2014; 49(2): 175-84.
9. AbouHaidar MG, Venkataraman S, Golshani A, Liu B and Ahmad T. Novel coding, translation, and gene expression of a replicating covalently closed circular RNA of 220 nt. Proc Natl Acad Sci U S A 2014; 111(40): 14542-7.
10. Salvato MS and Fraenkel-Conrat H. Translation of tobacco necrosis virus and its satellite in a cell-free wheat germ system. Proc Natl Acad Sci U S A 1977; 74(6): 2288-92.
11. Coffin JM, Hughes SH, Varmus HE, editors. Retroviruses. Cold Spring Harbor (NY): Cold Spring Harbor Laboratory Press; 1997.
12. Temin HM and Baltimore D. RNA-directed DNA synthesis and RNA tumor viruses. Adv Virus Res 1972; 17: 129-86.
13. Gilbert W. Origin of life: The RNA world. Nature 1986; 319: 618.
14. Rao AL and Kalantidis K. Virus-associated small satellite RNAs and viroids display similarities in their replication strategies. Virology 2015; 479-480: 627-36.
15. Koonin EV and Dolja VV. A virocentric perspective on the evolution of life. Curr Opin Virol 2013; 3(5): 546-57.
16. Iwanowski D. "Über die Mosaikkrankheit der Tabakspflanze". Bulletin Scientifique Publié Par l'Académie Impériale des Sciences de Saint-Pétersbourg Nouvelle Serie III 1892; 35: 67-70.
17. Loeffler F and Frosch P. Berichte der kommission zur erforschung der maulund klauenseuche bei dem institut ftjr infektionskrankheiten in Berlin. Centb Bakt 1898; 23(1): 371-91.
18. Twort FW. An investigation on the nature of ultra-microscopic viruses. Lancet 1915; 2: 1241-3.
19. d'Herelle F. An invisible microbe that is antagonistic to the dysentery bacillus. Comptes Rendus Academie Sciences Paris, 1917; 165: 373-5.
20. Harada LK, Silva EC, Campos WF, Del Fiol FS, Vila M, Dąbrowska K, et al. Biotechnological applications of bacteriophages: State of the art. Microbiol Res 2018; 212-213:38-58.
21. Principi N, Silvestri E and Esposito S Advantages and Limitations of Bacteriophages for the Treatment of Bacterial Infections. Front Pharmacol 2019; 10: 513.
22. Jain S and Kumar S. Cancer immunotherapy: dawn of the death of cancer? Int Rev Immunol 2020; 39: 1-18.
23. Barquinero J, Eixarch H and Pérez-Melgosa, M. Retroviral vectors: new applications for an old tool. Gene Ther 2004; 11: 3-9.
24. Smith W, Andrewes CH and Laidlaw PP. A virus obtained from influenza patients. Lancet 1933; 2: 66-8.
25. Potter CW. A history of influenza. J Appl Microbiol 2001; 91(4): 572-9.
26. Taubenberger JK and Morens DM. Pandemic influenza--including a risk assessment of H5N1. Rev Sci Tech 2009; 28(1): 187-202.
27. Yin Y and Wunderink RG. MERS, SARS and other coronaviruses as causes of pneumonia. Respirology 2018; 23(2): 130-7.
28. Diener TO. Discovering viroids-a personal perspective. Nat Rev Microbiol 2003; 1(1): 75-80.
29. Davies JW, Kaesberg P and Diener TO. Potato spindle tuber viroid. XII. An investigation of viroid RNA as a messenger for protein synthesis. Virology 1974; 61: 281-6.
30. Owens RA and Hammond RW. Viroid pathogenicity: one process, many faces. Viruses 2009; 1(2): 298-316.
31. Adkar-Purushothama CR and Perreault J. Current overview on viroid–host interactions. Wiley Interdisciplinary Reviews: RNA 2019; 11: e1570.
32. Randles J, Davies C, Hatta T, Gould A and Francki R. Studies on encapsidated viroid-like RNA I. Characterization of velvet tobacco mottle virus. Virology 1981; 108(1): 111-22.
33. Aiewsakun P and Katzourakis A. Time-Dependent Rate Phenomenon in Viruses. J Virol 2016; 90(16): 7184-95.
34. Koonin EV, Dolja VV and Krupovic M. Origins and evolution of viruses of eukaryotes: The ultimate modularity. Virology 2015; 479-480: 2-25.
35. Louten J. Virus Structure and Classification. Essential Human Virology 2016; 19-29.
36. International Committee on Taxonomy of Viruses Executive Committee. The new scope of virus taxonomy: partitioning the virosphere into 15 hierarchical ranks. Nature microbiology 2020; 5(5): 668-674. https://doi.org/10.1038/s41564-020-0709-x
37. Elena SF, Dopazo J, Flores R, Diener TO and Moya A. Phylogeny of viroids, viroidlike satellite RNAs, and the viroidlike domain of hepatitis delta virus RNA. Proc Natl Acad Sci U S A 1991; 88(13): 5631-4.
38. Flores R, Gago-Zachert S, Serra P, Sanjuan R and Elena SF. Viroids: survivors from the RNA world? Annu Rev Microbiol 2014; 68: 395-414.
39. Choi H, Jo Y, Cho WK, Yu J, Tran PT, Salaipeth L, et al. Identification of Viruses and Viroids Infecting Tomato and Pepper Plants in Vietnam by Metatranscriptomics. Int J Mol Sci 2020; 21(20): 7565.
40. Bester R, Cook G, Breytenbach JHJ, Steyn C, De Bruyn R, Maree HJ. Towards the validation of high-throughput sequencing (HTS) for routine plant virus diagnostics: measurement of variation linked to HTS detection of citrus viruses and viroids. Virol J 2021; 18: 61.
41. Di Serio F, Li SF, Matoušek J, Owens RA, Pallás V, Randles JW, et al. ICTV Virus Taxonomy Profile: Avsunviroidae. J Gen Virol 2018; 99(5): 611-2.
42. Di Serio F, Owens RA, Li SF, Matoušek J, Pallás V, Randles JW, et al. ICTV Virus Taxonomy Profile: Pospiviroidae. J Gen Virol 2021; 102(2): 001543.
43. Tsagris EM, Martinez de Alba AE, Gozmanova M and Kalantidis K. Viroids. Cell Microbiol 2008; 10(11): 2168-79.
44. ICTV (2011). Satellites and Other Virus-dependent Nucleic Acids, ICTV 9th Report.
45. Alves C, Branco C and Cunha C. Hepatitis delta virus: a peculiar virus. Adv Virol 2013; 560105.
46. Durzyńska J and Goździcka-Józefiak A. Viruses and cells intertwined since the dawn of evolution. Virol J 2015; 12: 169.
47. d' Herelle F.The bacteriophage: its rôle in immunity. Baltimore: Williams & Wilkins. 1922.
48. Wessner DR. The Origins of Viruses. Nature Education 2010; 3(9):37.
49. Koonin EV, Senkevich TG and Dolja VV. Compelling reasons why viruses are relevant for the origin of cells. Nat Rev Microbiol 2009; 7(8): 615.
50. Nasir A, Kim KM and Caetano-Anolles G. Giant viruses coexisted with the cellular ancestors and represent a distinct supergroup along with superkingdoms Archaea, Bacteria and Eukarya. BMC Evol Biol 2012; 12: 156.
51. Salehi-Ashtiani K, Lupták A, Litovchick A and Szostak JW. A genomewide search for ribozymes reveals an HDV-like sequence in the human CPEB3 gene. Science 2006; 313(5794):1788-92.

52. La Scola B, Audic S, Robert C, Jungang L, de Lamballerie X, Drancourt M, et al. A giant virus in amoebae. Science 2003; 299(5615): 2033.
53. Krupovic M and Koonin EV. Multiple origins of viral capsid proteins from cellular ancestors. Proc Natl Acad Sci U S A 2017; 114(12): 2401-10.
54. Domingo E, Escarmís C, Sevilla N, Moya A, Elena SF, Quer J, et al. Basic concepts in RNA virus evolution. FASEB J 1996; 10(8): 859-64.
55. Sanjuán R and Domingo-Calap P. Mechanisms of viral mutation. Cell Mol Life Sci 2016; 73(23): 4433-48.
56. Taubenberger JK and Kash JC. Influenza virus evolution, host adaptation, and pandemic formation. Cell Host Microbe 2010; 7(6): 440-51.
57. Spreeuwenberg P, Kroneman M and Paget J. Reassessing the Global Mortality Burden of the 1918 Influenza Pandemic. Am J Epidemiol 2018; 187(12): 2561-67.
58. Shao W, Li X, Goraya MU, Wang S and Chen JL. Evolution of Influenza A Virus by Mutation and Re-Assortment. Int J Mol Sci 2017; 18(8).
59. Russell RJ, Kerry PS, Stevens DJ, Steinhauer DA, Martin SR, Gamblin SJ, et al. Structure of influenza hemagglutinin in complex with an inhibitor of membrane fusion. Proc Natl Acad Sci U S A 2008; 105(46): 17736-41.
60. Tong S, Zhu X, Li Y, Shi M, Zhang J, Bourgeois M, et al. New world bats harbor diverse influenza A viruses. PLoS Pathog 2013; 9(10): e1003657.
61. Mostafa A, Abdelwhab EM, Mettenleiter TC and Pleschka, S. Zoonotic Potential of Influenza A Viruses: A Comprehensive Overview. Viruses 2018; 10(9).
62. Das SR, Hensley SE, Ince WL, Brooke CB, Subba A, Delboy MG, et al. Defining influenza A virus hemagglutinin antigenic drift by sequential monoclonal antibody selection. Cell Host Microbe 2013; 13(3): 314-23.
63. Webster RG and Govorkova EA. Continuing challenges in influenza. Ann N Y Acad Sci 2014; 1323: 115-39.
64. Taubenberger JK. The origin and virulence of the 1918 "Spanish" influenza virus. Proc Am Philos Soc 2006; 150(1): 86-112.
65. Urbaniak K and Markowska-Daniel I. In vivo reassortment of influenza viruses. Acta Biochim Pol 2014; 61(3): 427-31.
66. Neumann G, Noda T and Kawaoka Y. Emergence and pandemic potential of swine-origin H1N1 influenza virus. Nature 2008; 459(7249): 931-9.
67. Gracia JCM. Novel insights in the adaptation of avian H9N2 influenza viruses to swine. (Doctor of Philosophy (Ph.D.), 2017); Ghent University, Belgium.
68. Orlich M, Gottwald H and Rott, R. Nonhomologous recombination between the hemagglutinin gene and the nucleoprotein gene of an influenza virus. Virology 1994; 204(1): 462-5.
69. Dahourou G, Guillot S, Le Gall O, Crainic R. Genetic recombination in wild-type poliovirus. J Gen Virol 2002; 83: 3103-10.
70. Diener TO. Origin and evolution of viroids and viroid-like satellite RNAs. Virus Genes 1995; 11(2-3): 119-31.
71. Cervera A and De la Peña, M. Eukaryotic penelope-like retroelements encode hammerhead ribozyme motifs. Mol Biol Evol 2014; 31(11): 2941-7.
72. Cervera A, Urbina D and De la Peña M. Retrozymes are a unique family of non-autonomous retrotransposons with hammerhead ribozymes that propagate in plants through circular RNAs. Genome Biol 2016; 17: 135.
73. Kiefer MC, Owens RA and Diener TO. Structural similarities between viroids and transposable genetic elements. Proc Natl Acad Sci U S A 1983; 80(20): 6234-8.
74. Diener TO . Circular RNAs: relics of precellular evolution? Proc Natl Acad Sci U S A 1989; 86(23): 9370-4.
75. Gago S, Elena SF, Flores R and Sanjuán, R. Extremely high mutation rate of a hammerhead viroid. Science (New York, N.Y.) 2009; 323(5919): 1308.
76. López-Carrasco A, Ballesteros C, Sentandreu V, Delgado S, Gago-Zachert S, Flores R, et al. Different rates of spontaneous mutation of chloroplastic and nuclear viroids as determined by high-fidelity ultra-deep sequencing. PLoS pathogens 2017; 13(9): e1006547.
77. Wu J and Bisaro DM. Biased Pol II fidelity contributes to conservation of functional domains in the Potato spindle tuber viroid genome. PLoS pathogens 2020; 16(12): e1009144.
78. Eigen M and Schuster P.The hypercycle. A principle of natural self-organization. Part C: the realistic hypercycle. Naturwissenschaften 1978; 65: 341-69.
79. Dinter-Gottlieb G. Viroids and virusoids are related to group I introns. Proc Natl Acad Sci U S A 1986; 83(17): 6250-4.
80. Mothes W, Sherer NM, Jin J and Zhong P. Virus cell-to-cell transmission. J Virol 2010; 84(17): 8360-8.
81. Thorley JA, McKeating JA and Rappoport JZ. Mechanisms of viral entry: sneaking in the front door. Protoplasma 2010; 244(1-4): 15-24.
82. Madshus IH, Olsnes S and Sandvig K. Mechanism of entry into the cytosol of poliovirus type 1: requirement for low pH. J Cell Biol 1984; 98(4): 1194-200.
83. Zhou P, Yang XL, Wang XG, Hu B, Zhang L, Zhang W, et al. A pneumonia outbreak associated with a new coronavirus of probable bat origin. Nature 2020; 579 (7798): 270-3.
84. Li W, Moore MJ, Vasilieva N, Sui J, Wong SK, Berne MA, et al. Angiotensin-converting enzyme 2 is a functional receptor for the SARS coronavirus. Nature 2003; 426(6965): 450-4.
85. Guo Y, Korteweg C, McNutt MA and Gu J. Pathogenetic mechanisms of severe acute respiratory syndrome. Virus Res 2008; 133(1): 4-12.
86. Plemper R. K. Cell entry of enveloped viruses. Curr Opin Virol 2011; 1(2): 92-100.
87. Cohen FS. How Viruses Invade Cells. Biophys J 2016; 110(5): 1028-32.
88. Sieczkarski SB and Whittaker GR. Differential requirements of Rab5 and Rab7 for endocytosis of influenza and other enveloped viruses. Traffic (Copenhagen, Denmark) 2003; 4(5): 333-43.
89. Walsh D and Mohr I. Viral subversion of the host protein synthesis machinery. Nat Rev Microbiol 2011; 9: 860-75.
90. Rampersad S and Tennant P. Replication and Expression Strategies of Viruses. Viruses 2018; 55-82.
91. Keen EC and Dantas G. Close Encounters of Three Kinds: Bacteriophages, Commensal Bacteria, and Host Immunity. Trends Microbiol 2018; 26(11): 943-54.
92. Desfarges S and Ciuffi A. Viral Integration and Consequences on Host Gene Expression. Viruses: Essential Agents of Life 2012; 147-75.
93. Chung BN and Pak HS. Seed transmission of Chrysanthemum stunt viroid in Chrysanthemum. Plant Pathol J 2008; 24(1): 31-5.
94. Ding B, Zhong X and Flores R. Viroids/Virusoids. Reference Module in Life Sciences 2017. DOI: 10.1016/B978-0-12-809633-8.13120-6.
95. Daròs JA, Elena SF and Flores R. Viroids: an Ariadne's thread into the RNA labyrinth. EMBO reports 2006; 7(6): 593-8.
96. Branch AD and Robertson HD. A replication cycle for viroids and other small infectious RNA's. Science 1984; 223(4635): 450-5.
97. Flores R, Gas ME, Molina-Serrano D, Nohales MÁ, Carbonell A, Gago S, et al. Viroid replication: rolling-circles, enzymes and ribozymes. Viruses 2009; 1(2): 317-34.

98. Roossinck MJ, Sleat D and Palukaitis P. Satellite RNAs of plant viruses: structures and biological effects. Microbiol Rev 1992; 56(2): 265-79.
99. Gellatly D, Mirhadi K, Venkataraman S and AbouHaidar MG. Structural and sequence integrity are essential for the replication of the viroid-like satellite RNA of lucerne transient streak virus. J Gen Virol 2011; 92(Pt 6): 1475-81.
100. Sheldon CC and Symons RH. Is hammerhead self-cleavage involved in the replication of a virusoid in vivo? Virology 1993; 194(2): 463-74.
101. Matoušek J, Steinbachová L, Drábková LZ, Kocábek T, Potěšil D, Mishra AK, et al. Elimination of Viroids from Tobacco Pollen Involves a Decrease in Propagation Rate and an Increase of the Degradation Processes. Int J Mol Sci 2020; 21(8): 3029.
102. Carbonell A, Martinez de Alba AE, Flores R and Gago S. Double-stranded RNA interferes in a sequence-specific manner with the infection of representative members of the two viroid families. Virology 2008; 371(1): 44-53.

ISTANBUL UNIVERSITY PRESS

REVIEW ARTICLE

Eur J Biol 2022; 81(1): 96-106

Black Fungus Mutilating COVID-19 Pandemic in India: Facts and Immunological Perspectives

Anushka Mondal[1], **Mylari Gireeshwar**[1], **Lekha Govindaraj** [1]

[1]Indian Institute of Science Education and Research Kolkata, Department of Biological Sciences, Mohanpur, India

ORCID IDs of the authors: A.M. 0000-0002-5231-9422; M.G. 0000-0002-2496-3384; G.L. 0000-0002-0729-2152

Please cite this article as: Mondal A, Gireeshwar M, Govinderaj L. Black Fungus Mutilating COVID-19 Pandemic in India: Facts and Immunological Perspectives. Eur J Biol 2022; 81(1): 96-106. DOI: 10.26650/EurJBiol.2022.1083922

ABSTRACT

While the world is still struggling with the severe acute respiratory syndrome coronavirus-2 (SARS-CoV-2) infection, an aggressive and rare fungal infection which is commonly ascribed as the black fungus has emerged as a new medical challenge in India. India had already experienced the devastating consequences of the COVID-19 and, being a rare "opportunistic" fungal infection, black fungus infection has severely complicated the post-COVID-19 recoveries. Together with the uncertain treatment modalities at the beginning of the pandemic, indiscriminate use of a plethora of medications has driven the surging cases of black fungus-associated complications. Moreover, low oxygen, high iron levels, and prolonged hospitalization with mechanical ventilators created a superlative condition for contracting black fungus infection. The disease mainly spreads through the respiratory tract and erodes facial structures. Since mucormycosis specifically attacks immunosuppressed patients, the disease started spreading rapidly, with an average mortality rate of 54 %. Common symptoms include blackening over the nose, blurred or double vision, breathing difficulties, chest pain and hemoptysis. Although not contagious, the outcome of the disease is often very frightful.

If the infection disseminates systematically, the risk of affecting the vital organs such as the spleen and heart is substantially high. We have tried to provide an epidemiological overview of black fungus infection in India. We focused on drawing a comprehensive fact check of the current situation through an immunological perspective to better understand the infection as a major co-infection in patients affected by COVID-19 and its impact on India's fight against the COVID-19 pandemic.

Keywords: Black fungus, COVID-19, Mucormycosis, Epidemiology, India

INTRODUCTION

As a rare "opportunistic" fungal disease, the black fungus infection has severely impacted the post-COVID-19 recoveries and imposed an additional burden on our medical and healthcare management system. Together with the uncertain treatment modalities at the beginning of the pandemic, the indiscriminate use of a plethora of medications, including steroids and antibiotics, have helped drive the surging cases of black fungus-associated complications. However, the persistent low oxygen level in blood with high iron levels, along with prolonged hospitalization of COVID-19 patients under the aid of mechanical ventilators, are the key contributors to contracting the black fungus infection. A black fungus is a group of molds commonly known as mucormycetes, while the resultant infection is termed mucormycosis. Mucormycosis is reported to be more prevalent among COVID-19 patients with precedent medical conditions like hyperglycemia with prescribed medications, including steroids. Mucormycosis usually spreads through the respiratory tract, predominantly erodes the facial structures, causes discoloration or blackening over the nose, and blurred or double vision. In addition to these, the infected patient often exhibits chest pain, breathing difficulties and hemoptysis (coughing up blood). Although not contagious, the outcome of the disease is often frightful as it causes gastrointestinal bleeding with severe respiratory distress. Moreover, if

Corresponding Author: Lekha Govindaraj E-mail: lekhag@iiserkol.ac.in

Submitted: 07.03.2022 • **Accepted:** 10.05.2022 • **Published Online:** 30.05.2022

the infection disseminates systematically, the risk of affecting vital organs such as the spleen and heart is substantially high.

Considering the high population density and the high-speed dissemination rate of mucormycosis, we have tried to provide an epidemiological overview of black fungus infection in India in the first part of the review. In the second part, we have focused on drawing a comprehensive fact check of the current situation from the immunological perspectives.

EPIDEMIOLOGICAL BACKGROUND of COVID-19

Originating from Wuhan, in Hubei province, China, the Severe Acute Respiratory Syndrome Coronavirus-2 (SARS-CoV-2) virus has led to the global COVID-19 pandemic. However, SARS-CoV-2 is not the first to cause a global emergency; there are six other variants of coronavirus that are known to have originated from animals. Among them, four coronaviruses are endemic in humans which include almost 10-15% of common colds. The other coronavirus variants, NL63 and 229E, probably originated from bats, whereas the sources for OC43 and HKU1 virus seem to be rodents (1). The Severe Acute Respiratory Syndrome (SARS) caused by a human coronavirus (SARS-CoV) was the first non-endemic coronavirus to be recognized, which was for the first time reported in China (November 2002) followed by Vietnam (2003) and attracted significant attention worldwide. However, the outbreak was in the same year, with the last cases reported in April 2004 from China. An estimated total of 8098 cases of SARS-CoV positive were reported worldwide, of which 774 casualties were recorded (2). The subsequent report suggested that the SARS-CoV originated from horseshoe bats and that it may be transmitted to humans through some specific kind of cats.

The next outbreak related to the SARS-CoV infection was Middle Eastern Respiratory Syndrome (MERS), first reported in Saudi Arabia in 2012 (3) which spread across 27 countries. Similar to SERS-CoV, a flu-like illness with mild to severe pneumonia and acute respiratory distress was found in MERS-CoV with symptoms varying from mild to severe pneumonia and acute respiratory distress syndrome. SARS-CoV-2 resembles the wild bat virus more than SARS-CoV or MERS-CoV. This strongly suggests that it is a novel coronavirus in humans (4). SARS-CoV-2 is one of37 members of coronaviruses in their Coronaviridae family, belonging to the order Nidovirales, and it is presently a major cause of pandemic affecting lots of people globally (5). Cell entry of the virus is mediated by binding the target receptor with the help of spike proteins. This requires six amino acids among which only one of these is with SARS-CoV (6). The spike protein regulates viral infectivity and host range which is different from SARS-CoV.

These little viruses are extremely powerful and possess unique mechanisms to enter into the host cells. These viruses enter the host cells through the angiotensin-converting enzyme 2 (ACE2) receptor (7), which is expressed in various human organs. These receptors interact with the spike protein of SARS-CoV-2. Studies suggest that SARS-CoV spike protein and R. sinicus ACE2 might have co-evolved over time and experienced a selection pressure from each other, triggering the evolutionary arms race dynamics (8).

The first reported case of COVID-19 was in Wuhan, China, in December 2019 and the first case was reported in Kerala, India. During the first pandemic wave in April 2020, almost 5 million people in India were significantly affected, while nearly 1.57 lakh deaths were reported globally. However, a significant improvement in the early post-first wave time led pseudo confidence to push us to a riskier situation, causing the second wave's advent. The impact of the second wave was substantially high in both the number of cases and mortality, reporting many deaths (9).

COMMON MICROBIAL CO-INFECTIONS in COVID-19

Common co-infection of the SARS-CoV-2 significantly affects the diagnosis, treatment, and recovery of COVID-19 and often worsens the disease symptoms and mortality rate. Moreover, co-infection can also alter the gut homeostasis of the patients by promoting a relative abundance of opportunistic pathogens and subsequently destabilizing the host immune system. Specifically, a marked reduction in the lymphocytes count, particularly helper T-cells and cytotoxic T-cells due to COVID-19 infection, seems to make the individual highly exposed to secondary bacterial and fungal co-infections (10,11). Although not common, co-infection with other respiratory viruses such as respiratory syncytial virus (RSV) and influenza virus infection were also reported in the recent past (12). In a contemporary study, it was found that around 7% of hospitalized COVID-19 patients and around 14% of the total ICU patients in India, were affected by bacterial co-infection (12). The two most common types of COVID-19 associated bacterial co-infections are caused by *Acinetobacter baumannii* and two *Staphylococcus aureus* strains, presumably due to their acquired hypervirulence and antibiotic resistance. The source of co-infection includes bacterial infections including *Mycoplasma pneumoniae, Pseudomonas aeruginosa, Haemophilus influenzae* and *Klebsiella pneumoniae* (13,14).

BLACK FUNGUS and COVID-19

Apart from bacterial co-infections, India has also witnessed a rather daunting and terrifying epidemic outbreak of mucormycosis and other fungal co-infections, adding to India's growing COVID-19 woes during the second wave. While black fungus or mucormycosis is non-contagious in nature, a significant number of patients who at some point either suffered from COVID-19 or recovered from COVID-19 are found to be the target for black fungus infection.

Hierarchical Classification of Black Fungus

Black fungus is a disease caused by moulds known as mucormycetes (15). These moulds are abundant in natural environments with a greater percentage in soil, specifically in soil rich in decaying organic matter, which includes compost piles, leaves, and animal dung. They may cause serious fungal infections in human beings, although chances of being attacked were rare in earlier times. To know more about this disease, we have to know about the types of mucormycosis.

Position in classification:
Black fungus has the following taxonomic position: -

Order: Mucorales

Family: Mucoraceae

Genus: Mucor Fresen

Mucormycosis was previouslyknown as "zygomycosis" and was first discovered by Friedrich Küchenmeister in 1855 (16). However, Max Carl Anton Fürbringer was the first to describe the disease in the lungs (17). In 1884, Lichtheim explained the development of mucormycosis disease in rabbits and explained two species -*Mucor rhizopodiformis* and *Mucor corymbifera*, which later came to be known as *Rhizopus* and *Lichtheimia*. In 1943, the association of this disease with uncontrolled diabetes was reported in three cases with symptoms such as severe sinus, eye and brain involvement (16).

When cases of "zygomycosis" started to be reportedin the mid-1950sin the United States, it was thought to be a novel disease resulting from the extensive use of antibiotics, adrenocorticotropic hormone, corticotropin (ACTH) and steroids (18). Until the late 20th century, the only treatment that was available for treating "zygomycosis" (later named as mucormycosis) was potassium iodide (KI). Between 1970 and 2000, Amphotericin B was found to be more effective for the treatment of mucormycosis.

Common Symptoms of Mucormycosis
Until recently, the black fungus was a rare fungal ailment, with just a few cases documented around the world. However, it has now become a fresh catastrophe that requires prompt attention. Because black fungus infection has such a high mortality rate, itis critical to be aware of and warrants early diagnosis. One of the key issues associated with black fungus Infections is that of serious cosmetic problems as it affects different sections of the face. This is also known as "rhino-orbital-cerebral-mucormycosis" which is characterized by swelling and inflammation along the nasal line. In the following a brief overview of common signs are outlined:

a. **Formation of Black crust around the nose:** Swelling and black crust formation around the nasal tube are two of the most common symptoms of black fungus. If left untreated, the infection progresses to a more serious stage, resulting in nose mutilation and perhaps requiring surgery to repair the jawbone or other facial structures.

b. **Swelling and inflammation on cheeks and eyes:** Chronic swelling or inflammation around the eyes or cheeks, could also be signs of black fungus. As a result of black fungus infection patients often exhibit numbness or inflammation on one side of the face with necrosis-like symptoms, which could also be the outcome of black fungus infection.

c. **Acute headache:** Acute headaches, inflammation around the forehead, and redness are reported to be caused by black fungus when spreading to the brain. This is the most serious stage, where any lack of knowledge or inappropriate treatment modality may result in memory loss, cognitive function loss, or substantial brain injury.

d. **Partial or complete loss of vision:** If the black fungus targets the retinal nerves, it can cause partial or complete loss of vision. Any redness, irritation, or pain in one or both eyes are preliminary signs of such an outcome.

In addition, other consequences of black fungus infection include gastrointestinal bleeding, hemorrhage, shortness of breath, and even blindness. If the infection spreads inside the body through the blood, then it is known as disseminated black fungus (19). In such conditions, the severity of the disease reaches its peak, and the fungus starts to attack vital organs such as the heart and spleen. It can also lead to blood clotting in the lungs and brain, and in the worst case, it may affect the nervous system and cause some unpleasant mental changes leading to coma (20) or even death.

WHAT CAUSES A BLACK FUNGUS OUTBREAK IN INDIA?

Black fungus is a rising concern for South Asian countries. However, India has reported the highest number of cases of mucormycosis over the last year. To date, there have been over 40,000 cases, of which more than 3,129 people died, were reported to be caused by black fungus across India (21). The major concern is the rapid dissemination rate of mucormycosis among COVID-19 infected patients, while a little delay, even a few hours, could cost the patient's life. When searching for predisposing factors for the incidence of mucormycosis in COVID-19 patients, it was observed that (22) prolonged hospitalization with mechanical ventilators can create a perfect environment for mucormycosis. Together with early diagnosis, retaining diabetes and other associated health issues in check, treating patients with specific intravenous antifungal medications can control the dissemination of the infection. Moreover, along with wearing masks and using sanitizers, maintenance of hygiene, if added to the already existing treatment modalities, the better management of COVID-19 associated complications can be avoided. In the following, a comprehensive discussion is presented on how COVID-19 is associated with an increase in the risk of black fungus.

HAS COVID-19 INCREASED THE RISK OF BLACK FUNGUS?

Despite its best efforts, India is still at risk in terms of vaccinating such a huge population and has inadequate health care systems for saving thousands of people from the impending threat of a future outbreak of COVID-19 and associated illness. The black fungus outbreak as a post COVID-19complication has compelled us to realize that "misfortune never comes alone". Keeping in mind that (19) with an average mortality rate of 54%, black fungus infection in COVID-19 recovered patients is indeed alarming. The association of a black fungus and COVID-19 infection is illustrated in Figure 1, explaining why covid patients may get mucormycosis. Steroids are considered a good drug for critically ill COVID-19 patients, particularly in reducing inflamma-

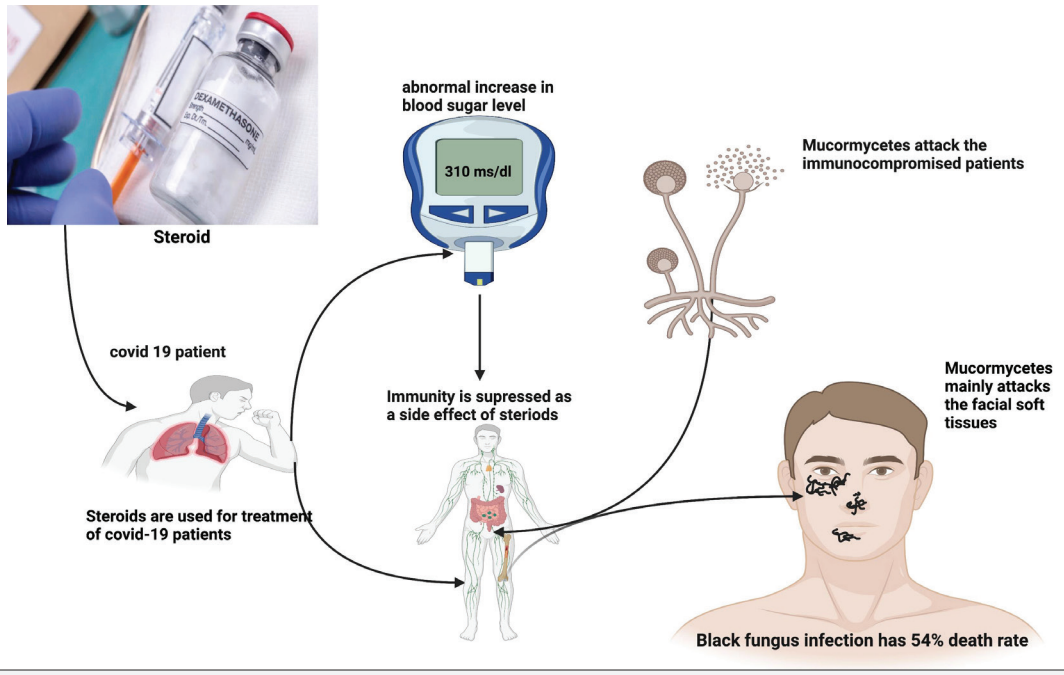

Figure 1. Illustration depicting the mechanism of attack of black fungus.

Steroids are used for the treatment of critically ill covid patients. As a result of this, the sugar level increases manifold in both diabetic and non-diabetic patients along with the suppression of immunity of those patients. The opportunistic fungus called black fungus releases its spores which if inhaled causes black coloration over the face.

tion in the lungs. Steroids are primarily used to suppress further tissue damage caused by one's immune system when it goes into overdrive response to fight against infections and can be used to control cytokine storms (23). However, while applying steroids, the other factors must be taken into account, particularly while treating high blood sugar conditions in both diabetics and non-diabetic COVID-19 patients. Since mucormycosis normally affects persons with an immunocompromised state, patients who have already recovered from COVID-19 are falling prey to such attacks by black fungus.

Types of mucormycosis

Mucormycosis can be classified as per the following types (24, 25)

a. Rhinocerebral mucormycosis: Rhinocerebral mucormycosis is also known as zygomycosis, is an infection which affects the nose, paranasal sinuses and can even spread to the brain (26). This type of mucormycosis is common in people with uncontrolled diabetes and in people who have undergone a kidney transplant. The infection starts in the nasal cavity at first and spreads towards the adjoined paranasal sinuses. Subsequently, implantation occurs in that area and grows at a faster rate in the sinuses and nasal cavity. The moist and humid environment inside the nasal cavity and paranasal sinuses are known to favor the growth and invasion of fungi.

Angioinvasion is another way through which the infection can reach the brain. In this case, the progression is very rapid and has a unique model of pathogenesis. Rhino cerebral mucormycosis symptoms include black lesions on the upper inside of the buccal cavity with induction of mild to severe fever. More serious consequences in the form of brain infarction, hematoma and orbital apex syndrome are not rare (27). Since vascular invasion is an important characteristic of this type of infection, the formation of intravascular thrombi often leads to infarction of the brain and ischemia (28). In some cases, if the aneurysmal blood vessels are ruptured, it may lead to hematoma along with intracerebral hemorrhages. Rhinocerebral mucormycosis also results in Meningitis which is a rare manifestation of this infection (27). The involvement of brain tissue leads to the formation of brain abscesses, especially in chronic cases (29). Brain abscess formation in such cases may be caused by some secondary bacterial infection (30). This infection may also affect the unilateral cranial nerves and cause hemiplegia (31). Mostly such outcome is mediated through the growth of mycelium along the invasion of leptomeningeal blood vessels (32). Diagnosis at an early stage, followed by proper treatment and surgical removal, if required, may help to save lives, and avoid permanent neurological complications.

b. Pulmonary mucormycosis: Pulmonary mucormycosis mostly attacks the lungs of individuals affected with black fungus. This is the most common type of mucormycosis in people who have had a stem cell transplant or an organ transplant which also includes cancer patients (33). Pul-

monary mucormycosis may develop due to inhalation of spores or lymphatic and hematogenous spread. The pathway of entry for *Mucorales* is primarily the respiratory tract where the fungi easily invade veins, arteries, and lymphatics and results in infarction and thrombosis which can be fatal (34). Patients suffering from haematological malignancies, diabetes mellitus, or who have received organ transplants and hematopoietic stem cell transplants are prone to invasive mucormycosis. The patients on corticosteroid-based therapy, chelation therapy and neonatal prematurity can be other reasons for infection. In addition, in low-income countries like India, malnutrition is a major issue that can play a vital role in acquiring mucormycosis infection (35). Angioinvasion and sometimes direct tissue injury of the respiratory tract, are some of the consequences of this infection which may even extend from the lungs into the great vessels (36). Clinical symptoms of the infection may include some nonspecific symptoms like fever, chest pain and dyspnea (37, 38).

In a large experimental set-up, whereof 929 cases of zygomycosis were reviewed, the overall mortality rate was found to be 44% in the diabetic patients with zygomycosis whereas there was a 76% mortality rate in the case of pulmonary zygomycosis patients. The most common species responsible for zygomycosis is *Rhizopus (39*).

c. Gastrointestinal mucormycosis: Gastrointestinal mucormycosis mostly affects the stomach and intestine and is highly prevalent among newborns, especially premature infants who are less than 1 month of age (40). There was a prevalence of gastrointestinal mucormycosis in industrialized nations. However, during the last few years, the number of cases of gastric and gastrointestinal mucormycosis has increased around the globe (41). Other rare causes of gastrointestinal mucormycosis were seen in immunocompromised patients who were suffering from AIDS, systemic lupus erythematosus and who had undergone organ transplantation (42). Some patients were seen to suffer from hepatic mucormycosis suggested an association with ingestion of herbal medications (43). A study was conducted by Morton and colleagues and they found a substantial increase in this infection in the 21st century (44). Recently, an outbreak of gastric mucormycosis occurred due to contamination of wooden applicators that had beenused to mix drugs for patients with nasogastric feeding tubes (45). These patients suffered from massive gastric bleeds.

d. Cutaneous mucormycosis: This type of infection primarily affects the skin, especially in cases of skin trauma or surgery. This is one of the most common types of mucormycosis which occurs even in people with an immunocompromising history (46). Cutaneous mucormycosis is comparatively a new emerging fungal infection that is caused by fungi belonging to the phylum Glomeromycota. The clinical presentation is usually nonspecific, but a rapidly evolving necrosis indicates the presence of this infection. In view of the occurrence of cutaneous mucormycosis, the strains that are most frequently isolated are *Rhizopus oryzae, Apophysomyces elegans* and *Lichtheimia corymbifera (47*) Other isolates reported to be responsible are *Saksenaea vasiformis, Mucor* sp, *Cunninghamella bertholletiae, Rhizopus microspores* and *Rhizomucor* spp. (48). Reports are available to indicate that this type of fungus is associated with nitroglycerine patches and vascular devices (49). In a review that was done of 196 cases of healthcare-associated mucormycosis, it was found that 57% involved the skin. Among them, a predominant number of the population included surgical patients, premature infants and immunocompromised hosts (50). Cutaneous mucormycosis is classified into two types- primary and secondary type infection. In the primary type of disease, the skin is often infected by direct inoculation and in the secondary form, the infection is caused by dissemination from other locations. According to the pattern of infection, it can be categorized as localized, deep or disseminated. In a review that was conducted with 929 cases, 176 patients were found with skin involvement. The most affected areas of the skin due to this infection are the arms and legs (51). Other locations for spreading include the scalp, breast, neck and gluteal area, face, thorax, back, abdomen and perineum (52).

e. Disseminated mucormycosis: It is a type of infection that spreads via the bloodstream to affect other parts of the body. The infection commonly affects the brain. It also can affect other organs such as the heart, skin and spleen (53). Mucormycosis is a rapidly spreading infection that is associated with extensive angioinvasion, thrombosis, tissue infarction and necrosis (54). In worse cases, it leads to haematogenous dissemination of the fungi (55). Dissemination may occur in up to 40% of patients who are suffering from haematological malignancies (56). In a review about children, it was found that dissemination increases the risk of death sevenfold (57). Patients with disseminated infection in the brain can even develop stress or coma in worse cases.

HOW COMMON IS MUCORMYCOSIS?

Mucormycosis is actually a very rare infectious disease. In 1992–1993, a population-based study was performed which suggested a yearly rate of 1.7 cases per 1 million population were affected by black fungus (47). Prospective surveillance among 16,808 transplant recipients was performed during 2001–2006 and it was found that, in stem cell transplant recipients, mucormycosis was the third most common type of invasive fungal infection. It accounted for 8% of all invasive fungal infections (54). Moreover, it was also observed in the case of solid organ transplant recipients, that mucormycosis accounted for nearly 2% of all invasive fungal infections (28 mucormycetes cases among 1,208 solid organ transplant recipients who developed any fungal infection) (58). Although mucormycosis outbreaks on a global scale have not been reported yet, the risk of a mucormycosis endemic through healthcare-associated systems cannot be overruled. The risk of black fungus spread through

improper disposal adhesive bandages, wooden tongue depressors, and hospital linens is potentially high. Pathogen transmission in health care establishments via negative pressure rooms, water leakage, poor air filtration, non-sterile medical devices and hospital building construction are also found to be equally responsible (59, 60).

ORGAN WISE PATHOGENICITY OF BLACK FUNGUS INFECTION

Exposure to mucor is commonly associated with mould infestation of soil, plants, manure, and decaying vegetation. It usually spreads through the respiratory tract and erodes facial structures and in severe cases, surgical removal of the eye becomes necessary to prevent the fungus from spreading to the brain. The ethmoid sinus has proved to be a vital route of infection because mucormycosis can invade through the thin lamina papyracea and then eventually gain access to the orbit. The infection in some cases may extend posteriorly to the orbital apex, which ultimately leads to orbital apex syndrome. The optic nerve affected due to this infection results in loss of vision involving superior orbital fissure as well as the cranial nerves III, IV, and VI, and branches of V1 and V2. This altogether causes ophthalmoplegia, diplopia, and sensory loss to the areas corresponding to the cornea and face. If the infection spreads posteriorly and gains access to the cavernous sinus and the brain parenchyma, vascular thrombosis and infarction in the posterior part can also be noticed.

THE EPIDEMIOLOGICAL PERSPECTIVE OF BLACK FUNGUS

In India, an estimated 0.14 mucormycosis cases were recorded per 1000 population as per a recent report (61). Organ transplantation, diabetes and blood cancers are also common underlying problems in many developed countries (61). Even before the COVID-19 pandemic, the mucormycosis incidence in India was estimated to be around 70 times more than the rest of the world (62). In fact, the rapidly growing number of cases of mucormycosis in some parts of India declared it to be an epidemic. The mortality rate for black fungus is close to 54% which is much greater than the ongoing pandemic of COVID-19. The mortality rate of patients suffering from various types of mucormycosis is given below in Figure 2. The mortality rate varies with the type of fungus that has attacked or even with the present condition of the patient as well as the site of infection (52).

HOST IMMUNE RESPONSE AGAINST BLACK FUNGUS

Exposure to fungi by inhalation, digestion, and even by traumatic inoculation of pathogens or allergens causes fungal infection in our everyday life. However, antifungal host defense protects the host either by killing the pathogen or restricting further spread in a coordinated way via both innate and adaptive immune responses. However, some Pathogenic fungi, including black fungus, use multiple strategies to subvert or exploit the host immune defense and successfully colonize and spread further. The immune evasion of black fungus is schematically represented in Figure 3.

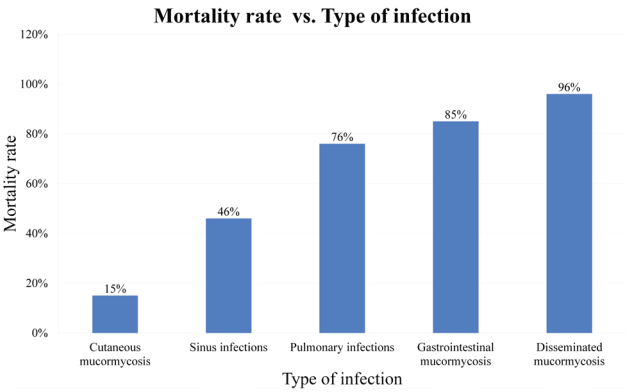

Figure 2. Representation of mortality rate of patients affected by mucormycosis.

The data for the graph was taken from a trusted journal (63). It represents the mortality rate of patients with respect to the type of mucormycosis infection.

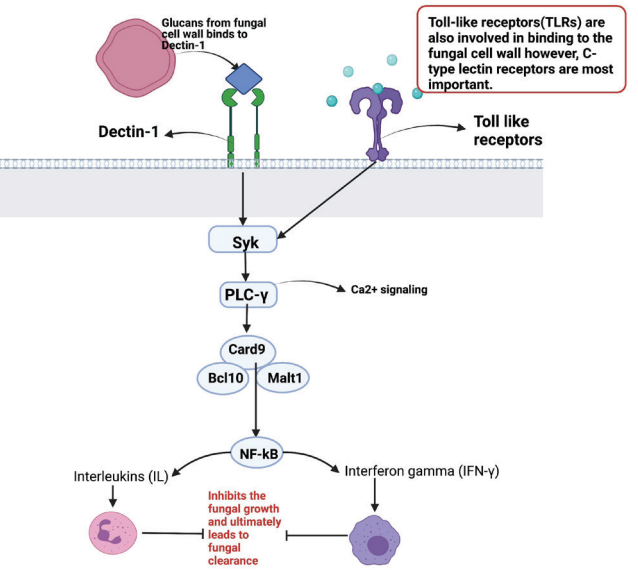

Figure 3. Host cell immune response pathway against fungal infection.

This is a schematic representation of the host immune response pathway via CARD9 molecule. When the glucans from the fungal cell wall bind to DEctin-1 receptor then a series of reactions are initiated leading to NF-kB localization which ultimately results in release of cytokines that inhibit and destroy the fungal cells.

Fungal recognition and immune activation

The cell wall of the fungi is composed of polysaccharides and lipid moieties to activate innate immune responses via binding to Toll-like receptor 4 (TLR4) expressed by major antigen-presenting cells (64). Like other prokaryotic cells, the fungal cell wall lies to the exterior of the plasma membrane and is arranged in bi-layers - the innermost layer consists of chitin. It

also consists of the adjacent layer that lies on the external side which is formed by β-(1,6) glucans and immunoreactive β-(1,3) (65). While entering the host cells, fungal cells bind to soluble pattern recognition receptors (PRRs). Subsequently, these interactions facilitate signalling responses by membrane-bound receptors to activate the antifungal effector response (66). The C-type lectin receptor (CLR) dectin-1 binds β-glucans from the fungi. The binding of β-Glucan displaces regulatory phosphatases such as CD45 and CD148 (67) and induces SRC-dependent phosphorylation of the intracellular ITAM-like motif while recruiting the SHP-2 phosphatase (68). The SYK docks to this scaffold and then transduce signals through a family of Guanine nucleotide exchange factors (GEFs) (69) to CARD9, to activate the NF-κB pathway via the subunits p65 and c-REL (70). Thus, CARD9 is considered very important for activating antifungal immune responses.

Alternatively, Dectin-1 also plays an important role in innate immunity activation primarily by triggering Th17 differentiation. IL-17 produced by Innate lymphoid, Th17 and γδ T cells at the mucosal surfaces is critical for antifungal immunity. In addition, other Dectin-1 dependent cytokines, such as IL-6, IL-23, IL-1β and TNF (71) are expressed following fungal infection. Neutrophils rapidly direct the production of reactive oxygen species (ROS) to the fungal phagosome (72). Fungal invasion of endothelial and epithelial cells promotes disease dissemination and tissue damage. In mucormycosis, the endothelial receptor glucose-regulated protein 78 (GRP78) enables the fungal hyphae to bind to endothelial cells (73) via spore coat protein surface proteins (CotH). Often metabolic changes associated with diabetic ketoacidosis (DKA) and hyperglycemia enhance the endothelial GRP78 expression and results in tissue invasion in the fungi (74).

COVID-19 ASSOCIATED MUCORMYCOSIS: WHY IT IS MORE IMPORTANT THAN OTHER FUNGAL DISEASES

Low oxygen, diabetes, high iron levels, and immunosuppression are predisposing conditions that make the COVID-19 affected person more vulnerable to black fungus infection. Various other factors, including prolonged hospitalization under mechanical ventilation, can create an ideal milieu for contracting mucormycosis. Similar to cryptococcosis or oral candidiasis (oral thrush) in HIV-infected patients, COVID-19 patients are also vulnerable to opportunistic pathogens such as black fungus which suggests some similarity between SARS-COV-2 and HIV infection where the patient's immunity is compromised (75). In contrast, since opportunistic infections breach the host defenses due to weakened host immunity (76), any viral attack that doesn't weaken the immune system won't attract further attacks by opportunistic fungi such as the influenza virus.

HOST SUSCEPTIBILITY TO MUCORMYCOSIS

For the current scenario, in the following section, we discuss the predisposing factor that makes the COVID-19 patient more vulnerable to black fungus infection:

A pre-existing condition such as diabetes, specifically diabetic ketoacidosis, organ transplant, and Cancer. Injection drug use, excessive iron in the body (commonly known as hemochromatosis), skin injury which may occur as a result of surgery, burns, or wounds and prematurity due to low birthweight, stem cell transplant, long-term corticosteroid use and low number of white blood cells and neutropenia (77).

MUCORMYCOSIS: A THERAPEUTIC CHALLENGE/TREATMENT OPTIONS

The ray of hope for us to battle this dangerous disease is our dedicated doctors and researchers who have put all their efforts into identifying a suitable drug of choice. If treatment is initiated in a timely manner, it reduces the mortality rate. Treatment of Mucormycosis involves a combination of surgical removal and antifungal therapy. The appropriate treatment and medications suggested are as follows (Table 1).

This treatment protocol has to be followed until clinical signs of infection are resolved with the elimination of predisposing risk factors such as hyperglycemia, immunosuppression etc. For the treatment of mucormycosis, it is vital to understand the mechanism of drug action for mucormycosis. Amphoter-

Table 1. Treatment modalities.

1.	Amphotericin B deoxycholate (D-AmB)- should be given for 1.0-1.5 mg/kg/day
2.	Liposomal amphotericin B (L-AmB) is the preferred treatment- 5- 10mg/kg/day that has to be continued till an appropriate response is achieved and the disease reachesa stabilized condition. It may even take several weeks, following which,step down to oral Posaconazole of 300 mg dose del tablets twice a day for 1 day which is then followed by 300 mg daily or Isavuconazole of 200 mg 1 tablet 3 times daily for 2 days followed by 200 mg dose of a tablet daily would be a good drug of choice.
3.	Injection of Amphotericin B Lipid Complex may also be given as a drug of choice for - 5mg/kg/day
4.	We need to reduce the dose of steroids if the patient is still taking it and discontinue it rapidly.
5.	Discontinue other immunomodulating drugs. The earlier the Surgical debridement is performed, the better, is pivotal in the management of mucormycosis.
6.	Surgical debridement involves an extensive process to remove all necrotic material
7.	Exenteration of eye can be performed if there is involvement of the eyes
8.	Immediate management has to be done to control diabetes & diabetic ketoacidosis.

icin B is currently considered the best drug of choice for the treatment of mucormycosis. The mechanism of drug action is given in Figure 4. Along with traditional antifungal agents and surgery methods, some other therapies include reversing immunosuppression and correcting metabolic deficits and involve strategies of immune augmentation for controlling mucormycosis beneficially (78). Some popular adjunctive therapies include immunomodulation strategies, iron chelation and hyperbaric oxygen (79). Hyperbaric oxygen is known to be an effective treatment for diabetic patients who have rhino cerebral or severe cutaneous mucormycosis (80). High concentrations of oxygen may also improve wound healing by releasing enhanced tissue growth factors (81). Other techniques, such as immune augmentation strategies, which include interferon-γ and granulocyte colony-stimulating factor (G-CSF), have been stated as adjunctive therapies for improving host response (82).

FUTURE PERSPECTIVE

Although fungi evolved 400 million years ago and played an important role on Earth, some of them have evolved to become pathogenic (83). The great Irish famine of 1845 that affected millions of people resulted from the fungus *Phytophthora infestans*, which wiped out the country's staple potato crop. Although fungal diseases are common among plants, only a tiny fraction of them tends to attack humans and animals. However, our immune system gets compromised due to other illnesses, and fungi, which are otherwise harmless, immediately take advantage to invade the hosts (84). This opportunistic nature of fungi has often hindered COVID-19 recovery of affected patients and makes them more vulnerable to several other secondary bacterial and fungal infections. There are three main ways humans can contract fungal infection: inhaling spores, swallowing fungal spores in food or medicines, or when spores contaminate wounds. Specifically, in the case of black fungus, mucor spores, when they attack the sinuses, spread to the lungs and brain, and then finally affect the central nervous system. Though many other secondary bacterial and fungal infections may attack Covid patients, the black fungus remains a fatal fungal infection. Although mucormycosis is not contagious, it spreads from fungal spores circulating in the air or the environment, hence, it is almost impossible to avoid. However, in addition to maintaining personal hygiene, basic precautions such as avoiding contact with soil, moss, and dusty construction sites along with wearing shoes, long trousers, and long-sleeved shirts while doing professional activi-

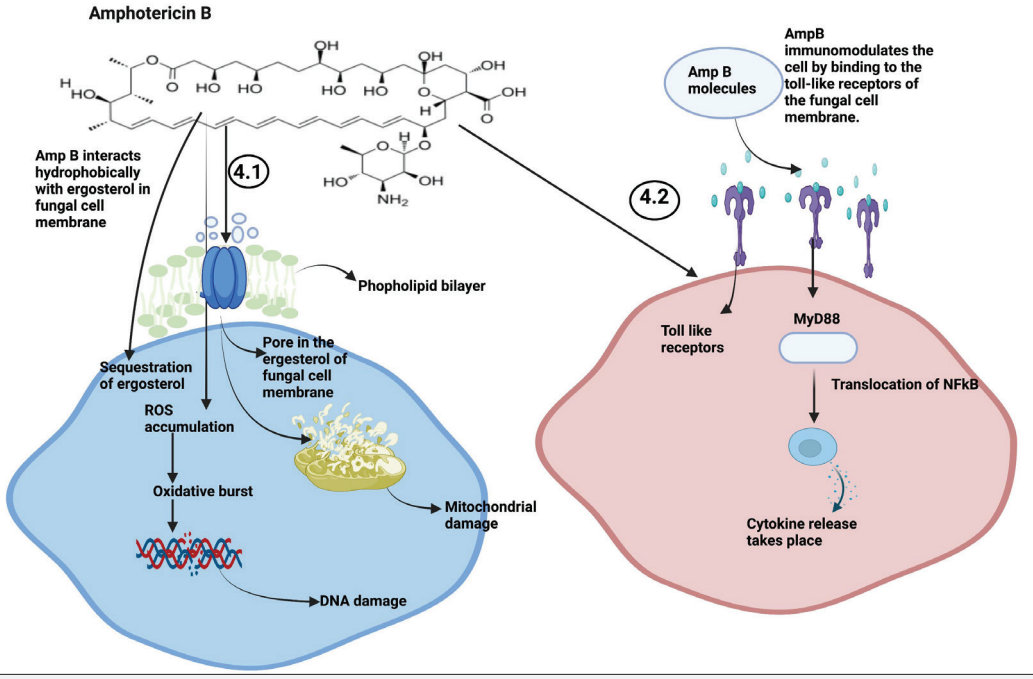

Figure 4. Mechanism of drug of choice.

We can see 2 pathways through which Amphotericin B can damage the fungal cell. In the pathway marked in Figure 4.1. we can see that Amphotericin B interacts hydrophobically with the ergosterol present in the fungal cell membrane and leads to the formation of pores. As soon as it forms pores, the molecules inside the fungal cell start to leak out through the pores. Figure 4.1. also demonstrates that Amphotericin B leads to Reactive Oxygen Species accumulation which leads to oxidative burst ultimately resulting in mitochondrial damage and DNA damage. In the pathway marked in Figure 4.2., it is demonstrated that Amphotericin B molecules bind to the toll-like receptors, specifically TLR-2, TLR-4 and CD-14 on the fungal cell membrane. The adapter protein or MyD88 gets activated and helps to translocate NF-KB to the nucleus which leads to cytokine release in the end step. Cytokines modulates the fungal cell immunologically and help in damaging the cell.

ties may provide us with enough protection to stop us getting affected by black fungus (85). Regular steam inhalation and maintaining nasal and oral hygiene also contribute to avoiding infections, especially from those suffering from COVID-19. Patients, especially those with diabetes or taking steroids because of COVID-19 or any condition that affects the immune system, need to control high blood sugar levels, and regularly monitor blood sugar levels. Other preventive measures to be followed are to regularly clean and replace humidifiers for those using oxygen concentrators and to change masks daily. Further progress in research and exploring novel methods of diagnosis and antifungal treatment modality should continue for better therapeutic and preventive measures against black fungus (86).

CONCLUSION

Educating patients about the symptoms will act as a very helpful armament in the early detection of the condition. Although it is a life-threatening disease, we shouldn't lose hope as early diagnosis and rigorous treatment may control the situation to a great extent. Liposomal amphotericin B is the best quality antifungal to be used for the treatment of this infection.

In this review article, we have mainly tried to highlight all the necessary points we all need to know about this deadly disease. Our main aim through this article is to create awareness among people instead of creating panic. We all need to understand that while biological systems are definitely unpredictable, we can prevent them by taking a few simple precautions and that is true for both covid and black fungus infections. Let's try to win this evolutionary arms race by bravely fighting this battle with covid and the deadly fungal disease "The black fungus".

Acknowledgement: We want to thank the Indian Institute of Science Education and Research Kolkata for the support they provided us for writing this article. We are also grateful to our colleagues for their suggestions and scientific communications throughout our writing tenu

Peer Review: Externally peer-reviewed.

Author Contributions: Conception/Design of Study- A.M., M.G., G.L.; Data Acquisition- A.M., M.G., G.L.; Drafting Manuscript- A.M.; Critical Revision of Manuscript- M.G., G.L.; Final Approval and Accountability- A.M., M.G., G.L.

Conflict of Interest: Authors declared no conflict of interest.

Financial Disclosure: Authors declared no financial support.

REFERENCES

1. Bar-Or I, Yaniv K, Shagan M, Ozer E, Weil M, Indenbaum V, et al. Regressing SARS-CoV-2 sewage measurements onto COVID-19 burden in the population: A Proof-of-Concept for quantitative environmental surveillance. Front Public Health 2022; 9: 561710.
2. Sahu RK, Salem-Bekhit MM, Bhattacharjee B, Almoshari Y, Ikbal AMA, Alshamrani M, et al. Mucormycosis in indian covid-19 patients: Insight into its pathogenesis, clinical manifestation, and management strategies. Antibiotics (Basel) 2021;10(9): 1079.
3. Valente Aguiar PD, Carvalho B, Monteiro P, Linhares P, Camacho Ó, Vaz R. Hyperbaric oxygen treatment: Results in seven patients with severe bacterial postoperative central nervous system infections and refractory mucormycosis. Diving Hyperb Med 2021; 51(1): 86-93.
4. Afzal ProfS, Nasir M. Aspergillosis and Mucormycosis in COVID-19 Patients; a Systematic Review and Meta-analysis. medRxiv. Published online 2021.
5. Domingo FR, Waddell LA, Cheung AM, Cooper CL, Belcourt VJ, Zuckermann AME, et al. Prevalence of long-term effects in individuals diagnosed with COVID-19: a living systematic review. medRxiv. Published online 2021.
6. Chavda VP, Apostolopoulos V. Mucormycosis – An opportunistic infection in the aged immunocompromised individual: A reason for concern in COVID-19. Maturitas 2021; 154: 58-61.
7. Russell CD, Fairfield CJ, Drake TM, Turtle L, Seaton RA, Wootton Dan G, et al. Co-infections, secondary infections, and antimicrobial use in patients hospitalised with COVID-19 during the first pandemic wave from the ISARIC WHO CCP-UK study: a multicentre, prospective cohort study. Lancet Microbe 2021; 2(8): e354-e365
8. Musuuza JS, Watson L, Parmasad V, Putman-Buehler N, Christensen L, Safdar N. Prevalence and outcomes of co-infection and superinfection with SARS-CoV-2 and other pathogens: A systematic review and meta-analysis. PLoS One 2021; 16(5): e0251170.
9. Kalfaoglu B, Almeida-Santos J, Tye CA, Satou Y, Ono M. T-cell dysregulation in COVID-19. Biochem Biophys Res Commun 2021; 538: 204-210.
10. Graichen H. What is the difference between the first and the second/third wave of Covid-19? – German perspective. J Orthop 2021; 24: A1-A3.
11. Kanungo R. Mucormycosis: New actor in the saga of COVID-19. J Curr Res Sci Med 2021; 7(1).
12. Chowdhary S, Alexander A, Ganesan S, Raj JV, Chakkalakkoombil SV, Lakshmanan J, et al. Cavernous sinus thrombosis in COVID-19 associated rhino-orbital Mucormycosis: A Retrospective Audit in the First Wave of the Pandemic, 2021, PREPRINT (Version 1) available at Research Square. Doi: 10.21203/rs.3.rs-693804/v1
13. Ademe M. Immunomodulation for the treatment of fungal infections: Opportunities and challenges. Front Cell Infect Microbiol 2020; 10: 469.
14. Jenks JD, Gangneux JP, Schwartz IS, Alastruey-Izquierdo A, Lagrou K, Thompson GR, et al. Diagnosis of breakthrough fungal infections in the clinical mycology laboratory: An ecmm consensus statement. J Fungi (Basel) 2020; 6(4): 216.
15. Skiada A, Pavleas I, Drogari-Apiranthitou M. Epidemiology and diagnosis of mucormycosis: An update. J Fungi (Basel) 2020; 6(4): 265.
16. Mekki SO, Hassan AA, Falemban A, Alkotani N, Alsharif SM, Haron A, et al. Pulmonary Mucormycosis: A Case Report of a Rare Infection with Potential Diagnostic Problems. Case Rep Pathol 2020: 5845394.
17. Ragab D, Salah Eldin H, Taeimah M, Khattab R, Salem R. The COVID-19 Cytokine Storm; What We Know So Far. Front Immunol 2020; 11: 1446.
18. Lansbury L, Lim B, Baskaran V, Lim WS. Co-infections in people with COVID-19: a systematic review and meta-analysis. J Infect 2020;81(2):266-275.
19. Guo H, Hu BJ, Yang XL, Zeng LP, Li B, Ouyang S, et al. Evolutionary Arms Race between Virus and Host Drives Genetic Diversity in Bat Severe Acute Respiratory Syndrome-Related Coronavirus Spike Genes. J Virol 2020; 94(20): e00902-20.

20. Cuervo NZ, Grandvaux N. Ace2: Evidence of role as entry receptor for sars-cov-2 and implications in comorbidities. Elife 2020; 9: e61390.
21. Huang Y, Yang C, Xu X feng, Xu W, Liu S wen. Structural and functional properties of SARS-CoV-2 spike protein: potential antivirus drug development for COVID-19. Acta Pharmacol Sin 2020; 41(9): 1141-9.
22. Lu R, Zhao X, Li J, Niu P, Yang B, Wu H, et al. Genomic characterisation and epidemiology of 2019 novel coronavirus: implications for virus origins and receptor binding. Lancet 2020; 395(10224): 565-574.
23. Reid G, Lynch III JP, Fishbein MC, Clark NM. Mucormycosis. Semin Respir Crit Care Med 2020; 41(1): 99-114.
24. Bhandari J, Thada PK and Nagalli S. Rhinocerebral mucormycosis. StatPearls.; 2020.
25. Yao H, Liu Y, Ma ZF, Zhang H, Fu T, Li Z, et al. Analysis of nutritional quality of black fungus cultivated with corn stalks. J Food Qual 2019; 2019.
26. Cornely OA, Alastruey-Izquierdo A, Arenz D, Chen SCA, Dannaoui E, Hochhegger B, et al. Global guideline for the diagnosis and management of mucormycosis: an initiative of the European Confederation of Medical Mycology in cooperation with the Mycoses Study Group Education and Research Consortium. Lancet Infect Dis 2019; 19(12): e405-e421.
27. Azhar EI, Hui DSC, Memish ZA, Drosten C, Zumla A. The Middle East Respiratory Syndrome (MERS). Infect Dis Clin North Am 2019;33(4):891-905.
28. Hui DSC, Zumla A. Severe Acute Respiratory Syndrome: Historical, Epidemiologic, and Clinical Features. Infect Dis Clin North Am 2019; 33(4): 869-89.
29. Bennett M, Kaide CG, Matheson E, Bari V. Hyperbaric Oxygen Therapy and Utilization in Infectious Disease. Curr Emerg Hosp Med Rep 2018; 6(3).
30. Warnatsch A, Tsourouktsoglou TD, Branzk N, Wang Q, Reincke S, Herbst S, et al. Reactive Oxygen Species Localization Programs Inflammation to Clear Microbes of Different Size. Immunity 2017; 46(3): 421-32.
31. Castrejón-Pérez AD, Miranda I, Welsh O, Welsh EC, Ocampo-Candiani J. Cutaneous mucormycosis. An Bras Dermatol 2017; 92(3): 304-11.
32. Lionakis MS, Iliev ID, Hohl TM. Immunity against fungi. JCI Insight 2017; 2(11): e93156.
33. Yamin HS, Alastal AY, Bakri I. Pulmonary mucormycosis over 130 years: A case report and literature review. Turk Thorac J 2017; 18(1): 1-5.
34. Schroeder MR, Stephens DS. Macrolide resistance in Streptococcus pneumoniae. Front Cell Infect Microbiol 2016; 6: 98.
35. Gebremariam T, Lin L, Liu M, Kontoyiannis DP, French S, Edwards JE, et al. Bicarbonate correction of ketoacidosis alters host-pathogen interactions and alleviates mucormycosis. J Clin Invest 2016; 126(6): 2280-94.
36. Roth S, Bergmann H, Jaeger M, Yeroslaviz A, Neumann K, Koenig PA, et al. Vav Proteins Are Key Regulators of Card9 Signaling for Innate Antifungal Immunity. Cell Rep 2016; 17(10): 2572-83.
37. Erwig LP, Gow NAR. Interactions of fungal pathogens with phagocytes. Nat Rev Microbiol 2016; 14(3): 163-76.
38. Wang XM, Guo LC, Xue SL, Chen Y bin. Pulmonary mucormycosis: A case report and review of the literature. Oncol Lett 2016; 11(5): 3049-53.
39. Yang HN, Wang CL. Looks like tuberculous meningitis, but not: A case of rhinocerebral mucormycosis with garcin syndrome. Front Neurol 2016; 7: 181.
40. Mattingly JK, Ramakrishnan VR. Rhinocerebral Mucormycosis of the Optic Nerve. Otolaryngol Head Neck Surg 2016;155(5):888-9.
41. Paczosa MK, Mecsas J. Klebsiella pneumoniae: Going on the Offense with a Strong Defense. Microbiol Mol Biol Rev 2016; 80(3): 629-61.
42. Alaa Abdul-Hussein Al-Daamy, Haider Abd-Al Ameer, Hasan Zuher, Hussein Monather, Bashaer Ahmmed, Niesreen Kadhim. Antifungal activity of propolis against Dermatophytes and Candida albicans isolated from human mouth. J contemp med sci 2015; 1(3).
43. Deng Z, Ma S, Zhou H, Zang A, Fang Y, Li T, et al. Tyrosine phosphatase SHP-2 mediates C-type lectin receptor-induced activation of the kinase Syk and anti-fungal T H 17 responses. Nat Immunol 2015; 16(6): 642-52.
44. Underhill DM, Pearlman E. Immune Interactions with Pathogenic and Commensal Fungi: A Two-Way Street. Immunity 2015;43(5):845-58.
45. Shin S, Jung S, Menzel F, Heller K, Lee H, Lee S. Molecular phylogeny of black fungus gnats (Diptera: Sciaroidea: Sciaridae) and the evolution of larval habitats. Mol Phylogenet Evol 2013; 66(3): 833-46.
46. Guymer C, Khurana S, Suppiah R, Hennessey I, Cooper C. Successful treatment of disseminated mucormycosis in a neutropenic patient with T-cell acute lymphoblastic leukaemia. BMJ Case Rep 2013; 2013: bcr2013009577.
47. Lewis RE, Kontoyiannis DP. Epidemiology and treatment of mucormycosis. Future Microbiol 2013; 8(9): 1163-75.
48. Ibrahim AS, Spellberg B, Walsh TJ, Kontoyiannis DP. Pathogenesis of mucormycosis. Clin Infect Dis 2012; 54(Suppl 1): S16-22.
49. Neblett Fanfair R, Benedict K, Bos J, Bennett SD, Lo YC, Adebanjo T, et al. Necrotizing Cutaneous Mucormycosis after a Tornado in Joplin, Missouri, in 2011. N Engl J Med 2012; 367(23): 2214-25.
50. Petrikkos G, Skiada A, Lortholary O, Roilides E, Walsh TJ, Kontoyiannis DP. Epidemiology and clinical manifestations of mucormycosis. Clin Infect Dis 2012; 54(Suppl 1): S23-34.
51. Rammaert B, Lanternier F, Zahar JR, Dannaoui E, Bougnoux ME, Lecuit M, et al. Healthcare-associated mucormycosis. Clin Infect Dis 2012; 54(Suppl 1): S44-54.
52. Lalayanni C, Baliakas P, Xochelli A, Apostolou C, Arabatzis M, Velegraki A, et al. Outbreak of cutaneous zygomycosis associated with the use of adhesive tape in haematology patients. J Hosp Infect 2012; 81(3): 213-5.
53. Skiada A, Rigopoulos D, Larios G, Petrikkos G, Katsambas A. Global epidemiology of cutaneous zygomycosis. Clin Dermatol 2012; 30(6): 628-32.
54. Morton J, Nguyen V, Ali T. Mucormycosis of the intestine: A rare complication in Crohn's disease. Gastroenterol Hepatol (N Y) 2012; 8(2): 137-40.
55. Spellberg B. Gastrointestinal mucormycosis: An evolving disease. Gastroenterol Hepatol (N Y) 2012; 8(2): 140-2.
56. Walsh TJ, Gamaletsou MN, McGinnis MR, Hayden RT, Kontoyiannis DP. Early clinical and laboratory diagnosis of invasive pulmonary, extrapulmonary, and disseminated mucormycosis (zygomycosis). Clin Infect Dis 2012; 54(Suppl 1): S55-60.
57. Goodridge HS, Reyes CN, Becker CA, Katsumoto TR, Ma J, Wolf AJ, et al. Activation of the innate immune receptor Dectin-1 upon formation of a Phagocytic synapse-TM. Nature 2011; 472(7344): 471-5.
58. Liu M, Spellberg B, Phan QT, Fu Yue Fu Yong Lee AS, Edwards JE, Filler SG, et al. The endothelial cell receptor GRP78 is required for mucormycosis pathogenesis in diabetic mice. J Clin Invest 2010; 120(6): 1914-24.
59. Pappas PG, Alexander BD, Andes DR, Hadley S, Kauffman CA, Freifeld A, et al. Invasive fungal infections among organ transplant recipients: results of the transplant-associated infection surveillance network (Transnet). Clin Infect Dis 2010;50(8):1101-11.

60. Cano P, Horseman MA, Surani S. Rhinocerebral mucormycosis complicated by bacterial brain abscess. Am J Med Sci 2010;340(6):507-10.
61. Mezhir JJ, Mullane KM, Zarling J, Satoskar R, Pai RK, Roggin KK. Successful nonoperative management of gastrointestinal mucormycosis: Novel therapy for invasive disease. Surg Infect (Larchmt) 2009; 10(5): 447-51.
62. Simbli M, Hakim F, Koudieh M, Tleyjeh IM. Nosocomial post-traumatic cutaneous mucormycosis: A systematic review. Scand J Infect Dis 2008; 40(6-7): 577-82.
63. Page A v., Evans AJ, Snell L, Liles WC. Primary cutaneous mucormycosis in a lung transplant recipient: Case report and concise review of the literature. Transpl Infect Dis 2008; 10(6): 419-25.
64. Garg R, Marak Rungmei SK, Verma S, Singh J, Sanjay, Prasad R. Pulmonary mucormycosis mimicking as pulmonary tuberculosis : A case report. Lung India 2008; 25(3): 129-31.
65. LeibundGut-Landmann S, Groß O, Robinson MJ, Osorio F, Slack EC, Tsoni SV, et al. Syk- and CARD9-dependent coupling of innate immunity to the induction of T helper cells that produce interleukin 17. Nat Immunol 2007; 8(6): 630-8.
66. Rappleye CA, Eissenberg LG, Goldman WE. Histoplasma capsulatum α-(1,3)-glucan blocks innate immune recognition by the β-glucan receptor. Proc Natl Acad Sci U S A 2007; 104(4): 1366-70.
67. Zaoutis TE, Roilides E, Chiou CC, et al. Zygomycosis in children: A systematic review and analysis of reported cases. Pediatr Infect Dis J 2007; 26(8): 723-7.
68. Ward AB. Hemiplegic shoulder pain. J Neurol Neurosurg Psychiatry 2007; 78(8): 789.
69. Thapar VK, Deshpande A, Jain VK, Bhowate P, Madiwale C. Isolated breast mucormycosis. J Postgrad Med 2006; 52(2): 134-5.
70. Pellacchia V, Terenzi V, Moricca LM, Buonaccorsi S, Indrizzi E, Fini G. Brain abscess by mycotic and bacterial infection in a diabetic patient: Clinical report and review of literature. J Craniofac Surg 2006; 17(3): 578-84.
71. Rogers NC, Slack EC, Edwards AD, Nolte MA, Schulz O, Schweighoffer E, et al. Syk-dependent cytokine induction by dectin-1 reveals a novel pattern recognition pathway for C type lectins. Immunity 2005; 22(4): 507-17.
72. Roden MM, Zaoutis TE, Buchanan WL, Knudsen TA, Sarkisova TA, Schaufele RL, et al. Epidemiology and outcome of zygomycosis: A review of 929 reported cases. Clin Infect Dis 2005; 41(5): 634-53.
73. Spellberg B, Edwards J, Ibrahim A. Novel perspectives on mucormycosis: Pathophysiology, presentation, and management. Clin Microbiol Rev 2005; 18(3): 556-69.
74. Maraví-Poma E, Rodríguez-Tudela JL, de Jalón JG, Manrique-Larralde A, Torroba L, Urtasun J, et al. Outbreak of gastric mucormycosis associated with the use of wooden tongue depressors in critically ill patients. Intensive Care Med 2004; 30(4): 724-8.
75. Pagano L, Offidani M, Fianchi L, Nosari A, Candoni A, Picardi M. & GIMEMA (Gruppo Italiano Malattie EMatologiche dell'Adulto) Infection Program. Mucormycosis in hematologic patients. Haematologica 2004; 89(2): 207-14.
76. Boxer L, Dale DC. Neutropenia: Causes and consequences. Semin Hematol 2002; 39(2): 75-81.
77. Chander J. Textbook of Medical Mycology.; 2002.
78. Hosseini M. Gastrointestinal mucormycosis mimicking ischemic colitis in a patient with systemic lupus erythematosus. Am J Gastroenterol 1998; 93(8): 1360-2.
79. Raleigh AB. Hepatic mucormycosis in a bone marrow transplant recipient who ingested naturopathic medicine. Clin Infect Dis 1996; 22(3): 521-4.
80. Brullet E, Andreu X, Elias J, Roig J, Cervantes M. Gastric mucormycosis in a patient with acquired immunodeficiency syndrome. Gastrointest Endosc 1993; 39(1): 106-7.
81. Helenglass G, Elliott JA, Lucie NP. An unusual presentation of opportunistic mucormycosis. Br Med J (Clin Res Ed) 1981; 282(6258): 108-9.
82. Ho KL. Acute subdural hematoma and intracerebral hemorrhage: Rare complications of Rhinocerebral Mucormycosis. Arch Otolaryngol 1979; 105(5): 279-81.
83. Baker RD. Mucormycosis—a new disease? J Am Med Assoc 1957; 163(10): 805-8.

ISTANBUL UNIVERSITY PRESS

SHORT COMMUNICATION

Eur J Biol 2022; 81(1): 107-116

Identification of *Fusarium graminearum* and *Fusarium culmorum* Isolates via Conventional and Molecular Methods

Beliz Yuksektepe[1], Ozlem Sefer[2], Gulin Inci Varol[3], Tugba Teker[4], Mehmet Arslan[4], Busra Nur Cetin[4], Figen Mert[5], Emre Yoruk[2], Gulruh Albayrak[3]

[1]Istanbul University, Institute of Sciences, Programme of Molecular Biology and Genetics, Istanbul, Turkiye
[2]İstanbul Yeni Yüzyıl University, Faculty of Arts and Sciences, Department of Molecular Biology and Genetics, Istanbul, Turkiye
[3]Istanbul University, Faculty of Sciences, Department of Molecular Biology and Genetics, Istanbul, Turkiye
[4]Istanbul University, Institute of Sciences, Programme of Molecular Biotechnology and Genetics, Istanbul, Turkiye
[5]Canakkale Onsekiz Mart University, Faculty of Agriculture, Department of Plant Protection, Canakkale, Turkiye

ORCID IDs of the authors: B.Y. 0000-0001-7703-2981; O.S. 0000-0002-2711-5938; G.I.V. 0000-0003-0091-1245; T.T. 0000-0001-9892-8429; M.A. 0000-0003-0613-8978; B.N.C. 0000-0002-3917-867X; F.M. 0000-0002-1603-0226; E.Y. 0000-0003-2770-0157; G.A. 0000-0002-4499-8912

Please cite this article as: Yuksektepe B, Sefer O, Varol GI, Teker T, Arslan M, Cetin BN, Mert F, Yoruk E, Albayrak G. Identification of *Fusarium graminearum* and *Fusarium culmorum* Isolates via Conventional and Molecular Methods. Eur J Biol 2022; 81(1): 107-116. DOI: 10.26650/EurJBiol.2022.1078448

ABSTRACT

Objective: *Fusarium* spp. cause Fusarium head blight (FHB) and crown rot (CR) diseases. They also have harmful effects on animal and human health through their mycotoxins. Within the scope of this study, *F. graminearum* and *F. culmorum* isolates were purified from wheat ears and stalks contaminated with phytopathogens, which had been collected from various regions of Turkey, were identified and characterized by conventional and molecular methods.

Materials and Methods: Sixty-eight *Fusarium* samples were isolated by single spore analysis and classified according to their macroconidia shape and size. Morphologically characterized samples were verified by amplification of SCAR markers. Their mating types (MAT) and chemotypes were also determined through polymerase chain reaction (PCR).

Results: Thirty-eight *F. graminearum* and 30 *F. culmorum* isolates were identified via amplification of UBC85 and OPT18 SCAR markers, respectively. All isolates were determined as trichothecene producers by amplification of the *tri5* gene. All *F. graminarum* isolates carry both *MAT-1* and *MAT-2* loci, whereas 7 of *F. culmorum* isolates were also determined as MAT-1 and 23 of them as MAT-2 mating types. Deoxynivalenol production capacity of all isolates was identified by *tri13* amplification for chemotype determination.

Conclusion: Routine monitoring of phytopathogens and their mycotoxin levels is a requirement since their annual levels may vary depending on environmental factors. This work provides knowledge about the distribution of *Fusarium* spp. leading to FHB and CR in different regions of Turkey between 2010 and 2020. Also, their chemotypes were demonstrated. Our studies will contribute to disease profiling and it is the first step in disease management.

Keywords: *Fusarium* spp., macroconidia, SCAR marker, mating types, trichothecene producers, chemotyping

INTRODUCTION

The soilborne genus *Fusarium* involves a high number of phytopathogenic fungal species that are able to cause diseases by infecting agriculturally important crops including cereals, tobacco, bananas, and carnations, and can also induce health issues in humans and animals through their mycotoxins (1-5). *Fusarium* species are responsible for various dominant diseases on plants including Fusarium head blight (FHB), crown root (CR), or Fusarium wilt via the involvement of different organs like roots, flowers, and spikes in cereal crops. *F. graminearum* and *F. culmorum* are prevalent species causing FHB and CR diseases worldwide as well as in Turkey (6-9). *Fusarium* spp. are widely distributed

Corresponding Author: Gulruh Albayrak E-mail: gulruh@istanbul.edu.tr
Submitted: 24.02.2022 • **Revision Requested:** 21.03.2022 • **Last Revision Received:** 24.03.2022 • **Accepted:** 28.03.2022 • **Published Online:** 13.04.2022

in soil, aerial plant parts, plant debris, and other organic substrates and the causal agents may vary from one agro-ecological region to another (10-12). They are able to produce various mycotoxins at one and the same time. The best known of these endotoxins are trichothecenes, fumonisins, zearalenone, and gibberellic acids. The trichothecenes are divided into four types (A-D) in terms of their additional radical groups onto the heterocyclic core skeleton (13). Deoxynivalenol (DON), nivalenol (NIV), diacetoxyscirpenol, T-2 toxin, and NX-2 are the most studied and well-known trichothecene mycotoxins (14-17). Their toxicity arises from their effects on different cellular mechanisms. Trichothecenes are responsible for oxidative stress-mediated DNA damage, induction of apoptosis through mitochondria-mediated or -independent pathways, and inhibition of protein synthesis by inhibiting the peptidyl transferase activity via binding to the large ribosomal subunit (60S) of eukaryotic cells. Therefore, mycotoxin accumulation as a result of the consumption of contaminated plants and animal products as food leads to potentially severe health problems in humans (18,19). Besides the health concerns based on toxicoses, *Fusarium* spp.-based diseases have both economic effects on agricultural areas and a remarkable number of risks for the vegetation. By considering all these risks, chemotyping, carried out by chemical profile determination of distinct mycotoxins, which are represented by a family or group of related preliminary compounds, is a requirement for the detection of effective methods to cope with the diseases directly caused by pathogens and toxication on animals or humans caused by its natural metabolites. It also has great importance in the characterization of phytopathogenic fungi (20,21).

The fundamental step in the taxonomy of any fungal species is morphological characterization. The classification of closely related *Fusarium* species is carried out according to the distinction of asexual spore types; macroconidia, microconidia and chlamydospores. Remarkable expertise in morphological analyses in *Fusarium* taxonomy is required. Some *Fusarium* species consist of very closely related members. Because differences among them are unclear, they are mentioned as members of the species complex (22). Therefore, the classification of a species complex based on morphological analyses is insufficient for taxonomic characterization. Hence, molecular approaches along with morphological characterization are effectively used in this field, as they provide rapid access to delicate and accurate findings for the identification of species. The amplification of a targeted definite genomic region also known as genotyping, nucleic acid sequencing both any specific regions or the whole genome and chemotyping carried out by using DNA amplification methods or chromatographic-based methods are efficiently used for classification and characterization of *Fusarium* species (2,21,23).

In the current study, a total of 68 isolates belonging to *Fusarium* species collected from infected cereal plants were identified and characterized based on conventional and molecular approaches. After the classification of the fungal isolates was carried out according to their macroconidia types, genus and species identifications were performed by using molecular assays. Also, their mating types (MAT) and chemotypes were determined through amplification methods.

MATERIALS AND METHODS

Single Spore Isolation and Growth Conditions

Wheat ears and stalks with FHB and CR symptoms were collected from different agricultural regions of Turkey (Çanakkale, Balıkesir, Tekirdağ, Amasya) between 2010 and 2020 (Figure 1). Thirty-eight *F. graminearum* (Table 1) and 30 *F. culmorum* (Table 2) samples included for analysis were isolated by the single spore isolation technique (24). After plant samples were treated with 15% NaOCl for 3 minutes, surface sterilization was completed by washing with sterile distilled water three times. Explants, which were dehumidified on blotting paper, were transferred to potato dextrose agar (PDA) medium (4 g/L potato extract, 20 g/L dextrose, 15 g/L agar) and incubated for 3 days at 25±2°C with 60% humidity. After incubation, 0.25 cm^2 diameter plates taken from *in vitro* fungal cultures were suspended

Figure 1. The isolates used in the study were obtained from where marked on the map.

Table 1. The list of *Fusarium graminearum* isolates originated from infected wheat ears and stalks. Their agroecological distributions, mating types and chemotypes.

Species	Isolate	Region/ Year	Mating Type		DON Chemotype
			MAT-1	*MAT-2*	
F. graminearum	Fg19W1	Amasya (2019)	+	+	+
	Fg19W2	Amasya (2019)	+	+	+
	Fg19W3	Amasya (2019)	+	+	+
	Fg19W4	Amasya (2019)	+	+	+
	Fg19W5	Amasya (2019)	+	+	+
	Fg19W6	Amasya (2019)	+	+	+
	Fg19W7	Amasya (2019)	+	+	+
	Fg19W8	Amasya (2019)	+	+	+
	Fg19W9	Amasya (2019)	+	+	+
	Fg19W10	Amasya (2019)	+	+	+
	Fg19W11	Amasya (2019)	+	+	+
	Fg19W12	Amasya (2019)	+	+	+
	Fg19W13	Amasya (2019)	+	+	+
	Fg19W14	Amasya (2019)	+	+	+
	Fg19W15	Amasya (2019)	+	+	+
	Fg19W16	Amasya (2019)	+	+	+
	Fg19W17	Amasya (2019)	+	+	+
	Fg19W18	Amasya (2019)	+	+	+
	Fg19W19	Amasya (2019)	+	+	+
	Fg19W20	Amasya (2019)	+	+	+
	Fg19W21	Amasya (2019)	+	+	+
	Fg19W22	Amasya (2019)	+	+	+
	Fg19W23	Amasya (2019)	+	+	+
	Fg19W24	Amasya (2019)	+	+	+
	Fg19W25	Amasya (2019)	+	+	+
	Fg19W26	Amasya (2019)	+	+	+
	Fg19W27	Amasya (2019)	+	+	+
	Fg20W28	Amasya (2020)	+	+	+
	Fg20W29	Amasya (2020)	+	+	+
	Fg20W30	Amasya (2020)	+	+	+
	Fg20W31	Amasya (2020)	+	+	+
	Fg20W32	Amasya (2020)	+	+	+
	Fg20W33	Amasya (2020)	+	+	+
	Fg20W34	Amasya (2020)	+	+	+
	Fg20W35	Amasya (2020)	+	+	+
	Fg20W36	Amasya (2020)	+	+	+
	Fg20W37	Amasya (2020)	+	+	+
	Fg20W38	Amasya (2020)	+	+	+

Table 2. The list of *Fusarium culmorum* isolates originated from infected wheat ears and stalks. Their agroecological distributions, mating types and chemotypes.

Species	Isolate	Region/ Year	Mating Type		DON Chemotype
			MAT-1	*MAT-2*	
F. culmorum	CM61	Çanakkale (2014)	+	-	+
	BB7	Balıkesir (2014)	-	+	+
	BB18	Balıkesir (2014)	-	+	+
	BG14	Balıkesir (2014)	-	+	+
	BH149	Çanakkale (2010)	-	+	+
	BH192	Tekirdağ (2010)	+	-	+
	BBR15	Balıkesir (2014)	-	+	+
	BBR16	Balıkesir (2014)	+	-	+
	BBR7	Balıkesir (2014)	-	+	+
	BBR8	Balıkesir (2014)	-	+	+
	D823	Çanakkale (2010)	-	+	+
	C606	Çanakkale (2010)	+	-	+
	L901	Balıkesir (2010)	-	+	+
	CE291	Çanakkale (2014)	-	+	+
	CE293	Çanakkale (2014)	-	+	+
	CB205	Çanakkale (2014)	+	-	+
	M211	Balıkesir (2010)	-	+	+
	M213	Balıkesir (2010)	-	+	+
	M214	Balıkesir (2010)	-	+	+
	TK309	Tekirdağ (2014)	-	+	+
	N201b	Balıkesir (2010)	-	+	+
	TC13	Tekirdağ (2014)	-	+	+
	BH226	Çanakkale (2010)	-	+	+
	TY13	Tekirdağ (2014)	-	+	+
	TY21	Tekirdağ (2014)	-	+	+
	TY82	Tekirdağ (2014)	-	+	+
	CA202	Çanakkale (2014)	-	+	+
	D815	Çanakkale (2010)	+	-	+
	CB206	Çanakkale (2014)	+	-	+
	TC14	Tekirdağ (2014)	-	+	+

in 1 mL of phosphate buffered saline. Forty microliters of the suspension was transferred to water-agar (WA) for 16 hours under the same conditions, explained above. Single spores were selected and transferred to PDA medium for a 7-day incubation with the same environmental conditions above and pure cultures were obtained.

Species Description Based on Morphological Characters

Species identification of isolates was carried out *in vitro* cultures grown on PDA medium from a single spore according to their macroconidia structures under the light microscope by following the characteristics explained below (16). Macroconidia of *F. graminearum* are relatively rare *in vitro* cultures while sporodochia are abundant. The macroconidium is medium length and thick-walled. Its ventral surface is moderately curved to straight while the dorsal side is neatly arched. Macroconidia of *F. culmorum* are uniform in shape and size. Their sporodochia are abundant. The macroconidium is relatively short, and thick-walled. Its midpoint is wide. The dorsal side is somewhat curved,

but the ventral is nearly straight. It is quite wide in comparison to its size.

Genomic DNA (gDNA) Isolation and Analysis

In this study, gDNAs were extracted from 40 mg mycelium for each sample by using Nucleospin Tissue, Mini Kit for DNA from Cells and Tissue (Macherey-Nagel™, Germany) with the manufacturer's instructions. The quality and quantity of gDNAs were spectrophotometrically determined by using NanoDrop™ 2000 (Thermo Fisher Scientific, USA). Also, their integrity was controlled by agarose gel electrophoresis conducted at 65V for 60 min. Amplicons were visualized under a UV transilluminator (Avegene X-Lite 200).

Classification of Isolates by Using Polymerase Chain Reaction (PCR)

Classification of all isolates at species level, identification of their mating types and chemotypes were determined by using PCR. The Tox 5-1/2 primer set (Table 3) was used for the classification of the *Fusarium* genus. Species-level determination was performed with two different sets. The UBC85F/R and OPT18F/R primer pairs (Table 3) were used for the identification of *F. graminearum* and *F. culmorum* isolates, respectively. Amplification reactions were carried out in a volume of 25 µL containing; 50 ng gDNA, 1×PCR buffer, 2.5 mM $MgCl_2$, 10 pmol for each primer, 0.4 mM for dNTP mix and 1 U *Taq* DNA polymerase (Thermo Fisher Scientific, Germany) under conditions at 94°C for 5 min as predenaturation and followed by 30 cycles as denaturation, annealing and extension steps at 94°C for 45 sec, 55°C for 45 sec and 72°C for 1.5 min, respectively. Finally, 72°C for 5 min was applied as the final extension step. Amplification products were observed on agarose gel as described in section "Genomic DNA (gDNA) Isolation and Analysis".

The fusαF/R and fusHMGF/R primer pairs targeting the *MAT-1* and *MAT-2* loci, respectively, were used for the determination of the mating types of the isolates (Table 3). The reaction volume was adjusted as 25 µL including 50 ng gDNA, 1×PCR buffer, 1.5 mM $MgCl_2$, 5 pmol for each primer, 0.5 mM for dNTP mix and 1 U *Taq* DNA polymerase. The mixtures were incubated at 94°C for 2 min as predenaturation and followed by 30 cycles as denaturation, annealing and extension steps at 94°C for 30 sec, 55°C for 30 sec and 72°C for 30 sec, respectively. The final extension was obtained at 72°C for 5 min. Amplification products and Gene Ruler 100 bp DNA ladder (Thermo Fisher Scientific, Germany) were run on agarose gel electrophoresis and visualized as previously mentioned in "Genomic DNA (gDNA) Isolation and Analysis".

Chemotype determination was performed by amplifying the *tri13* gene region of isolates. For that purpose, the primer pairs of Tri13NIVF/Tri13R and Tri13F/Tri13DONR were chosen for the determination of NIV and DON chemotypes, respectively (Table 3). PCR mixtures were prepared for 25 µL containing 50 ng gDNA, 1×PCR buffer, 2 mM $MgCl_2$, 5 pmol for each primer, 0.4 mM for dNTP mix and 1 U *Taq* DNA polymerase. PCR conditions were set at 94°C for 2 min as predenaturation, 30 cycles as denaturation, annealing and extension steps at 94°C for 30 sec, 53°C for 45 sec and 72°C for 1.5 min, respectively, and 72°C for 5 min as a final extension. Amplification products were controlled as described above in "Genomic DNA (gDNA) Isolation and Analysis".

RESULTS AND DISCUSSION

F. graminearum and *F. culmorum* are the predominant species responsible for FHB and CR infections in Turkey. Accurate identification of the causal agents is the fundamental step in the diagno-

Table 3. Primers, their target regions on gDNA, their nucleotide sequences and product sizes used for PCR analysis (*gene region, **marker, ***locus)

Primer	Target	Sequence 5' - 3'	Band Size (bp)	References
Tox 5-1 **Tox 5-2**	*tri5**	GCTGCTCATCACTTTGCTCAG CTGATCTGGTCACGCTCATC	658	Niessen and Vogel (1998) (25)
UBC85F **UBC85R**	SCAR**	GCAGGGTTTGAATCCGAGAC AGAATGGAGCTACCAACGGC	332	Schilling et al. (1996) (26)
OPT18F **OPT18R**	SCAR	GATGCCAGACCAAGACGAAG GATGCCAGACGCACTAAGAT	472	
fusαF **fusαR**	*MAT-1****	CGCCCTCTKAAYGSCTTCATG GGARTARACYTTAGCAATYAGGGC	210	Kerényi et al. (2004) (27)
fusHMGF **fusHMGR**	*MAT-2****	CGACCTCCCAAYGCYTACAT TGGGCGGTACTGGTARTCRGG	260	
Tri13NIVF **Tri13R**	*tri13**	CCAAATCCGAAAACCGCAG TTGAAAGCTCCAATGTCGTG	312	Chandler et al. (2003) (28)
Tri13F **Tri13DONR**	*tri13**	CATCATGAGACTTGTKCRAGTTTGGG GCTAGATCGATTGTTGCATTGAG	282	

sis of plant diseases. At the same time, it also aids in establishing efficient methods to understand and control them. Macroconidia of fungi play an important role in the dissemination of fungal diseases (29). Their shape and size are the main primary morphological features used for the differentiation of *Fusarium* species as a conventional classification approach (16,30).

Since traditional morphological techniques are time-consuming and inaccurate, preferring new techniques for the diagnosis of disease and characterization of pathogens has become obligatory. Within this context, nucleic acid amplification-based methods provide accurate and reliable diagnosis and classification of species, identified by conventional approaches, in a short time. In the current study, at first, 38 *F. graminearum* and 30 *F. culmorum* samples isolated from wheat ears and stalks with FHB and CR symptoms collected from different agricultural regions of Turkey were identified at species level based on their macroconidia shape and size (Figure 2). PCR-based molecular methods, targeting the amplification of different genomic regions, were used for the classification of all isolates at species level and the determination of their mating types and chemotypes. Within this context, after the gDNA isolation of 68 *Fusarium* isolates, their amount (70-120 ng/µl) and purity (1.7-1.9) were controlled and found to be convenient for use in PCR amplification. Since, SCAR markers were generated from cloned RAPD or AFLP fragments, linked to a trait of interest or not, those species-specific DNA fragments are amplified for use in species determination (26). Schilling et al. (1996) developed species-specific oligonucleotide primers, that are capable of differentiating two *Fusarium* species (*F. graminearum* and *F. culmorum*) by the amplification of species-specific SCAR markers derived from RAPD fragments (26). Since amplicons with 332 bp specific to *F. graminearum* were amplified in this study from 38 isolates by using a UBC85 primer pair, they were classified as *F. graminearum* (Figure 3). Similarly, 30 isolates were diagnosed as *F. culmorum* by amplifying the 472 bp SCAR marker region specific to *F. culmorum* by using OPT18 primers (Figure 4). In this manner, the identification of both species, already

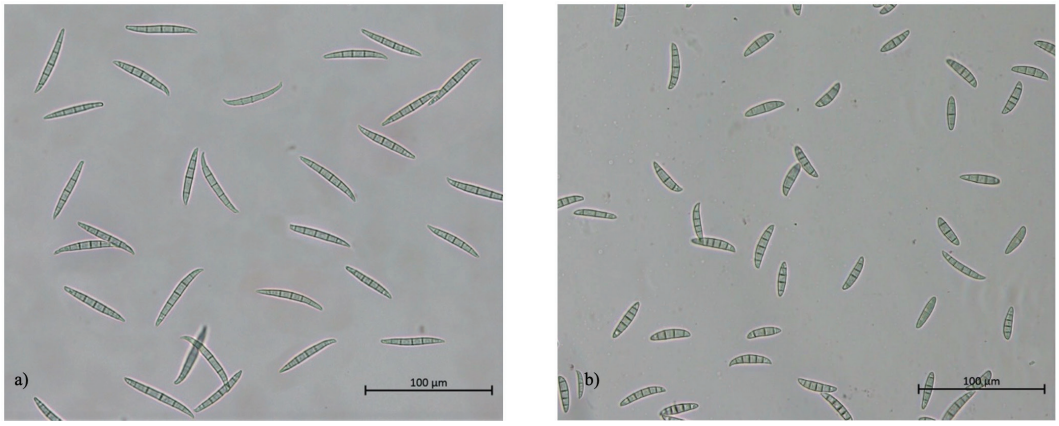

Figure 2. Macroconidia structures of a) *Fusarium graminearum* b) *Fusarium culmorum* under light microscope with total 40X magnification (Eclipse E100, Nikon Instruments, Japan).

Figure 3. PCR products with 332 bp length obtained by using UBC85 F/R primers for species diagnosis of *Fusarium graminearum*. PH-1 was used as positive control. M: 100 bp (Thermo Scientific, ABD), NC: Negative control.

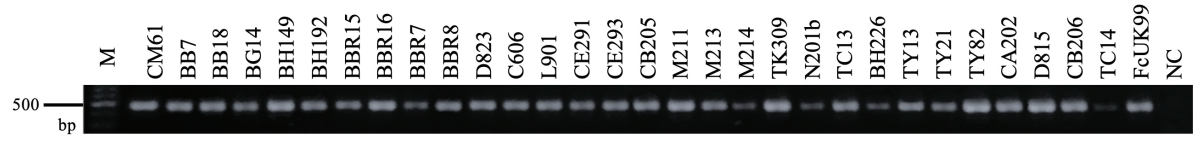

Figure 4. Fragments with 472 bp amplified with OPT18 F/R primers for *Fusarium culmorum* species diagnosis. Electrophoresis was conducted at 65V for 60 min. Fragments were visualized under UV transilluminator (Avegene X-Lite 200). FcUK99 was used as positive control. M: 100 bp (Thermo Scientific, ABD), NC: Negative control.

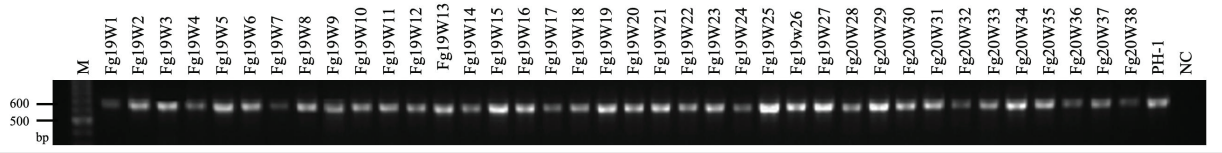

Figure 5. PCR products of 658 bp, amplified with Tox5-1/2 primers for genus diagnosis purpose. Electrophoresis was conducted at 65V for 60 min. Fragments were visualized under UV transilluminator (Avegene X-Lite 200). PH-1 was used as positive control. M: 100 bp (Thermo Scientific, ABD), NC: Negative control.

carried out based on morphological characters, were verified by using molecular methods. In the same way, Yörük and Albayrak (2012) described 12 fungal isolates as *F. graminearum* with a UBC85 primer pair, while 20 were identified as *F. culmorum* with OPT18 primers (20). In another study, Yörük et al. (2014) described eight *F. graminearum* and four *F. culmorum* isolates among 17 fungal samples by targeting the same SCAR regions (21). Moreover, Abedi-Tizaki and Sabbagh (2012) identified 51 *F. culmorum* isolates among 344 studied specimens by using the OPT18 primer pair for amplification of the SCAR marker (31).

Trichothecenes are toxic secondary metabolites produced by various fungal species belonging to *Fusarium*, *Myrothecium*, *Stachybotrys* and *Trichoderma* genera. The *tri5* gene, encoding the trichodiene synthase, is located at the beginning of the trichothecene biosynthetic gene cluster and has highly conserved nucleotide sequences. Those sequences enable the detection of trichothecene producers based on amplification (25, 32-34). Therefore, in the current study, the amplification of the *tri5* gene was carried out for the characterization of trichothecene producing *F. graminearum* and *F. culmorum* isolates. A 658 bp fragment belonging to the *tri5* gene was amplified from all isolates with the Tox 5-1/2 primer pair designed by Niessen and Vogel (1998) (25) (Figure 5). Hence, it was shown that isolates of both *Fusarium* species were trichothecene producers. Similarly, trichothecene producers among different *Fusarium* species, isolated from infected crops and fast food, were confirmed by using Tox5 primers (35,36). As can be understood from these studies, *tri5* amplification with Tox5 primer pair is a suitable approach for characterization in terms of the mycotoxin production patterns of phytopathogenic *Fusarium* species obtained directly from crops or processed products.

Biological species concepts can not be used for many species including *Fusarium* as the sexual stage has not been observed under laboratory conditions. Therefore, the determination of MAT alleles via PCR amplification is required to provide information about the sexual stage and compatibility between haploid individuals in heterothallic ascomycetes (37,38). Kerényi et al. (2004) accomplished the determination of mating types in several *Fusarium* species including *F. graminearum* and *F. culmorum* by developing degenerated and semi degenerated primer pairs targeting the conserved α-box and the high-mobility-group (HMG) domains of *MAT-1* and *MAT-2* alleles, respectively. They reported that *F. graminearum*, which is a homothallic species, carries both *MAT-1* and *MAT-2* idiomorphs together whereas heterothallic *F. culmorum* carries only one of the MAT alleles (27). With the aim of isolates' MAT determination, two primer sets for targeting the alleles which were two idiomorphs found in a single locus were used for PCR analysis in the present study. Likewise, it was determined that all *F. graminearum* isolates carried both the *MAT-1* and *MAT-2* loci (Table 1). The 210 bp long amplification products obtained from seven *F. culmorum* isolates with the fusαF/R primer pair revealed these isolates contained only the *MAT-1* allele (Figure 6). The 260 bp long fragments, amplified with fusHMGF/R primers, demonstrated that the remaining 23 *F. culmorum* samples bear only the *MAT-2* locus (Figure 7). These findings obtained from the study were exactly compatible with

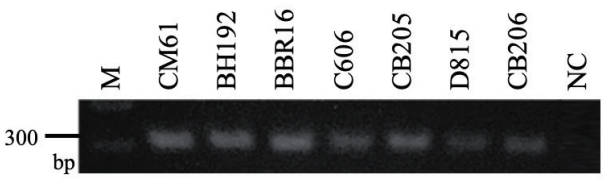

Figure 6. Agarose gel electrophoresis image of PCR products displayed amplicons (210 bp) were obtained from reaction with fusαF/R primers for mating type diagnosis purpose. M: 100 bp (Thermo Scientific, ABD), NC: Negative control.

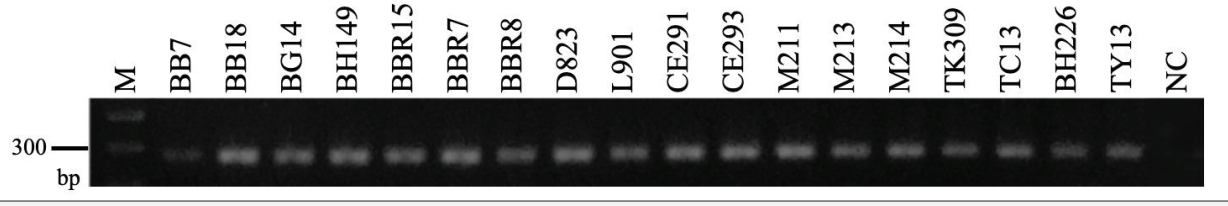

Figure 7. Agarose gel electrophoresis image of PCR products displayed amplicons (260 bp) were obtained from reaction with fusHMG-F/R primers for mating type diagnosis purpose. M: 100 bp (Thermo Scientific, ABD), NC: Negative control.

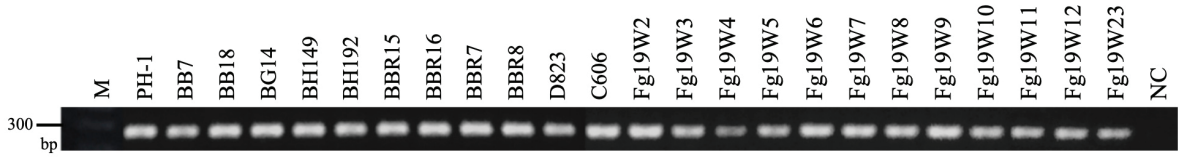

Figure 8. Agarose gel electrophoresis image of PCR products displayed amplicons (282 bp) were obtained from reaction with Tri13F/ Tri13DONR primers for chemotype diagnosis purpose. M: 100 bp (Thermo Scientific, ABD), NC: Negative control.

that of Kerényi et al. (2004) (27). Likewise, it was reported in the previous studies that both *MAT-1* and *MAT-2* alleles were carried together in *F. graminearum* whereas either the *MAT-1* or *MAT-2* idiomorph was detected in *F. culmorum* (39,40).

Since the mycotoxin type and quantity have a considerable effect on epidemics, the designation of mycotoxin production pattern has an influence on the development of control strategies against pathogenic organisms (20). Trichothecenes are the largest group of mycotoxins known to date. In this context, chemotyping of *Fusarium* species is carried out by targeting conserved functional genes located in the *Tri5* gene cluster via PCR-based molecular methods (41). Therefore, for the discrimination of mycotoxins, researchers developed various PCR methods based on revealing the sequence differences of genes that are responsible for the encoding of mycotoxin production enzymes.

Discrimination between DON and NIV-producing isolates was mainly determined from *tri7* and *tri13* genes in the *Tri5* gene cluster in *Fusarium* species. NIV-producing isolates carry functional copies of both genes (28,42), whereas DON producers have deleted regions on both of them (42-44). However, it was also reported that there are certain DON-producing isolates with full-length *tri7* while carrying nonfunctional *tri13* (44). Therefore, as functional *tri7* is a rare event for DON producers, targeting *tri13* instead of *tri7* became a more consistent strategy in chemotyping for isolates in terms of detection of DON or NIV producing capacity (28,45-47). Chandler et al. (2003) performed chemotyping of *Fusarium* isolates by amplifying the *tri13* gene region encoding P450 monooxygenase (28). In the current study, all *Fusarium* isolates were identified according to the amplification of two different regions of the *tri13* gene. For that purpose, two different primer sets designed by Chandler et al. (2003) were chosen (28). The potential of NIV production was not determined because the expected 312 bp amplicons could not be obtained from any of the isolates by PCR using Tri13NIVF/ Tri13R primers. However, all isolates were determined as having potential DON production via obtaining 282 bp amplicons by PCR assay which was performed with the Tri13F/Tri13DONR primer pair (Figure 8). Similarly, Tóth et al. (2004) identified the DON and NIV producer *F. graminearum* and *F. culmorum* isolates based on *tri13* amplification (40). Although it is known that the DON chemotype is common in Turkey (48,49), after the *F. graminearum* isolate with NIV production capacity was reported by Yörük and Albayrak (2012) for the first time (20), this chemotype was also detected by different researchers (50,51).

Species identification of phytopathogenic fungal agents and their chemotyping via PCR assay ensure a reliable diagnosis, and also provide developing influential struggle strategies against pathogens (20). For that purpose, genotypic and chemotypic identification of 68 *Fusarium* isolates, purified by single spore analysis, through different amplification strategies was performed in this study. Since studied isolates originated from four different populations of Turkey (Tekirdağ, Çanakkale, Balıkesir and Amasya) and their geographical discrimination inferred two different regions (Marmara and Black Sea), data became supportive for revealing the agro-ecological distribution of *Fusarium* spp. chemotypes.

Since the annual levels of phytopathogenic fungi spread and their produced mycotoxin levels may vary depending on environmental factors, continuous monitoring of phytopathogenic profile and levels of mycotoxins is essential for controlling diseases and ensuring risk assessment arising from contaminated food products. According to these findings from the present study, it could be said that PCR becomes a significant tool for screening plant infecting mycotoxigenic fungi. In addition, determination of mycotoxin distribution via chemotyping in agro-ecological regions is an effective approach for understanding the severity and spread of pathogens. Lastly, further research from other regions of Turkey with more isolates will improve the identification of the regional distribution of both *F. graminearum* and *F. culmorum* and their produced mycotoxins. Through this research, a new wild-type culture collection including *F. graminearum* and *F. culmorum* isolates was established from different agricultural areas with the aim of being utilized in future projects.

Acknowledgement: Reference fungal isolates *F. graminearum* PH-1 and *F.culmorum* FcUK99 were used as positive control and they were provided kindly by Dr. Tapani Yli-Mattila (University of Turku/ Finland) and Dr. Pierre Hellin (Walloon Agricultural Research Centre/ Belgium), respectively.

Peer Review: Externally peer-reviewed.

Author Contributions: Conception/Design of Study- G.A., E.Y., F.M., T.T., O.S.; Data Acquisition- B.Y., O.S., G.I.V., T.T., M.A., B.N.C.; Data Analysis/Interpretation- G.A., E.Y., F.M.; Drafting Manuscript- G.A., B.Y., G.I.V.; Critical Revision of Manuscript- G.A., T.T., E.Y., F.M.; Final Approval and Accountability- B.Y., O.S., G.I.V., T.T., M.A., B.N.C., F.M., E.Y., G.A.

Conflict of Interest: Authors declared no conflict of interest.

External financing: This work was supported by The Scientific and Technological Research Council of Turkey, Project No: 119Z366.

REFERENCES

1. Bottalico A. *Fusarium* diseases of cereals: species complex and related mycotoxin profiles, in Europe. J Plant Pathol 1998; 80(2): 85-103.
2. Moretti, A. Taxonomy of Fusarium genus: A continuous fight between lumpers and splitters. Zb Matice Srp Prir Nauk 2009; 117: 7-13.
3. Antonissen G, Martel A, Pasmans F, Ducatelle R, Verbrugghe E, Vandenbroucke V, et al. The Impact of *Fusarium* mycotoxins on human and animal host susceptibility to infectious diseases. Toxins 2014; 6(2): 430-52.
4. LaMondia JA. Fusarium wilt of tobacco. Crop Prot 2015; 73: 73-7.
5. Basallote-Ureba MJ, Vela-Delgado MD, Capote N, Melero-Vara JM, López-Herrera CJ, Prados-Ligero AM, et al. Control of Fusarium wilt of carnation using organic amendments combined with soil solarization, and report of associated *Fusarium* species in southern Spain. Crop Prot 2016; 89: 184-92.
6. Tunali B, Ozseven I, Buyuk O, Erdurmus D, Demirci, A. Fusarium head blight and deoxynivalenol accumulation of wheat in Marmara region and reactions of wheat cultivars and lines to *F. graminearum* and *F. culmorum*. Plant Pathol J 2006; 5(2): 150-6.
7. Yli-Mattila, T, Rämö S, Hietaniemi V, Hussien T, Carlobos-Lopez A, Cumagun C. Molecular quantification and genetic diversity of toxigenic *Fusarium* species in Northern Europe as compared to those in Southern Europe. Microorganisms 2013; 1(1): 162-74.
8. Pasquali M and Migheli Q. Genetic approaches to chemotype determination in type B-trichothecene producing *Fusaria*. Int J Food Microbiol 2014; 189: 164-82.
9. Ölmez F and Tunali B. *Fusarium* species isolated from wheat samples showing root and crown rot. Plant Prot Bull 2019; 59(3): 31-7.
10. Yoruk E, Albayrak G, Sharifnabi B, Candar B. Molecular characterization of *Fusarium graminearum* and *F. culmorum* isolates of wheat, barley and maize using ISSR markers. Curr Opin Biotechnol 2011; 22: S132.
11. Liu YY, Sun HY, Li W, Xia YL, Deng YY, Zhang AX, et al. Fitness of three chemotypes of *Fusarium graminearum* species complex in major winter wheat-producing areas of China. PLoS One 2017; 12(3): e0174040.
12. Bahadur A. Current status of *Fusarium* and their management strategies. Mirmajlessi SM editor. *Fusarium* - An Overview on Current Status of the Genus. IntechOpen Book Series; 2021. p.1-17.
13. Chen Y, Kistler HC, Ma Z. *Fusarium graminearum* trichothecene mycotoxins: Biosynthesis, regulation, and management. Annu Rev Phytopathol 2019; 57: 15-39.
14. Miller JD, Greenhalgh R, Wang YZ, Lu M. Trichothecene chemotypes of three *Fusarium* species. Mycologia 1991; 83: 121-30.
15. Desjardins AE and Proctor RH. Molecular biology of *Fusarium* mycotoxins. Int J Food Microbiol. 2007; 119(1-2): 47-50.
16. Leslie JF and Summerell BA. Species descriptions. The *Fusarium* Laboratory Manual. John Wiley & Sons; 2006. p.158-80.
17. Varga E, Wiesenberger G, Hametner C, Ward TJ, Dong Y, Schöfbeck D., et al. New tricks of an old enemy: isolates of F*usarium graminearum* produce a type A trichothecene mycotoxin. Environ Microbiol 2015; 17(8): 2588-600.
18. Pestka JJ and Smolinski AT. Deoxynivalenol: toxicology and potential effects on humans. J Toxicol Environ Health - B 2005; 8(1): 39-69.
19. Arunachalam C and Doohan FM. Trichothecene toxicity in eukaryotes: Cellular and molecular mechanisms in plants and animals. Toxicol Lett 2013; 217(2): 149-58.
20. Yörük E and Albayrak G. Chemotyping of *Fusarium graminearum* and *F. culmorum* isolates from Turkey by PCR assay. Mycopathologia 2012; 173(1): 53-61.
21. Yörük E, Gazdağli A, Albayrak G. Class B trichothecene chemotyping in *Fusarium* species by PCR assay. Genetika 2014; 46(3): 661-9.
22. van der Lee T, Zhang H, van Diepeningen A, Waalwijk C. Biogeography of *Fusarium graminearum* species complex and chemotypes: a review. Food Addit Contam Part A Chem Anal Control Expo Risk Assess 2015; 32(4): 453-60.
23. Lacmanová I, Pazlarová J, Kostelanská M, Hajšlová J. PCR-based identification of toxinogenic *Fusarium* species. Czech J Food Sci 2009; 27(Special Issue 2): 90-4.
24. Booth C. *Fusarium*: laboratory guide to the identification of the major species. Commonwealth Mycological Institute, Kew, Surrey, England; 1977. p. 58.
25. Niessen ML and Vogel RF. Group specific PCR-detection of potential trichothecene-producing *Fusarium*-species in pure cultures and cereal samples. Syst Appl Microbiol 1998; 21(4): 618-31.
26. Schilling AG, Möller EM and Geiger HH. Polymerase chain reaction-based assays for species-specific detection of *Fusarium culmorum*, *F. graminearum* and *F. aveneceaum*. Mol Plant Pathol 1996; 86: 515-22.
27. Kerényi Z, Moretti A, Waalwijk C, Oláh B, Hornok L. Mating type sequences in asexually reproducing *Fusarium* species. Appl Environ Microbiol 2004; 70(8): 4419-23.
28. Chandler EA, Simpson DR, Thomsett MA, Nicholson, P. Development of PCR assays to Tri7 and Tri13 trichothecene biosynthetic genes, and characterisation of chemotypes of *Fusarium graminearum, Fusarium culmorum* and *Fusarium cerealis*. Physiol Mol Plant Pathol 2003; 62(6): 355-67.
29. Harris SD. Morphogenesis in germinating *Fusarium graminearum* macroconidia. Mycologia 2005; 97(4): 880-7.
30. Nelson PE, Dignani MC, Anaissie EJ. Taxonomy, biology, and clinical aspects of *Fusarium* species. Clin Microbiol Rev 1994; 7(4):479-504.
31. Abedi-Tizaki M and Sabbagh SK. Morphological and molecular identification of Fusarium head blight isolates from wheat in north of Iran. Aust J Crop Sci 2012; 6(9):1356-61.
32. Doohan FM, Parry DW, Jenkinson P, Nicholson P. The use of species specific PCR assays to analyse Fusarium ear blight of wheat. Plant Pathol 1998; 47: 197-205.
33. Edwards SG, Pirgozliev SR, Hare MC, Jenkinson P. Quantification of trichothecene-producing *Fusarium* species in harvested grain by competitive PCR to determine efficacies of fungicides against Fusarium head blight of winter wheat. Appl. Environ. Microbiol 2001; 67: 1575-80.
34. Niessen L, Schmidt H, Vogel RF. The use of *tri5* gene sequences for PCR detection and taxonomy of trichothecene-producing species in the *Fusarium* section *Sporotrichiella*. International Journal of Food Microbiology 2004; 95(3): 305-19.
35. Brancão MF, Bianchi VJ, de Farias CRJ, dos Santos J, Rosseto EA. Caracterização genética de *Fusarium graminearum* Schwabe através de técnicas moleculares. Curr Agric Sci Technol 2008; 14(3).
36. Agodi A, Barchitta M, Ferrante M, Sciacca S, Niessen L. Detection of trichothecene producing *Fusarium* spp. by PCR: adaptation, validation and application to fast food. Ital J Public Health 2005; 2(1).
37. Leslie JF and Summerell BA. An Overview of *Fusarium*. Brown DW & Proctor RH, editors. *Fusarium*: Genomics, Molecular and Cellular Biology. Caister Academic Press; 2013.p.1-9.

38. Wallace MM and Covert SF. Molecular mating type assay for *Fusarium circinatum*. Appl Environ Microbiol. 2000; 66(12):5506-8.
39. Albayrak G, Yörük E, Gazdağli A, Sharifnabi B. Genetic diversity among *Fusarium graminearum* and *F. culmorum* isolates based on ISSR markers. Arch Biol Sci 2016; 68(2):333-43.
40. Tóth B, Mesterházy Á, Nicholson P, Téren J, Varga J. Mycotoxin production and molecular variability of European and American isolates of *Fusarium culmorum*. In Molecular Diversity and PCR-detection of Toxigenic *Fusarium* Species and Ochratoxigenic Fungi Springer, Dordrecht; 2004. p.587-99.
41. Kimura M, Tokai T, O'Donnell K, Ward TJ, Fujimura M, Hamamoto H, Shibata T, Yamaguchi I. The trichothecene biosynthesis gene cluster of *Fusarium graminearum* F15 contains a limited number of essential pathway genes and expressed non-essential genes. FEBS Lett 2003; 539:105-10.
42. Li HP, Wu AB, Zhao CS, Scholten O, Löffler H, Liao YC. Development of a generic PCR detection of deoxynivalenol- and nivalenol-chemotypes of *Fusarium graminearum*. FEMS Microbiol Lett 2005; 243:505-11.
43. Brown DW, Dyer RB, McCormik SP, Kendra DF, Planttner RD. Functional demarcation of the *Fusarium* core trichothecene gene cluster. Fungal Genet Biol. 2004; 41:454-62.
44. Lee T, Han YK, Kim KH, Yun SH, Lee YW. *Tri13* and *Tri7* determine deoxynivalenol- and nivalenol-producing chemotypes of *Gibberella zeae*. Appl Environ Microbiol 2002; 68(5):2148-54.
45. Jennings P, Coates ME, Walsh K, Turner JA, Nicholson P. Determination of deoxynivalenol- and nivalenol-producing chemotypes of *Fusarium graminearum* isolated from wheat crops in England and Wales. Plant Pathol 2004; 53:643-52.
46. Jennings P, Coates ME, Turner JA, Chandler EA, Nicholson P. Determination of deoxynivalenol and nivalenol chemotypes of *Fusarium culmorum* isolates from England and Wales by PCR assay. Plant Pathol 2004; 53:182-90.
47. Haratian M, Sharifnabi B, Alizadeh A, Safaie N. PCR analysis of the *Tri13* gene to determine the genetic potential of *Fusarium graminearum* isolates from Iran to produce nivalenol and deoxynivalenol. Mycopathologia 2008; 166:109-16.
48. Tunali B, Nicol J, Erol FY, Altıparmak G. Pathogenicity of Turkish crown and head scab isolates on stem bases on winter wheat under greenhouse conditions. Plant Pathol J 2006; 5(2):143-9.
49. Tunali B, Özseven İ, Büyük O, Erdurmus D, Demirci A. Fusarium head blight and deoxynivalenol accumulation of wheat in Marmara region and reactions of wheat cultivars and lines to *F. graminearum* and *F. culmorum*. Plant Pathol J 2006; 5(2):150-6.
50. Mert-Türk F and Gencer R Distribution of the 3-AcDON, 15-AcDON, and NIV chemotypes of *Fusarium culmorum* in the North-West of Turkey. Plant Prot Sci 2013; 49(2):57-64.
51. Tok FM and Arslan M. Distribution and genetic chemotyping of *Fusarium graminearum* and *Fusarium culmorum* populations in wheat fields in the eastern Mediterranean region of Turkey. Biotechnol Biotechnol Equip 2016; 30(2):254-60.